Functional role of the Reinitiation Supporting Protein (RISP) in plant translation initiation and reinitiation

Eder Alberto Mancera-Martinez

UNIVERSITÉ DE STRASBOURG

ÉCOLE DOCTORALE DES SCIENCES DE LA VIE ET DE LA SANTÉ

INSTITUT DE BIOLOGIE MOLÉCULAIRE DES PLANTES UPR-CNRS 2357

THÈSE

présentée par :

Eder Alberto MANCERA-MARTÍNEZ

soutenue le : **24 novembre 2014**

pour obtenir le grade de : **Docteur de l'Université de Strasbourg**

Mention : Sciences de la Vie et de la Santé

Discipline : Aspects Moléculaires et Cellulaires de la Biologie

Fonction de la protéine cellulaire RISP (Reinitiation Supporting Protein) dans la reinitiation de la traduction chez les plantes

THÈSE dirigée par :

Mme. RYABOVA Lyubov	Directrice de recherche, Université de Strasbourg, IBMP-CNRS

RAPPORTEURS :

M. MEYER Christian	Directeur de recherche, INRA-Centre Versailles-Grignon
M. ROBAGLIA Christophe	Professeur, Université Aix Marseille, CEA-CNRS

AUTRES MEMBRES DU JURY :

M. WESTHOF Eric	Professeur, Université de Strasbourg, IBMC-CNRS
M. MARTIN Franck	Chargé de recherche, Université de Strasbourg, IBMC-CNRS
M. POOGGIN Mikhail	Directeur de recherche, Université de Bâle

Dédicace

A Marie…

“Esta vez volvíamos,
el amanecer te daba en la cara como la expresión más viva de ti misma,
tus cabellos llevaban la brisa,
el puerto era una flor cortada en nuestras manos”. José Carlos Becerra

A mis padres Martha Laura y Rosendo y a mi hermano Fernando Evair…

“A veces tu ausencia forma parte de mi mirada, mis manos contienen la lejanía de las tuyas y el otoño es la única postura que mi frente puede tomar para pensar en ti”. José Carlos Becerra

Los amo, gracias por siempre alumbrar con su presencia los momentos más bellos de mi vida.

Acknowledgements

The work described in this thesis was accomplished in a large part due to the many people who have given me guidance and support through the years. First, I would like to thank my advisor, Dr. Lyuba Ryabova, for accepting me into her lab and providing me with support and a fantastic intellectual environment. I would not have even arrived here at Strasbourg University if it were not due to her support. I am also thankful for the excellent example she has provided as a successful researcher.

In particular, I would like to thank ever so much my friends Mikhail Shchepetilnikov and Jean-Michel Daviere. I appreciate all their contributions of time, ideas, and training to make my Ph.D. experience productive and stimulating. The joy and enthusiasm they have for their own research was contagious and motivational for me, even during tough times in the Ph.D. pursuit. I am absolutely sure that without their valuable help and advice I would not have been able to go further in my research.

If this research represents anything, it is that it is possible for a student to reach beyond the boundaries of his/her previous training. I definitely started my Ph.D. research as a pure chemist who wished to learn more about plant molecular biology. Any 'rounding' of my abilities that I have obtained is due in large part to the patience of my lab colleagues from IBMP, and their ability to explain new concepts and to suggest good ideas: Mario Keller, Angèle Geldreich, Clément Bouton, Nina Lukhovitskaya and Maria Dimitrova. To them, I am really grateful.

I would also like to thank my committee members Drs. Christian Meyer, Christophe Robaglia, Eric Westhof, Franck Martin and Mikhail Pooggin. It is a multidisciplinary committee and it matches my work. Their different perspectives on the important issues in my research have been invaluable.

However, I would not have even been able to overcome this challenge if it was not due to the love, happiness and efforts my wife and parents share with me.

Résumé

Des études dans notre laboratoire ont démontré que la protéine cellulaire appelée RISP est un composant de la machinerie de traduction cellulaire. Cette dernière est détournée par le virus de la mosaïque du chou-fleur (CaMV) pour assurer, ensemble avec la protéine virale TAV (transactivator/viroplasmin), la traduction de son ARN 35S polycistronique. TAV active le mécanisme de réinitiation après traduction d'un cadre de lecture ouvert (ORF, open reading frame) en interagissant avec le facteur d'initiation de la traduction eIF3 et avec RISP et en les recrutant au niveau des polysomes pour assurer la réinitiation de la traduction au niveau d'un ORF, situé en aval sur le même ARN messager. D'après les résultats que nous avons obtenus *in vitro*, le complexe formé par RISP et eIF3 peut s'associer avec la sous-unité ribosomique 40S alors que RISP est incapable de se lier au complexe eIF3-40S. Le CaMV est également le premier virus codant une protéine capable d'interagir directement avec la protéine kinase cellulaire TOR et ainsi activer sa voie de signalisation qui stimule la traduction. La protéine RISP a été identifiée comme une nouvelle cible de la voie de signalisation de TOR et il a été montré que cette phosphorylation de la sérine 267 (Ser267) est requise pour promouvoir la réinitiation de la traduction activée par TAV. Cependant, le rôle de RISP dans la traduction cellulaire de même que dans le processus d'activation par TAV fait encore l'objet d'investigations.

Les résultats que j'ai obtenus au cours de mon travail de thèse suggèrent que RISP intervient ensemble, avec eIF3, au niveau du complexe de pré-initiation 43S (43S PIC) pour recruter le complexe ternaire (TC ; eIF2/GTP/Met-tRNAi^{Met}), ainsi que dans le mouvement dynamique du ribosome 80S en cours de traduction, en faisant un pont entre les sous-unités ribosomiques 40S et 60S. Dans un premier temps j'ai démontré que RISP est capable d'interagir *in vitro* avec la sous unité β du facteur d'initiation eIF2 *in vitro* et qu'il peut être immunoprécipité spécifiquement avec des anticorps anti-eIF2α à partir d'extrait de plantes. Des résultats préliminaires indiquent que la phosphorylation de RISP n'est pas critique pour la formation du complexe entre RISP et eIF2β. Par conséquent, la mutation de la sérine 267 de RISP en alanine (RISP-S267A) qui empêche la phosphorylation, permet à RISP de s'associer à eIF2β plus efficacement que la substitution de cette même sérine par un acide aspartique (RISP-S267D) qui mime l'état de phosphorylation de RISP. Notre modèle actuel propose que RISP relie

eIF3 et eIF2 au sein du complexe de pré-initiation 43S pour promouvoir le recrutement du TC au niveau de la sous-unité 40S.

La structure cristallographique du ribosome 80S de la levure a révélé que le domaine N-terminal de la protéine ribosomique eL24 qui fixe TAV, est localisé à l'interface de la sous-unité 60S alors que l'hélice α C-terminale d'eL24 qui interagit avec RISP, émerge de la sous-unité 60S en direction de la sous-unité 40S. L'analyse du ribosome suggère que la protéine eL24 de la sous-unité 60S et la protéine ribosomique eS6 de la sous-unité 40S pourraient former un pont entre les deux sous-unités du ribosome. La protéine eS6 est connue depuis longtemps pour être une cible de la voie de TOR mais la fonction de cette phosphorylation demeure inconnue. De ce fait, nous avons investigué l'interaction éventuelle entre eS6 et eL24 ainsi que le rôle de RISP dans l'association entre les sous-unités 40S et 60S. Bien que nous n'ayons trouvé aucun lien direct entre eS6 et eL24, il s'est avéré que RISP a la capacité, lorsqu'elle est phosphorylée, d'interagir non seulement avec eL24 mais également avec eS6 chez *Arabidopsis thaliana*. L'hélice C-terminale de la protéine eS6 d'*Arabidopsis thaliana* contient 5 sérines dont au moins trois pourraient être phosphorylées par la voie de TOR. Nos résultats suggèrent que la phosphorylation de la protéine eS6 joue un rôle dans sa liaison à RISP, ainsi que dans la transactivation traductionnelle chez le CaMV. En effet, des plantes d'*Arabidopsis thaliana*, dans lesquelles une des deux copies du gène codant eS6 a été inactivée (plantes knock-out), sont plus résistantes à l'infection par le CaMV et moins efficaces dans la transactivation traductionnelle assurée par TAV. Nos résultats indiquent que la liaison entre les sous-unités ribosomiques 60S et 40S sous l'effet de RISP, est régulée par la voie de TOR et qu'elle joue un rôle dans le contrôle de la réinitiation de la traduction.

Les résultats obtenus au cours de mon travail de thèse contribuent à clarifier le mécanisme d'initiation et de réinitiation de la traduction chez les plantes de même que la stratégie utilisée par les virus pour franchir les barrières qui limitent la réinitiation de la traduction chez les eucaryotes. De manière inattendue, mes résultats apportent également un éclaircissement sur le rôle de la protéine ribosomale eS6 et sa phosphorylation par la voie de TOR dans l'initiation de la traduction et lors de l'infection de la plante par le CaMV. Ainsi, nous commençons enfin à comprendre l'importance et le rôle des ORFs présents dans la région 5' non-traduite de près de 35% des ARNm qui sont traduits par un mécanisme de réinitiation chez *Arabidopsis thaliana*.

[Mots-clés]: (Reinitiation; Polycistronic mRNAs; sORF; Pararetrovirus; TAV; RISP; Ribosomal protein eS6, TOR signaling pathway)

Contents

List of figures

Liste of tables

List of abbreviations

Abbreviation	Term
CaMV	*Cauliflower mosaic virus*
TAV	Transactivator/viroplasmin
RISP	Reinitiation supporting protein
eIF	Eukaryotic initiation factor
TOR	Target of rapamycin
ORF	Open reading frame
uORF	Upstream open reading frame
UTR	Untranslated región
sORF	Short upstream open reading frame
ARF	Auxin-response factor
IRES	Internal ribosome entry site
pgRNA	Pre-genomic RNA
40S	Small ribosomal subunit
60S	Large ribosomal subunit
80S	80S ribosome
S6K1	Eukaryotic ribosomal protein eS6 kinase-1
tRNA	Transfer RNA
rRNA	Ribosomal RNA
Met-tRNA$^{Met}_{i}$	Methionine initiator transfer RNA
GTP	Guanosine-5'-triphosphate
TC	Ternary complex
PIC	Preinitiation complex
PABP	Poly-A binding protein
smFRET	Single molecule Fluorescence Resonance Energy Transfer
PTC	Ribosomal peptidyl transferase center
ABCE1	ATP-binding cassette protein-1
post-TCs	Post-termination complexes
ES	Ribosomal expansion segment
r-proteins	Ribosomal proteins
VR	Ribosomal variable region
eB	Eukaryotic ribosomal intersubunit bridge
GAP	GTPase-activating protein

Preface

Protein synthesis is a highly conserved process that links amino acids together on the ribosomal machinery according the sequence of an mRNA template. Protein synthesis in eukaryotes shares some similarities with that in bacteria, comprising four phases: initiation, elongation, termination and recycling. While the elongation phase is highly conserved, the initiation, termination and recycling events differ considerably. A unique feature of eukaryotic protein synthesis is that mRNAs are translated in the cytoplasm, making translation uncoupled from transcription in the nucleus. In eukaryotes, the majority of mature mRNAs is monocistronic, 5'-capped and 3'-polyadenylated, and these mRNAs are normally translated via 5'-cap dependent translation initiation. Translation initiation involves the binding of the 40S ribosomal subunit (40S) to the capped 5'-end of an mRNA and subsequent scanning of the 5' untraslated region (5' UTR) for searching an initiation codon.

Polycistronic mRNA translation is frequent in Eubacteria, although translation of the downstream cistrons may not involve coupled termination-reinitiation events. In contrast, translation of downstream open reading frames (ORFs) of polycistronic mRNAs via reinitiation is usually impaired in eukaryotes, where the translation terminating ribosome dissociates mRNA, unless there is an internal ribosome entry site (IRES) or unless the upstream ORF (uORF) is very short. After short uORF translation, the ribosome can resume scanning and initiate at further downstream ORF by a mechanism known as reinitiation. However, mRNAs that harbour uORFs within their 5' UTRs can finally produce their encoded protein albeit at lower levels indicating that eukaryotic ribosomes can conduct subsequent reinitiation events on the same mRNA. This is the case of proto-oncogene or transcription factor encoding mRNAs whose expression is apparently regulated at the post-transcriptional level in order to reduce synthesis of toxic or harmful proteins in cells.

Therefore, in addition to canonical translation control mechanisms, reinitiation of translation being the non-canonical event requires a special attention: about 30% of full-length mRNAs harbour one or more uORFs in their 5'-leader sequences in *Arabidopsis*. These uORFs

seem to be important regulators of gene expression required to control expression of genes coding for potent proteins such as cytokines, growth factors, protein kinases, and transcription factors. Reinitiation is normally less efficient than initiation at the first ORF, and uORFs are used to down-modulate production of the abovementioned critical effector proteins. Many important transcriptional factors that mediate responses to plant hormone auxin—auxin-responsive factors (ARFs)—contain multiple short ORFs (sORFs) and their translation requires reinitiation. Several disorders in humans, for example hereditary thrombocythemia, are due to perturbation in translation reinitiation.

Viruses, and particularly plant viruses, have developed through evolution several strategies to express their proteins from polycistronic mRNAs. Such mechanisms are often integral to viral translational and replicative programs (e.g., IRES) or regulatory mechanisms (e.g., ribosome shunting), or furnish a mode to enlarge the coding capacity within a restricted genome (e.g., readthrough, frameshifting). These strategies require RNA cis-elements and do not seem to alter the translational machinery of the host.

Cauliflower mosaic virus (CaMV), a plant *pararetrovirus* infecting a wide variety of Cruciferae plants and a few Solanaceae species, has developed a strategy to activate reinitiation after long ORF translation that under normal circumstances is prohibited in eukaryotes. Its circular double-stranded DNA genome code for six functional proteins: one of them, translation transactivator/viroplasmin protein (TAV)—mainly translated from a separate subgenomic 19S RNA—is essential for polycistronic translation of the 35S pregenomic RNA (35S pgRNA). 35S pgRNA acts as the pregenomic RNA—intermediate of reverse transcription-mediated DNA replication—, and the polycistronic mRNA for synthesis of viral proteins. Translation of this polycistronic 35S pgRNA occurs via a reinitiation mechanism under the control of TAV. To accomplish reinitiation, TAV interacts with a complex of cellular factors—the key translation initiation factor 3 (eIF3) and a novel plant ReInitiation Supporting Protein (RISP)—called as a reinitiation complex. TAV exceptionally promotes reinitiation through a mechanism involving retention of the reinitiation complex on 80S and re-use of eIF3 and RISP to regenerate reinitiation-competent ribosomes. Cellular and viral reintiation strategies are extremely complex and remain not well understood. Both the reinitiation and the canonical translation initiation strategies in eukaryotes are critical for understanding of translational control mechanisms and therefore CaMV is a great tool to study both translation initiation and reinitiation cellular strategies including analysis of essential host factors. Moreover, it has been shown that TAV function depends on interaction with the target-of-rapamycin (TOR) protein kinase, which plays

a key role in controlling cell growth in response to energy sufficiency, nutrients, hormones and growth factors. TAV binding to TOR triggers TOR hyperactivation and S6K1 phosphorylation in *Arabidopsis*. RISP is the TOR signaling pathway downstream target and is phoshorylated at Ser267 in response to TAV or phytohormone auxin. Phosphorylated RISP is active in TAV-mediated reinitiation.

The main aim of my thesis was to characterize and to understand the molecular mechanisms of RISP function in (1) initiation and (2) reinitiation of translation, including virus-activated reinitiation after long ORF translation. To better understand these mechanisms of translation initiation, a brief overview of translation steps and their control by canonical translation (re)initiation factors (eIFs) in eukaryotes will be presented in the Introductory part of my thesis. I will describe in details the main protagonists of (re)initiation such as ribosomes and main eIFs. Various mechanisms of polycistronic RNA translation, particularly in plant viruses, will also be discussed.

1. Introduction

In translation, the arrangement of nucleotides on mRNA directs the biosynthesis of a specific polypeptide chain with unique enzymatic or structural properties. This action occurs on the ribosome, and the movement of tRNA and mRNA through the ribosome is an intricate process that is characterized by both high speed and accuracy. In all living organisms the ribosome is the central element of the cell translational machinery—it accommodates mRNA and exhibits essential functions such as to receive a succession of tRNA molecules charged with proper amino acids, which have to recognize mRNA through base-pairing of their anti-codons with corresponding mRNA codons, to catalyze the formation of polypeptide bonds within the peptidyl transferase center and to promote translocation of the ribosome along the mRNA. This whole complex of processes is carried out by this giant ribonucleoprotein machine, the ribosome, which consists of two ribosomal subunits that are made of ribosomal RNA (rRNA), and up to 80 different proteins in higher eukaryotic cells.

However, numerous eukaryotic translation initiation factors (eIFs) have to assist the ribosome to initiate translation, particularly to load the ribosome on the mRNA 5'-end and encounter the AUG initiation codon (Pestova et al., 2007). That is in contrast to prokaryotes, where only few initiation factors assist the 70S ribosome in initiation of translation suggesting a more complex control of initiation in eukaryotes.

Table 1.1-1. Eukaryotic initiation factors

Name	Number of subunits and their molecular mass (kDa)	Function
Core initiation factors		
eIF2	3 (36.1, 38.4 and 51.1)	Forms an eIF2–GTP–Met-tRNAi ternary complex that binds to the 40S subunit, thus mediating ribosomal recruitment of Met-tRNAi
eIF3	13 (800 total)	Binds 40S subunits, eIF1, eIF4G and eIF5; stimulates binding of eIF2–GTP–Met-tRNAi to 40S subunits; promotes attachment of 43S complexes to mRNA and subsequent scanning; and possesses ribosome dissociation andanti-association activities preventing joining of 40S and 60S subunits
eIF1	1 (12.7)	Ensures the fidelity of initiation codon selection; promotes ribosomal scanning; stimulates binding of eIF2–GTP–Met-tRNAi to 40S subunits; and prevents premature eIF5-induced hydrolysis of eIF2-bound GTP and Pi release
eIF1A	1 (16.5)	Stimulates binding of eIF2–GTP–Met-tRNAi to 40S subunits and cooperates with eIF1 in promoting ribosomal scanning and initiation codon selection
eIF4E	1 (24.5)	Binds to the m7GpppG 5' terminal 'cap' structure of mRNA
eIF4A	1 (46.1)	DEAD-box ATPase and ATP-dependent RNA helicase
eIF4G	1 (175.5)	Binds eIF4E, eIF4A, eIF3, PABP, SLIP1 and mRNA and enhances the helicase activity of eIF4A
eIF4F	3 (246.1 total)	A cap-binding complex comprising eIF4E, eIF4A and eIF4G; unwinds the 5' proximal region of mRNA and mediates the attachment of 43S complexes to it; and assists ribosomal complexes during scanning
eIF4B	1 (69.3)	An RNA-binding protein that enhances the helicase activity of eIF4A
eIF4H	1 (27.4)	An RNA-binding protein that enhances the helicase activity of eIF4A and is homologous to a fragment of eIF4B
eIF5	1 (49.2)	A GTPase-activating protein specific for GTP-bound eIF2 that induces hydrolysis of eIF2-bound GTP on recognition of the initiation codon
eIF5B	1 (138.9)	A ribosome-dependent GTPase that mediates ribosomal subunit joining
eIF2B	5 (33.7, 39.0, 50.2, 59.7 and 80.3)	A guanosine nucleotide exchange factor that promotes GDP–GTP exchange on eIF2
Auxiliary factors		
DHX29	1 (155.3)	A DExH box-containing protein that binds 40S subunit and promotes ribosomal scanning on mRNAs with long highly structured 5' UTRs
Ded1	1 (65.6)	A DEAD box-containing NTPase and RNA helicase that potentially promotes scanning in *Saccharomyces cerevisiae*
eIF6	1 (26.6)	An anti-association factor that binds 60S subunits and prevents them from joining to 40S subunits
p97	1 (102.4)	Closely related to the carboxy-terminal two-thirds of eIF4G; binds eIF4A and eIF3; and promotes initiation in a potentially mRNA-specific manner
PABP	1 (70.7)	Binds to the 3' poly(A) tail of mRNA, eIF4G and eRF3; enhances binding of eIF4F to the cap; and might facilitate recruitment of recycled post-termination 40S subunits back to the 5' end of mRNA

1.1 Mechanisms of eukaryotic translation initiation

1.1.1 General overview of translation

Initiation phase

Translation initiation is the mechanism of association of the large (60S) and the small (40S) ribosomal subunits leading to the formation of the elongating-competent 80S ribosome (80S), in which the AUG start codon of the mRNA is base-paired with the anticodon loop of the initiator Methionyl-tRNA (Met-tRNA$^{Met}_{i}$) in the ribosomal P-site (Jackson et al., 2010). Initiation is promoted and highly regulated by at least twelve eIFs (Table 1.1-1), containing more than 30 different polypeptides (Pestova et al., 2007), many of which are known to be the downstream targets of potent regulatory pathways (Hinnebusch and Lorsch, 2012). However, there are still putative eIFs whose role and relevance in initiation are not well characterized.

The initiation phase of protein synthesis can be divided in several distinct steps including the assembly of the 48S pre-initiation complex (48S PIC) with Met-tRNA$^{Met}_{i}$ positioned over the start AUG codon in the P-site of 40S, and the joining of 48S PIC with 60S (Figure 1.1-1; Jackson et al., 2010). Initiation starts with the assembly of a ternary complex (TC) consisting of Met-tRNA$^{Met}_{i}$, eIF2 and GTP, which then is recruited on 40S already pre-bound with eIFs 1, 1A, 3 and 5 to mold a 43S pre-initiation complex (43S PIC, Majumdar et al., 2003). eIFs 1, 1A and 3 join the 40S subunit and produce an “open” state, to which TC binds readily (Aitken and Lorsch, 2012). 43S PIC is next recruited to the 5’ end of the mRNA, distinguished by a 7-methylguanosine (cap) pre-bound by the cap binding complex eIF4F composed of the cap-binding protein (eIF4E), an RNA helicase (eIF4A) and the scaffold protein eIF4G, via interactions between 40S-bound eIF3 and cap-bound eIF4G, eIF4B and the poly(A)-binding protein (PABP). The main player is the eIF4G scaffold protein that is able to interact with PABP, eIF4E, eIF4A and eIF3. These interactions enable eIF4G not only to coordinate the assembly of circular mRNAs, but also to establish a bridge between this “activated and partially unwound mRNP” and 43S PIC in order to guarantee the attachment of 43S PIC at the capped 5’ end of the mRNA (Hinnebusch and Lorsch, 2012). Once bound near the cap, 43S PIC scans the 5’UTR region until it encounters the AUG start codon in a suitable initiation context using perfect complementarity to the Met-tRNA$^{Met}_{i}$ anticodon loop (Hinnebusch, 2011). The codon-anticodon interaction provokes arrest of 40S scanning and triggers eIF5 (GTPase-activating protein, GAP)-dependent hydrolysis of eIF2-bound GTP to its GDP-associated state accompanied by phosphate release.

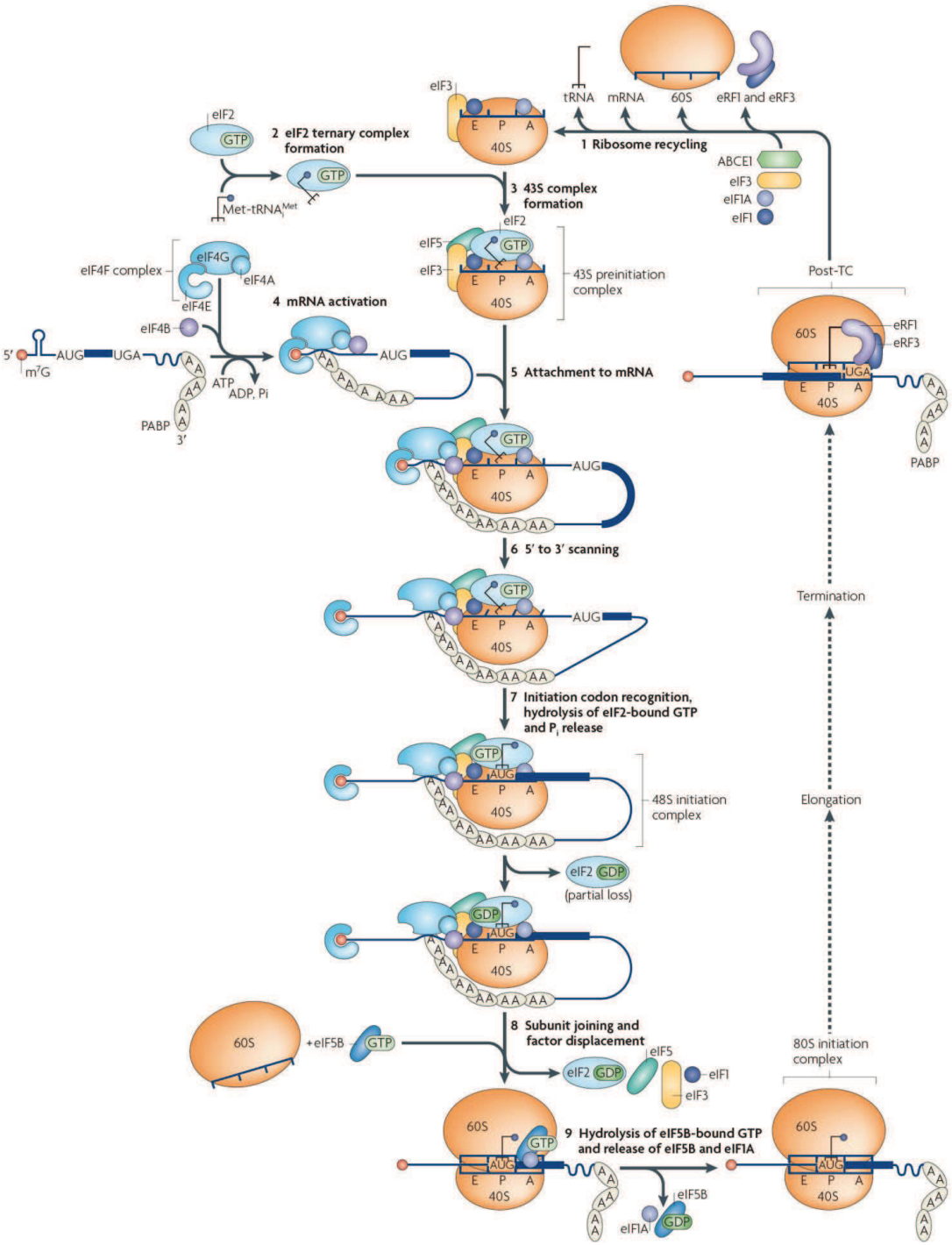

Figure 1.1-1 | **Model of the canonical pathway of eukaryotic 5' cap dependent translation initiation** (**1**) Recycling of post-termination complexes (post-TC) provides separated ribosomal subunits ready to initiate translation of new mRNA—the canonical initiation pathway can be dived into seven discrete stages (**2-9**). (**2**) Initiation begins with the formation of the ternary complex (TC) containing eIF2·GTP and the Met-tRNA$^{Met}_i$. (**3**) The TC is recruited to the 40S subunit bound to MFC (eIFs 1, 1A, 3 and 5) mainly via eIF3 that completes formation of 43S PIC. (**4**) Initiation-competent mRNA is pre-bound by the eIF4F complex and eIF4B at the capped 5'-end and PABP at the poly(A) tail. (**5**) 43S PIC is loaded at the cap structure mainly via interactions between eIF3 and eIF4F to form 48S PIC. (**6**) Once bound at the 5' end of the mRNA, 43S PIC scans to locate the start AUG codon in the optimal initiation context. (**7**) Codon-anticodon base pairing triggers hydrolysis of eIF2-bound GTP, eIF1 release and arrest of the scanning process. (**8**) eIF2·GDP dissociates followed by eIF5B binding that triggers 60S joining. (**9**) After 60S joining, eIF5B-bound GTP is hydrolysed and mediates eIF5B release and gradual dissociation of other factors. (**10**) The 80S ribosomal initiation complex is formed—Met-tRNA$^{Met}_i$ is base paired with the AUG codon in the ribosomal P-site. *Modified from Jackson et al. (2010), Nature Reviews Molecular Cell Biology 11, 113-127*

After removal of eIF2-GDP, another G-factor eIF5B catalyzes the joining of 60S resulting in the formation of an elongation-competent 80S complex with Met-tRNA$^{Met}_{i}$ in the 80S P site that is ready to initiate the elongation phase of protein synthesis (Hinnebusch and Lorsch, 2012; Pestova et al., 2007)

Elongation phase

The process of elongation is well conserved between eukaryotes and bacteria (Rodnina and Wintermeyer, 2009), and the mechanism of elongation has been studied mainly using bacterial models. Translation initiation ends with the mRNA-bound 80S ribosome with the Met-tRNA$^{Met}_{i}$ anticodon loop in the P (donor) site base-paired with the start codon (Figure 1.1-2). The next mRNA codon is present in the A (acceptor) site of the ribosome expecting binding of the correct aminoacyl-tRNA. The eukaryotic elongation factor 1A (eEF1A; its bacterial ortholog is known as EF-Tu), binds aminoacyl-tRNA in a GTP-dependent manner and then guide the tRNA molecule to the A site of the ribosome (Dever and Green, 2012). Interesting that the initial step in prokaryotes, the interaction of EF-Tu·GTP·aminoacyl-tRNA with the ribosome is a codon-independent, and probably is mediated by early interactions between EF-Tu and the 60S ribosomal stalk composed of L7/L12 ribosomal proteins (Rodnina et al., 2005).

The formation of the cognate codon-anticodon duplex leads to very complex conformational changes in the decoding site on 40S (Rodnina et al., 1994), and furnishes an activation signal that is communicated to the G domain of EF-Tu leading to the formation of the activated GTPase status of the ribosome·EF-Tu·aminoacyl-tRNA complex (Rodnina et al., 1995), which is followed by GTP hydrolysis. As a result, the conformation of EF-Tu changes from GTP- to the GDP-bound form (Gromadski and Rodnina, 2004), triggering elongation factor dissociation from the elongating machinery. All these arrangements enable the aminoacyl-tRNA to be placed into the A site.

Accommodation of the aminoacyl-tRNA into the A site “locks” the ribosome, and transpeptidation reaction between peptidyl-tRNA in the P site and aa-tRNA in the A-site— hydrolysis of the ester bond and transfer of a peptidyl moiety from P-site peptidyl-tRNA to A-site aa-tRNA— can occur rapidly (Dever and Green, 2012). The transpeptidation reaction proceeds spontaneously in the peptidyl transferase center (PTC), and results in formation of one-residue-elongated peptidyl-tRNA in the A-site, and deacylated tRNA in the P-site. PTC is formed of conserved rRNA elements on the 60S subunit, and functions to bring the substrates closer for catalysis.

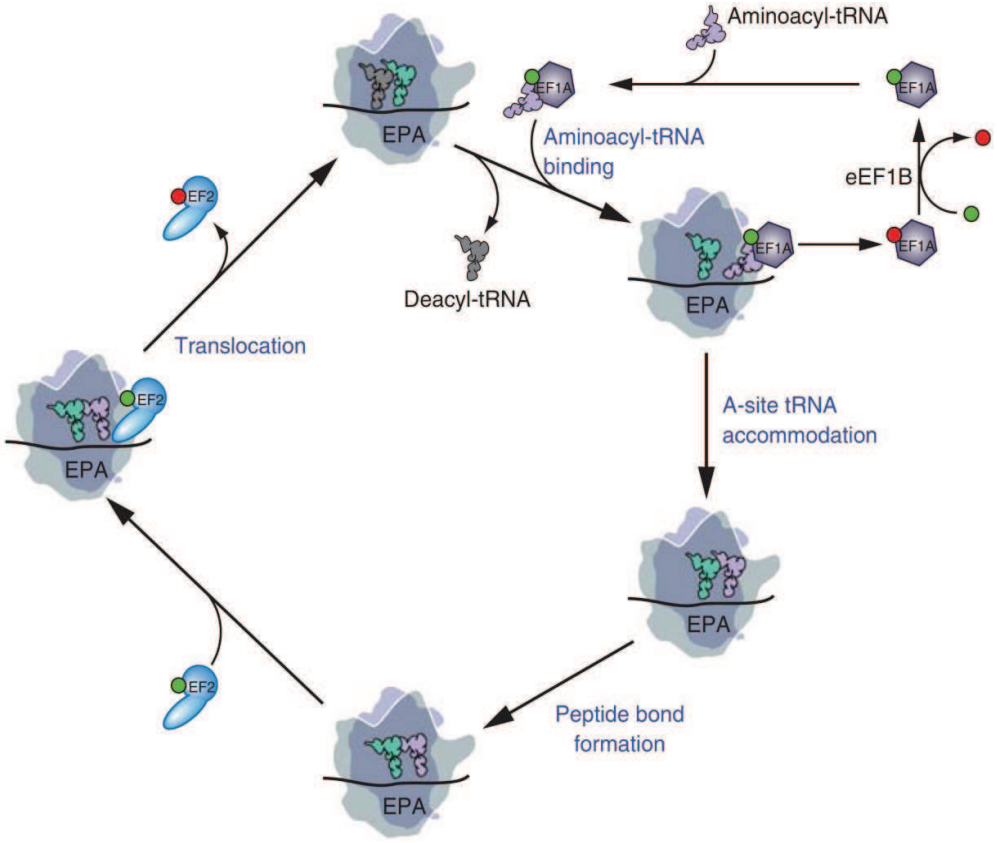

Figure 1.1-2 | **The eukaryotic translation elongation cycle**
(1) Binding of aminoacyl-tRNA—an eEF1A·GTP·aminoacyl-tRNA complex delivers aminoacyl-tRNA (aa-tRNA) into the A-site of the ribosome with the anticodon loop of tRNA in contact with the mRNA A-site codon.
(2) Transpeptidation reaction between peptidyl-tRNA in the P site and aa-tRNA in the A-site: hydrolysis of the ester bond and transfer of a peptidyl moiety from P-site peptidyl-tRNA to A-site aa-tRNA.
(3) Translocation—eEF2xGTP binds and triggers translocation—I step: acceptor ends move towards (60S), but not anticodons (40S), II step: GTP hydrolysis promotes couple movement of mRNA and its associated tRNA anticodon ends by 3 nucleotides and removal of eEF2.
Thus, eEF2 pushes the peptidyl-tRNA into the P-site and the deacylated tRNA into the E-site, freeing the A-site for another round of elongation. *Modified from Dever and Green (2012), Cold Spring Harb. Perspect. Biol. doi: 10.1101/cshperspect.a013706.*

After peptide bond formation, the marching-on of the ribosomal subunits triggers movement of the tRNAs into so called hybrid P/E (E-exit site) and A/P states with the acceptor ends of the tRNAs in the E and P-sites and the anticodon loops still being in the P and A sites, respectively. Translocation of tRNAs to the standard E and P sites requires the GTPase eEF2 in eukaryotes or its bacterial ortholog EF-G. Binding of eEF2-GTP stabilizes the hybrid state and triggers rapid hydrolysis of GTP. Conformational changes in eEF2 after GTP hydrolysis and Pi release are thought to alternatively "unlock" the ribosome permitting tRNA and mRNA movement (Dever and Green, 2012). It has been proposed that EF-G and eEF2 function to prevent backward movement of the tRNAs in the unlocked state of the ribosome. At this stage, a deacylated tRNA occupies the E site and the peptidyl-tRNA is in the P site. The A site is free and available for binding of the next aminoacyl-tRNA·eEF1A·GTP complex. The elongation cycle is repeated until the stop codon of the mRNA is loaded in the A site to trigger termination of translation. After GTP hydrolysis, the eEF1A-GDP complex is released and recycled to eEF1A-GTP by the eEF1B factor to participate in further rounds of peptide elongation.

Termination phase

Termination takes place when the ribosome reaches the 3' end of the ORF and a stop codon enters the A site (Jackson et al., 2012). The elongating process is terminated by one of the three stop codons (UAA, UAG and UGA), which, instead of being recognized by a tRNA, are sensed by proteins called class I release factors (RF; Nakamura and Ito, 2003). In eukaryotes, a single release factor, eRF1, identifies all three stop codons.

Upon stop-codon recognition, class I RFs catalyze hydrolysis of the ester bond that links the nascent polypeptide chain to P-site tRNA, through contact with the PTC of the ribosome (Figure 1.1-3). Class II release factor eRF3 is a GTPase, which couples stop-codon recognition and peptidyl-tRNA hydrolysis mediated by eRF1 to ensure rapid and efficient peptide release (Salas-Marco and Bedwell, 2004).

Eukaryotic translation recycling (and some connections to reinitiation)

After termination, the post-termination complexes (post-TC)—mRNA-bound ribosomes— can be recycled. In eukaryotes, besides the known termination factors, the highly conserved and essential ABC-type ATPase ABCE1 has recently been proposed as an important player in ribosome recycling (Figure 1.1-4; Pisarev et al., 2010).

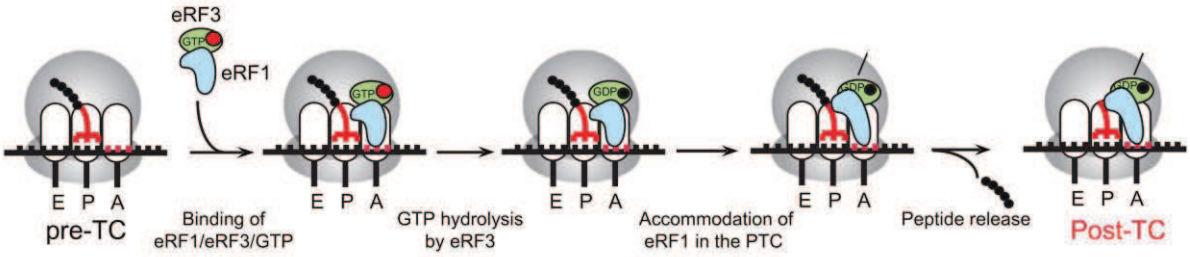

Figure 1.1-3 | **A model for translation termination in eukaryotes**
Pre-termination complexes (pre-TC) contain peptidyl-tRNA in the P-site.
eRF1 and eRF3 bind to pre-TCs as the eRF1·eRF3·GTP complex.
The stop codon is recognized by eRF1 in the A-site.
After GTP hydrolysis by eRF3, eRF1 induces peptide release. At least one release factor, eRF1, remains associated with post-termination complexes (post-TCs). *Modified from Jackson et al. (2012), Advances in Protein Chemistry and Structural Biology 86: 45–93.*

Although eRF3 most likely dissociates from the ribosomal machinery after GTP hydrolysis, eRF1 remains attached to post-TCs after peptide release (Pisarev et al., 2010). After ABCE1-mediated dissociation of post-TCs, deacylated P-site tRNA and mRNA remain attached to 40S (Pisarev et al., 2010). tRNA release is followed by dissociation of mRNA.

In some cases, post-TCs do not go through complete recycling. In these cases 40S subunits remain bound to mRNA, and termination is followed by reinitiation at a downstream ORF (Jackson et al., 2012). Recent genome-wide bioinformatic analyses revealed that more than 45% of mammalian mRNAs contain at least one uORF (Calvo et al., 2009) and ribosome profiles showed that these uORFs are likely translated (Ingolia, 2014). Similar studies indicate that only 13% of yeast mRNAs harbor uORFs, but that many of them are also translated (Ingolia et al., 2009). Reinitiation of translation requires a special attention also in plants since about 30% of mRNAs in *Arabidopsis* harbor one or more uORFs within their 5'-leader sequences. These uORF-containing mRNAs encode for transcriptional factors, including auxin-responsive factors (ARFs; Kim et al., 2007), and other potent proteins. Considering that reinitiation is usually less efficient than initiation at the first ORF, these uORFs are therefore used to down-modulate the production of critical effector proteins (Zhou et al., 2010). Reinitiation can be modulated in response to environmental or physiological changes (Jackson et al., 2012; Schepetilnikov et al., 2013).

1.1.2 The structure and function of the eukaryotic ribosome

The ribosomal machinery is built from ribosomal RNA (rRNA) and ribosomal proteins (r-protein), and thanks to remarkable achievements in the field of the bacterial 70S ribosome, we have a good knowledge of basic universal features of protein synthesis. However, the eukaryotic ribosome is much larger than its bacterial counterpart, and its activity is markedly different in many key ways. Usefully for my research, cryo-electron reconstructions and especially X-ray crystal structures of eukaryotic ribosomes have offered an opportunity to dissect eukaryotic translational-related mechanisms in an atomic detail. Furthermore, despite enormous efforts dedicated to structural modeling of eukaryotic ribosomes over the last fifteen years, the full assignment of the r-proteins in the eukaryotic ribosome only became possible with the improved resolution (3Å) resulting from the crystal structures of the *Saccharomyces cerevisiae* 80S ribosome (Figure 1.1-5 and Figure 1.1-6; Ben-Shem et al., 2011).

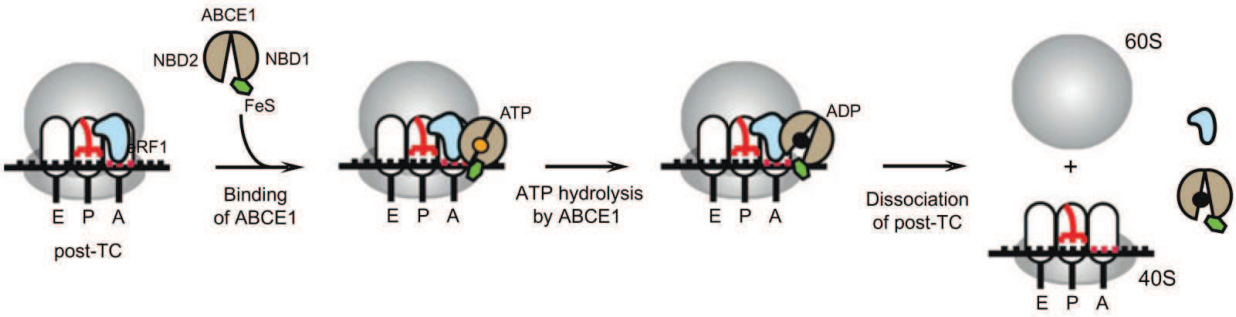

Figure 1.1-4 | **Ribosome recycling in eukaryotes**
After peptide release, eRF1 remains bound to post-TC and together with the ATP-binding cassette protein ABCE1, splits them into free 60S subunits and tRNA- and mRNA-associated 40S subunits. *Modified from Jackson et al. (2012), Advances in Protein Chemistry and Structural Biology 86: 45–93.*

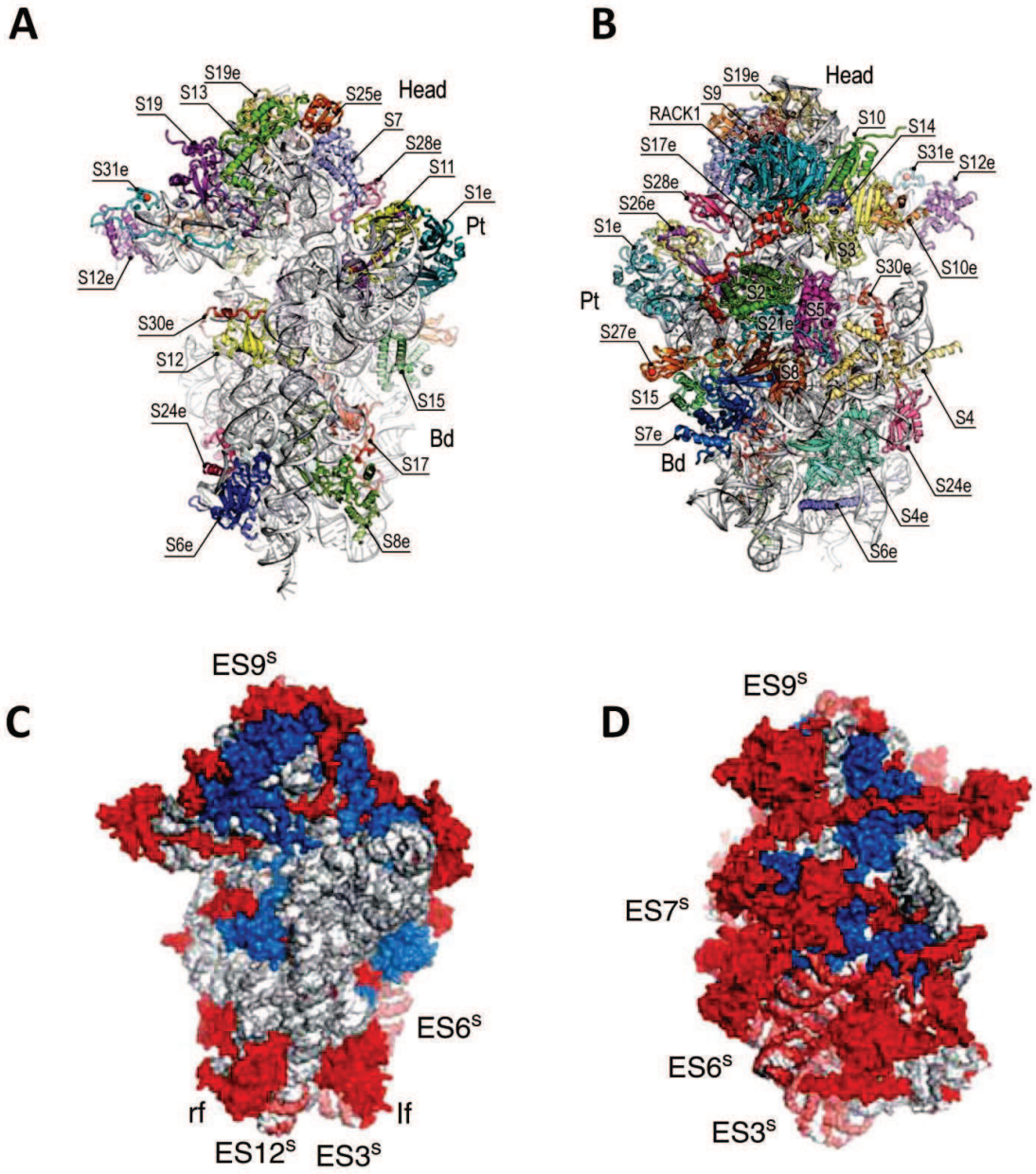

Figure 1.1-5 | **Architecture of the 40S small ribosomal subunit**
(**A**) Interface view of the 40S subunit. Landmarks include head, body (Bd) and platform (Pt) of 40S.
(**B**) Solvent side view of the 40S subunit.
(**C**) Interface and (**D**) solvent views of the eukaryotic 40S subunit, with eukaryotic-specific r-proteins (in red) and rRNA (in pink) shown relative to conserved rRNA (gray) and r-proteins (blue). *Modified from Ben-Shem et al. (2011), Nature 334 (6062): 1524-1529 and Rabl et al. (2011), Science 331:730-736.*

At first sight, comparisons between bacterial and eukaryotic ribosome structures reveal a universally conserved central core, which is involved in catalysis of peptide bond formation by 60S and translates genetic information encoded by mRNA on the mRNA decoding center (located on 40S). The 40S subunit can be divided into head, beak, platform, body, shoulder, left and right foot regions (Figure 1.1-5). Similarly, the superposed view of 60S shows that the core has a structure similar to the bacterial 50S, and key landmarks are conserved, including the central protuberance (CP), the two stalks (L1- and P-stalks in eukaryotes), and the sarcin-ricin loop (SRL) (Figure 1.1-6). During 40/60S joining, the head of the 40S particle is associated with the CP of the 60S subunit forming a cavity wide enough for the passage of a tRNA.

However, in contrast to their bacterial counterparts, eukaryotic ribosomes are about 40% larger due to additional rRNA elements known as expansion segments (ES) as well as many additional ribosomal proteins (r-proteins) and ribosomal protein extensions (Figure 1.1-5 and Figure 1.1-6).

Compared with the approximately 4500 nucleotides of rRNA and 54 r-proteins of the bacterial 70S ribosome, the eukaryotic 80S ribosome contains more than 5500 nucleotides within its rRNA (40S—18S rRNA; 60S—5S, 5.8S and 25S rRNA) and 80 r-proteins (Wilson and Doudna Cate, 2012). The vast majority of the 1.35 MDa of the eukaryote-specific moiety (350 KDa of rRNA ES, 800 kDa of proteins absent in bacteria and 200 kDa of eukaryotic-specific extensions in conserved proteins) is located on the solvent surface of the 80S ribosome, surrounding the universally conserved core (Figure 1.1-5 and Figure 1.1-6; Ben-Shem et al., 2011).

Ribosomal RNA of the 80S ribosome

Concerning rRNA, the major differences between bacterial and eukaryotic ribosomes is the presence of five expansion segments (ESs) and five variable regions (VRs) on 40S, as well as 16 ESs and two VRs on 60S (Figure 1.1-5 and Figure 1.1-6; Wilson and Doudna Cate, 2012). On the large subunit most ES are located on the back and sides of the particle, leaving its interface and the mRNA exit tunnel practically unaffected (Figure 1.1-6; Armache et al., 2010; Ben-Shem et al., 2011). The largest moiety of extra rRNA on 60S is located just behind the P stalk with a second piece located behind the L1 stalk. The main rRNA additions to the CP are due to $ES9^{L}$, composed of two co-axially stacked helices and to $ES12^{L}$, and both elements run parallel to 5S rRNA. On the yeast small subunit the larger part of supplementary rRNA comprises $ES3^{S}$ and $ES6^{S}$, which contact together to construct the left foot of the particle (Figure 1.1-5; Armache et al., 2010; Ben-Shem et al., 2011).

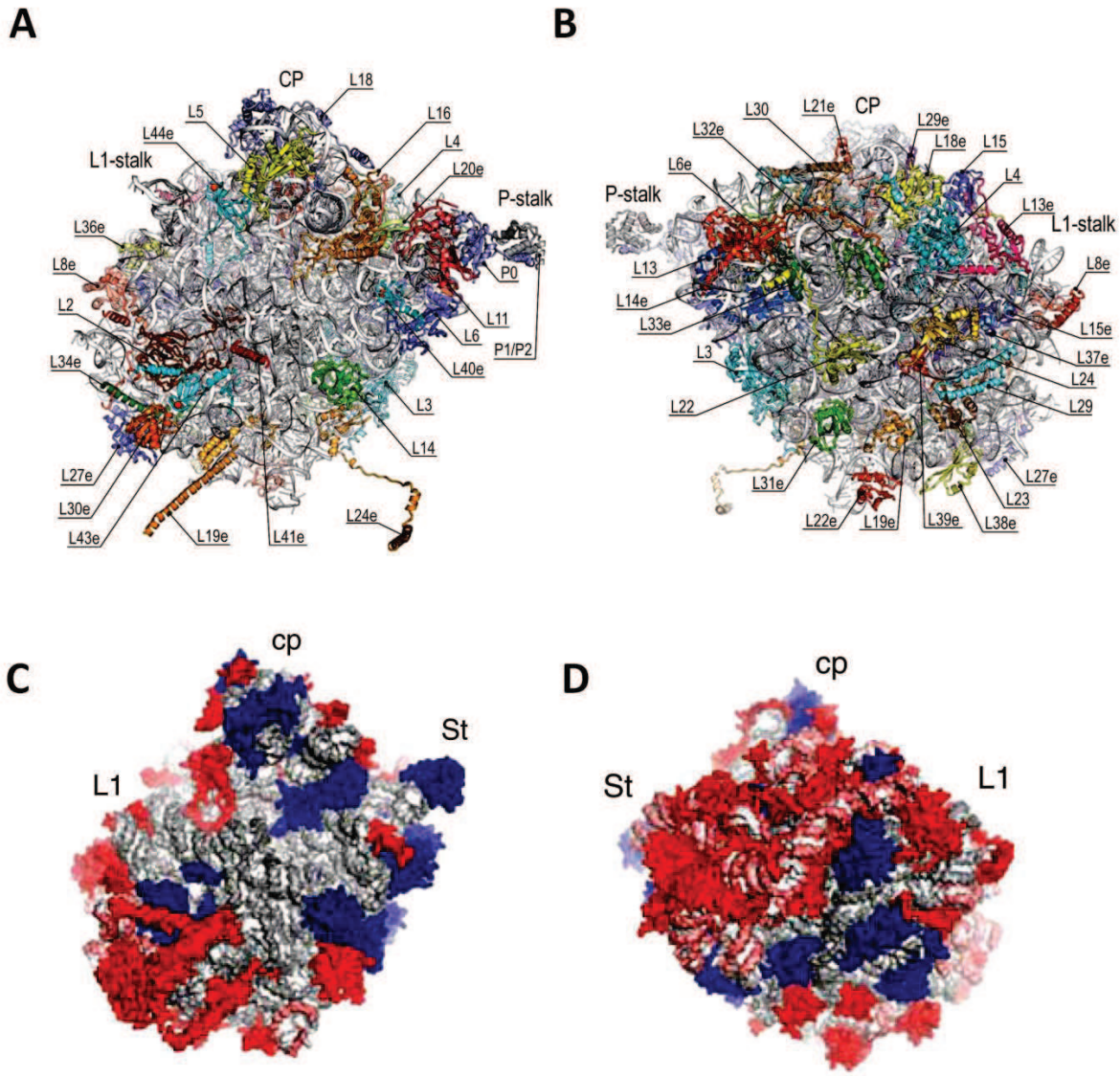

Figure 1.1-6 | **Architecture of the 60S large ribosomal subunit**
(**A**) Interface view of the 60S subunit. Landmarks include central protuberance (CP), L1 stalk, and P stalk of 60S.
(**B**) Solvent side view of the 60S subunit.
(**C**) Interface and (D) solvent views of the eukaryotic 60S subunit, with eukaryotic-specific r-proteins (in red) and rRNA (in pink) shown relative to conserved rRNA (gray) and r-proteins (blue). *Modified from Ben-Shem et al. (2011), Nature 334 (6062): 1524-1529 and Rabl et al. (2011), Science 331:730-736.*

In addition, cryo-EM reconstructions of mammalian ribosomes reveal little density for the longer ESs, indicating their high mobility (Budkevich et al., 2011; Spahn et al., 2004). However, the role for the majority of ES remains unclear. Their presence in eukaryotic ribosomes may reflect the enlarged complexity of translation regulation, providing binding surfaces for additional proteins such as translation factors or other translational regulatory effectors.

Ribosomal proteins of the eukaryotic 80S ribosome

The yeast 80S ribosome is composed of 79 r-proteins (80 in other higher eukaryotes: 33 small subunit r-proteins and 47 large subunit r-proteins), 35 of which have bacterial/archaeal homologs, whereas 32 have only archaeal homologs (Lecompte et al., 2002). Similar to ES, the extra r-proteins and r-protein extensions form a complex layer of additional RNA-protein mass that is located on the solvent sides of the ribosome (Klinge et al., 2012). More than half of the conserved r-proteins contain extensions, which in some cases, such as S5, L4, L7 and L30, establish long-distance interactions far (50-140Å; Ben-Shem et al., 2011) from the globular core of the protein. Physical communication between eukaryotic-specific extensions and conserved core proteins occurs via β-sheet mediated interprotein interactions, for example, between L14e and L6 as well as L21e and L30 (Ben-Shem et al., 2011).

60S r-proteins

Comparing with bacterial large subunit, the eukaryotic one contains 1 MDa of additional proteins. Most of this supplementary protein mass is located in a ring around the back and sides of the 60S, where it interacts with ES (Figure 1.1-6). One cluster of extra protein mass comprises five eukaryotic r-proteins (L6e, L14e, L28e, L32e and L33e), as well as eukaryotic-specific extensions of conserved r-proteins (L4, L13 and L30), which are positioned in the vicinity of the $ES7^{L}$ and $ES39^{L}$. Curiously, parallel rRNA/r-protein variability has been observed in this cluster among the species and it has been associated to co-evolutionary processes. For example, yeast $ES7^{L}$ is considerably shorter than wheat germ (plant) $ES7^{L}$, and surprisingly the extension of L6e is longer in wheat germ as compared with yeast and appears to wrap around $ES7^{L}$ (Armache et al., 2010). In addition, $ES7^{L}$ is stabilized by L28e in plants, whereas this helix is more flexible in yeast lacking L28e (Wilson and Doudna Cate, 2012). The second major ES/r-protein cluster is located at the back of the L1-stalk, and is closely associated with eukaryotic specific r-proteins L27e, L30e, L34e, L43e and L8e (Ben-Shem et al., 2011).

40S subunit r-proteins

The most part of the additional eukaryotic-specific r-proteins and ESs form a layer on the back of the particle (the solvent side of 40S; Figure 1.1-5; Ben-Shem et al., 2011). For example, the beak of 40S has acquired three r-proteins: S10e, S12e, and S31e. 40S-related r-proteins interact also with expansion segments $ES3^{S}$ and $ES6^{S}$, via r-proteins S4e, eS6, S7e, and S8e. The mRNA exit site on 40S also differs from the bacterial one because of the presence of S26e and S28 surrounding the 3' end of the 18S rRNA (Rabl et al., 2011). Here is the site for eIF3 and some viral IRES binding (Muhs et al., 2011; Siridechadilok et al., 2005). S30e locates at the mRNA entry site of 40S and its conserved lysine residues extend into mRNA tunnel suggesting that S30e together with S3, plays a role in unwinding mRNA secondary structure (Rabl et al., 2011). Interesting that S3 also has a long carboxyl-terminal prolongation that passes over S17e and contacts a receptor for activated C protein kinase 1 (RACK1; Rabl et al., 2011). RACK1 is a member of the tryptophan-aspartate repeat (WD-repeat) family of proteins that binds to many signaling proteins and seems to connect the translational machinery to different transduction pathways (Nilsson et al., 2004).

Eukaryote-specific intersubunit bridges

Several contact regions between 40S and 60S play essential structural and functional roles. These bridges keep the ribosomal subunits intercommunicated and enable the ribosome to coordinate its function (Figure 1.1-7; Ben-Shem et al., 2011). Strikingly, nearly all elements involved in intersubunit interactions are eukaryotic-specific. These bridges connect 40S and 60S at the area where rotation of 40S relative to the 60S platform leads to considerable conformational changes. Thus, the bridges might limit the dynamic capacity of 40S in the 80S ribosome.

The eukaryotic-specific bridge 8 (eB8) is formed by S1e, and the $ES31^{L}$. In the vicinity of this bridge, interaction network between S1e, helix 26 (h26), S11 and S26e forms the mRNA exit tunnel (Ben-Shem et al., 2011). The bridge eB11 is formed by eukaryotic-specific S8e and ES41L located on the large subunit (Figure 1.1-7). The only bridge present at the center of the ribosomal intersubunit surface is eB14 composed of L41e whose single α-helix protrudes from 60S into a 40S cavity in closest proximity to the decoding center. It is curious that L41e is more strongly associated with 40S than 60S within the 80S context (Ben-Shem et al., 2011).

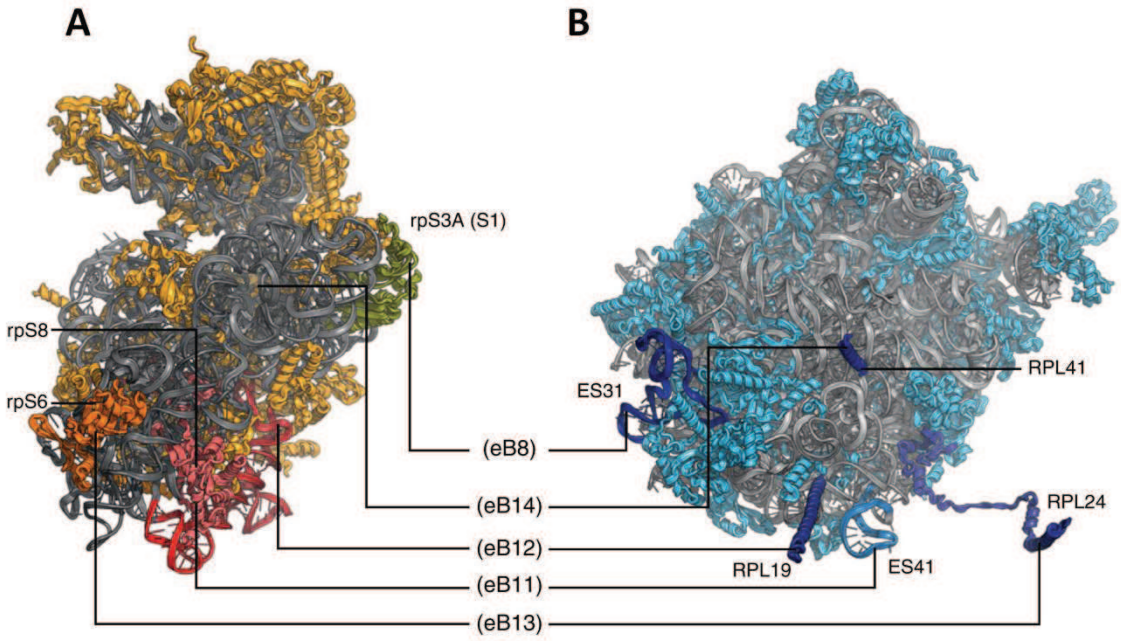

Figure 1.1-7 | **Eukaryote-specific intersubunit bridges**
(**A-B**) Views of the subunit interfaces of yeast 40S (**A**) and 60S subunit (**B**) with contact spots and resulting eukaryote-specific bridges (eBs) indicated. *Taken from Klingle et al. (2012), Trends in Biochemical Sciences 37 (5):189-198*

Exceptional cases of solvent-exposed intersubunit bridges

A distinctive feature of 60S is two long protein helices, which embrace the 40S small subunit from its left and right sides. These α-helices—large extensions in L19e and eL24— form two bridges, eB12 and eB13, respectively, which are accessible from the solvent (Figure 1.1-8). Bridge eB12, located below the mRNA exit tunnel is most likely situated near to the binding zone for initiation factor eIF4G, a protein that plays a central role in assembling of the 48S pre-initiation complex (Yu et al., 2011). This observation suggests that the regulation of the functional behavior of eB12 may play a role in particular subunit joining and shedding/releasing factors (Ben-Shem et al., 2011). eL24 is located at the periphery of the 60S subunit interface according to yeast 60S 3D structure and together with eS6 forms the bridge eB13 (Ben-Shem et al., 2011). The eL24 N-terminal domain resides mainly in 60S but it is also able to contact the N-terminal domain of eS6. Strikingly, the N-terminus of eL24 protrudes deep into the side of the 40S body to embraces the back of 40S. This external fragment of eL24 can be divided into two main domains: the small α-helical linker and long α helix, which may contact h10 of the 40S rRNA and the C-terminal fragment of eS6 (Ben-Shem et al., 2011). According to Ben-Shem et al. (2011), the solvent-exposed eL24 C-terminal region obeys the movements of 40S via its highly flexible linker as if it were a genuine 40S component. This intriguing architecture of the bridge eB13 should be considered in the light of recent research findings: eL24 is a critical factor in both translation reinitiation of uORF-containing mRNAs (Nishimura et al., 2005) and virus-induced polycistronic translation via reinitiation of the *Cauliflower mosaic virus* 35S pgRNA (Park et al., 2001). In the viral case the eL24 protein mediates pivotal interactions with viral and plant host factors—the translational TransActivator/ Viroplasmin protein (TAV) and the Reinitiation Supporting Protein (RISP)—in order to promote reinitiation after long ORF translation (Park et al., 2001; Thiébeauld et al., 2009). It is interesting that the C-terminal helix of eS6, which can be phosphorylated via the TOR signaling pathway (Ruvinsky and Meyuhas, 2006), is solvent exposed and, as it was proposed by Ben-Shem et al. (2011), may interact with factors that dock on $ES6^S$ and eL24 indicating a role in initiation/reinitiation.

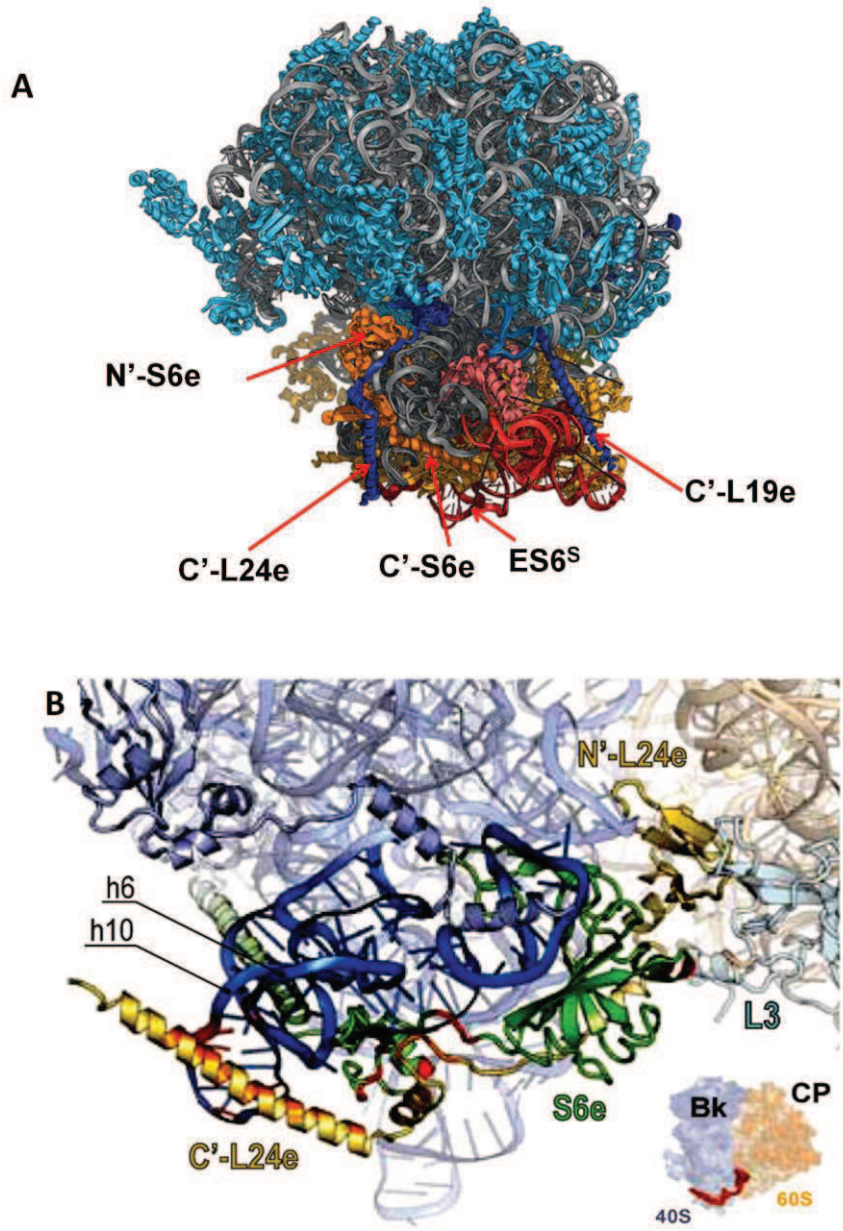

Figure 1.1-8 | | **Exceptional cases of solvent-exposed intersubunit bridges**
(**A**) View of yeast 80S structure with eukaryotic-specific elements involved in solvent-exposed intersubunit bridges with 60S (blue) and 40S (orange).
(**B**) eL24 extends from the 60S body to interact with eS6 on the 40S subunit.
Modified from Kingle (2012), Trends in Biochemical Sciences 37 (5):189-198 and Ben-Shem et al. (2011), Nature 334 (6062):1524-1529

1.1.3 Functional role of the initiation factors (eIFs)

eIF2 carries Met-tRNAMeti to the ribosome

Met-tRNA$^{Met}_{i}$ is delivered to the 40S subunit by eIF2·GTP (a ternary complex, TC; Hinnebusch and Lorsch, 2012). eIF2 is a heterotrimer composed of a large γ subunit and smaller α and β subunits. Although the structure of eIF2 has not yet been resolved, structural analyses of the individual subunits as well as of the analogous archaeal eIF2, aIF2 have revealed some structural and functional aspects of this Met-tRNA$^{Met}_{i}$ carrier (Figure 1.1-9 and Figure 1.1-11; Lorsch and Dever, 2010). The α subunit structure is conserved between eukaryotes and Archea, except that eukaryotic eIF2α possesses a short acidic extension of 29 residues in length at the C-terminus (Schmitt et al., 2012). But in contrast, an extension containing three lysine-rich segments (K-boxes) makes eIF2β twice the length of the archaeal protein (Figure 1.1-9 and Figure 1.1-11; Lorsch and Dever, 2010). The function of eIF2β K-boxes is probably to mediate the binding of eIF2 to GTPase-activating protein (GAP) eIF5, and the catalytic subunit of its guanine nucleotide exchange factor (eIF2B), eIF2Bε (Asano et al., 1999). eIF2γ harbors three domains and show high overall similarity to the structure of EF-Tu/eEF1A (GTPase that delivers aminoacyl-tRNAs onto the ribosome during elongation).

The e/aIF2α subunit is composed of three domains: a highly conserved N-terminal β barrel, a central α-helical domain, followed by a C-terminal α-β alternating domain. Domains I and II form a rigid body linked to the mobile domain III. In eukaryotes, a highly conserved serine residue (S51 in yeast) within a loop of domain 1 is the target of several eIF2α kinases (Schmitt et al., 2010). As we will describe below, phosphorylation of this residue is crucial for global translation control.

Plant eIF2 does not differ significantly in composition or amino acid sequence from mammalian eIF2, but there seem to be significant differences in the way eIF2 and protein synthesis are regulated in plants (Browning, 2004).

The α subunit

The C-terminal domain III of aIF2α interacts with aIF2γ and promotes Met-tRNA$^{Met}_{i}$ binding to aIF2 (Yatime et al., 2007). The highly conserved amino-terminal domain I contains a β-barrel “OB fold” with nonspecific RNA-binding activity (Yatime et al., 2004). The Domain I contains the regulatory phosphorylation site (Ser 51 in yeast that is highly conserved in eukaryotes).

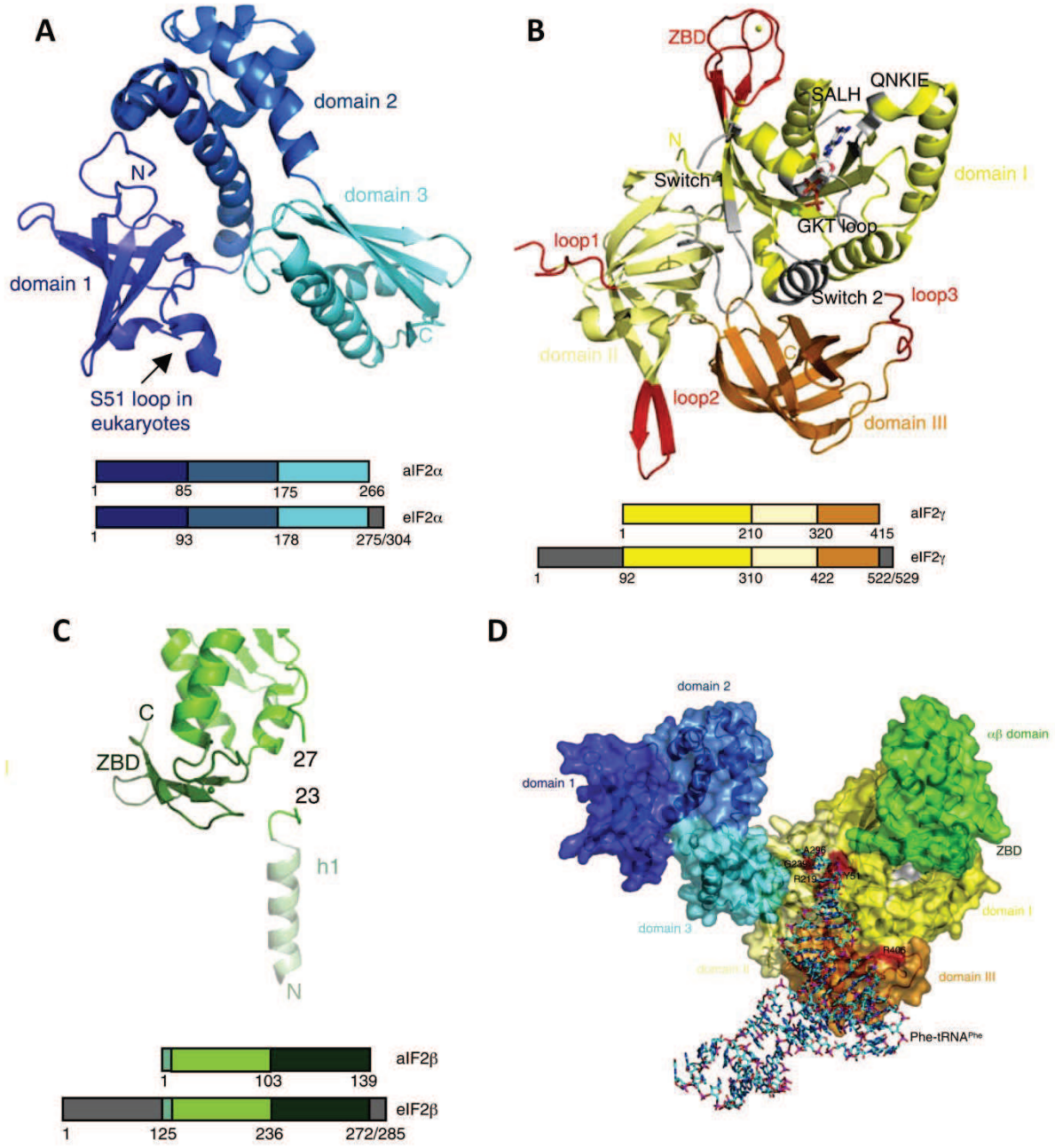

Figure 1.1-9 | **Eukaryotic and archaeal translation intiation factor 2 (eIF2/aIF2)**

(**A**) The α subunit. The three structural domains are colored as follows: domain 1 in dark blue, domain 2 in marine, and domain 3 in cyan. The loop carrying the S51 residue in eIF2α is indicated.

(**B**) The γ subunit. The three structural domains are colored as follows: domain 1 in yellow, domain 2 in pale yellow, and domain 3 in orange. GDP is shown as sticks, Mg^{2+} as a green sphere, and Zn^{2+} as a yellow sphere. Regions involved in the binding of the nucleotide are colored in grey and labeled. Regions characteristic of the initiation factor are colored in red and labeled.

(**C**) The β subunit. The three structural domains are colored as follows: helix 1 in pale green, domain 2 in green, and domain 3 in dark green. Zn^{2+} is shown as a green sphere. Residues 23–27 are not visible.

Below the cartoons we show the schematic representations of e/aIF2 subunits. Colors of the boxes are related to the colors of the structural domains. For archaeal subunits, numbering is that of aIF2 from *S. solfataricus* and for eukaryotic subunits, numbering is that of eIF2 from *S. cerevisiae*. Domains specific of eukaryotic subunits are shown in grey.

(**D**) Docking of Phe-$tRNA^{Phe}$ onto aIF2. A structure modeling of the full aIF2αβγ heterotrimer is shown in the surface representation. The color code is the same as in A, B and C. *Modified from Schmitt et al., (2010), FEBS Letters 584:405–412*

Following phosphorylation, the affinity of eIF2-GDP for eIF2B is highly increased, and eIF2 is converted from a substrate to an inhibitor of the GDP-GTP exchange factor. When the amount of eIF2-GTP is rapidly reduced, translation is inhibited in the cell. Four types of eIF2-Ser51 specific kinases have been identified: the double-stranded RNA-dependent protein kinase (PKR), heme-regulated kinase (HRI), PKR-like Endoplasmic Reticulum Kinase (PERK) and the General Control Non-derepressible kinase 2 (GCN2). These kinases share a conserved kinase-domain insuring high specificity for eIF2α (Dey et al., 2007), but they are activated by different input signals. The most widespread one, GCN2, is controlled by uncharged tRNA that accumulates during amino acid starvation (Dong et al., 2000). PKR (Meurs et al., 1993) is present in all vertebrates (Dar et al., 2005), and is induced by interferon and double-stranded RNA binding. As an inhibitor of protein synthesis, PKR participates in cell defense against virus propagation (Schmitt et al., 2010). PERK is found in animals, and is activated in response to ER stress in the case of an imbalance in the lumen between unfolded proteins and chaperones (Harding et al., 1999). Finally, HRI, present in vertebrates and yeast, is activated upon heme deprivation in erythrocytes and various oxidative stresses in different cell types (Schmitt et al., 2010).

The knowledge on the mechanism and regulation of Met-tRNA$^{Met}_{i}$ recruitment has been largely obtained thanks to genetic analysis on GCN2-dependent translational control of yeast GCN4 mRNA—an activator of amino acid biosynthetic pathways—whose translation is mediated by four uORFs in its 5'UTR. This particular mRNA escapes the global translation inhibition induced by low eIF2-GTP because at low active TC levels scanning ribosomes bypass the inhibitory for reinitiation uORFs, particulary uORF 4 and initiate at GCN4 ORF instead (Hinnebusch, 2005). Thus, mutations reducing the TC level or the rate of its binding to 40S derepress GCN4 translation by allowing ribosomes to bypass inhibitory uORFs in the absence of the starvation signal (Gcd^{-} phenotype). Mutations that impair scanning or AUG recognition generally impair GCN4 induction during amino acid starvation (Gcn^{-} phenotype; Lee et al., 2007). Some residues near to the Ser51 have been also implicated in regulating GDP-GTP exchange by eIF2B. Furthermore, cells lacking eIF2α can survive if eIF2 (β and γ) and Met-tRNA$^{Met}_{i}$ are overexpressed.

The β subunit

eIF2β contains two additional domains when compared with aIF2β. At the N-terminal region a domain containing lysine-rich boxes was shown to be responsible for the binding to the C-terminal domains of the GAP eIF5, and the catalytic subunit of eIF2B, eIF2Bε (Asano et al.,

1999). Therefore, the absence of the eukaryotic-specific N-terminal part of eIF2 in archaea could be related to the absence of archaeal eIF5 and eIF2B orthologues. The eukaryotic C-terminal is 15 residues longer compared to aIF2β and no role has been proposed for this part of eIF2β. The 3D crystal structure revealed that subunit β is bound to γ (Yatime et al., 2007). An N-terminal α-helix is connected by a flexible linker to a central α-β domain, followed by a C-terminal zinc-binding domain (Schmitt et al., 2010).

Whereas the archaeal eIF2 αγ heterodimer binds Met-tRNA$^{Met}_{i}$ with almost the same affinity when compared to aIF2 (Yatime et al., 2004), a mammalian eIF2αγ dimer binds nucleotide but is not able to form a stable complex with Met-tRNA$^{Met}_{i}$ (Flynn et al., 1993), suggesting that subunit β is more crucial than α for Met-tRNA$^{Met}_{i}$ binding in eukaryotes (Hinnebusch, 2014). Compatible with this, a *S264Y* mutation in yeast eIF2β abolishes Met-tRNA$^{Met}_{i}$ binding by eIF2 (Huang et al., 1997). Numerous genetic analyses have shown that cysteine residues within the Zn binding pocket at the C-terminal domain are essential for TC binding to 40S and regulation of GTP hydrolysis during AUG recognition (Huang et al., 1997). A fragment of yeast eIF2β is required and effective by itself for eIF2γ binding (amino acids 128-159), and substitutions of Tyr-131 and Ser132 disrupt binding of β to γ, exacerbating the hyperactive GTPase function or the defect in Met-tRNA$^{Met}_{i}$ binding conferred by *S264Y* mutation (Hashimoto et al., 2002). Finally, eIF2 can also bind mRNA via the K-boxes present in eIF2β and given their evolutionary conservation, only one of them was found to be sufficient to provide this functional behavior essential for translational efficiency (Laurino et al., 1999). A variety of *in vivo* and *in vitro* binding assays have revealed that the N-terminal region of the eIF2β subunit plays an important role in binding other initiation factors, such as eIF5 (via C-terminus), eIF3 (via a and/or c subunits) and eIF1, however it is not clear if all these interactions are conserved in other eukaryotes, and it is suspected that post-translational modifications that alter amino acid charges, such as phosphorylation, may play an influential role in 43 PIC formation (Asano et al., 2000; Dennis et al., 2009; Singh et al., 2004).

The γ subunit

eIF2γ binds directly to both GTP and Met-tRNA$^{Met}_{i}$ and it seems that α and β subunits can significantly increase the affinity of eIF2 for Met-tRNA$^{Met}_{i}$ (Naveau et al., 2010). *In vitro* assembly of a stable aIF2 trimer from purified subunits revealed that the core of aIF2, the subunit γ, plays a role of a bridge between subunits α and β (Figure 1.1-9 and Figure 1.1-11; Yatime et al., 2006). The eukaryotic homolog of aIF2γ—eIF2γ contains an N-terminal extension that varies in length depending on the species. In yeast this N-terminal domain without being critical for survival

confers a slow growth phenotype if mutated (Erickson et al., 2001). The eukaryotic version contains all the elements required for nucleotide and Met-tRNA$^{Met}_{i}$ binding which have been discovered thanks to similarity between eIF2 and the EF-Tu elongation factor.

aIF2γ is composed of three domains (Figure 1.1-9). The domain I harbors the guanine nucleotide binding site with classic G-protein related elements such as the GKT loop, switch 1-2 regions, and QNKIE and SALH sequences (Figure 1.1-9B; Vetter and Wittinghofer, 2001). Mobile switch regions allow conformational movements required for the transition from an active GTP-bound ("switch on") to an inactive GDP-bound state ("switch off"; Vetter and Wittinghofer, 2001) and thus modulate the eIF2γ affinity for Met-tRNA$^{Met}_{i}$. However, α and β subunits seem to play a predominant role in stabilization of the γ subunit binding to Met-tRNA$^{Met}_{i}$ (Schmitt et al., 2010). Site-directed hydroxyl radical footprinting suggests that eIF2γ, in addition to contacts with the acceptor stem of Met-tRNA$^{Met}_{i}$, is involved in binding to the 40S subunit via 18S rRNA helix h44 and the eIF2γ domain III. Accordingly, biochemical analyses strongly demonstrated that the eIF2γ domain III exhibits strong ribosome binding (Shin et al., 2011).

Binding of TC to 40S is assisted by eIF1, eIF1A, eIF5 and eIF3

In yeast TC is not able to bind 40S by itself, and instead it requires the support of eIFs 1, 1A, 5 and the eIF3 multisubunit complex (Hinnebusch and Lorsch, 2012). All of these factors, except for eIF1A, are part of the "multifactor complex" (MFC) and can interact with the 40S subunit in a cooperative way. Indeed, data from two groups suggest that modifying particular contacts between MFC components affects the TC recruitment to 40S in yeast (Nielsen et al., 2004; Valásek et al., 2004). However, *in vitro* analysis of reconstituted human MFC (similar to the MFC reported in yeast and plants, (Asano et al., 2000; Dennis et al., 2009) indicates that MFC binding to 40S·eIF1A and further delivery of Met-tRNA$^{Met}_{i}$ to the complex occurs at the same rate for TC binding to 40S·eIF1A preloaded with eIFs 1, 3 and 5 (Sokabe et al., 2012), suggesting the role of MFC components in TC recruitment. Moreover, MFC·GDP shows a highly reduced affinity to Met-tRNA$^{Met}_{i}$, when compared to that for eIF2·GDP, suggesting that MFC components are implicated in release of Met-tRNA$^{Met}_{i}$ from eIF2·GDP during AUG recognition, in addition to the role of eIF5 in eIF2-bound GTP-hydrolysis (Hinnebusch and Lorsch, 2012). Considering that the MFC·Met-tRNA$^{Met}_{i}$ complex can be detected in cell lysates, it may be responsible for Met-tRNA$^{Met}_{i}$ delivery to 40S *in vivo*. However the possibility of a direct Met-tRNA$^{Met}_{i}$ binding to the MFC·40S complex is not excluded since these distinct pathways for Met-tRNA$^{Met}_{i}$ delivery to 40S have been reported by Sokabe et al. (2012).

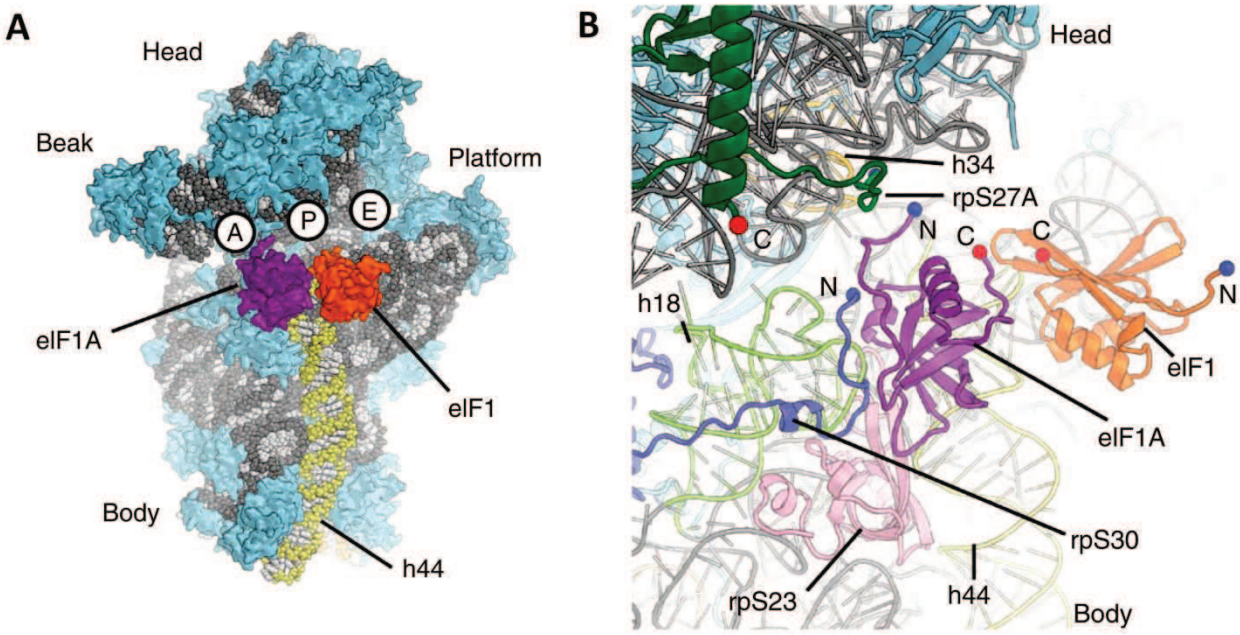

Figure 1.1-10 | **Modeling of eIF1A and eIF1 binding sites on 40S**
(**A**) Structure of eIF1A and eIF1 bound to the top of h44 of the 40S subunit (light blue, ribosomal proteins; gray, 18S rRNA). A, P and E sites are indicated
(**B**) Structure showing eIF1A contacts to h18, h34 and h44 and rpS27A (green), rpS30 (blue) and rpS23 (pink) but not to eIF1. Blue and red spheres indicate N and C termini, respectively.
Modified from Weisser et al., (2013), Nat Struct Mol Biol. 20 (8):1015-1017

eIF1A and eIF1

eIF1A and eIF1 are small proteins that bind cooperatively to the 40S subunit with high affinity (Figure 1.1-10; Kapp and Lorsch, 2004; Weisser et al., 2013). Both are essential for viability in yeast, and are highly conserved in eukaryotes. They synergistically enhance TC binding to 40S and create an scanning-competent complex by inducing conformational changes in the 40S subunit (Passmore et al., 2007). eIF1A and eIF3 are essential to generate a stable 43S PIC (Majumdar et al., 2003). Directed hydroxyl radical footprinting located the core of eIF1A in the A-site of 40S, where eIF1A N- and C-terminal tails protrude toward the P-site-bound Met-tRNA$^{Met}_{i}$ (Yu et al., 2009). Moreover, the eIF1A C-terminal domain contacts the P-site and may interfere with Met-tRNA$^{Met}_{i}$ accessing to the P-site within the active or open scanning complex (Saini et al., 2010). At the same time, eIF1, which plays a critical role in start codon selection, binds near the P-site where it might monitor codon-anticodon interactions during AUG site selection (Lomakin et al., 2003). Upon start codon recognition and conversion of PIC to the "closed", scanning-arrested state, Met-tRNA$^{Met}_{i}$ fully docks in the P-site, relegating both the eIF1A C-terminal domain and eIF1 (Yu et al., 2009).

eIF1A is characterized by the β-barrel OB-fold, the α-helical domain and two unstructured N and C-terminal extensions (Figure 1.1-10; Figure 1.1-11). Mammalian eIF1A can contact RNA via OB-fold and α-helical domains during 40S scanning, and mutations within these domains reduced RNA binding and thus impaired scanning *in vitro*. In yeast, eIF1A is essential for translation initiation *in vivo* and removal of its C-terminal domain impairs TC recruitment leading to a Gcd^{-} phenotype. Mutations within the OB-fold domain abolishes eIF1A binding to 40S reducing eIF2, eIF3 and eIF5 binding to 40S and thus TC recruitment (Fekete et al., 2007). The N-terminal domain of yeast eIF1A is involved in eIF2 and eIF3 binding, which may stabilize TC binding to 40S (Olsen et al., 2003). The crystal structure of the complex between 40S and eIF1 has shown that eIF1 binds to the interface side of 40S via h44 of the 18S rRNA (Figure 1.1-10; Figure 1.1-11). Interesting that eIF1 can be displaced by Met-tRNA$^{Met}_{i}$ upon completion of start codon-anticodon interactions (Voigts-Hoffmann et al., 2012). In addition, eIF1 also impairs the release of P_i from eIF2·GDP·P_i in 43S PIC (Algire et al., 2005).

eIF5

The main function of G-protein eIF5 is to promote GTP hydrolysis of eIF2-bound GTP in response to start codon recognition. A zinc finger motif within the eIF5 N-terminal domain is required for activation of the eIF2 GTPase (Figure 1.1-11; Alone and Dever, 2006; Nanda et al., 2013).

Currently it is neither clear at which initiation step eIF5 joins 43S PIC nor where it binds. However, eIF5 is involved in multiple interactions with other initiation factors (Luna et al., 2012).

The eIF5 C-terminal HEAT domain that interacts with eIF2β (Asano et al., 1999) is required for the guanosine nucleotide binding to eIF2 (Jennings and Pavitt, 2010). The yeast C-terminal domain of eIF5 interacts with the N-terminal tail of eIF2β, the N-terminal domain of eIF3c and eIF1, thereby linking eIF3 to eIF2 and eIF1 supporting MFC assembly. Thus, the C-terminal domain of eIF5 plays a role in PIC assembly possibly by stabilizing interactions between eIF1, eIF2 and eIF3 within the MFC (Sokabe et al., 2012).

In its other roles, eIF5 promotes the dissociation of eIF1 (Figure 1.1-11; Reibarkh et al., 2008) and may interact with eIF1A to improve eIF1A-dependent AUG selection. Recently, it was discovered that mutating the binding sites of eIF1 and eIF2β on the eIF5 C-terminal domain impairs start codon recognition and impede eIF1 release from the PIC (Luna et al., 2012) suggesting other role of eIF5-CTD's dynamic interplay with eIF1 and eIF2β in switching PICs from an open to a closed state at start codons. In Figure 1.1-11 from Lorsch and Dever (2010) a summary of the architecture and interaction network within PIC are presented.

eIF3

The approximately 800 kDa mammalian eIF3 consists of 13 subunits (eIF3a-eIF3m). Six eIF3 subunits (a, c, e, k, l and m) harbour a PCI (Proteasome, COP9/signalosome, eIF3) domains—several helical repeats followed by a winged helix tail—and two eIF3 subunits (f and h) contain a MPN (Mpr1-Pad1-N-terminal) domain—a β-barrel surrounded by α helices and additional β strands (Figure 1.1-12; Enchev et al., 2010; Hashem et al., 2013). Both PCI and MPN form a stable octamer (the PCI/MPN core) that functions in promoting assembly of two other multiprotein complexes such as the 26S proteasome lid (a multisubunit complex involved in proteasome-mediated deubiquitination) and the COP9/signalosome (CSN, possibly an alternative lid to the 26S proteasome that regulates ubiquitination and cell signaling) and in each case seem to have a conserved architecture, a five-lobule structure (Lingaraju et al., 2014). The rest of the eIF3-related subunits contain RRM domains (b, d and g), WD β-propeller domains (b and i), and a putative Zn-binding site (g) that are likely flexibly linked to the PCI/MPN core (Hashem et al., 2013). eIF3 is involved in almost all stages of cap-dependent translation initiation, promoting binding of TC to the 40S subunit, 43S PIC recruitment to mRNA at the 5'-cap structure by interacting with the eIF4G subunit of the eIF4F complex and other eIFs—1, 1A, 2, 4B and 5 (Hinnebusch, 2006).

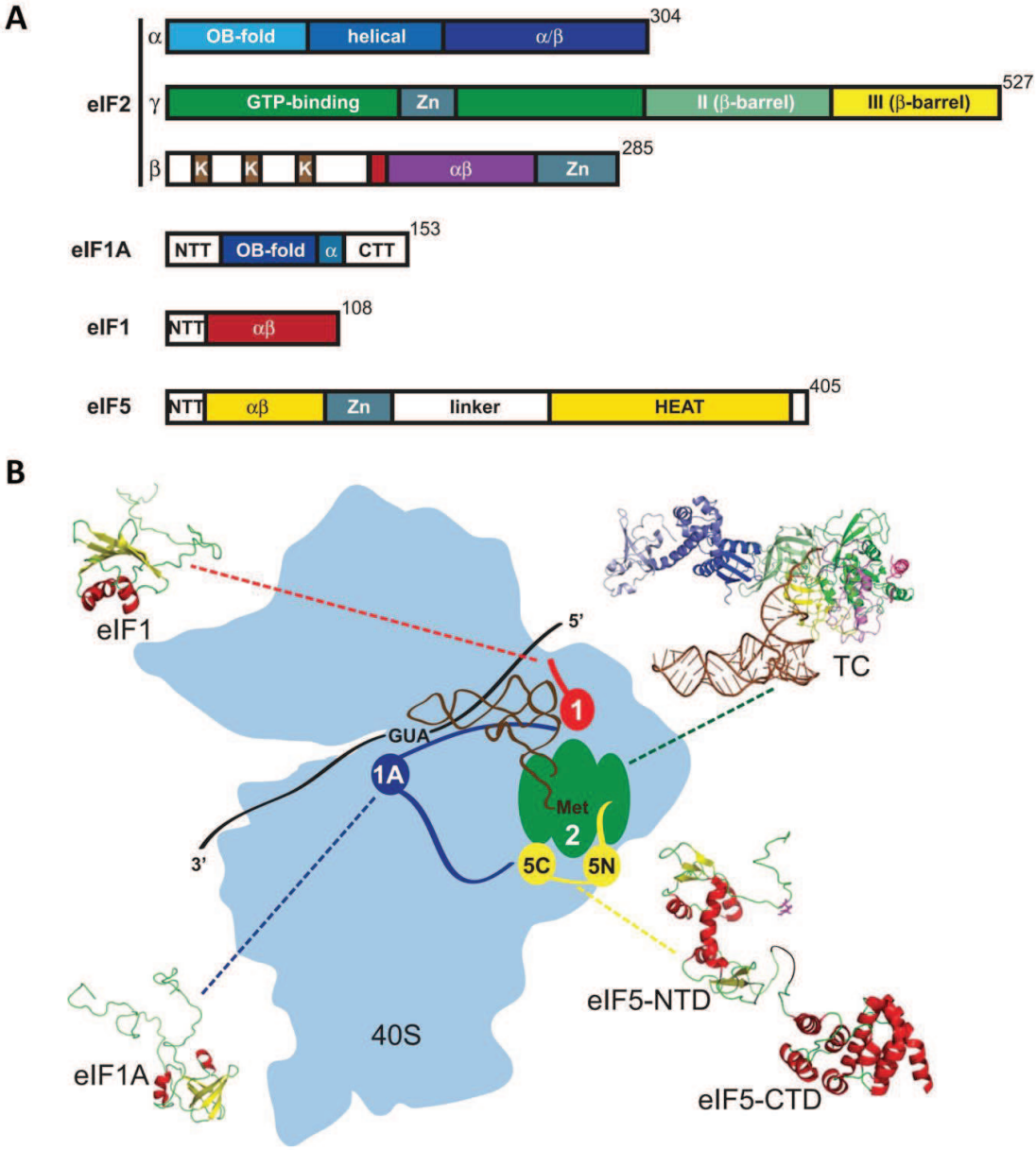

Figure 1.1-11 | Architecture of the 40S preinitiation complex (PIC)

(**A**) Schematic representations of the key PIC factors from yeast. eIF2 is composed of α, β and γ. eIF2 α consists of an OB-fold, an α-helical domain, and an α/β domain; the N-terminal half of eIF2β contains three Lys-rich (K) segments followed by a short unfolded domain (that adopts a helical structure when in the eIF2 complex, red), a core αβ domain, and a C-terminal zinc finger (gray) domain. eIF2γ has three domains: an N-terminal GTP-binding domain (G) and two β-barrel domains II and III; a zinc-binding knuckle is present within the G-domain.

eIF1A consists of a core OB-fold domain and long unstructured N- and C-terminal tails (NTT and CTT). eIF1 contains an unstructured N-terminal tail linked to anαβ core similar to eIF2β and the eIF5 NTD. eIF5 contains N-terminal αβand zinc finger domains connected by an unstructured linker to the C-terminal HEAT (Huntington, elongation factor 3, PR65/A, TOR) domain.

(**B**) 43S PIC is shown including 40S (light blue) and PIC component structures as indicated. Structures of human eIF1, eIF1A, eIF5 (yeast-CTD and human-NTD), and an archaeal TC. TC structure consists of archaeal aIF2 and yeast tRNAi (see details in **Figure 1.1-9**). Structures of eIF1, eIF1A, and eIF5 are displayed with α-helices in red and β-strands in yellow. *Modified from Lorsch and Dever, (2010), J. Biol. Chem., 285 (28): 21203–21207*

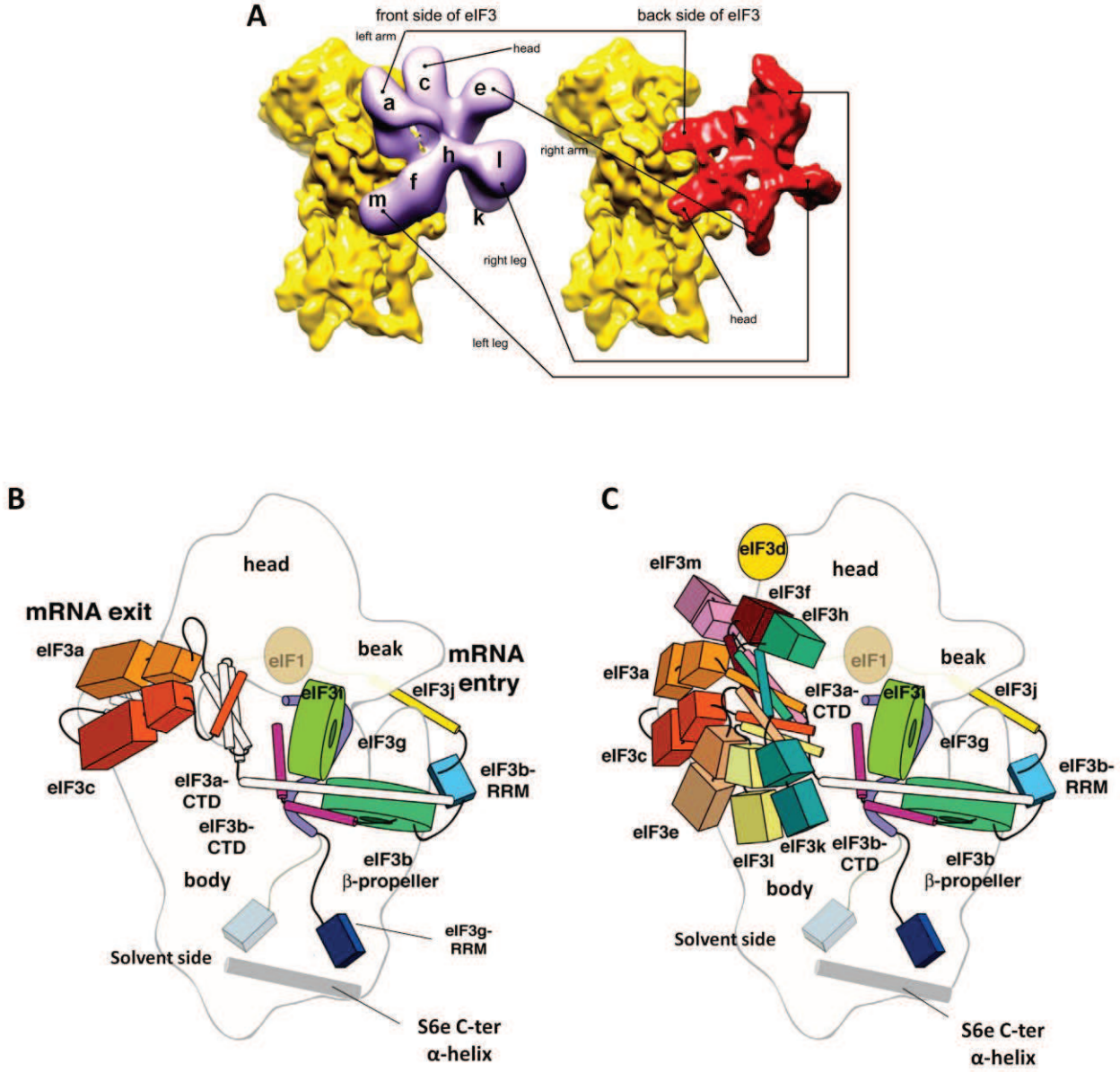

Figure 1.1-12 | 3D structures of the human and yeast eIF3-40S complexes obtained by cryo-electron microscopy-based modeling

(A) Side-by-side comparison of human eIF3-40S subunit interactions modeled by Siridechadilok et al. (2005; left structure) and cryo-EM based reconstruction (right) reported by Hashem et al. (2013).

(**B-C**) Integrative modeling of the yeast (**B**) and human 40S-eIF1-eIF3 complexes (**C**) reported by Erzberger et al. (2014). Localization densities for eIF3 subunits superposed on the 40S cryo-EM reconstruction. Linker regions are represented by thin tubes. The position of eIF1, located in the intersubunit surface, is indicated in light brown. *Modified from Hashem et al. (2013), Cell 153:1108–1119 and Erzberger et al. (2014), Cell 158:1123–1135*

Results from negative-stain electron microscopy (EM) modeling indicate that eIF3 resides on the solvent side of 40S and eIF3 binding is preferentially maintained through the contacts between the left leg and the platform of 40S (Figure 1.1-12; Siridechadilok et al., 2005). Recent cryo-EM structure of the mammalian 43S complex at 11,6 Å resolution (Hashem et al., 2013) suggested a notably different orientation for the eIF3 core within 40S than that modeled in Siridechadilok et al. (2005). First, the model confirmed the five-lobed conformation adopted by eIF3 within 40S. In the reconstruction of 43S (Hashem et al., 2013) 40S-bound eIF3 is rotated and flipped so that its head (the subunit c) and the left arm (the subunit a), but not the left leg, face the 40S subunit platform area involving r-proteins S13e, S27e, S1e and S26e near the head of 40S (Figure 1.1-12A). These observations are strengthened by some studies in yeast (reviewed in Hinnebusch, 2006) showing that deletion of eIF3c N- and C- terminal domains or the eIF3a N-terminal domain impairs 40S binding by otherwise intact eIF3 complexes.

Strikingly, the octamer composed of the PCI/MPN core that contains truncated versions of eIF3 a and c and full-length eIF3 subunits e, k, l, m, f and h seems to occur in native eIF3, 26S proteasome lid and COP9/signalosome assembly models that are structurally similar (Figure 1.1-12; Lingaraju et al., 2014; Sun et al., 2011). This led to the suggestion that significant parts of b, d, g, and i subunits constitute flexible and highly mobile regions of eIF3 that were averaged out during reconstitution. However, these mobile subunits together with the a and c flexible regions apparently protrude out from the structural core and embrace the 40S subunit during 43S PIC formation (Sun et al., 2011). The recent excellent publication of (Erzberger et al., 2014) indeed confirmed that non-core eIF3 subunits have extended secondary structures on 40S (Figure 1.1-12).

In addition, the 43S PIC cryo-EM model of Hashem et al. (2013) resolved the continuous mass on the back of 40S that is not enough to explain the entire eIF3 structure. Therefore, two additional masses near to the right foot of 40S and to the head behind the r-protein RACK1 were attributed to flexible eIF3 peripheral domains outside of its structural core. The additional mass near to RACK1 on the back side of the 40S head may correspond to a residual density of eIF3a, while the additional mass may correspond to the eIF3b WD β-propeller domain and eIF3i. Accordingly, the eIF3b RRM domain was shown to be required for eIF3 binding to 40S in yeast (Nielsen et al., 2006; Figure 1.1-12). Finally, Erzberger et al. (2014) showed a correlation in attributions of eIF3g, eIF3b, eIF3i and eIF3j when compared to previous models, being predominantly located in the vicinity of the mRNA entry site and the right foot (Figure 1.1-12).

eIF4F promotes recruitment of mRNA to 43S PIC

43S PIC loading at the 5'-cap of the mRNA is orchestrated by interactions between the eIF4F complex and 43S PIC. The eIF4F complex stimulates this step through interaction of its subunit eIF4E with the cap structure, drafting eIF4A to the 5'UTR (Pestova et al., 2007). eIF4G stimulates the activity of the DEAD box protein eIF4A (Nielsen et al., 2011), enabling it to melt the mRNA leader secondary structure to prepare a single-stranded mRNA region for 43S PIC binding to the 5' end. It is thought that eIF4G also helps to recruit the 43S PIC through direct interactions with eIF3 within 43S PIC (Pestova et al., 2007).

In addition to recruiting and activating eIF4A, there is evidence that a region of mammalian eIF4G participate in recruitment of 43S PIC to the mRNA 5' end via interaction with the eIF3 subunit e (LeFebvre et al., 2006). Although eIF3 and eIF4G do no directly interact, another eIF4F-bound protein eIF4B that interacts with eIF3 subunit g (tif35) is involved in 43S PIC recruitment in yeast (Vornlocher et al., 1999). In addition, complex formation between eIF4G and eIF5 can settle the bridge between eIF4F and 43S PIC in yeast (Asano et al., 2001; Mitchell et al., 2010).

eIF4E/eIF4G

Simultaneous loading of both eIF4G-bound eIF4E and Poly(A) Binding Protein (PABP) within the eIF4G N-terminal domain to the cap and poly(A) tail, respectively, results in creating the so called "closed loop" configuration of mRNA that is required for efficient attachment of 43S PIC to mRNA. However, the relevance of the PABP-eIF4G interaction in translation seems to vary with the cell type (Hinnebusch and Lorsch, 2012). In mammals the RNA-binding domain in the middle region of eIF4G is also required for eIF4F binding to the 5' end of mRNA (Yanagiya et al., 2009). In yeast two other RNA-binding domains of eIF4G (RNA2 in the middle and RNA3 at the C-terminus) seem to display key functions downstream from eIF4F-mRNA-PABP assembly (Park et al., 2011). Interestingly, RNA3 harbors a binding site for the DEAD-box RNA helicase Ded1/Dx3, a protein, which has been implicated in 40S scanning (Hinnebusch, 2011). Recent studies in yeast proposed that RNA-binding sites within eIF4G work together for settling 5' to 3' directionality of 43S PIC scanning (Rajagopal et al., 2012).

Plants posses an isoform of eIF4F, known as eIFiso4F, which is not present in other eukaryotes. eIFiso4F, similar to eIF4F, consists of two subunits, a small cap-binding protein (eIFiso4E) and a large subunit eIFiso4G, and has *in vitro* activities similar to eIF4F. The cap-binding subunits eIF4E and eIFiso4E display about 50% of similarity in their amino acid sequences, and the molecular mass of both is around 24 kDa. However, the eIF4G and eIFiso4G

subunits differ substantially in mass (180 kDa and 86 kDa respectively). eIFiso4G lacks a significant region in the N-terminal domain when compared with eIF4G and may not mediate mRNA circularization due to the lack of the PABP binding site (Browning, 1996). This substantial difference in the mass of eIF4G and eIFiso4G suggests that these proteins may have different roles in regulation of plant translation (Browning, 2004). The functional significance of having two forms of eIF4F has not been elucidated, but evidence suggests that these two versions may discriminate between mRNAs that have internal initiation elements or secondary structure (Mayberry et al., 2011).

The cap-binding subunits eIF4E and eIFiso4E have been shown to have a variety of roles during plant viral infection, primarily through interaction with the viral VPg (Ruffel et al., 2002). eIF4E and eIFiso4E have been shown to interact directly with RNA elements in the 3'-UTR of satellite tobacco necrosis virus RNA (Gazo et al., 2004) and barley yellow dwarf virus (W.A. Miller, personal communication). An *Arabidopsis* knockout for the single eIFiso4E gene shows a normal phenotype, but is characterized by elevated accumulation of eIF4E. In addition, both eIF4E/ iso4E and eIF4G/ iso4G proteins seem to be important determinants in the outcome of viral infections (Robaglia and Caranta, 2006). Viruses affected by these genes belong mainly to potyviruses. For example, eIFiso4E knockout plants are resistant to infection by some potyviruses (Duprat et al., 2002). eIF4E/ eIF4G virus resistance genes in plants are normally recessively inherited, but their role in plant resistance is not yet known.

eIF4A

eIF4A is the member of the DEAD-box family protein that consists of a helicase core only formed by two RecA-like domains that carries a number of very conserved motifs contributing to ATP binding and hydrolysis. DEAD-box helicases are non-processive, and belong to RNA-stimulated ATPases that catalyze the ATP-dependent unwinding of RNA duplexes. Concerning eIF4A, when bound to ATP, it is believed to melt short helices in the 5'UTR of the mRNA by binding to an unpaired RNA strand. The role of the ATP hydrolysis has not been established but it seems either to serve disruption of surrounding duplexes or to release eIF4A for subsequent rounds of RNA unwinding (Parsyan et al., 2011). eIF4A interacts with the "HEAT" domain of eIF4G via RecA-like domains in a conformation that is suitable to bind substrates and release products (Hilbert et al., 2011). Recent biochemical and physicochemical analyses revealed that another helicase-like protein eIF4B (see above chapter) stimulates RNA unwinding by eIF4A, but does not affect eIF4A conformation. The eIF4G middle domain enhances eIF4A stimulatory effect and promotes the formation of a "closed" eIF4A conformation in the presence of ATP and RNA

(Harms et al., 2014). Cross-linking experiments have revealed that both eIF4A and eIF4B are bound to the 5' leader up to 52 nucleotides downstream of the cap to play their roles during scanning (Lindqvist et al., 2008).

In plants, eIF4A is loosely associated with the cap-binding complexes, and eIF4B is not found within these complexes. eIF4F and eIFiso4F show RNA-dependent ATPase activity that is increased in the presence of eIF4A (Lax et al., 1986), and ATP dependent helicase activity in the presence of eIF4A (Browning et al., 1989). Interesting that the interaction between PABP and eIF4G and eIF4B also stimulates the unwinding of secondary structure in the 5' UTR of mRNA by the eIF4A·eIF4B·eIFiso4F complex. eIF4A was reported to be associated with a cyclin-dependent kinase during active cell proliferation (Hutchins et al., 2004). This finding opens a whole new area for the regulation of translation during plant cell growth and development.

eIF4B

eIF4B is an RNA-binding protein (approximately 59 kD) that functions to enhance the helicase activity of eIF4A and eIF4F (Parsyan et al., 2011) and to organize the assembly of the translation initiation machinery. Accordingly, PIC recruitment to mRNA and scanning of structured mRNAs in vitro was shown to be highly dependent on eIF4B, particularly its C-terminal RNA-binding region. There is evidence that eIF4B promotes binding of both ATP and RNA by eIF4A (Rozovsky et al., 2008). Although eIF4B function in scanning is conserved among plants, animals, and yeast, the protein is one of the least conserved among initiation factors in terms of sequence.

Strikingly that eIF4B is a scaffold protein that binds multiple eIFs and RNA. To promote recruitment of 43S PIC to the mRNA 5'-end, mammalian eIF4B interacts with eIF3 via its subunit a through its internal hydrophilic region rich in aspartic acid, arginine, tyrosine and glycine residues (DRYG), which is also responsible for dimerization. Mammalian eIF4B contains a C-terminal RNA binding domain and a C-proximal serin-rich region. Thus eIF4B can bridge *in vitro* mRNA and the 18S rRNA through its two distinct RNA-binding domains and thus creates additional bridges that may function in concert with the eIF3-eIF4G bridge.

Plant eIF4B is playing a role of a scaffold protein since it interacts with eIF4A, eIF3, PABP, RNA and in addition with eIFiso4G (Cheng and Gallie, 2006). Despite the pure conservation of eIF4B primary sequence, plant orthologues largely maintain the domain organization of mammalian eIF4B. Wheat eIF4B contains RNA binding motifs found in mammalian factor—RRM and the C-terminal RNA binding domain, and harbors one additional domain—the lysine-rich sequence at the N-terminus (Cheng and Gallie, 2006). Each RNA binding domain in wheat eIF4B requires dimerization to display RNA binding activities. The interaction between eIFiso4G and

eIF4B was shown for the first time and the eIFiso4G binding domain lies within the N-proximal RNA binding domain of eIF4B. Two PABP binding sites are located within the conserved domains on either side of the C-terminal RNA binding domain. eIF4A is bound to an adjacent region within the PABP binding C-terminal domain. These and other results support the notion that eIF4B plays a role of a scaffold protein by organizing multiple interactions within components of the translational machinery (Cheng and Gallie, 2006). Finally, eIF4Bs from mammals and plants are known to be highly phosphorylated, suggesting that phosphorylation plays a role in the regulation of translation initiation. Indeed, it was demonstrated that the interaction between plant eIF4B and PABP depends on the phosphorylation status of both eIF4B and PABP (Le et al., 2000). Although in mammals eIF4B interacts with eIF3 subunit a in yeast (Vornlocher et al., 1999), the plant eIF4B binds eIF3 subunit g via the DRYG domain (Park et al., 2004).

The role of eIF3 in 43S PIC recruitment to mRNA

Thus eIF3 plays a key role in mRNA recruitment to 43S PIC. Recent studies in yeast have revealed a direct role for eIF3, particularly PCI domains of eIF3c and eIF3a in recruitment of 43S PIC on capped, native mRNA *in vitro* and *in vivo* independently of eIF4G (Chiu et al., 2010; Jivotovskaya et al., 2006; Khoshnevis et al., 2014; Mitchell et al., 2010). In this case both eIF3a and eIF3c subunits have been located using UV-cross-linking approach at the mRNA exit channel (Pisarev et al., 2008), suggesting that eIF3 subunits a and c constitute an extension of the mRNA exit channel. Mutations within the yeast eIF3a subunit revealed defects in 43S PIC binding to mRNA, scanning and AUG recognition (see below; Chiu et al., 2010). The putative model states that interaction between eIF3a C-terminal domain and some 40S structural elements (h16 and r-protein S3) promote opening of the mRNA channel (Passmore et al., 2007). However, these interactions may stimulate helicase activities required to remove RNA secondary structure elements at the entry channel.

Ribosome scanning and initiation codon recognition

Once at the 5’ end of the mRNA, the 43S PIC must scan over the 5’UTR (less than thousand nucleotides) until it will encounter the start codon (Mignone et al., 2002). Until now the nature of scanning and mechanisms by which eIFs orchestrate scanning remains unclear. Anyway, unwinding the 5’-UTR secondary structure and the 43S PIC movement along RNA are two linked processes occurred during scanning.

It has been observed that 43S PIC can move along unstructured 5' UTRs without the presence of other RNA-unwinding related factors and thus the 40S complex may be capable of scanning along the mRNA by itself. Two initiation factors, eIF1 and eIF1A are critically required to induce the 40S scanning-competent conformation, and omission of eIF1 almost annuls scanning of 40S (Passmore et al., 2007). Although it has been difficult to discriminate between eIF3 function in scanning, TC recruitment and 43S PIC binding to mRNA, eIF3i and eIF3g subunits have been implicated in scanning since their mutants impede reinitiation after uORF1 translation of the GCN4 mRNA preventing GCN4 ORF derepression due to defects in scanning of posttermination 40S ribosomes (Cuchalová et al., 2010).

Unwinding secondary structure in proximity to the 5'-cap during scanning may require eIF4F and ATP, suggesting that eIF4F plays multiple functions during initiation of translation (Pestova and Kolupaeva, 2002). Accordingly, mutations in eIF4G affecting its capacity to bind mRNA or the other eIF4F-related factors also seem to affect scanning efficiency (Watanabe et al., 2010). Even the scanning of 5' leaders containing weak secondary structures requires ATP and eIF4A, eIF4G and eIF4B (Jackson et al., 2010), and the requirement for ATP and eIF4A is proportional to the degree of secondary structure (Svitkin et al., 2001). Strikingly, ATP-dependent RNA helicase DHX29 is required in addition to eIF4A for translation initiation of mRNAs carrying long structured 5'UTRs in mammals (Berthelot et al., 2004; Hashem et al., 2013).

When the start codon enters to the P-site, the 43S PIC has to employ an intensive molecular network to accomplish start codon recognition and trigger the transition to its scanning-arrested state. Once the start codon is recognized, the 40S movement is arrested at this codon. This commitment stage is controlled by the eIF2-specific GAP eIF5. In response to codon-anticodon base-pairing eIF5 binds the eIF2 subunit β triggering hydrolysis of GTP bound to eIF2γ within 40S-bound TC.

A more detailed model of start codon recognition has been propose based on genetic, biochemical and structural data (Aitken and Lorsch, 2012). This model states that eIF1 dissociation is the key step that triggers P_i release and 48S PIC closing, which is accompanied by movements of eIF1A tails and eIF5. eIF1 release occurs in response to start codon recognition, and may be induced by transition of the initiator tRNA from the P_{out} state to the fully accommodated P-site state (P_{in} state). Very recent structural analyses demonstrated that 40S rRNA arrangement in the $tRNA_i$ binding pockets of PIC1 (40S·eIF1), PIC2 (40S·eIF1·eIF1A) and 48S PIC differs significantly and is thus affected by eIF1 and eIF1A, reflecting the differences

between the scanning-competent and scanning-incompetent complex conformations (Lomakin and Steitz, 2013). Together with eIF1, the C-terminal domain of eIF1A must be ejected from the P-site upon Met-tRNA$^{Met}_i$ installation (Yu et al., 2009). Interesting that eIF5 by itself can enhance the dissociation of eIF1 from 48S PIC (Nanda et al., 2009), and eIF5 C-terminal domain mutations can impair start codon recognition and impede eIF1 release from 48S PIC (Luna et al., 2012). A current model has proposed that eIF1 can modulate recognition of the start-codon by restricting $tRNA_i$ binding to AUG only in an optimal context (Lomakin and Steitz, 2013). But $tRNA_i$ binding to AUG triggers the dissociation of eIF1 followed by the release of the P_i from the eIF2·GDP·P_i complex (Algire et al., 2005).

60S ribosomal subunit joining

Joining of the 60S ribosomal subunit and dissociation of eIF2·GDP are mediated by the GTPase eIF5B (Pestova et al., 2000). eIF5B promotes 80S assembly followed by hydrolysis of eIF5B bound GTP that triggers eIF5B dissociation from assembled 80S (Jackson et al., 2010). In principle, binding of the eIF5B C-terminal domain IV to the eIF1A C-terminal tail can promote GTP hydrolysis and thus subunit joining (Acker et al., 2006). eIF1A binding to to eIF5B may become possible after the eIF1A C-terminus is displaced from the P-site by tRNAi after Pi release. Thereby eIF1A plays the essential role in 60S joining. Consistent with its key role in scanning, AUG recognition and 60S joining, eIF1A is present on the ribosome throughout the initiation process and dissociates after eIF5B release (Acker et al., 2009). In contrast to eIFs located on the intersubunit interface that must be released at subunit joining, solvent surface-bound factors such as eIF3 or eIF4G may remain attached to 80S during a few elongation events and participate in downstream reinitiation (Szamecz et al., 2008).

1.2 Regulation of mRNA translation by the TOR/S6K1 signaling pathway in plants

mRNA translation is the most energy consuming process in living organisms. In addition, it plays an essential role in the control of gene expression and is therefore tightly regulated. Translational regulation provides cells with a mechanism to rapidly control gene expression in a reversible manner in response to environmental and developmental cues. It involves the dynamic, coordinated activity of numerous factors that direct the synthesis of proteins with precision in space and time. Translational control is primarily regulated at the level of initiation, and as such, mechanisms that regulate translation most often target the initiation machinery.

Translation in plants is fundamentally similar to that of other eukaryotes. However, there are some differences in number of translation factors and their associated proteins, while translation regulation mechanisms are largely unknown in plants. Here we summarize current knowledge on the role of cellular signaling pathways in translation control, focusing on the role of the Target of Rapamycin TOR in translation—the TOR well conserved pathway regulates the phosphorylation and function of a multitude of eIFs and associated factors. In particular, we portray the role of the TOR signaling pathway in the regulation of plant translation.

1.2.1 TOR complexes

The large evolutionarily conserved Ser/Thr protein kinase TOR belongs to the phosphoinositide 3-kinase (PI3K)-related kinase family, and regulates cell proliferation and growth in response to cellular energy sufficiency, growth factors, hormones, and nutrient availability (Beauchamp and Platanias, 2013).

In mammals TOR (mTOR) interacts with several proteins to form two structurally different and functionally distinct complexes named TOR complex 1 (mTORC1) and TOR complex 2 (mTORC2). However, these mTOR complexes have different sensitivities to the immunosuppressive and anticancer drug rapamycin, distinct upstream effectors and downstream outputs (Figure 1.2-1; Laplante and Sabatini, 2012). The yeast and mammalian TORC1 complexes are normally sensitive to rapamycin (Hay and Sonenberg, 2004; Heitman et al., 1991). Rapamycin forms a complex with its intracellular receptor, FKBP12, which binds to the FRB domain of mTOR and inhibits mTORC1 function (Chen et al., 1995).

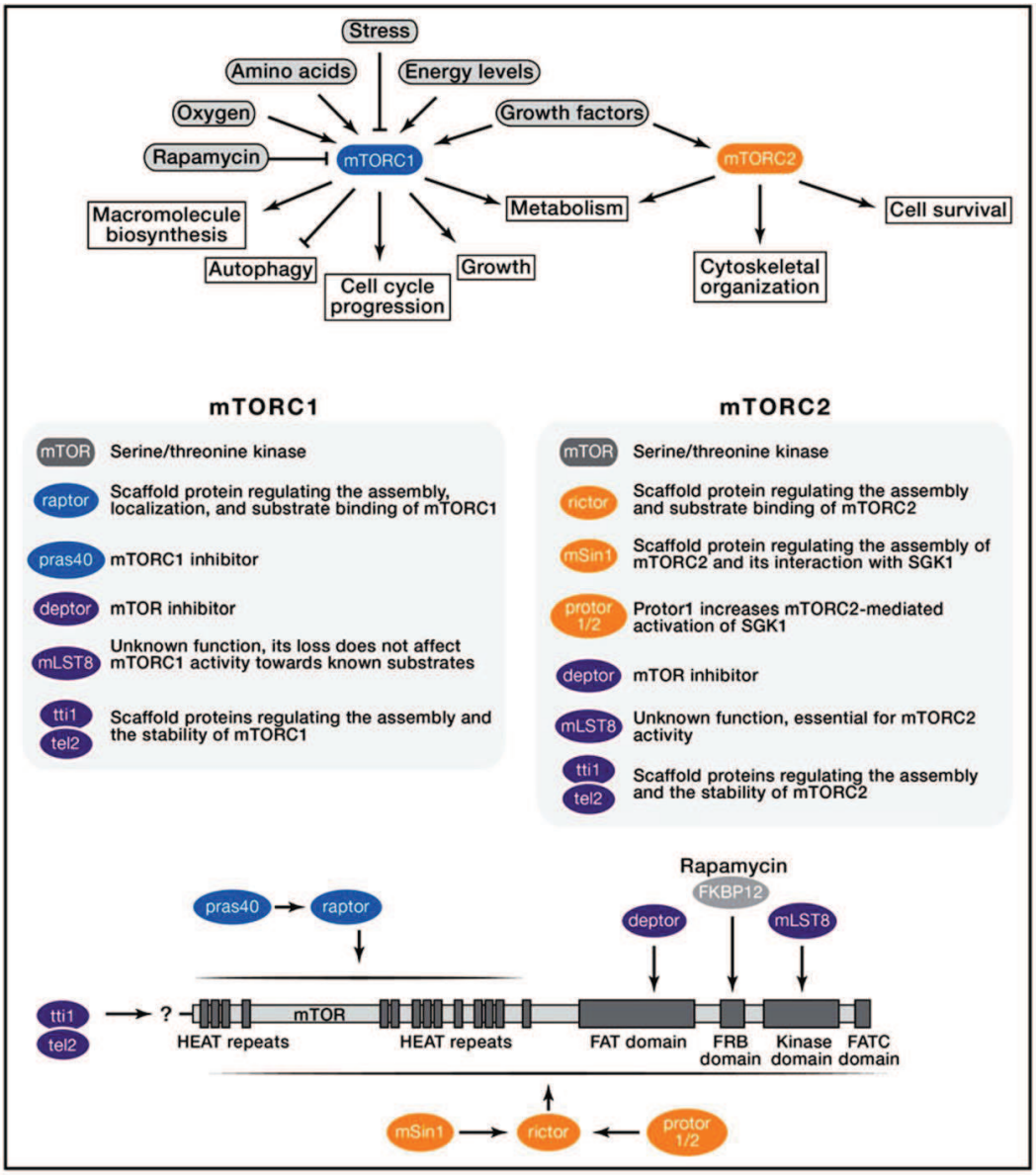

Figure 1.2-1 | **mTORC1 and mTORC2 Complexes**

The mTOR kinase is the core of two distinct protein complexes named mTORC1 and mTORC2.

Upper panel mTORC1 upstream effectors and downstream targets are presented. It promotes cell growth by inducing and inhibiting anabolic and catabolic processes, respectively, and also drives cell-cycle progression.

mTORC2 responds to growth factors and regulates cell survival and metabolism, as well as the cytoskeleton.

Middle panel mTORC1 and mTORC2 complex composition is presented; the known functions are depicted.

Bottom panel Schematic representation of TOR domains and their interaction partners within TORC1 (blue) and TORC2 (orange).

The following abbreviations are used: FAT domain, FAT-carboxy terminal domain; FATC domain, FRAP-ATM-TTRAP domain; FRB domain, FKBP12-rapamycin binding domain; HEAT repeats, Huntingtin-Elongation factor 3-regulatory subunit A of PP2A-TOR1 repeats.

Modified from Laplante and Sabatini (2012), Cell 149:274-293.

However, due to use of rapamycin as a pharmacological tool, TOR was identified as a regulatory hub integrating environmental inputs—the availability of nutrients, the integrity of the cell and the presence of proliferation stimuli—to orchestrate cell growth and cell proliferation. In contrast, TORC2 function is less known due to its resistance to rapamycin.

The mTORC1 complex consists of the catalytic core protein mTOR, the platform protein RAPTOR (regulatory-associated protein of TOR; its yeast ortholog is KOG1), the GTPase β-subunit like protein (gβL/ mLST8), the proline-rich AKT substrate of 40 kDa (PRAS40) and the DEP domain-containing mTOR-interacting protein (DEPTOR), and the Tti/Tel2 complex (Figure 1.2-1; Zoncu et al., 2011). RAPTOR, PRAS40 and Tti/Tel2 seem to be the unique mTORC1-related components, while other proteins are shared with mTORC2. In contrast, the rapamycin-insensitive companion of mTOR (RICTOR, whose yeast ortholog is AVO3), the mammalian stress-activated MAP kinase-interacting protein 1 (mSIN1) and the protein observed with RICTOR 1 and 2 (PROTOR1/2) are found exclusively in mTORC2 (Thedieck et al., 2007); Pearce et al., 2011). The well-known mTORC1 substrates are eIF4E-binding proteins (4E-BPs), the 70 kDa ribosomal protein eS6 kinases 1 and 2 (S6Ks), the PRAS40 protein, the Ser/Thr kinase Ulk1, and the growth factor receptor-bound protein 10 (Grb10; Roux and Topisirovic, 2012). TORC1 mediates temporal control of cell growth by activating anabolic processes such as ribosome biogenesis, protein synthesis, transcription, and nutrient uptake and by inhibiting catabolic processes such as autophagy and ubiquitin-dependent proteolysis. mTORC2 phosphorylates targets and regulates some AGC kinase family members, such as AKT, protein kinase C (PKC) and serum/glucocorticoid regulated kinase 1 (SGK1) and thus controls cytoskeletal organization and cell survival (Beauchamp and Platanias, 2013).

Genes coding for putative TORC1-related orthologs have been identified in plant and algal genomes, including TOR, RAPTOR, LST8 and FKBP12 (Díaz-Troya et al., 2008; Moreau et al., 2012; Robaglia et al., 2012), but TORC2-related homologs are not yet discovered in plant genome. Additionally, plants (*Arabidopsis thaliana; At*) and worms (*C. elegans*) are notable exceptions of FKBP12-rapamycin dependent TORC1 inhibition (Makky et al., 2007; Moreau et al., 2010). Rapamycin, even at high concentrations, does not cause growth retardation phenotypes in land plants. This might be due to the absence of ternary complex formation, caused by mutations in the plant FKBP12 ortholog (Menand et al., 2002; Sormani et al., 2007). It has been reported that disruption of AtTOR causes a premature arrest of endosperm and embryo development (Menand et al., 2002). Partial or inducible RNA silencing, or inhibition of

TOR activity by rapamycin or Torin-1, a potent ATP-competitive TOR inhibitor, has made possible the study of TOR signaling pathway in plants (Deprost et al., 2007; Ren et al., 2012; Schepetilnikov et al., 2013). *Arabidopsis* plants silenced for the *AtTOR* expression display leaf senescence, arrest organ growth, reduction of rRNA synthesis and are characterized by a significant reduction in polysome abundance (Deprost et al., 2007) and increase in constitutive autophagy (Liu and Bassham, 2010). Rapamycin treatment of *Arabidopsis* lines expressing the yeast FKBP12 protein also affects polysomes levels but at lesser extend (Sormani et al., 2007). When the expression of *AtTOR* was abolished by an ethanol-inducible RNAi, plants growth was arrested and senescence-linked markers (genes and metabolites) became up-regulated (Dobrenel et al., 2011). It was further found that the plant TOR pathway can modulate the structure of the cell wall (Leiber et al., 2010). It should be stressed that TOR inhibition by RNAi is likely to reveal a larger spectrum of phenotypes than rapamycin since this drug is known to inhibit only a subset of TORC1 activities (Guertin and Sabatini, 2009). Moreover, mutations in *raptor* are conditionally lethal (Anderson et al., 2005; Deprost et al., 2005), *lst8* mutants are viable (Moreau et al., 2012), but both present a wide range of developmental defects. *Arabidopsis* also encodes a major target of TOR in yeast and animals, the ribosomal protein eS6 kinases (S6K; Mahfouz et al., 2006; Figure 1.2-2) and a downstream phosphatase subunit, Tap46 (Ahn et al., 2011).

The upstream effectors of the plant TOR pathway include energy balance and glucose status (Robaglia et al., 2012). Photosynthesis-derived glucose triggers target-of-rapamycin (TOR) signalling activation through glycolysis and mitochondrial bioenergetics (Xiong et al., 2013). Plant hormone auxin is revealed to be other TOR upstream effector, where treatment of *Arabidopsis* seedlings by auxin triggers TOR phosphorylation that results in its activation and phosphorylation of S6K1 at Thr 449 (Figure 1.2-2; Schepetilnikov et al., 2013; Zhang et al., 1994). When fully activated, S6K1 phosphorylates its downstream target, the r-protein eS6 (Turck et al., 2004), and two recently discovered downstream targets of the TOR signaling pathway in plants: subunit h of eIF3 (eIF3h) and a novel plant protein, reinitiation supporting protein (RISP) implicated in reinitiation after short and long ORFs, respectively (Schepetilnikov et al., 2011, 2013; Thiébeauld et al., 2009) in a manner sensitive to the TOR inhibitor, Torin-1. In addition to Torin-1, two specific phosphoinositide 3-kinase (PI3K) inhibitors wortmannin and LY294002 can suppress S6K1 activity in plants (Turck et al., 2004).

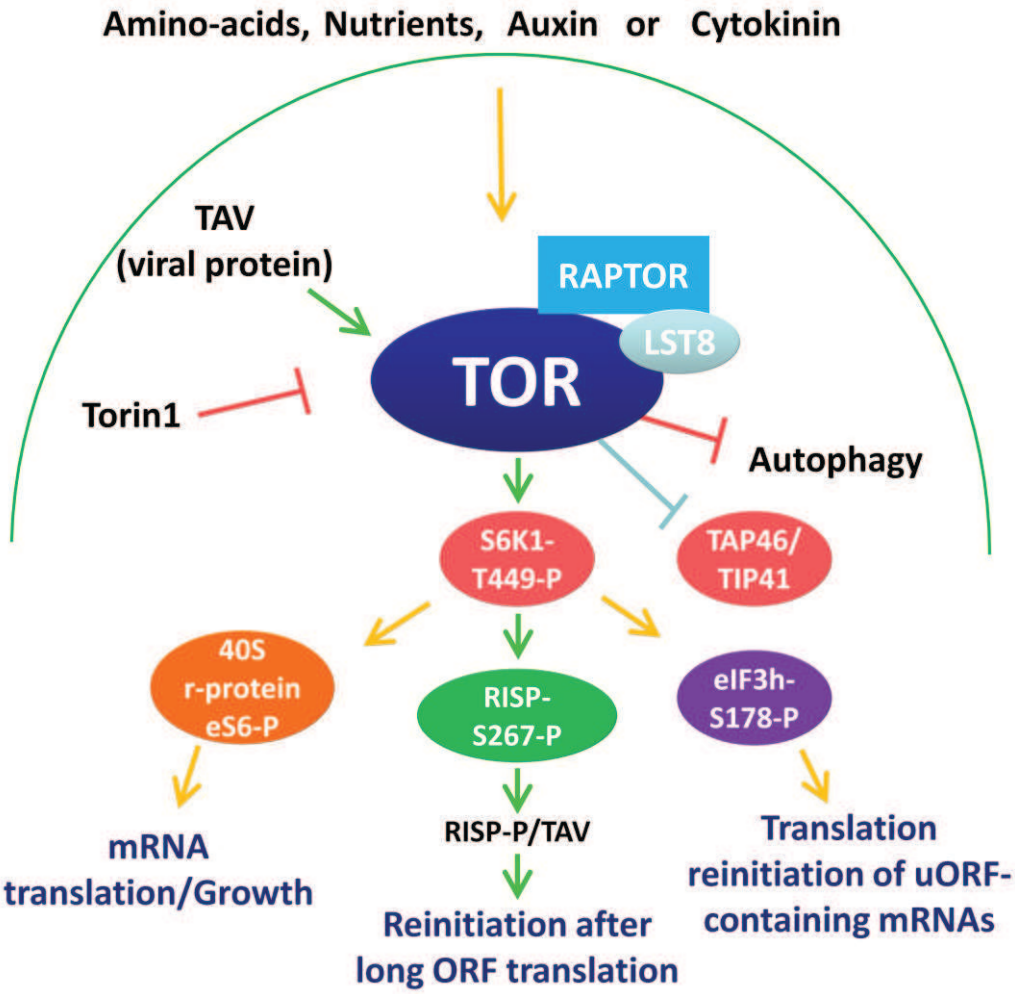

Figure 1.2-2 | **A current model of the TOR signaling pathway in plant translation**
Overview of plant TOR signaling pathway components have been implicated in cellular translation control, Cauliflower mosaic virus (CaMV)-activated reinitiation after long ORF translation and cellular reinitiation after short uORF translation. Phosphorylation events that favour CaMV-activated reinitiation are shown by green arrows.

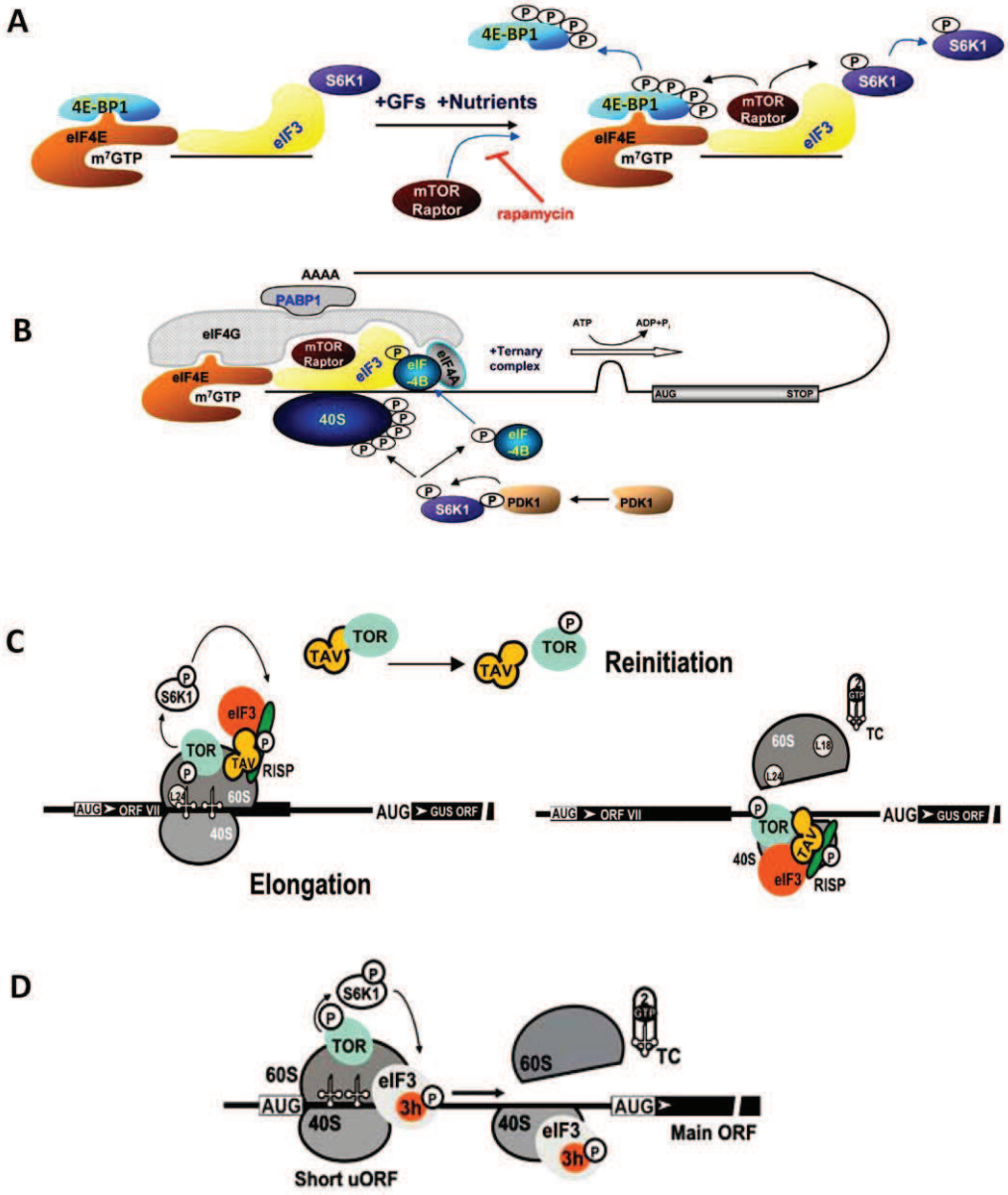

Figure 1.2-3 | TOR regulates the cell translation machinery in initiation and reinitiation of translation

(**A**) eIF3 is a multifactor complex used for S6K1 phosphorylation by mTORC1. When activated, mTOR is recruited to the S6K1-eIF3 complex and phosphorylates S6K1. Phosphorylation triggers S6K1 dissociation from eIF3 and its further activation by PDK1.

(**B**) These phosphorylation events lead to preinitiation-complex assembly and initiation of protein translation.

(**C**) CaMV TAV-mediated reinitiation after long ORF translation. The model of transactivator-viroplasmin (TAV)/TOR function in TAV-induced reinitiation (see text for detailes). TAV ensures retention of reinitiation factors—eIF3/RISP on the translating ribosome during long elongation event. TAV mediates TOR activation. TOR is loaded into polysomes, where it activates S6K1, which maintains the high phosphorylation status of RISP and likely other eIFs.

(**D**). To accomplish reinitiation after short ORF translation, active TOR is targeted to polysomes, where it mantains high phosphorylation levels of other TOR downstream target—the reinitiation factor eIF3h subunit. eIF3h phosphorylation is essential for reinitiation after short ORF translation. *Modified from Holz et al. (2005), Cell 123:569–580* and *Schepetilnikov et al. (2013), 32:1087–1102.*

1.2.2 TORC1 signaling to the translational machinery

Cap-dependent translation initiation is up-regulated by the mTORC1 signaling pathway in response to high levels of amino acids and other nutrients, high energy status or other stimuli via its two main translation-related downstream targets. These best characterized substrates for TORC1 are proteins that binds to the eucaryotic initiation factor 4E (eIF4E, the cap binding protein) which is a limiting factor in translation initiation and the p70 ribosomal protein S6 kinase, S6K (Ma and Blenis, 2009). eIF4E-binding proteins targeted by TOR have been found in yeast and animals but not in plants (Gingras et al., 1999), whereas orthologs of S6K are known in plants (Turck et al., 2004) and are phosphorylated by TOR (Mahfouz et al., 2006; Schepetilnikov et al., 2013). 4E-BPs have been recently implicated in mTOR-dependent translation initiation control of mRNAs that harbor 5' terminal oligopyrimidine (TOP) motifs within the leader region (Thoreen et al., 2012). Activation of S6K1 deploys its phosphorylating potential at multiple translation-initiation related downstream targets, including its major client the 40S r-protein eS6 (Ma and Blenis, 2009), eIF4B (Holz et al., 2005; Raught et al., 2004) and eIF3 (Figure 1.2-3; Martineau et al., 2014).

eIF3 assists phosphorylation of S6K1 and apparently 4E-BPs by mTOR within the 43S preinitiation complex, where eIF3 serves as a scaffold for either inactive S6K1 or active mTOR binding (Figure 1.2-3; Holz et al., 2005). In conditions of low energy/ amino acids, S6K1 is inactivated and binds the eIF3 complex via at least eIF3 subunit f. mTORC1 enters the cell translation machinery likely at the 43S pre-initiation step via association with the multisubunit initiation factor eIF3 (Holz et al., 2005). Upon activation, mTORC1 is recruited to the S6K1/eIF3 complex and phosphorylates S6K1 at Thr389. Phosphorylation triggers S6K1 detachment and further activation by phosphoinositide-dependent kinase 1 (PDK1; Holz et al., 2005; Magnuson et al., 2012). Activated S6K1 may facilitate formation of the translation preinitiation complex and unwinding of highly structured mRNAs by phosphorylating downstream targets and dissociating eIF3 (Ma and Blenis, 2009). mTORC1 directly phosphorylates 4E-BP1 and its subsequent release from the cap complex strongly indicating mTORC1 localization in close proximity to the mRNA cap 5'-end (Clemens, 2001).

mTORC1 was implicated in recruitment of eIF3 subunit j, which is not stably bound to eIF3 and moreover, when it interacts with eIF1A reduces 40S affinity for mRNA. Thus eIF3j under control of mTORC1 may initiate the assembly of 43S PIC (Fraser et al., 2004).

Plant eS6 kinases and their downstream targets in translation initiation

S6Ks belong to a family of basophilic serine/threonine kinases known as AGC kinases, which phosphorylate at basophilic motifs, particularly RXRXXS*/T* for S6K1 (Dempsey et al., 2010). The well known S6K target is the r-protein eS6, although the function of eS6 phosphorylation remains unclear. In mammals, S6 phosphorylation is regulated by $p70^{s6k}$/$p85^{s6k}$ protein kinase isoforms that rely on multiple phosphorylations (Thr389 is a TOR-specific phosphorylation site) for activation (Pullen and Thomas, 1997). The $p85^{s6k}$ isoform is expressed from the same transcript as $p70^{s6k}$ via an alternative translational initiation start site, and thus has a 23-amino acid extension at the N-terminus that targets it to the nucleus (Dufner and Thomas, 1999). Two putative S6K homologs have been identified in *Arabidopsis* and named as S6K1 and S6K2 (Turck et al., 1998; Zhang et al., 1994). The two key phosphorylation sites of mammalian S6K1 (Thr229 and Thr389) seem to be conserved between plants and mammals. S6K1 has been identified as an ortholog of p70 S6 kinase: it has cytoplasmic localization and phosphorylates r-protein eS6 (Mahfouz et al., 2006). S6K2 is exclusively nuclear and has been suggested to phosphorylate the chromatin-bound nuclear form of r-protein eS6 (Franco and Rosenfeld, 1990). Indeed, Mahfouz et al. (2006) identified that $p70^{S6K}$, which is mostly cytoplasmic, is involved in the phosphorylation of r-protein eS6 on the cytoplasmic ribosome. It was shown that two putative bipartite nuclear targeting signals within S6K2 sequence mediate its localization in the nucleus of BY2 tobacco cells (Mahfouz et al., 2006). AtS6K1 is a TOR direct downstream target—it is phosphorylated at Thr449 in response to TOR activation and, when fully activated, phosphorylates eS6 in a Torin-1 sensitive manner (Schepetilnikov et al., 2011). The catalytic domain of S6K1 could be phosphorylated by *Arabidopsis* 3-phosphoinositide-dependent kinase-1 (PDK1; Mahfouz et al., 2006).

Phosphorylation status of r-protein eS6

R-protein eS6 was identified as a substrate of S6Ks. Six phosphorylation sites have been reported within the C-terminal α helix of eS6 in frog, human and mouse (Ser235, Ser236, Ser240, Ser242, Ser244 and Ser247; Figure 1.2-4; Meyuhas, 2008). In mammals there are several major eS6 phosphorylation sites—Ser235/Ser236 (both are conserved in yeast) that are phosphorylated by both $p70^{S6K}$ kinase as well as RSK (via the MAPK signaling pathway) and Ser240/Ser244 which are thought to only be phosphorylated by $p70^{S6K}$ (Hutchinson et al., 2011; Meyuhas, 2008; Roux et al., 2007). A similar distribution of phosphorylation sites within the C-terminal α helix was described for *Drosophila melanogaster* r-protein eS6 (Radimerski et al.,

2000). However, yeast r-protein eS6 harbors only two phosphorylatable serine residues, Ser232 and Ser233 that correspond to mammalian ortholog Ser235 and Ser236 residues (Meyuhas, 2008). It has been proposed that phosphorylation in mammals occurs in an ordered fashion, with Ser236 being a primary phosphorylation site (Hutchinson et al., 2011). In yeast, eS6 is strongly phosphorylated after relocation into fresh nutrient medium and at an early stage of germination (Jakubowicz, 1985; Szyszka and Gasior, 1984).

In plants, eS6 is presented by two isoforms, eS6a and eS6b, and several phosphorylation sites in eS6 have been reported in *Arabidopsis* and maize. Phosphorylation of Ser240 was demonstrated for two eS6 isoforms in *Arabidopsis* cell culture (Carroll et al., 2008). A large-scale phosphoproteome revealed phosphorylation of Thr127, Ser237, Ser240, Ser247, Thr249 for eS6a and phosphorylation of Thr127, Ser237, Ser240 for eS6b for *Arabidopsis* seedlings (Reiland et al., 2009). Comparative proteomic analyses by Turkina et al. (2012) detected eS6 phosphorylation at the previously unknown site—Ser231 in *Arabidopsis*. Recently, from similar comparative phospho-proteomic analyses, Boex-Fontvieille et al., (2013) revealed additional phosphorylation sites in the two isoforms of *Arabidopsis* r-protein eS6 at Ser229 and Ser231, with mono and bis-phosphorylated peptides Ser229 and Ser229/Ser231, respectively (Figure 1.2-4). Multiple phosphorylations of the two isoforms of eS6 in maize roots had also been characterized (Williams et al., 2003). Five potential phosphorylation sites in the C-terminal helix of the maize eS6 protein isoforms were suggested and at least two sites have been shown to correspond to *Arabidopsis* eS6 sites, Ser237 and Ser240 (Williams et al., 2003). However, these five phosphorylation sites are more comparable with that of vertebrate r-protein eS6, yet this set of sites is not confined to serines, as it include also a threonine residue (Williams et al., 2003). The phosphorylation level of eS6 in plants is significantly higher during the day than at night (Boex-Fontvieille et al., 2013; Turkina et al., 2011), and is up-regulated by cold (Williams et al., 2003), UV-B exposure (Casati and Walbot, 2004), high CO_2 concentration (Boex-Fontvieille et al., 2013) and auxin (Beltrán-Peña et al., 2002; Schepetilnikov et al., 2013; Turck et al., 2004). In contrast, eS6 phosphorylation is reduced by conditions that suppress translation such as heat (Scharf and Nover, 1982), hypoxia (Williams et al., 2003), reactive oxygen (Khandal et al., 2009), low CO_2 concentration and darkness (Boex-Fontvieille et al., 2013). In light of the pan-eukaryotic nature of this phosphorylation event, it is surprising that its biological meaning for translation remain largely mysterious. Despite numerous reports showing a direct correlation between stimulation of TOR/S6K1 pathway and high S6 phosphorylation levels, more evidence on the role of eS6 phosphorylation in translation is required.

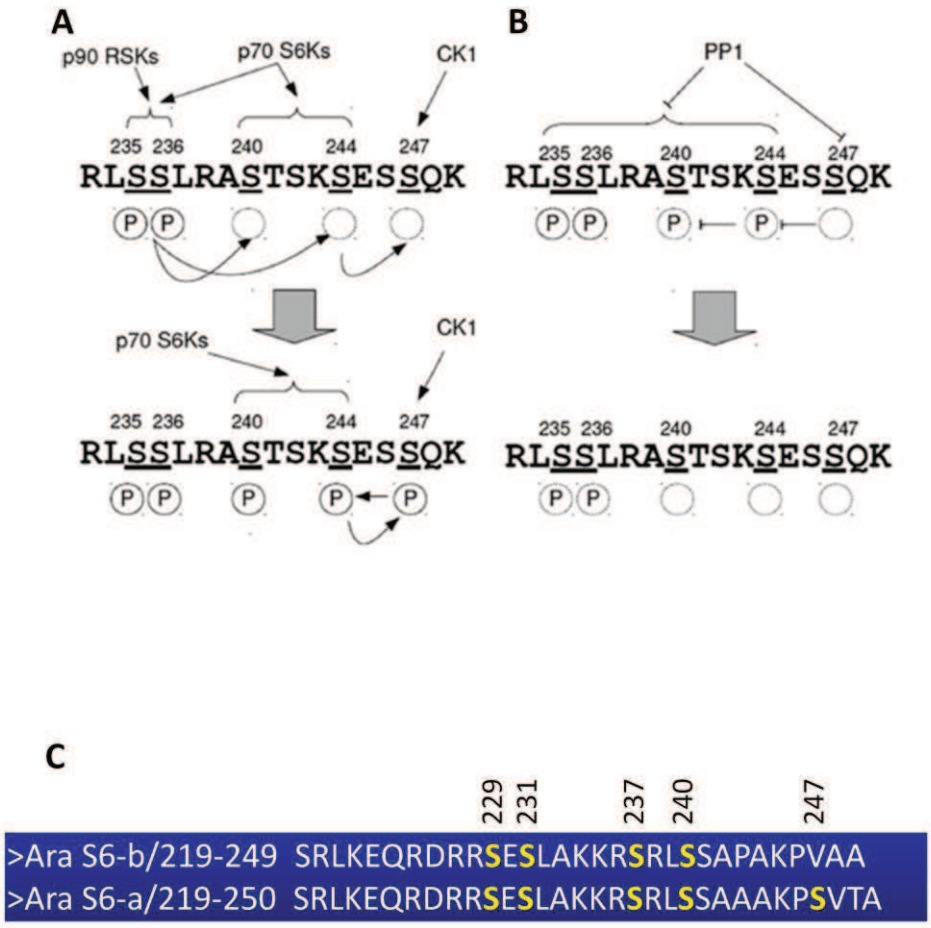

Figure 1.2-4 | **Phosphorylation and dephosphorylation events operating at the eS6 C-terminal domain**

(**A**) Initiation and maintenance of eS6 phosphorylation in mammals. Upon mitogenic stimulation, p90 RSK and p70 S6K kinase families phosphorylate Ser235/236. Ser235/236 phosphorylation (*circled P*) promotes p70 S6K-dependent phosphorylation of Ser240 and Ser244. Ser244 phosphorylation then promotes Casein Kinase 1 (CK1)-dependent phosphorylation of Ser247. Phospho-Ser247 triggers feedback phosphorylation of Ser240/244, which supports eS6 phosphorylation.

(**B**). Dephosphorylation of rpS6 by PP1. After cessation of mitogenic stimuli and inactivation of eS6 kinases, phosphatase 1 (PP1) rapidly dephosphorylates eS6 beginning with Ser247. Phosphorylation sites are underlined.

(**C**) Number of phosphorylated serines reported for *Arabidopsis* eS6 paralogs are indicated. Positions of five serine residues that can be found phosphorylated in eS6a and eS6b proteins from *Arabidopsis thaliana* are indicated by a yellow. S. *Modified from Hutchinson et al. (2011) Journal of Biological Chemistry 286(10): 8688–8696.*

1.3 Plant translation reinitiation

1.3.1 Reinitiation after uORF translation

Eukaryotic cells react to environmental inputs by availing itself of a complex signaling transduction network. Regulation can take place at the transcriptional level as well as post-transcriptionally, for example, via regulation of particular messages (Nilsson et al., 2004). Translational regulation of mRNAs that harbor upstream ORFs (uORFs) within their leader regions has been largely accepted as a mechanism controlling levels of potent proteins such as growth factors, protein kinases and transcription factors (Morris and Geballe, 2000). uORFs are highly abundant in angiosperms, being present in at least 30% of full-length mRNAs (Zhou et al., 2010), and 28% of plant uORF-containing genes encode proteins involved in signal transduction and/or gene regulation (Kawaguchi and Bailey-Serres, 2005). By capturing scanning ribosomes, uORFs decrease the translation levels of downstream protein-coding genes (Ingolia, 2014).

However, when the translational repression by the uORF is attenuated in response to specific signals, translation of the main ORF becomes regulated (Hanfrey et al., 2005). For example, in *Arabidopsis*, an uORF-encoded peptide, located in the 5' leader of the basic leucine zipper transcription factor-encoding mRNA (AtbZip11) mediates translational repression by high sucrose (Rahmani et al., 2009). In yeast, combination of four uORFs within the 5' leader of the bZip transcription factor GCN4 cause a translational derepression in response to amino acid starvation (Hinnebusch, 2005). uORFs also function in complex regulatory switches dedicated to IRES remodeling (Yaman et al., 2003) as well as translation reinitiation or shunting (Park et al., 2001, 2004; Ryabova et al., 2006).

Reinitiation after short uORF translation in mammalian cells was noticed by Kozak in 1987 during her investigations leading to formulation of the scanning ribosome model. In this study, M. Kozak observed that insertion of an in-frame stop codon a few codons after the 5'-proximal AUG strongly activated initiation at the next downstream AUG of a reporter ORF. The efficiency of initiation at this second AUG augmented with increasing the intercistronic distance, reaching a ceiling at a distance of 79 nucleotides ((Kozak, 1987). This led to the idea that some of the ribosomes that translate the uORF can resume scanning likely as 40S subunits, but initially without a ready-to-start TC (eIF2·Met-tRNA$^{Met}_{i}$·GTP), which could, however, be recruited during the course of this rescanning. In this way, successful for reinitiation intercistronic distance will therefore depend on the TC availability and/ or the capacity of the reinitiating-ribosomal machinery to recruit *de novo* a "fresh" TC. However, reinitiation is quite rare event in yeast.

Reinitiation efficiency decreases quite acutely with increasing length of the uORF (Luukkonen et al., 1995), but a single very short uORF often does not interfere with downstream translation initiation. Normally the 35-codon uORF abolishes translation reinitiation downstream (Rajkowitsch et al., 2004). A detailed *in vivo* study in human cells with >25 uORFs that inhibited protein expression between less than 5% and 100% did not reveal a strong correlation between uORF length and protein levels (Calvo et al., 2009). Surprisingly, a fraction of *Arabidopsis* mRNAs harbour uORFs that exceed this length (Zhou et al., 2010). Comparable analysis of uORF length and protein levels revealed a direct correlation between uORF length and inhibition of gene expression, where uORFs of more than 16 codons are expected to inhibit translation (Roy and von Arnim, 2013). In the majority of eukaryotic cases reinitiation after translation of uORF less than 30 codons in size can occur and thus the reinitiation permitted upstream short ORF (sORF) size could be 30 codons or less. However, it seems that some plant uORF-containing mRNAs are the exception to this rule, such as the ARF3/ETTIN-encoding mRNA (see below), which contains 90-codon-uORF1 encoding 10 kDa protein (Nishimura et al., 2005).

The reinitiation efficiency is reduced if the rate of uORF elongation is slowed down by chemical agents or by adding a pseudoknot into the uORF (Kozak, 2001; Pöyry et al., 2004). These observations imply that it is the time required for translation of the uORF that is critical determinant of rescanning and reinitiation efficiency. This is in accord with the hypothesis stating that some of the initiation factors that promote initiation at the uORF AUG might remain transiently associated with the ribosome after 80S assembly, and might then be released stochastically during a few elongation cycles (Jackson et al., 2012; Kozak, 1987), explaining why reinitiation is permitted only after a short elongation event. As a result, the initiation factor-retaining ribosomes would be reinitiation-competent capable of resumption of scanning, recruiting a TC-associated Met-tRNA$^{Met}_{i}$ and the 60S subunit *de novo*. However, these reinitiation promoting factors (RPFs) and especially mechanisms of their functions are only starting to emerge.

Reinitiation promoting factors, RPFs

Thanks to the discovery of alternative mechanisms of initiation that do not require all the canonical eIFs (e.g., IRES-dependent initiation), new insights on the critical reinitiation-promoting factors have been obtained by investigating whether reinitiation depends on factors assisting the uORF initiation event. By placing different types of IRESes upstream of the uORF start codon, it has been observed that reinitiation *in vitro* can occur only if the eIF4F complex (or

at minimum the central domain of eIF4G plus eIF4A) participated in the uORF initiation event. This study predicts that the interaction between eIF4G and the 40S that is established during 43S PIC loading on mRNA is maintained during the time taken to translate the uORF (Pöyry et al., 2004). Since eIF4G builds an indirect bridge with the 40S subunit, by a firm hold provided by eIF3, this may imply that the eIF4G-eIF3-40S interaction network is required for reinitiation after short uORF translation.

How is it to remove eIFs after the initiation event? The only factors that dissociate 40S before elongation can start are G-proteins eIF2 and likely eIF5B as soon as their bound molecules of GTP are hydrolysed. As mentioned before, the factors involved in the 43S PIC formation—eIF1A, eIF1 and eIF5—play their functional roles on the interface of the 40S subunit. Thus, there seems little doubt that all the aforementioned eIFs dissociate from the ribosome after 60S joining or might remain associated with 40S within the multifactor complex. Consequently, only eIF3 and eIF4F-related factors preferentially attached to the 40S solvent surface remain as factors whose interaction with 40S could persist during the time invested to translate the uORF (Jackson et al., 2012). Accordingly, in the last years the mammalian eIF4G and eIF4A (Pöyry et al., 2004), eIF3 (Cuchalová et al., 2010; Park et al., 2001) and probably an insect eIF5-ortholog (Hiraishi et al., 2014) have been identified, as RPFs.

In plants, eIF3 non-core subunit h (eIF3h) and the 60S r-protein eL24 have been proposed to be key players in reinitiation after uORF translation in plants. Both eL24b and eIF3h are required for translation of uORF-containing mRNAs that encode two families of transcriptional factors, the auxin response factors (ARFs) and the basic zipper transcription factors (bZIPs), via as yet unknown mechanisms (Kim et al., 2004; Nishimura et al., 2005; Schepetilnikov et al., 2013; Zhou et al., 2010). Critically, translation reinitiation and auxin-mediated organogenesis are compromised severely by deletion mutagenesis of either eIF3h or eL24b (see above). In plants, eIF3 is recruited to promote a special case of reinitiation after long ORF translation by the *Cauliflower mosaic virus* (CaMV) protein translational transactivator/ viroplasmin (TAV; Park et al., 2001; see above). Thanks to CaMV, other RPF have been highlighted—reinitiation supporting protein (RISP) that is a subject of my research.

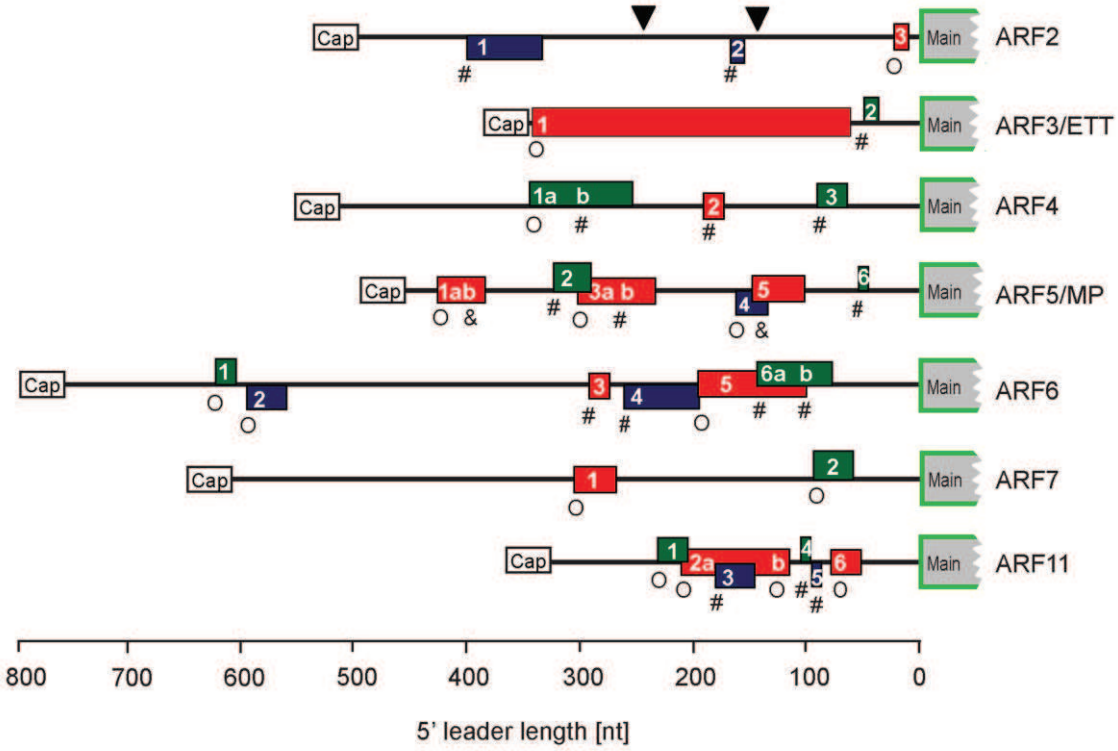

Figure 1.3-1 | Schematic representation of auxin response factor (ARF)-encoding mRNAs that harbor multiple uORFs within their leader regions

Many mRNAs coding for ARFs containing one or more upstream short ORFs within their leader regions, their translation depends on reinitiation mechanisms.

Rectangles represent uORFs that are in frame (red) with the main ORF, in the -1 position (green), or in the +1 position (blue).

Start codon contexts are illustrated as weak (O, NNNAUGN), moderate (#, RNNAUGN or NNNAUGG) and strong (&, RNNAUGG).

The cDNA sequences shown generally correspond to the longest known gene model displayed at http://www.arabidopsis.org/ in November 2009: ARF2 (AT5G62000.1); ARF3 (AT2G33860.1); ARF4 (AT5G60450.1); ARF5 (AT1G19850.1); ARF6 (AT1G30330.1); ARF7 (AT5G20730.1); ARF11 (AT2G46530.1). A splice variant known for ARF2 retains uORF1 and uORF3 (intron flanked by black triangles). *Taken from Zhou et al. (2010), BMC Plant Biology 10:193.*

The role of eIF3h and eL24-b in gene regulation in plants

mRNAs that encode members of the ARF protein family are particular enriched by uORFs within their leader regions (Figure 1.3-1; Kim et al., 2007, 2004). Auxin response factors or ARFs are family of transcriptional factors that bind specifically to auxin response elements in promoters of primary or early auxin-responsive genes and activate their transcription in response to auxin (Tiwari et al., 2003). Auxin is one of phytohormones that plays critical roles in the initiation and specification of postembryonic organs emerging from the apical meristems as well as in the establishment of the apical-basal axis (Friml et al., 2003). The short-range directional auxin transport governs primordium initiation on the shoot apical meristem (SAM), thereby affecting phyllotaxis (Heisler et al., 2005; Reinhardt et al., 2003). While PIN proteins guide directional auxin transport, ARFs can sense the local auxin concentration to activate a gene expression response (Teale et al., 2006).

ARF3/ETTIN (*ETT*; regulates leaf polarity and reproductive development) and *ARF5/MONOPTEROS* (*MP*; regulates embryo and shoot apical development; Hardtke and Berleth, 1998; Sessions et al., 1997; Figure 1.3-1), contain two and six uORFs, respectively, that strongly reduce expression of ARF proteins (Zhou et al., 2010). Strikingly that either deletion of one of the eL24-encoding genes, *eL24b* (*stv-1* mutant), or mutations in the auxin response factor (ARF) genes *ETTIN* (*ETT*) and *MONOPTEROS* (*MP*) display defects in the apical-basal patterning of the gynoecium, in addition to phenotypes induced by ribosome deficiency (Nishimura et al., 2005). Interestingly, transformation of *stv-1* plants with a uORF-eliminated ETT construct suppresses the gynoecium phenotype, implying that r-protein eL24 could play a direct role in uORF-containing mRNA translation reinitiation. Analyses of 5'-leader-reporter gene fusions showed that the presence of uORFs within ETT and MP UTRs negatively regulate the translation of the downstream main ORFs and suggest the role of translation reinitiation in *ETT* and *MP* expression (Nishimura et al., 2005). Indeed, the expression of ETT and MP seems to occur by the translational reinitiation mechanism that is broken in eIF3h or eL24b deficient plants (Kim et al., 2004; Park et al., 2001; Schepetilnikov et al., 2013).

Moreover, Roy and von Arnim (2014) considered the suppression of the strong phenotype observed in eL24 deficient plants with a single "subject" gene as an extraordinary result, because according to their unpublished data, the *stv-1* mutant mistranslates more than a hundred mRNAs.

Similar to eL24, eIF3h counteracts the translational repression by uORFs (Kim et al., 2007) and plants with eIF3h deficiency display severe defects in auxin-mediated organogenesis

(Zhou et al., 2010). In the same report, a protoplast transformation assay based on *in vitro* transcribed mRNA showed that the translation efficiency of a reporter containing 5' ARF-related leaders with multiple uORFs was strongly affected in the *eif3h* mutant. The mutant phenotypes observed in *stv-1* and *eif3h-1* plants denote a role of translation reinitiation in developmental gene regulation.

Schepetilnikov et al. (2013) demonstrated the role of auxin in TOR signalling activation and reinitiation after uORF translation. Auxin triggers TOR and thus S6K1 activation that results in efficient loading of uORF-mRNAs onto polysomes in a manner sensitive to the TOR inhibitor Torin-1. Moreover, TOR/S6K1 signals to eIF3h that becomes phosphorylated and active in translation reinitiation (Schepetilnikov et al., 2013).

1.3.2 Virus-activated reinitiation after long ORF translation in plants

In contrast to short uORFs, reinitiation after a long ORF translation is an extremely rare event in eukaryotes. But many viruses code for polycistronic mRNAs and thus have engineered sophisticated mechanisms of their translation. Plant viruses have developed multiple strategies to express their compact genomes, including various types of polycistronic translation, such as leaky scanning, frame-shifting, read-through, and virus-activated reinitiation/transactivation of polycistronic translation. The latter is the main focus of this last chapter of introduction.

There seems to be no evidence that plant viruses can specifically shutdown translation of host cellular mRNAs. However, non-conventional translation mechanisms that help to compete with cellular mRNAs for the host translational machinery are employed by plant viruses. Such mechanisms include ribosomal shunting (Ryabova et al., 2006) and internal initiation (Dreher and Miller, 2006) to avoid scanning through structural elements of mRNA leaders that are required for other aspects of the viral cell cycle. Some viruses may avoid using of host translational machinery-related factors taking advantage of their translation strategies. In contrast, eIF4F/eIFiso4F cap-binding factors are essential for many plant viruses to infect cells (Robaglia and Caranta, 2006; Wang and Krishnaswamy, 2012). Furthermore, some viruses can counteract the high 5'-cap-dependent initiation efficiency (if lacking cap structure) by delivering eIF4F to their viral 5'-leaders through particular and really sophisticated elements within 3'-UTRs of viral mRNAs (Treder et al., 2008). However, caulimoviruses not only interact with the host translational machinery to exploit its properties but also they are capable to modify cell programs.

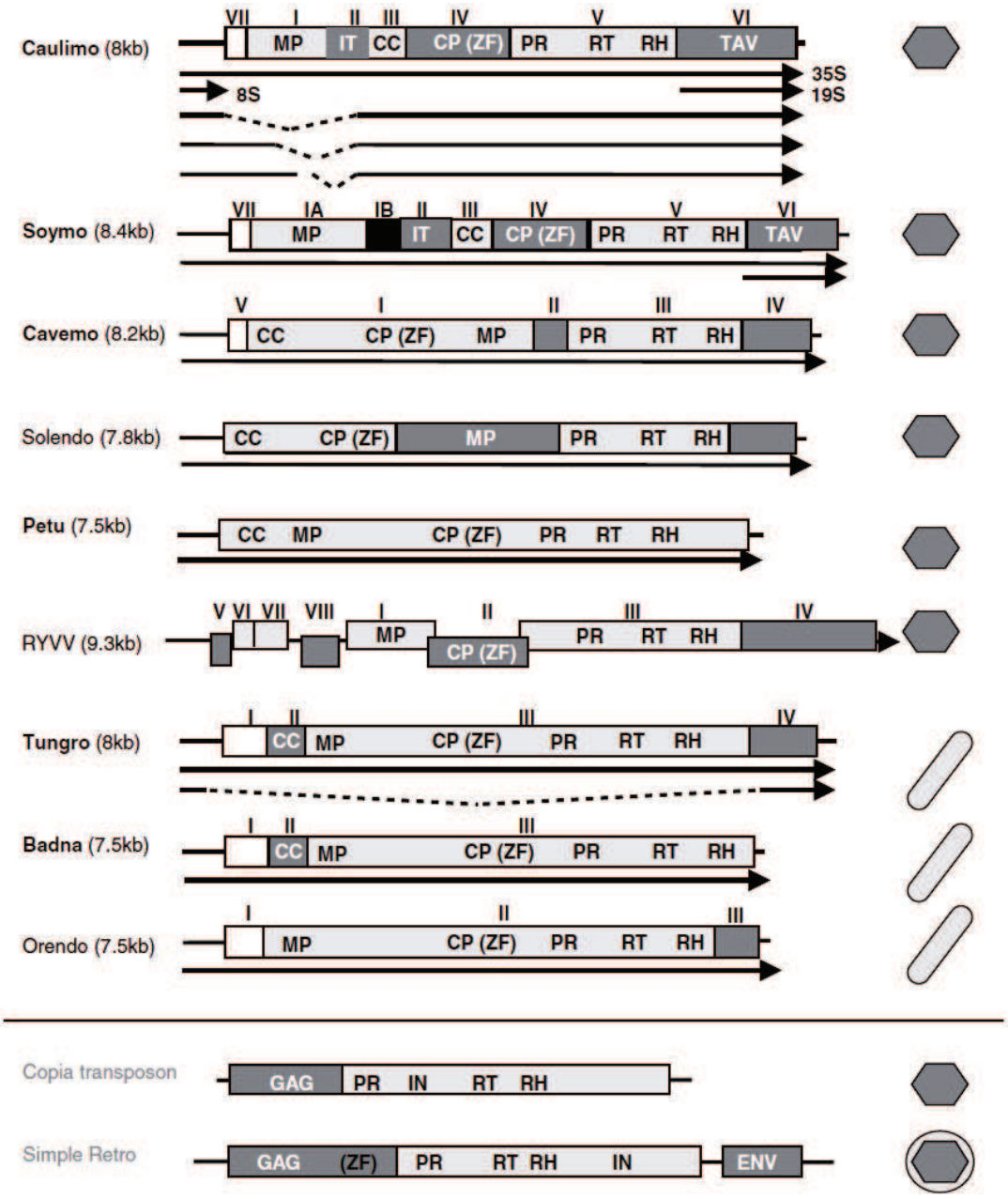

Figure 1.3-2 | **Schematic representation of pararetroviral genoms and their expression strategies**

Top panel: The most representative RNAs with specific ORF arrangement and features are shown. Arrows beneath each viral sequence indicate transcripts (dotted lines indicate introns). MP: movement protein, IT: insect transmission, CC: coiled coil, CP: coat protein, ZF: zinc finger, PR: protease, RT: reverse transcriptase, RH: RNAse H, and TAV: transactivator/viroplasmin.

Lower panel: Comparison with a canonical retrotransposon and a simple mammalian retrovirus

Plant pararetroviruses and their translation strategies

The plant pararetroviruses, named Caulimoviridae, include the icosahedral caulimo-, soymo-, cavemo-, and petu viruses and the bacilliform badna- and tungro viruses. Members of the *Caulimoviridae* are distinct in some aspects of their genome arrangement and expression strategies. Plant pararetroviruses, replicate via transcription/reverse transcription much like mammalian retroviruses but differ from the latter in that they do not integrate into the host genome (Pfeiffer and Hohn, 1983) excluding petu-viruses (their long integrated sequences have been found; Richert-Pöggeler et al., 2003). Instead, they accumulate as DNA episomal copies in the host cell nucleus, as redundant RNA in the cytoplasm, and as open circular dsDNA in virions. All pararetroviruses discovered until now encode a POL-fusion protein much like that of mammalian retroviruses, consisting of protease (PR), reverse transcriptase (RT) and RNAse H (RH) (but lacking integrase) domains, that is cleaved into its constituent parts by the viral (aspartic) protease (Figure 1.3-2; Torruella et al., 1989). Genes encoding a movement protein (MOV) and an aphid transmission factor (ATF) are involved in intra- and inter- plant spreading together with a viron-associated protein (VAP) which is required for both movement and insect transmission (Plisson et al., 2005; Stavolone et al., 2005).

In general, eukaryotic mRNAs are monocistronic, but pregenomic pararetrovirus transcripts are polycistronic. Strikingly, all genera of plant pararetroviruses, except for the Petunia vein clearing virus (PVCV) genus, encode polycistronic RNAs [PVCV has only one large ORF encoding a polyprotein precursor for all viral proteins (Richert-Pöggeler et al., 2003). Consequently, these viruses have designed programs to multiply their functions encoded in a single translation product, the number of mRNAs and/or the number of translation initiation sites harbored in a single mRNA. The strategic solutions encompass the production of polyproteins that are cleaved by a virus-encoded protease, the use of alternative subgenomic promoters, the alternative splicing of viral RNAs, and/or the deployment of multiple forms of polycistronic translation (Hohn and Rothnie, 2013).

CaMV encodes translation transactivator/ viroplasmin, TAV to accomplish its translation strategies

Two major viral transcripts accumulate in CaMV-infected turnip (Figure 1.3-3): (1) the 35S RNA that covers the whole genome with a 180 nt terminal repeat and acts as the pregenomic RNA and the polycistronic mRNA for six of the seven ORFs, and (2) the subgenomic 19S RNA that codes for translation transactivator/viroplasmin (TAV; ORF VI).

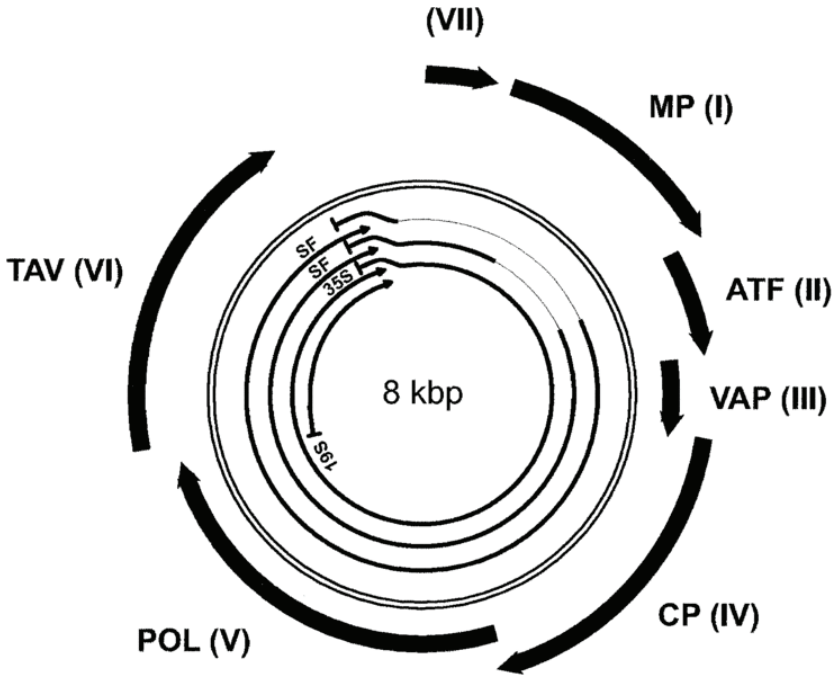

Figure 1.3-3 | **Schematic representation of CaMV genome**
Circular map of CaMV DNA (doubled circle).
ORFs are indicated by black arrows in the outer circles [VII (function unknown), I (MP, cell-to-cell movement protein), II (ATF, aphid-transmission factor), III (VAP, virion-associated protein, transmission function), IV (CP, capsid protein precursor, structural function) and V (POL, protease, reverse transcriptase, RNase H, enzymic functions)].
The inner circles represent the transcripts, the 35S RNA (35S) and 19S RNA (19S) transcripts and two distinct spliced forms (SF).

These two RNAs are transcribed from separate promoters but share the same 3'-terminus. Thus, TAV can be considered an early viral protein. Similar to majority of cellular mRNAs, the polycistronic 35S pgRNA is capped and polyadenylated. All seven long ORFs within the 35S pgRNA are translated by the same ribosome one by one via the reinitiation mechanism under exclusive control of TAV protein (Futterer and Hohn, 1992; Park et al., 2001; Schepetilnikov et al., 2011). Thus, expression of most of the viral proteins depends on TAV.

TAV

TAV, which we widely use as a tool to study translational control in plants, is an intrinsic multifunctional protein, present in most of the icosahedral plant pararetroviruses. TAV is highly expressed from the monocistronic subgenomic 19S RNA and forms so called viroplasms in the cytoplasm of infected cells, in which virus particles accumulate and which are the sites of virion assembly, intracellular virus replication, and likely translation of the full-length polycistronic RNA. TAV is a nuclear shuttle protein (Haas et al., 2005), whose function in the nucleus is largely unknown. It binds to itself and to the capsid protein (Himmelbach et al., 1996), to RNA (De Tapia et al., 1993), and to the translational machinery (Park et al., 2001; Ryabova et al., 2006). Finally, it is a pathogenicity determining factor, responsible for host range and symptom severity (Broglio, 1995; Kobayashi and Hohn, 2004; Schoelz and Wintermantel, 1993; Stratford and Covey, 1989) and, as a transgene, it strongly affects plant development and morphology (Baughman et al., 1988; Takahashi et al., 1989; Zijlstra et al., 1996). Another function for TAV is once viral proteins accumulate in inclusion bodies, and TAV might be responsible for this type of sequestration and for promoting the assembly process, or being involved in other aspects of intracellular replication (Kobayashi and Hohn, 2003). TAV may also control some aspects of systemic spread (Kobayashi and Hohn, 2004). However, I am interested to investigate the mechanisms TAV-controlled reinitiation after long ORF translation.

Host factors in TAV-mediated transactivation.

TAV-activated reinitiation has been studied largely in CaMV. Interestingly, specific *cis*-sequence modules do not play any role in transactivation of reinitiation as TAV can activate reinitiation after translation of the first ORF in an artificial bicistronic RNA containing two reporter ORFs (Fütterer and Hohn, 1991). Consequently, a stem structure at the cap-site inhibits expression of both reporters, while a stem between the two ORFs abolishes expression of only the second reporter (Fütterer and Hohn, 1991).

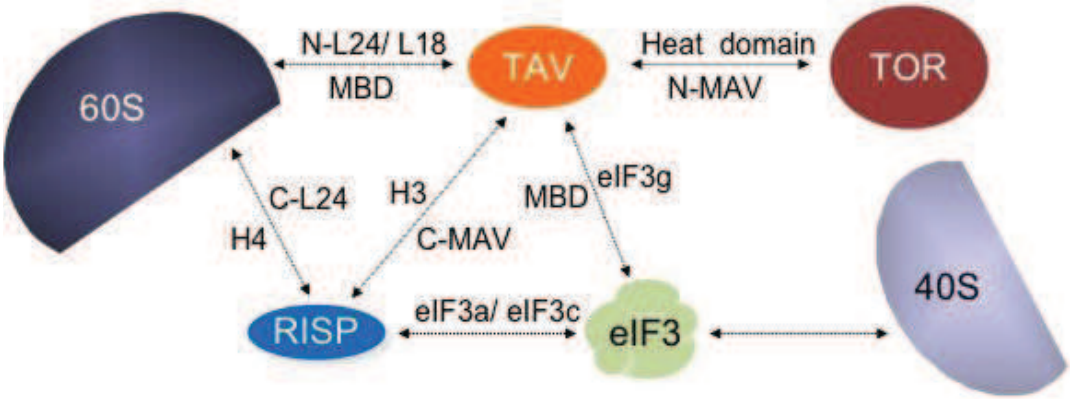

Figure 1.3-4 | **Protein-protein interactions between TAV and its partners**
TAV can bind 60S (via r-proteins L18 and eL24), RISP, and eIF3 (via the eIF3 subunit g). RISP interacts with 60S (via r-protein eL24), TAV, and eIF3 (via subunits a and c). RISP and TAV are two co-factors that are involved in complex formation with 40S via eIF3 and 60S via eL24. TAV interacts and activates TOR.
Interacting proteins are connected by thin interrupted lines. Proteins or protein domains mediating the above interactions are indicated. C-L24 (the eL24 C-terminus), N-L24 (the eL24 N-terminus), H4 (RISP α-helix 4), H3 (RISP α-helix 3), MBD (the multiple protein binding domain of TAV), MAV (the minimal transactivation domain of TAV), N-MAV (the MAV N-terminal domain), C-MAV (the MAV C-terminus), and Heat domain (the N-terminal heat repeat domain of TOR) are depicted.

Differently from the case of GCN4, TAV mediated reinitiation is not dependent on the length of the intercistronic region and takes place in an equal and efficient way either immediately after translation termination, when the two ORFs are linked by an AUGA quadruplet, or when the second ORF is positioned as far as 600 nt further downstream (Fütterer and Hohn, 1991).

Considering that reinitiation is not so much affected by the distance between the two consecutive cistrons, it has been proposed that reiniation promoting factors, RPFs, do not have to be recruited *de novo* but they must remain attached with the TAV-associated elongating ribosomal complexes, and thus could be reutilized during the reinitiation event to promote 48S PIC formation and/or 60S subunit recruitment (Park et al., 2001). Surprinsingly, Schepetilnikov et al. (2011) discovered that to achieve virus-activated polycistronic translation, it is required not only a simple binding of RPFs with the TAV-associated translating machinery, but also a change in the phosphorylation status of TAV interacting host factors.

Several host factors have now been reported to interact with TAV (Figure 1.3-4). TAV can interact directly with the 60S ribosomal subunit via multiple r-proteins such as eL24 (Park et al., 2001), L18 (Leh et al., 2000) and L13 (Bureau et al., 2004), and with eIF3 via subunit g (Park et al., 2001). Furthermore, eIF3 complex was found to serve as a bridge between 40S and TAV *in vitro* (Park et al., 2001), indicating the formation of a complex between TAV and the eIF3-bound 40S ribosomal subunit. More recently, two new TAV interacting partners were identified and characterized: the 45 kDa reinitiation-supporting factor, RISP (Thiébeauld et al., 2009), and TOR kinase (Schepetilnikov et al., 2011). As it can be seen in Figure 1.3-4, while TOR and RISP associates within the minimal domain of TAV (MAV domain), eIF3g and r-protein eL24 bind the multiple binding domain (MBD), and these two TAV domains were shown to be essential for TAV-mediated transactivation (Park et al., 2001; De Tapia et al., 1993). A novel putative reinitiation/initiation factor called RISP promotes TAV functions in reinitiation as well (Thiébeauld et al., 2009). The TAV and RISP interacting networks are quite similar, thus it has been proposed that RISP plays the role of a TAV cofactor, whereby both can associate with the 60S ribosomal subunit via the same 60S r-protein eL24 and eIF3 (Thiébeauld et al., 2009). As it can be seen in Figure 1.3-4, RISP binds the C-terminal α helix of eL24, while TAV binds the eL24 N-terminal domain. On the other hand, RISP and TAV binding to eIF3 occurs via distinct subunits. The a and c eIF3 subunits are responsible for binding to RISP, while eIF3 g subunit interacts to TAV. Finally, mutations abolishing mutual interaction between TAV and RISP negatively affect, or even abolish, transactivation and viral amplification. Despite the

observation of synergy between TAV and RISP in promoting reinitiation after long ORF translation, no bicistronic-reporter signal enhancement is observed with RISP alone (Thiébeauld et al., 2009).

In addition, new insights about the role of other TOR/S6K1 downstream targets in translation reinitiation have been unveiled by Schepetilnikov et al. in 2011 and 2013. First, in 2011, Schepetilnikov et al. showed that TOR/S6K1 signaling pathway plays a role in CaMV-activated reinitiation after long ORF translation. Virus accumulation triggers TOR activation as manifested by phosphorylation of S6K1 at TOR specific T499. To activate TOR the complex formation between TAV and TOR is required. What are TOR downstream targets in virus-activated reinitiation? TOR, when activated by TAV triggers phosphorylation of RISP at Ser267, a novel downstream target of the TOR/S6K1 signaling pathway. In *Arabidopsis* plants transgenic on TAV or TAV mutant lacking the TOR binding site RISP accumulates in polyribosomes either highly phosphorylated or nonphosphorylated, respectively, strongly suggesting that TOR is required to maintain high phosphorylation status of RPFs during the translation event.

Moreover, in 2013, Schepetilnikov et al. uncovered the role of the TOR/S6K1 signalling pathway in promoting reinitiation after uORF translation in *Arabidopsis*. These data show that TOR and S6K1 contribute to assembly of reinitiation-competent ribosomes in response to auxin. It has been suggested that TOR functions in reinitiation via maintenance of the eIF3h phosphorylation status in polysomes. Thus eIF3h is another downstream target of TOR in the reinitiation complex. Indeed, the presence of auxin triggers TOR activation followed by S6K1 phosphorylation at T449 and efficient loading of uORF-mRNAs onto polysomes in a manner sensitive to the TOR inhibitor Torin-1. Torin-1 inhibits TOR activation and thus triggers S6K1 dephosphorylation and its binding to polysomes. In contrast, auxin triggers TOR activation and recruitment of active TOR to polysomes, where TOR phosphorylates S6K1 triggering its dissociation from polysomes for further activation by PDK1. A putative target of TOR/S6K1—eIF3h—is phosphorylated and detected in polysomes in response to auxin. In TOR-deficient plants, polysomes were prebound by inactive S6K1, phosphorylation of eIF3h was impaired and loading of uORF-mRNAs and eIF3h was abolished.

These data suggest that activation of virus-activated polycistronic and uORF-containing mRNA translation in plants is a complex process depending on a dynamic sequence of events that served by the same RPFs and thus may rely on similar strategies.

My aim was to understand the role of RISP and its phosphorylation in promoting the initiation events and dissect the mechanism of RISP function in TC recruitment and/ or 60S loading during initiation and reinitiation with and without TAV.

2. Results

2.1 Article 1: A reinitiation supporting protein (RISP) can interact with eIF2 and the eS6—eL24 ribosomal intersubunit bridge to promote virus-activated translation reinitiation

Eder Mancera-Martínez[1], Joelle Makarian[1], Philippe Hammann[2], Mikhail Schepetilnikov[1] and Lyubov A. Ryabova[1,*]

[1]Institut de Biologie Moléculaire des Plantes du CNRS, Université de Strasbourg, 67084 Strasbourg CEDEX, France
[2]Institut de Biologie Moléculaire et Cellulaire du CNRS, Université de Strasbourg, 67084 Strasbourg CEDEX, France

A reinitiation supporting protein (RISP) can interact with eIF2 and the eS6—eL24 ribosomal intersubunit bridge to promote virus-activated translation reinitiation

Eder Mancera-Martínez[1], Joelle Makarian[1], Philippe Hammann[2], Mikhail Schepetilnikov[1] and Lyubov A. Ryabova[1,*]

[1]Institut de Biologie Moléculaire des Plantes du CNRS, Université de Strasbourg, 67084 Strasbourg CEDEX, France

[2]Institut de Biologie Moléculaire et Cellulaire du CNRS, Université de Strasbourg, 67084 Strasbourg CEDEX, France

*To whom correspondence should be addressed:

lyuba.ryabova@ibmp-cnrs.unistra.fr

Tel: +33 (0)3 67 15 53 31

Fax: +33 (0)3 88 61 44 42

Running title: RISP regulates translation via eIF2 and eS6

Keywords: 60S joining, TOR, S6K1, CaMV, eIF3, gravitropic response

2.1.1 Abstract

A complex arrangement of factors is required to recruit the initiator tRNA (Met-tRNAiMet) and a 60S ribosomal subunit to the 40S ribosomal subunit preinitiation complex (40S PIC) initiating translation. This recruitment is normally strictly limited during reinitiation of translation if factors recruited during the primary translation event are shed from 40S. However, factor retention can occur during short ORF translation, or during long ORF translation if the *Cauliflower mosaic virus* (CaMV) reinitation factor TAV is present. TAV, together with retention of eIF3 and a cellular reinitiation-supporting factor (RISP) on the translating ribosome, mediates activation of the protein kinase TOR (Target of Rapamycin) to maintain ribosome-associated factors in their active phosphorylated state. RISP is a downstream target of TOR and found either within the 43S preinitiation complex (43S PIC), if bound to eIF3, and/or attached to 60S, if phosphorylated by TOR. We show here that RISP interacts physically with subunit β of eukaryotic initiation factor 2 (eIF2β) *in vitro* and *in vivo*. RISP lacking its phosphorylation site (RISP-S267A) binds eIF2β significantly more strongly. Thus RISP may function together with eIF3 in eIF2 recruitment to 43S PIC before being phosphorylated. In contrast, a RISP phosphorylation mimic interacts preferentially with the 40S ribosomal protein eS6. Full-length RISP is required to interact specifically with the eS6 C-terminal alpha helix. Critically, TOR activation up-regulates phosphorylation of both RISP and eS6 at its C-terminus as well as the binding of both factors. Since phosphorylated RISP also associates with the C-terminal α-helix of eL24, it may link both C-terminal tails, forming or stabilizing an intersubunit bridge within 80S. Importantly, eS6-deficient plants are less active in TAV-mediated reinitiation after long ORF translation and are thus less susceptible to CaMV infection. In addition, S6a-knockout plants display defects in root gravitropism typical of TOR-deficient plants as would be expected for TOR downstream targets. It is attractive to propose that eS6 phosphorylation contributes to retention and re-use of 60S during 40S scanning.

2.1.2 Introduction

Translation initiation on most eukaryotic mRNAs begins with loading of the 43S preinitiation complex (43S PIC) at the capped 5'-end prebound with the multisubunit translation initiation factor 4F (eIF4F)—4E, 4G, 4A and 4B—to form a new 48S complex (48S PIC) on the mRNA. The 48S PIC then scans linearly along the mRNA until it encounters the most 5'-proximal AUG codon in a favorable initiation context, where the 60S then joins (Kozak, 1999). In mammals, the 43S PIC is formed through either sequential binding of eIFs 1, 1A, 5 and 3 followed by eIF3-assisted recruitment of a ternary complex (TC, eIF2/GTP/Met-tRNAi^{Met}) to 40S (Sokabe et al., 2012), or binding of a pre-bound multifactor complex consisting of eIFs 1, 1A, 5, 3-TC to 40S (Hinnebusch and Lorsch, 2012). The initiator tRNA, Met-tRNAi^{Met}, is recruited to 40S as a complex with GTP-bound eIF2—a conserved heterotrimer comprised of three subunits: α (a competitive inhibitor of 2B—phosphorylation at Ser51 determines the rate of formation of the translation initiation competent ternary complex), β (binds eIF5, 2B and mRNA), and γ (binds GTP and Met-tRNAi^{Met}). After delivery of Met-tRNAi^{Met} to the AUG codon, codon–anticodon base pairing triggers eIF5-dependent hydrolysis of eIF2-bound GTP and dissociation of eIF2-GDP from the ribosome. The GTPase eIF5B mediates 60S joining to assemble the 80S complex (Pestova et al., 2000). eIF5B dissociates from 80S after hydrolysis of eIF5B-bound GTP (Jackson et al., 2010). The removal of other eIFs seems to occur gradually after 60S joining within a few elongation cycles (Kozak, 2001).

After termination of translation, ribosomes dissociate from the mRNA, except if the first translated upstream ORF (uORF) is less than ~30 codons; in the latter case, ribosomes resume scanning and can reinitiate at a further downstream ORF (Morris and Geballe, 2000). uORFs are highly abundant in mammals and angiosperms, being present in at least 30% of full-length mRNAs (Calvo et al., 2009; Zhou et al., 2010). Many uORF-containing genes, especially in plants, encode potent proteins involved in signal transduction and/or gene regulation (Kawaguchi and Bailey-Serres, 2005). Often, but not always, the presence of a uORF decreases the translation levels of downstream protein-coding mRNAs by triggering dissociation of terminating ribosomes (Ingolia, 2014). The efficiency of reinitiation is constrained by structural features in the mRNA, the size of the uORF, and by the availability of initiation factors (Hinnebusch, 1997; Kozak, 2001). Nevertheless, reinitiation can occur if the complement of canonical initation factors that were involved in promoting primary initiation at the uORF initiation codon remain bound to the ribosome during the short initiation event and thus can resume scanning and reinitiate on the same mRNA. Reinitiation will be either abolished or delayed by the time needed for ribosome

recharging if eIFs necessary for reinitiation are shed from the ribosome. These reinitiation-promoting factors (RPFs) seem to either support resumption of scanning and/or facilitate recruitment of TC and 60S *de novo* at each initiation event on the same mRNA. One such RPF, eIF3, is composed of 13 distinct subunits in humans and plants, and orchestrates assembly of the 43S and 48S preinitiation complexes on mRNA (Burks et al., 2001; Hinnebusch, 2006). In reinitiation, eIF3 can stimulate binding of the ternary complex to the 40S ribosome in mammals, yeast and plants (Cuchalová et al., 2010; Hershey and Merrick, 2000; Munzarova et al., 2011; Park et al., 2001). The RPF function of eIF4F was demonstrated *in vitro* in mammals (Pöyry et al., 2004), and eIF3 non-core subunit h (eIF3h) and the 60S ribosomal eukaryotic protein L24 (eL24) are required for translation of uORF-containing mRNAs (uORF-RNAs) in plants (Kim et al., 2004; Nishimura et al., 2005). Translation reinitiation and auxin-mediated organogenesis in two families of plant transcriptional factors—auxin response factors (ARFs) and basic zipper transcription factors (bZIPs)—are compromised severely by mutations in either eIF3h or eL24 (Kim et al., 2004; Nishimura et al., 2005; Schepetilnikov et al., 2013; Zhou et al., 2010). Yeast eL24, which is implicated in the 60S subunit-joining step during translation initiation (Baronas-Lowell and Warner, 1990; Dresios et al., 2000), together with the eukaryotic 40S ribosomal protein S6 (eS6), forms a bridge point between the yeast 40S and 60S ribosomal subunits (Anger et al., 2013; Armache et al., 2010; Ben-Shem et al., 2011), which is another indication for eL24 and eS6 function in 60S joining.

Recent data have revealed that reinitiation after translation of a short uORF in plants depends on the large serine/threonine protein kinase TOR (Target of Rapamycin, (Schepetilnikov et al., 2013). TOR is a critical sensor of nutritional and cellular energy sufficiency and a main regulator of cell growth (Gingras et al., 2001; Senguptaet al., 2010; Dobrenel et al., 2011). In plants, TOR initiates phosphorylation of ribosomal protein S6 kinase 1 (S6K1) at TOR-specific T449, resulting in the formation of a binding site for phosphoinositide-dependent kinase 1 (PDK1), which completes activation of S6K1 (Ma and Blenis, 2009). When activated by the phytohormone auxin, TOR phosphorylates its downstream target eIF3h at Ser178, triggering subunit h activation and thus translation of uORF-mRNAs via an as yet unknown mechanism (Schepetilnikov et al., 2013).

Plant pararetroviruses have to modify the cell translation apparatus to effect translation of several ORFs from the same pregenomic RNA via reinitiation (virus-induced reinitiation; Ryabova et al., 2006). The first, and best studied, example of viral transactivation of repeated initiation events occurs on the polycistronic pregenomic 35S RNA (35S pgRNA) of *Cauliflower*

mosaic virus (CaMV; Futterer et al., 1990; Ryabova et al., 2006). The CaMV protein translational transactivator/viroplasmin (TAV)—a single protein mainly produced from the 19S subgenomic RNA—is sufficient to deregulate the cellular translation machinery towards reinitiation. To promote reinitiation after long ORF translation, TAV interacts with several host factors to form a reinitiation complex—eIF3, the reinitiation supporting protein (RISP) and eL24—that allows this complex to travel with elongating ribosomes through the long ORF, thus ensuring regeneration of reinitiation-competent ribosomal complexes after translation termination (Park et al., 2001; Thiébeauld et al., 2009). Retention in polyribosomes (polysomes) of eIF3 and RISP after the long elongation event is supported by their high accumulation in polyribosomes in the presence of TAV (Schepetilnikov et al., 2011).

The finding that TAV interacts with TOR and promotes TOR signaling activation by an as yet unknown mechanism is striking (Schepetilnikov et al., 2011). In addition to eIF3h, RISP is another TOR downstream target among RPFs; TOR-responsive RISP phosphorylation at Ser267 by S6K1 strongly promotes TAV-mediated transactivation (Schepetilnikov et al., 2011). The function of TOR in reinitiation seems to be to maintain the high phosphorylation status of RISP and eIF3h in polyribosomes (Schepetilnikov et al., 2011, 2013). Another intriguing finding is that 60S is involved in intensive interactions with the reinitiation complex—two ribosomal proteins at the exposed side of 60S, L18 and L13 can bind TAV *in vitro* (Leh et al., 2000; Bureau et al., 2004; respectively), but eL24 interacts both with TAV via its N-terminus, and with RISP via its C-terminus, strongly indicating complex formation on the 60S interface, especially taking into account the interaction between TAV and RISP. RISP alone can serve as a scaffold protein that is able to interact with eIF3 via subunits a/c, 40S (if RISP is already paired with eIF3), and 60S via the C-terminus of ribosomal protein eL24, suggesting that it has its own function in initiation of translation (Thiébeauld et al., 2009). *In vivo*, RISP is co-immunoprecipitated not only with eIF3 and 40S, but also with eIF2α, strongly suggesting that RISP can be part of the 43S PIC. In contrast, RISP is found in the 60S ribosomal fraction from wheat germ, and is co-localized with a 60S fraction in BY-2 cells, suggesting that RISP can also be part of 60S-containing complexes (Thiébeauld et al., 2009).

Here, we report two novel interactions of RISP that help it to achieve its functions within the 43S preinitiation complex and on 60S to promote TC recruitment and 60S recycling. Due to its extensive coiled-coil structural domains, RISP interacts with either eIF2 or the eS6-eL24 intersubunit bridge in a dynamic order of events depending on RISP and eS6 phosphorylation status. Therefore, our results are compatible with the idea that, in plants, RISP can affect

translation initiation and reinitiation within two distinct initiation complexes—the 43S PIC through eIF3 and eIF2 to ensure eIF2 recruitment, and eS6 and eL24 interactions within 80S to promote 60S recycling during repeated reinitiation events.

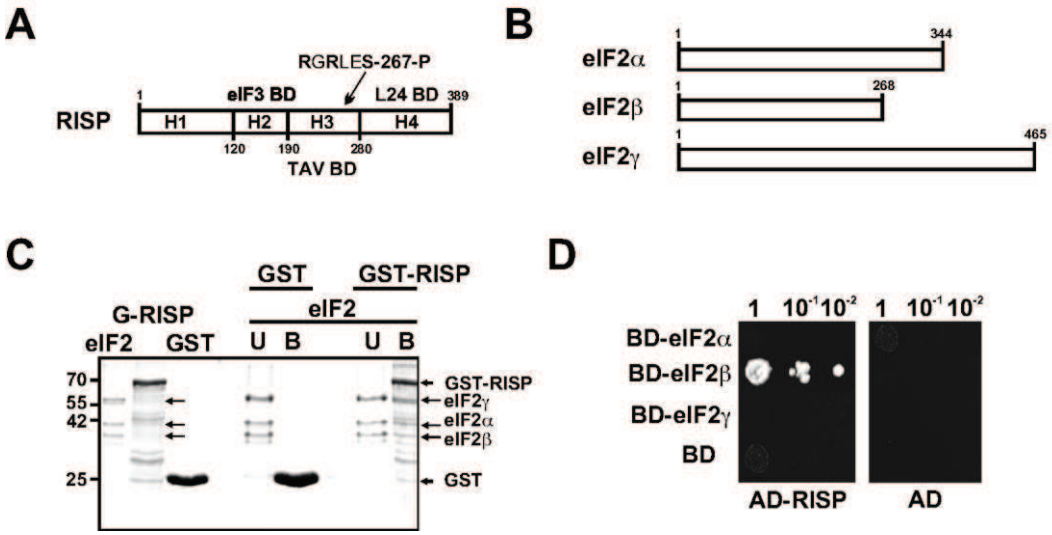

Figure 2.1-1 | **RISP binds wheat germ eIF2**

(**A**) Schematic representation of RISP. Alpha helical domains H1-H4, and the phosphorylation site Ser267 are indicated. eIF3, TAV and eL24 binding domains are shown. (**B**) Schematic presentation of Arabidopsis eIF2 subunits α, β and γ. (**C**) GST, GST-RISP were overexpressed in E. coli and purified by affinity chromatography; eIF2 was purified from wheat germ. The left panel of the gel shows the purified components. For the pull-down experiments, GST and GST-RISP were bound to glutathione beads and incubated with the eIF2 to be tested. The beads were then washed and the unbound (U) and bound (B) fractions assayed by SDS-PAGE and stained with Coomassie blue. (**D**) Yeast two-hybrid interactions between Gal4 binding domain (BD) fused to each subunit of eIF2 (BD-eIF2α, BD-eIF2β and BD-eIF2γ) and AD-RISP.

2.1.3 Results

RISP interacts with eIF2 via its subunit ß

In order to find out how RISP (see Figure 2.1-1A for a schematic representation) might support repeated reinitiation events on the same mRNA (Thiébeauld et al., 2009; Schepetilnikov et al., 2011), we tested its possible involvement in recruitment of the eIF2-containing ternary complex to 40S *de novo*. Because our earlier data pointed to *in planta* complex formation between eIF3 and RISP and the involvement of eIF3 in the ability of RISP to bind the 40S ribosomal subunit *in vitro* (Thiébeauld et al., 2009), we tested the possibility that RISP is the part of the 43S PIC with which eIF2 interacts directly.

To test this hypothesis, RISP was purified in *E. coli* and assayed for interaction with the entire eIF2 complex isolated from wheat germ extract using a GST-pull down assay. All three eIF2 subunits (α, β and γ Figure 2.1-1B) were present in the bound fraction after incubation with GST-RISP, but not in the unbound fraction after incubation with GST alone (Fig. Figure 2.1-1C). Next, we assayed the capacity of each eIF2 subunit in interaction with RISP using the yeast two-hybrid assay (Figure 2.1-1D). Only subunit β fused to Gal4 binding domain (BD) interacted strongly with AD-RISP, while α and γ were inactive, suggesting that subunit β is primarily responsible for eIF2 binding.

A 3D model of *Arabidopsis* RISP, generated by PyMOL (Sali et al., 1995), revealed four parts, each characterized by a coiled-coil structure predicted with high probability by computer analysis (helices H1–H4; Figure 2.1-2A; Schepetilnikov et al., 2011). The 3D structure of archaebacterial aIF2β shows possible folding of the conserved C-terminal half of the plant subunit (aa 114–268; Figure 2.1-2B). RISP and eIF2β truncation and deletion mutants fused to the Gal4 activation (AD) or binding (BD) domain, respectively, shown in Figure 2.1-2C and D (left panels), were tested to delineate regions important for binding. The N-terminal part of RISP (aa 1–190) binds eIF2β strongly, while the C-terminal part (aa 190–389) was inactive (Figure 2.1-2C). The binding activity was stronger between eIF2β and a RISP lacking H1, but an internal deletion of H2 (aa 120–190) abolished RISP binding to eIF2β (Figure 2.1-2B). Thus, RISP domain H2 seems to be a key contact for eIF2 subunit β and, as previously shown, eIF3 subunits a/c (Thiébeauld et al., 2009).

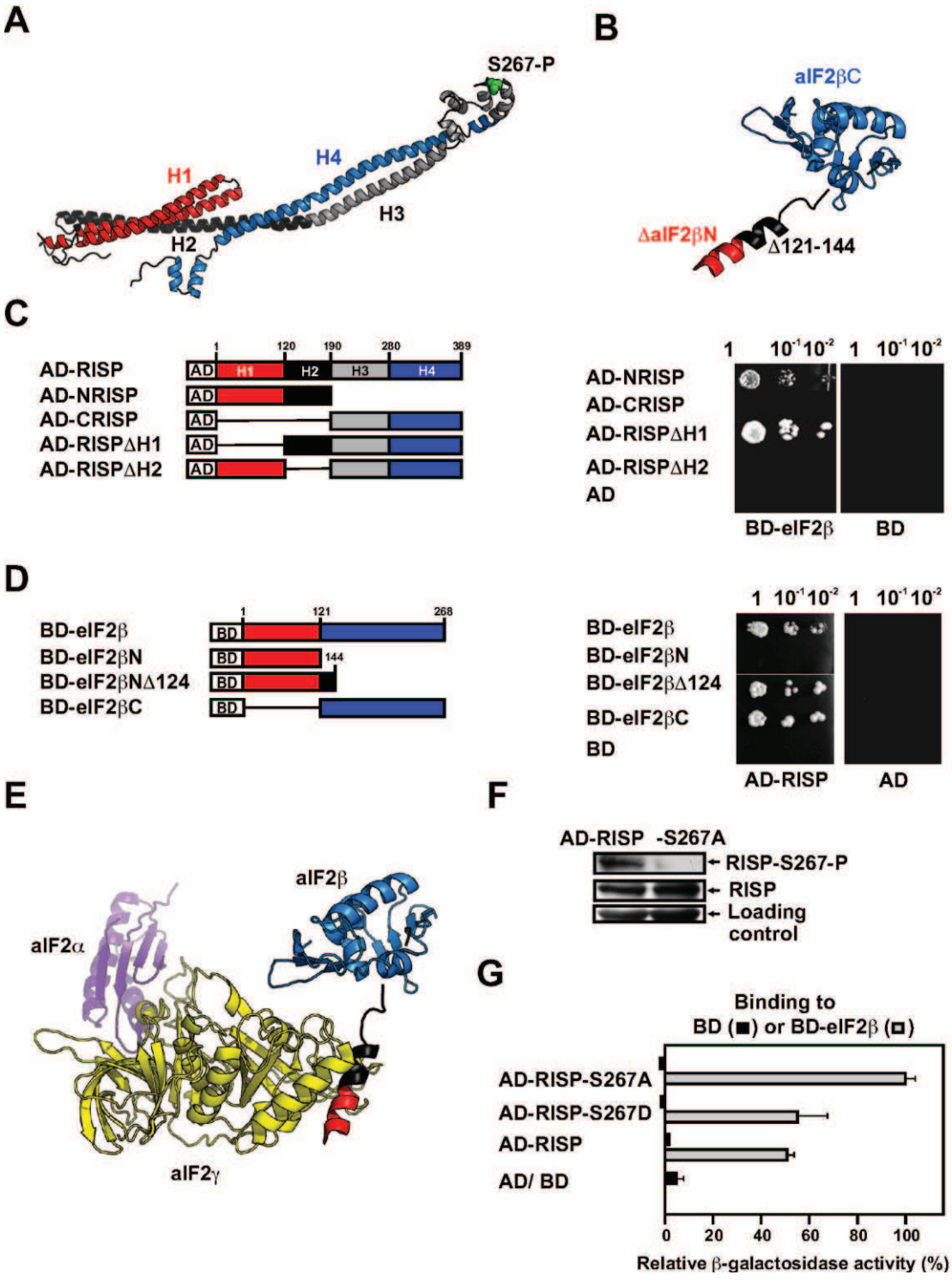
A
S267-P
H1
H4
H3
H2
B
aIF2βC
ΔaIF2βN
Δ121-144
C
AD-RISP
AD-NRISP
AD-CRISP
AD-RISPΔH1
AD-RISPΔH2
AD
H1
H2
H3
H4
1
120
190
280
389
AD-NRISP
AD-CRISP
AD-RISPΔH1
AD-RISPΔH2
AD
BD-eIF2β
BD
D
BD-eIF2β
BD-eIF2βN
BD-eIF2βΔ124
BD-eIF2βC
BD
1
121
268
144
BD-eIF2β
BD-eIF2βN
BD-eIF2βC
BD-eIF2βΔ124
BD
AD-RISP
AD
E
aIF2α
aIF2β
aIF2γ
F
AD-RISP -S267A
RISP-S267-P
RISP
Loading control
G
Binding to BD (■) or BD-eIF2β (□)
AD-RISP-S267A
AD-RISP-S267D
AD-RISP
AD/ BD
0
20
40
60
80
100
Relative β-galactosidase activity (%)

Figure 2.1-2 | **Mapping of RISP and eIF2β interacting regions**

(**A**) The putative *At*RISP 3D-structure was generated by PyMOL. The Ser267-P position within the conserved loop is highlighted in green. Color code: *red* N-terminal Helix 1, H1; *black* H2 helix; *grey* H3 helix; *blue* H4 helix. (**B**) The archaeal eIF2β 3D-structure resembles the part of the central and the C-terminal half of *At*eIF2β (114-268; PDB number: 2QMU; Yatime et al., 2007). Color code: *blue* C-terminal domain of aIF2 β homologous to that of *At*eIF2βC; *black* central helix that is homologous to fragment *At*eIF2β (aa 121-144); *red* fragment homologous to the *At*eIF2β N-terminal fragment. (**C**) *left panel* Schematic representation of *Arabidopsis* AD-RISP and its four fragments designated as helices I-IV fused to AD. The colored boxes indicate structural domains as in (A). *right panel* Yeast two-hybrid interactions between BD-eIF2β and RISP deletion mutants fused to BD. Equal OD_{600} units and 1/10 and 1/100 dilutions were used for one experiment. (**D**) *left panel* Schematic representation of *Arabidopsis* BD-eIF2β and its fragments fused to BD. Color code: *red* N-terminal domain of eIF2β; *black* central helix (aa 121-144); *blue* C-terminus. *right panel* Yeast two-hybrid interactions between AD-RISP, BD-eIF2β, and eIF2β deletion mutants fused to BD. (**E**) The archaeal aIF2 structure (Yatime et al., 2007). Color code: *blue* subunit β C-terminus; *black* central alpha helix of subunit β; *red* the N-terminal fragment of aIF2β; *yellow* γ; *pink* α. (**F**) Immunoblot analysis of RISP accumulation levels or its phosphorylation in yeast transformed with either pAD-RISP or pAD-RISP-S267A. (**G**) Yeast two-hybrid interactions between BD-eIF2β and AD-RISP phosphorylation mutants. Quantification of interactions between either RISP or RISP-S267A or RISP-Ser267-D fused to Gal4 AD and BD-eIF2β. Results represent the mean values from triplicates +/- standard deviation. Interactions were scored by measuring β-galactosidase activity in liquid assay. The highest value of β-galactosidase activity in the yeast transformed with the AD-RISP-S267A constructs is set to 100%.

eIF2βC binds RISP as strongly as full-length eIF2β, while the N-terminus (aa 1–121) does not (Figure 2.1-2D). However, elongation of the eIF2β N-terminal fragment by an additional 23 aa (aa 1–144; eIF2βNΔ124) restored the interaction, suggesting that a segment spanning residues 121–144 is strictly required for RISP binding (Figure 2.1-2D). On the 3D structure of archaebacterial aIF2 (Figure 2.1-2E) the N-terminal alpha helix shown in black probably corresponds to this putative RISP binding fragment (aa 121–144).

eIF2 interacts preferentially with unphosphorylated RISP

Strikingly, S6K1 and apparently RISP manoeuvre on and off the eIF3-containing initiation complex in a TOR signal-dependent manner (Holz et al., 2005; Schepetilnikov et al., 2011). Indeed, phosphorylation of RISP seems to regulate its interaction with eIF3 and the 60S ribosomal protein eL24—when inactive, RISP associates preferentially with eIF3, while TOR activation followed by RISP phosphorylation at Ser267 results in preferential RISP binding to eL24 (Schepetilnikov et al., 2011). These data suggest a sequential order of events in RISP binding controlled by TOR.

Here, we tested if the phosphorylation knockout RISP mutant (RISP-S267A) or its mimic (RISP-S267D) have different capacities to interact with eIF2β using the yeast two-hybrid quantitative β-galactisidase assay. Normally, RISP is highly phosphorylated upon overexpression in yeast two-hybrid extracts (Figure 2.1-2F). As shown in Figure 2.1-2G, the phosphorylation

inactive mutant of RISP (RISP-S267A) has a reproducibly stronger interaction with eIF2β than wild type RISP or its phosphorylation mimic RISP-S267D. Thus non-phosphorylated RISP is preferentially required to interact with both eIF3 and eIF2 apparently within 43S PIC, suggesting that RISP phosphorylation instead triggers its dissociation from 43S PIC.

RISP phosphorylated at Ser267 interacts with the eS6 C-terminal alpha helix

The data presented above provide evidence that RISP, when not phosphorylated, governs its binding to eIF2 and eIF3 within preinitiation complexes. However, TOR-mediated RISP phosphorylation favors RISP translocation towards 60S via association with the C-terminus of eL24 (Schepetilnikov et al., 2011), which is positioned on 60S very close to the 60S main factor-binding site. Strikingly, a recent 3D structure of *S. cerevisiae* 80S revealed that 60S-bound eL24 and the 40S-bound ribosomal protein eS6 form an inter-subunit bridge via their C-terminal tails and may interact (Ben-Shem et al., 2011). Strikingly, the eL24 N-terminal domain—the CaMV TAV binding site—is bound to the interface of 60S, while the C-terminal α-helix—the RISP binding site—protrudes out of 60S towards 40S ribosomal protein eS6 (Reinhardt et al., 2003); 40S-bound eS6 3D structure is shown in Figure 2.1-3A) thus raising the possibility that RISP may interfere with the formation of such a bridge.

After all our attempts to reveal direct interaction between eL24 and eS6 failed, we tested if RISP can provide additional contacts between eL24 and eS6 using the yeast two-hybrid system. Although AD-RISP interacts strongly with BD-S6 under our yeast two-hybrid system conditions, none of the RISP fragments assayed interacted with full-length eS6 (Figure 2.1-3B), probably indicating the critical importance of RISP tertiary structure for this interaction.

Taking advantage of the known 3D conformation of ribosome-bound eS6 (Ben-Shem et al., 2011), eS6 was dissected into three fragments (Figure 2.1-3A), and mapping of their interaction with RISP was first assayed in the yeast two-hybrid system (Figure 2.1-3C). Surprisingly, two fragments of eS6—the central fragment, MS6 (aa 83–177) and the C-terminal alpha-helix, CS6 (aa 177–249) bind RISP as strongly as a full-length protein (cf Figure 2.1-3B and C). However, the longer C-terminal fragment of eS6, ICS6 (aa 130–249) failed to interact, indicating that RISP binding is precluded by inserting the 47 aa fragment (which may display binding to CS6 in solution) instead of binding to rRNA on the 40S ribosomal subunit. Although both CS6 and MS6 seem to interact with RISP, we hypothesized that MS6 may participate in stabilization of the CS6 interaction with RISP and concentrated on studying the CS6 interaction network. The interaction between RISP and CS6 was confirmed in a GST-pull down assay using

GST-CS6 and RISP (Figure 2.1-3D)—RISP was present in the bound fraction after incubation with GST-CS6, and in the unbound fraction after incubation with GST alone, indicating no interaction.

RISP is phosphorylated at Ser267 within the motif RGRLES^{267}—a pattern found in many Akt or S6K1 substrates (R/KxR/KxxS/T)—in a TOR-sensitive manner (Schepetilnikov et al., 2011). Therefore, we analysed whether the S267A or S267D mutations of RISP would alter complex formation between RISP and CS6 in the yeast two-hybrid system. Figure 2.1-3E demonstrates that wild type RISP and the phosphorylation active mutant of RISP (RISP-S267D) interact reproducibly more strongly with CS6 than the RISP phosphorylation inactive mutant, RISP-S267A. These results suggest that phosphorylation of RISP might favour its interactions with 40S-bound eS6 and 60S-bound eL24 via their C-terminal alpha helixes, since both are accessible from the solvent side (Ben-Shem et al., 2011).

Phosphorylated RISP interacts preferentially with phosphorylated eS6

Mass spectrometry analysis indicated several significant well-conserved phosphorylation sites within the C-terminal tail of eS6: Ser231, Ser237 and Ser240 (Figure 2.1-4A; Boex-Fontvieille et al., 2013). Strikingly, seedlings treated with auxin to increase active TOR and thus active S6K1 levels (Schepetilnikov et al., 2011) display phosphorylation at Ser231, Ser237 and Ser240 sites according to our phosphoproteomic MS-MS analysis (see below). Interestingly, two of these sites are characterized by a partial pattern found in many plant S6K1 substrates (Ser231, DRRSES and Ser237, LAKKRS) that can support phosphorylation within these sites by S6K1 (Figure 2.1-4A). Strikingly, corresponding sites within mammalian eS6 are characterized by the perfect S6K1 phosphorylation context—Ser235 and Ser236. Thus, we prepared several phosphorylation knockout and mimic mutants corresponding to Ser231, Ser237 and Ser240 and tested their effect on interaction capacity of full-length eS6 and the eS6 C-terminus with either WT RISP or RISP-S267D (Figure 2.1-4B and C, respectively).

Overall, RISP or RISP-S267D have reproducibly stronger interactions with CS6 phosphorylation mimic mutants (Figure 2.1-4B-C). Not surprisingly, full-length eS6 and its phosphorylation mutants are not efficient in RISP binding (Figure 2.1-4B, left panel), probably due to differences in eS6 folding on the ribosome and in solution. Surprisingly, WT CS6 is less efficient than its phosphorylation mimics in either RISP or RISP-S267D binding, which may indicate hierarchical phosphorylation of CS6 in yeast, and would definitely require complementary testing of these mutations *in planta*.

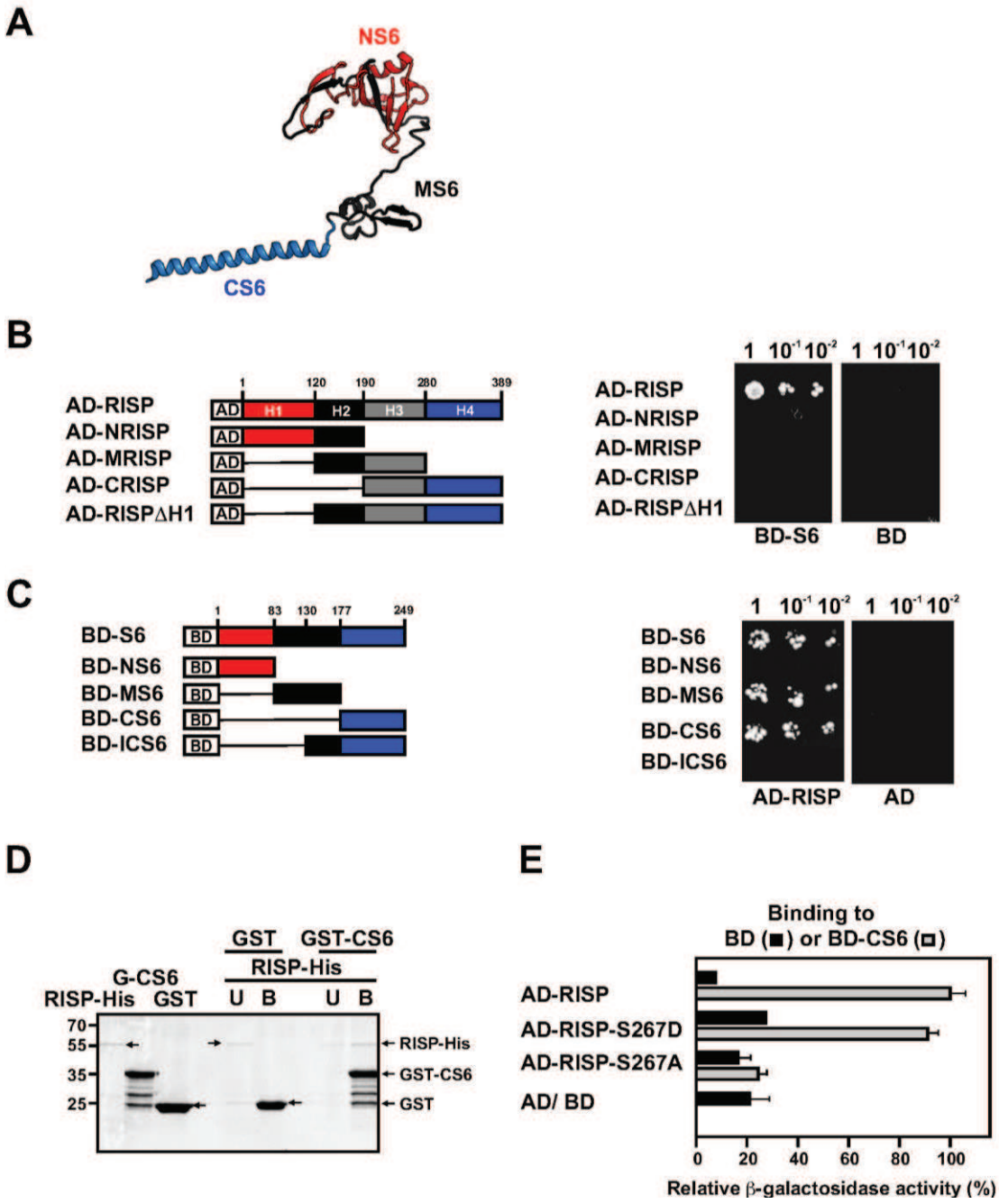

Figure 2.1-3 | **Mapping of RISP and eS6 interacting regions**

(**A**) Structure of *S. cerevisiae* ribosomal protein eS6 on the 40S ribosomal subunit (Ben-Shem et al., 2011). Color code: *red* N-terminus; *black* central fragment; *blue* C-terminal helix. (**B**) *left panel* Schematic representation of *Arabidopsis* BD-S6 and AD-RISP and its deletion mutants fused to AD. The colored boxes indicate structural domains as in Fig. 2A. *right panel* Yeast two-hybrid interactions between BD-S6 and AD-RISP and its deletion mutants fused to AD. Equal OD_{600} units and 1/10 and 1/100 dilutions were used for one experiment. (**C**) *left panel* Schematic representation of *Arabidopsis* eS6 and its fragments fused to BD. Color code: *red* N-terminal domain of eS6; *black* central domain; *blue* C-terminus;. *right panel* Yeast two-hybrid interactions between AD-RISP, BD-S6, and eS6 fragments fused to BD. (**D**) GST, GST fused to the eS6 C-terminus (CS6) and RISP-His were overexpressed in *E. coli* and purified by affinity chromatography. The left panel of the gel shows the purified components. For the pull-down experiments, GST and GST-CS6 were bound to glutathione beads and incubated with the RISP-His to be tested. The beads were then washed and the unbound (U) and bound (B) fractions assayed by SDS-PAGE and stained with Coomassie blue. (**E**) Quantification of interactions between either RISP or RISP-S267A or RISP-S267D fused to Gal4 AD and BD-CS6. Results represent the mean values from triplicates +/- standard deviation. Interactions were scored by measuring β-galactosidase activity in liquid assay. The highest value of β-galactosidase activity in the yeast transformed with the AD-RISP constructs is set to 100%.

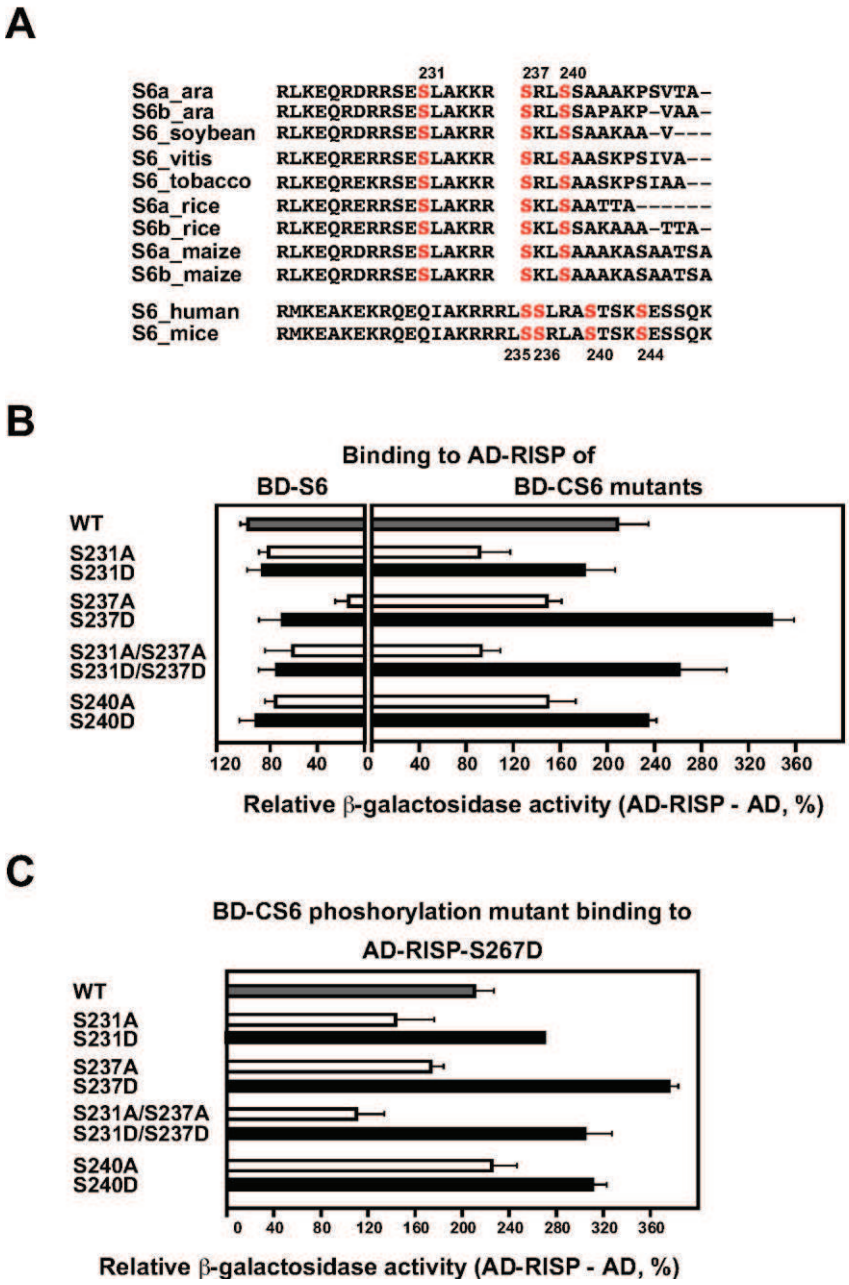

Figure 2.1-4 | **Interactions between RISP and the C-terminal helix of eS6 are controlled by each protein's phosphorylation status**

(**A**) Alignment of the C-terminal eS6 domains from eS6 homologues. Three plant Ser phosphorylation sites (Ser231, Ser237 and Ser240 at the top) and four sites in human eS6 (Ser235, Ser236, Ser240 and Ser244; at the bottom) are shown in red.(**B**) Yeast two-hybrid interactions between AD-RISP and BD-S6 or BD-CS6 phosphorylation mimic and knockout mutants. Quantification of interactions between AD-RISP and BD-S6 or BD-CS6 phosphorylation mutants. Interactions were scored by measuring β-galactosidase activity in liquid assay. Results represent the mean values from triplicates +/- standard deviation. The highest value of β-galactosidase activity in the yeast transformed with the wild BD-S6 (left panel) is set to 100%. (**C**) Quantification of interactions between AD-RISP-S267D and BD-CS6 or CS6 phosphorylation mutants fused to BD. Results represent the mean values from triplicates +/- standard deviation. The highest value of β-galactosidase activity in the yeast transformed with the wild BD-S6 (in B) is set to 100%.

Our data support the hypothesis that *Arabidopsis* TOR, and thus S6K1, activation triggers phosphorylation of RISP and its relocation on 60S-bound eL24. Thus, phosphorylation of 40S-bound eS6 at the C-terminal alpha helix might tighten the association between 60S and 40S and, for example, promote retention or recruiment of 60S on the mRNA for a reinitiation event rather than interfere with a ligand binding to the ribosome during the elongation phase of translation.

eS6a knockout plants are deficient in supporting CaMV infection and TAV-mediated transactivation of reinitiation

The regulated phosphorylation of the ribosomal protein eS6 has attracted much attention, yet its physiological role has remained obscure. However, viable and fertile knock-in mice, whose eS6 contains alanine substitutions at all five phosphorylatable serine residues [*rpS6(P-/-)*], display an increased rate of protein synthesis and are characterized by significantly smaller cells than those of *rpS6(P+/+)* mutants, reflecting a growth defect (Ruvinsky et al., 2005).

Although eS6-mediated defects in translation or translational control have not been reported in mammals and plants, we decided to test if eS6 defects would interfere with the reinitiation capacity of eukaryotic cells. Up-regulation by CaMV TAV of these strictly prohibited repeated reinitiation events might be less powerful in plants lacking, or deficient in, eS6.

Thus, we focused our *in planta* study on the two *RPS6* genes, *RPS6A* and *RPS6B*. Knock-out of both genes is lethal; however, we took advantage of two existing RPS6 knock-out *Arabidopsis* lines; *rps6a* and *rps6b* are single mutants that, together with the double heterozygous *RPS6A/rps6a*, *RPS6B/rps6b* plants, confer a slow growth phenotype, reduced leaf size and delayed flowering time (Creff et al., 2010). First, we compared the level of eS6 accumulation in *rps6a* and *rps6b* single mutants with that in WT plants (Figure 2.1-5A). The level of eS6 was reduced by about five-fold in *rps6b* and at least ten-fold in *rps6a* mutant plants. Accordingly, the *rps6a* mutant has slightly more elongated and pointed leaves (Figure 2.1-5B, upper panels).

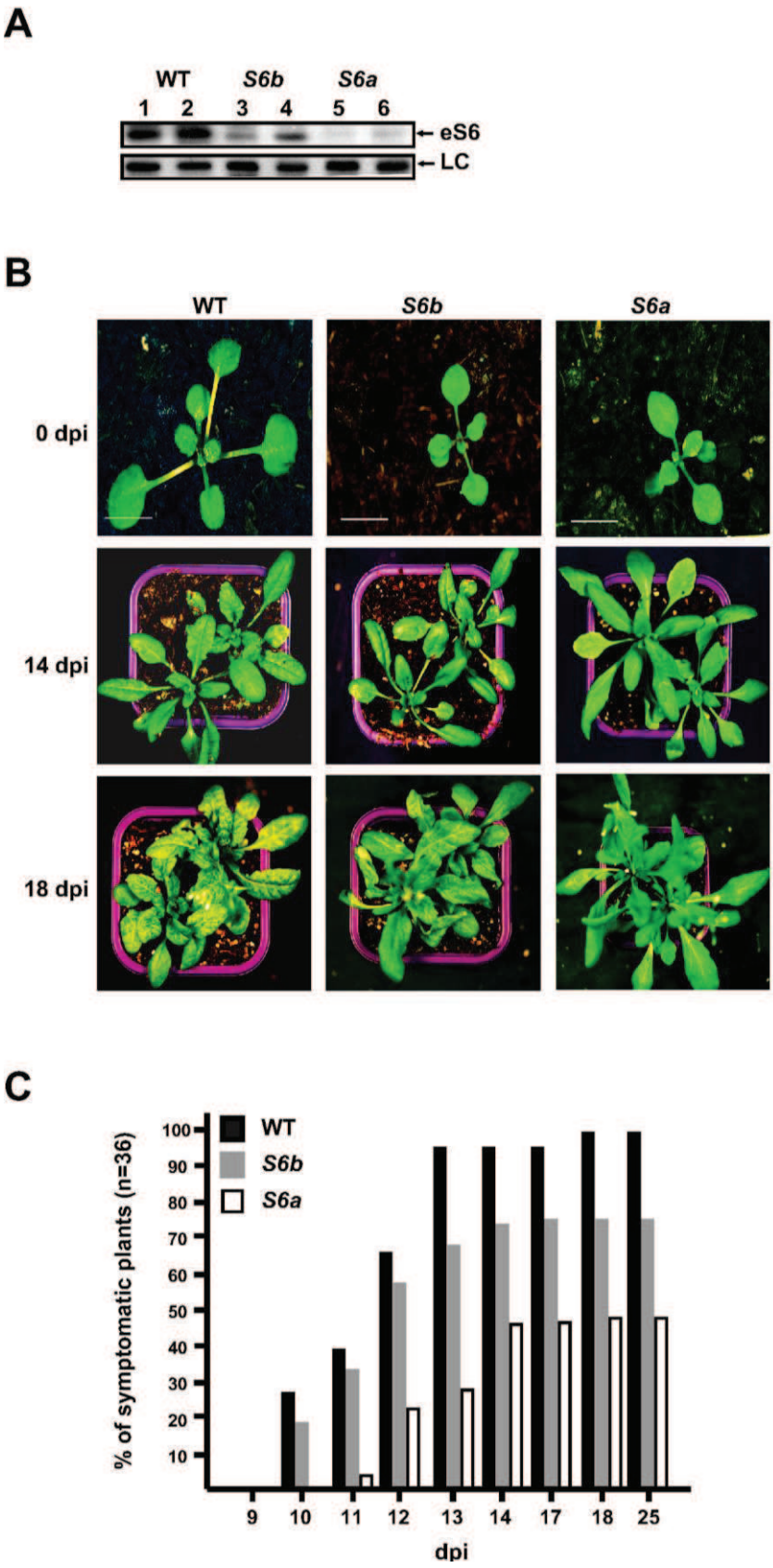

Figure 2.1-5 | CaMV symptom appearance is delayed in *S6a* knockout *Arabidopsis* plants

(**A**) eS6 protein levels in wild type, *S6a* and *S6b* knockout *Arabidopsis* plants. eS6 expression levels were analyzed by immunoblot.(**B**) CaMV symptom appearance in WT, *s6b* and *s6a Arabidopsis* plants at 0, 14, 18 dpi. The *S6a* knockout plant without symptoms up to 18 dpi is shown. (**C**) Kinetics of symptom appearance in WT and eS6-deficient plants.

To test whether CaMV indeed recruits eS6 to overcome cell resistance, we studied susceptibility to CaMV infection of WT, *rps6a* and *rps6b* mutant plants. The appearance of symptoms (Figure 2.1-5B and C) and virus replication kinetics Figure 2.1-6B in wild type and mutant plants agroinfiltrated with a CaMV infectious clone were compared in two independent experiments. Of 36 WT or *rps6a* or *rps6b* plants tested, 100% of WT, 80% of *rps6b* and 50% of *rps6a* plants were infected (Figure 2.1-5C). Although symptom appearance was strong in wild-type plants (typical vein-clearing symptoms indicative of systemic infection) and moderate in *rps6b* plants at 10 dpi, *rps6a* plants started to display symptoms only at 12 dpi (Figure 2.1-5C). Strikingly, 50% of *rps6a* plants displayed no signs of infection, the remainder displaying mild symptoms up to 25 dpi, suggesting some resistance of *rps6a* plants to CaMV infection.

Viral replication in each mutant plant was monitored and compared to that in WT plants (Figure 2.1-6A-B). TAV and viral coat protein (CP) accumulation was first observed at 10 dpi for the majority of WT plants and at 14 dpi on average for *rps6b* mutant plants according to our Western blot results. 50% of *rps6a* plants displayed neither symptoms nor accumulation of TAV and CP (S6a NI), with the remaining 50% of infected *rps6a* plants characterized by mild symptoms up to 22 dpi (see Figure 2.1-6A, the S6a I plant) and appearance of TAV and CP only at 18 dpi (Figure 2.1-6B, S6a I panel). These results strongly suggest significant down-regulation of CaMV replication in plants lacking one isoform of eS6. We concluded that this partial resistance to CaMV is due to low eS6 availability limiting viral replication in *Arabidopsis* plants.

To investigate this replication defect further, we next tested if these *rps6a* knockout plants are able to support TAV-mediated transactivation in mesophyll protoplasts. Protoplasts were prepared from wild type and *rps6a* mutant plants and transformed with two reporter plasmids: p*monoGFP*, containing a single GFP ORF [initiation at GFP ORF proceeds via cap-independent mechanism (Zeenko and Gallie, 2005); control for transformation efficiency], and either p*monoGUS* with GUS (β-glucuronidase) as a marker of cap-dependent translation initiation efficiency, or p*biGUS* containing two consecutive ORFs: CaMV ORF VII and GUS (Bonneville et al., 1989), where GUS serves as a marker of transactivation (Figure 2.1-6C). In addition, plants were co-transformed with reporter plasmids encoding TAV. Surprisingly, upon transfection of protoplasts with *pmonoGFP* and *pmonoGUS*, the *monoGUS* construct produced GUS activity reproducibly 1.5-fold higher in *rps6a* than in WT protoplasts (Figure 2.1-6D, lanes 1 and 4), indicating that removal of eS6 positively affects expression rates.

The biGUS construct did not give rise to any significant GUS activity without TAV (Figure 2.1-6D, lanes 2 and 5), indicating that OFRVII is intact and suppresses reinitiation at the GUS

ORF. Transient expression of GUS was activated only upon co-transfection with the pTAV vector (Figure 2.1-6D, lanes 3 and 6). In contrast to *monoGUS* translation, protoplasts prepared from *rps6a* plants had reproducibly lowered capacity to mediate reinitiation of the downstream GUS ORF in the presence of TAV—at least two-fold reduction was detected—while GFP internal translation initiation was largely unaffected. *biGUS* RNA transcript length and levels were monitored by semiquantitative RT-PCR (Figure 2.1-6D, bottom panel). Based on these results, we conclude that S6 has a positive effect on TAV function in reinitiation after long ORF translation.

eS6 mutant plants display defects in root gravitropic responses

Our results thus far suggest that the TOR downstream target eS6 belongs to reinitiation supporting factors that include TOR and its downstream target eIF3h—both critically required for reinitiation after short ORF translation; both eS6 (this study) and eIF3h (unpublished data of J. Makarian and L. Ryabova) promote virus-activated reinitiation after long ORF translation. The fact that TOR-deficient and eIF3h knockout plants (*TOR RNAi* and *eif3h-1*, respectively) display strong defects in root gravitropism (Schepetilnikov et al., 2013) raises the possibility that our eS6 mutants could mediate the link between TOR signaling and root gravitropic response.

After 6 days of growth [days after germination (dag)], root development for *rps6a*, *rps6a*/+, *rps6b*/+ and the *rps6b* mutants was delayed, with *rps6a* mutant growth most significantly affected (Figure 2.1-7A; Creff et al., 2010). Gravitropic defects were seen mainly in *rps6a* after 24 hours of 90° gravity stimulation (bigger bending angle; Figure 2.1-7B). Strikingly, at 8 dag, *rps6a*/+, *rps6b*/+ and *rps6a* seedlings grown for 24 h on agar plates lost gravity perception after turning the seedlings through 90°, showing no bending angle (*rps6a*/+, *rps6b*/+ and *rps6b*; drawn schematically in Figure 2.1-7C). These results indicate that, being downstream of TOR, eS6 may exert its effects on gravity sensing by triggering translation reinitiation of mRNAs that encode members of the ARF family, and thus auxin-responsive gene expression (Schepetilnikov et al., 2013).

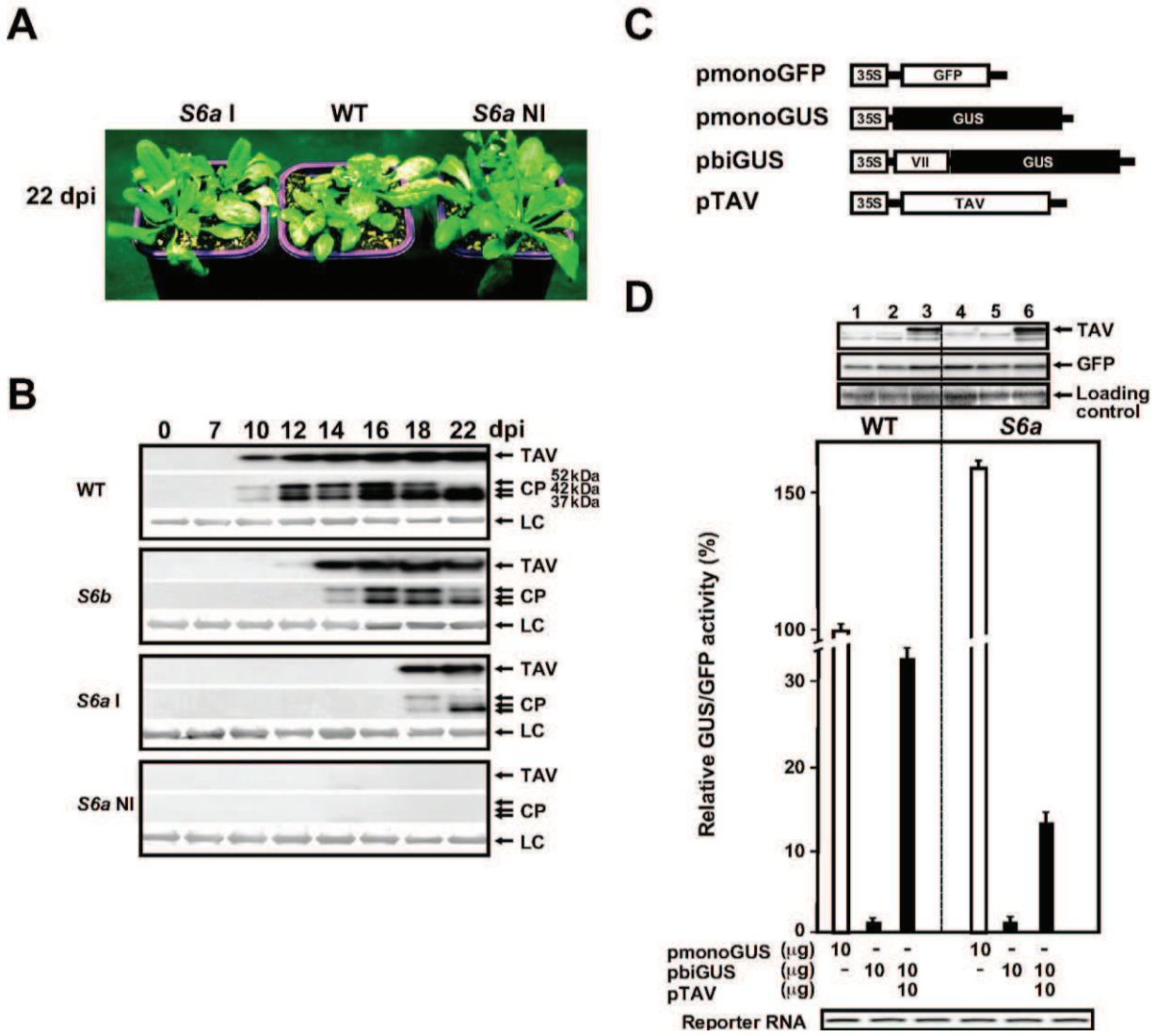

Figure 2.1-6 | *S6a* knockout plants are partly resistant to CaMV and fail to promote TAV-mediated transactivation of reinitiation after long ORF translation

(**A**) Analysis of healthy and *s6a* plant phenotypes at 22 dpi. *s6a* I—the example of *s6a* infected plant (show relatively mild symptoms), *s6a* NI—the example of non-infected plant are presented. (**B**) TAV and CP protein accumulation in CaMV-infected wild type, *S6b* and *S6a* knockout plants. TAV and CP accumulation was tested in *S6a* I and *S6a* NI. (**C**) Three reporter plasmids p*monoGFP*, p*monoGUS* and pbiGUS are shown, as well as the effector plasmids, pTAV in the amounts indicated below the graphs in D. (**D**) TAV-mediated transactivation is efficient in mesophyll protoplasts prepared from WT and reduced in *S6a* knockout plants. Stimulation of reinitiation after long ORF translation by TAV. GUS/GFP ratios from p*monoGUS* was set as 100% and shown as open bars, GUS/GFP rations from pbiGUS are shown by black bars. TAV, GFP expression levels were analyzed by immunoblot and shown by upper panels. *biGUS* and *monoGUS* mRNA levels were analyzed by semiquantitative RT-PCR. The data shown are the means of three independent assays: error bars indicate sd.

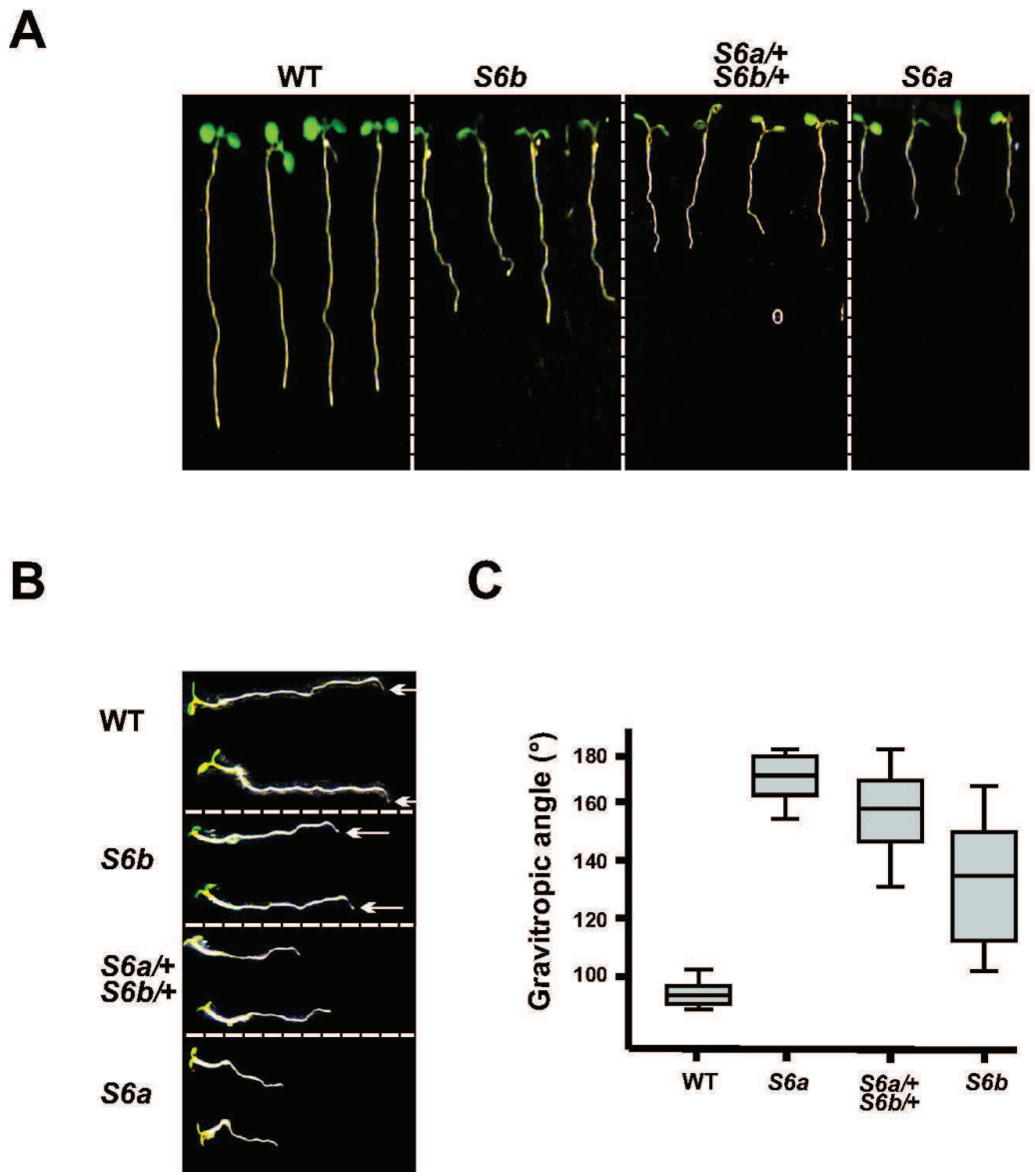

Figure 2.1-7 | eS6-deficient plants are defective in root gravitropic responses

(**A**) Root growth of *s6b*, *s6a*/+, *s6b/+* and *s6a* seedlings is delayed as compared to that of WT *Arabidopsis* plants. (**B**) *s6b*, *s6a*/+, *s6b/+* and *s6a* plants display agravitropic phenotype. Seedlings were grown 7 days after germination (dags) and analyzed 24 h after gravity stimulation. (**C**) Analysis of curvature in root gravitropic response 24 hours after gravity stimulation. Data are means +/- sd (n=50).

2.1.4 Discussion

Until now it has been unclear how RISP participates in translation initiation and particularly in the virus-activated reinitiation process. RISP has been suggested to assist eIF3 in recruitment of the ternary complex within 43S PIC and to mediate the link between 40S-bound eIF3 and the 60S ribosomal subunit during the 60S joining step. Here, we identified RISP as a dynamic scaffold that can interact with eIF2 possibly for eIF3-mediated assembly of 43S PIC and the eS6-eL24 intersubunit bridge for 60S joining to promote 80S assembly. Strikingly, the interaction between RISP and either eIF2 and/ or eIF3 is modulated by phosphorylation of RISP on the TOR/S6K1-responsive motif residue Ser267. Moreover, Ser267 phosphorylation can trigger RISP to bind preferentially to phosphorylated ribosome-bound eS6 and eL24 instead. However, how phosphorylation of RISP Ser267 disrupts eIF2/eIF3 binding and promotes the alternative interaction with phosphorylated eS6 and eL24 on the ribosome remains to be determined.

RISP and its interactions with 43S PIC

RISP is stably and specifically attached to 40S-PICs, and indeed RISP can be specifically immunoprecipitated from *Arabidopsis* extracts with antibodies against eIF2α, eIF3c and eS6 (Thiébeauld et al., 2009). RISP binds eIF2 subunit β within its central helix somewhere within contact points for subunit γ binding via helix–helix interaction (see archaebacterial aIF2 3D structure in Figure 2.1-2E; Schmitt et al., 2010). If RISP may contact both eIF3 and eIF2 within the 43S complex, we conclude that eIF3-bound RISP may assist eIF3 in capture of eIF2 via subunit β, thus stimulating recruitment of the ternary complex to 43S PIC.

In animal cells, phosphorylation of S6K1 by mTORC1 occurs within eIF3-containing PICs (Holz et al., 2005). *Arabidopsis* S6K1 is similarly fully activated by PDK1 (Mahfouz et al., 2006; Otterhag et al., 2006) and can phosphorylate eS6 and RISP. This is of importance as it places S6K1 in a position to phosphorylate RISP in close proximity to eIF3.

RISP, when phosphorylated binds the C-terminal helix of eS6. Although the C-terminal eS6 TOR-responsive phosphorylation sites in plants are not yet confirmed, Ser231 and Ser237 site patterns correspond in part to those found in many plant S6K1 substrates, and together with Ser240 were selected for interaction analysis. According our data phosphorylation of these sites can strongly contribute to eS6 ability to bind RISP. However, the functional significance of these phosphorylation sites and the effect of their mutation on plant development will require further exploration *in planta*.

RISP and its interaction with the 60S ribosomal subunit

The series of results obtained before and during this study suggest that RISP can interact with 60S-bound eL24 and 40S-bound eS6. The observation that a RISP phosphorylation mimic interacts preferentially with phosphorylation mimics of the eS6 C-terminal alpha helix has further importance in that it places the elongated coiled-coil structure of RISP in a position to interact with 60S-bound eL24 via protrusion out of the 60S C-terminal alpha helix. Again, binding of RISP to the eS6-eL24 intersubunit bridge may proceed via helix–helix interactions.

Recently published 3D structures of 80S (Ben-Shem et al., 2011) demonstrate that 40S and 60S are connected by two long protein helices extending from the left eL19 (eB12 bridge) and right sides of the 60S subunit interface eL24 (eB13, located near the main factor binding site of 60S). The eB13 bridge is formed by the C-terminal helix of eL24 and another helix of the eS6 C-terminus protruding from the 40S subunit interface. Although an eS6–eL24 interaction has been proposed, up to now we found no experimental proof for this contact in plants. Our results suggest a role for the eB13 bridge in the last stages of translation initiation, in particular subunit joining. This architecture of eL24 indicates a role for eL24 in translation reinitiation; its C-terminal domain was proposed to mediate retention of eIF3 on the ribosome and S6e may interact with factors that dock on $ES6^{S}$ or are involved in initiation/re-initiation (Ben-Shem et al., 2011). RISP may be one such factor.

Different *in vitro* approaches did not reveal stable RISP binding to 40S rather than to 60S (which has been demonstrated to form a complex with RISP; Thiébeauld et al., 2009). However, the fact that eS6 often could not be localized and thus modeled within the 80S structure may indicate that eS6 is not always present within 40S and/or that it is not available for interaction. Taking into account the fact that TOR phosphorylation levels are low in wild type plants (TOR phosphorylation is barely detected by the antibodies used; Schepetilnikov et al., 2013), and eS6 phosphorylation would also be expected to below and would thus diminish RISP binding to 40S especially *in vitro*. In contrast, auxin treatment of *Arabidopsis* seedlings positively affects RISP binding to 40S (Schepetilnikov et al., 2011).

The regulated phosphorylation of eS6 that is critical *in vivo* has attracted much attention since its discovery, but so far little is known about the possible role(s) of eS6 phosphorylation in eukaryotes. Our data suggest that, in response to TOR activation, phosphorylation of eS6 can tighten the 40S–60S association by binding of phosphorylated RISP to the eS6-eL24 bridge in response to TOR activation. This may negatively affect ligand binding during elongation of

translation, but in contrast promote 60S recycling or re-use of the same 60S for a reinitiation event.

At this stage we can propose a working model for the role of RISP in 43S PIC assembly and TAV-mediated reinitiation of translation (Figure 2.1-8). RISP is recruited to 43S PIC as a complex with eIF3, where RISP helix 2 contacts eIF3 subunits a and/ or c (Figure 2.1-8A; Thiébeauld et al., 2009). According to Holz et al. (2005), TOR, when activated, can phosphorylate eIF3-bound S6K1 within 48S PIC. One might expect that phosphorylation of RISP by activated S6K1 would also proceed in close proximity to 48S PIC (see Schepetilnikov et al., 2011). Although RISP is attached to eIF2-eIF3 before phosphorylation, its phosphorylation could trigger RISP-P binding to TAV and RISP-P or RISP-P/TAV complex relocation to the eS6 C-terminus (Figure 2.1-8B). An interesting possibility is that the link between eS6-RISP-TAV could be used for retention of eIF3 (via the eIF3g N-terminus) within polyribosomes during the long elongation event. Later (Figure 2.1-8C), during resumption of scanning, newly discovered contacts between RISP and the 40S ribosomal protein eS6 could ensure retention and re-use of 60S via the eS6/RISP/eL24 interaction network. If both RISP and TAV participate in stabilization of the eS6-eL24 intersubunit bridge, the same 60S could be used for repeated reinitiation events. However, this would require re-activation of TOR signaling. Indeed, in the presence of TAV, constitutively active S6K1 maintains the high phosphorylation status of RISP within polysomes (Schepetilnikov et al., 2011). Recruitment of TC *de novo* can be achieved either via eIF3 alone or via its complex with RISP, if nonphosphorylated RISP is available. Interestingly, functional roles in reinitiation for eIF3 subunits were proposed in yeast, where subunits a/Tif32, g/Tif35 and i/Tif34 were shown to support resumption of scanning of postterminating ribosomes in addition to their essential roles in translation initiation in mammals and yeast (Cuchalová et al., 2010; Munzarova et al., 2011).

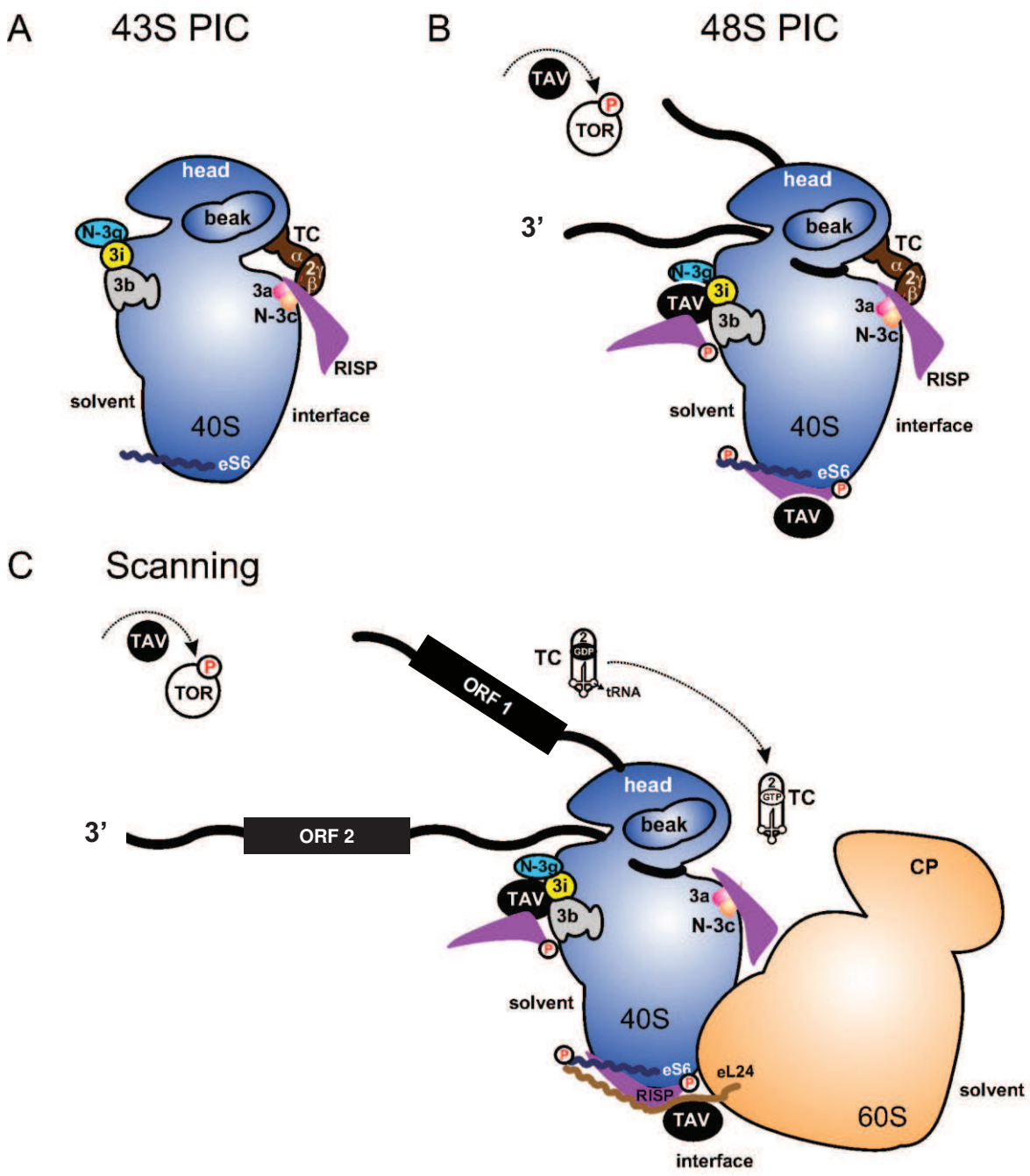
A
43S PIC
head
beak
N-3g
3i
3b
TC
α
2
γ
β
3a
N-3c
RISP
solvent
40S
interface
eS6
B
48S PIC
TAV
P
TOR
3'
head
beak
TC
N-3g
3i
TAV
3b
3a
N-3c
RISP
solvent
40S
interface
eS6
TAV
C
Scanning
TAV
P
TOR
ORF 1
TC
2
GDP
tRNA
3'
ORF 2
head
beak
2
GTP
TC
CP
N-3g
3i
TAV
3b
3a
N-3c
solvent
40S
eS6
eL24
RISP
TAV
60S
solvent
interface

Figure 2.1-8 | **Current model of RISP function in recruitment of initiator tRNA and 60S during virus-activated reinitiation of translation (see text for details)**

(**A**) RISP, together with eIF3, participates in recruitment of TC. (**B**) 48S PIC: upon TOR activation mediated by TAV, RISP is phosphorylated and locates to either eIF3 (via subunit g)-bound TAV or 40S-eS6, in response to TOR activation by TAV. RISP, if not phosphorylated, can still associate with eIF3 (subunits a and/or c). (**C**) 80S-scanning: RISP-P/ TAV stabilizes a bridge between 40S and 60S through the eS6-eL24 intersubunit bridge, preventing removal of 60S. During scanning, the RISP-P/TAV complex bridges relaxed 40S–60S interactions (open conformation of 80S). This open 80S conformation allows eIF3-bound 40S to continue scanning, and allows recruitment of TAV via either eIF3 alone or together with RISP. 40S (blue)—60S (yellow) orientation in 40S (beak and 60S P-stalk view), the position of TC and eIF3 subunits on 40S are shown schematically according to Ben-Shem et al., (2011), Hashem et al., (2013), and Erzberger et al., (2014), respectively. The solid black line represents the path of mRNA, boxes represent ORFs. eIF3, TC, RISP, TAV, eL24, eS6, 40S and 60S are indicated.

RISP and TAV-mediated reinitiation of translation

Our data suggest that eS6 plays a role in TAV-mediated reinitiation after long ORF translation and it is also clearly indispensible for CaMV infection. Since TAV maintains TOR in a constitutively phosphorylated state, RISP and eS6 are also likely to be phosphorylated.Thus, active TOR would create favorable conditions for RISP binding to 60S-bound eL24 and either stabilize or establish its interactions with 40S-bound eS6. To this end, TAV would further strengthen the link between subunits by binding to the N-terminus of eL24 and RISP H4. Once bound close to the main factor-binding site on the 60S interface, TAV might interfere with elongation events but could promote scanning of 80S in 40S-60S open conformation as we have proposed previously (Thiébeauld et al., 2009). Scanning of 80S was proposed later by Pestova's group (Skabkin et al., 2013). TAV-mediated reinitiation after long ORF translation is up-regulated by overexpression of eL24 in a free form (Park et al., 2001). In plants, some heterogeneity within the ribosomal population has been reported (Giavalisco et al., 2005), and production of eL24 may increase the fraction of eL24-bound ribosomes. Consistent with this notion, knockout of one copy of eS6a negatively affects TAV transactivation function (Figure 2.1-6D).

Although reinitiation after long ORF translation is essential for viral replication, knockout of cell non-essential protein eIF3h, or knockdown of essential proteins like TOR and eS6 that are critical for reinitiation to occur diminish or limit CaMV infection. Overall, virus resistance genes in plants are often inherited recessively, making such genes advantageous as tools to control plant diseases caused by pathogenic viruses. A growing number of recessive resistance genes encode translation initiation factors of the 4E (eIF4E) and 4G (eIF4G) families (Robaglia and Caranta, 2006). Here, the knockout of one copy of *eS6a* limits CaMV infection by inhibiting TAV transactivation function. Again *eS6a* knockout plants have no obvious defects in cap-dependent

translation and rather affects it positively (Figure 2.1-6D). Thus, the loss-of-susceptibility mutants identified to date correspond to mutations in the host translation machinery.

eS6, eL24 and other RPFs in plants

Statistical analysis has revealed that the length of plant uORFs is somewhat longer than that of other organisms, suggesting increased reinitiation capacity. Mutations in two known plant RPFs—eL24 and eIF3h, which cooperate to foster reinitiation in plants—both display some common defects in development (the cotyledon vasculature and the valves of the fruit; Zhou et al., 2010). However, in addition to reinitiation abnormalities, other defects that affect ribosome functioning and thus protein synthesis may contribute to the observed phenotypes. Indeed, mutations in several ribosomal proteins that affect plant development in a similar way (Byrne, 2009) are maybe not related to the reinitiation process *per se*. On the other hand, all proven reinitiation mutants—TOR-deficient and *eif3h-1* (Schepetilnikov et al., 2013) as well as eS6 mutants (*rps6a*, *rps6a*/+, *rps6a*/+; this study)—display gravitropic defects, suggesting a role for reinitiation in transporting TOR signals towards production of potent genes that harbor upstream ORFs within their leader region. We predict that other reinitiation-related mutants will have defects in gravity sensing.

2.1.5 Materials and Methods

Plant material, growth conditions and expression vectors.

Arabidopsis thaliana ecotype Columbia (Col-0) was used as the wild-type model in this study. SALK_048825 (*S6a*), SALK_012147 (*S6b*) and the *S6a*/+,*S6b*/+ double heterozygote lines were kindly provided by Dr. Thierry Desnos (CEA-Université Aix-Marseille-II, Marseille, France); all have a Col-0 background. Genotype details of these lines are described by Creff et al., (2010). Plasmids and expression constructions are described in Supplementary data. For seedling growth, cell culture details, extract preparation and production of recombinant His-tagged or GTS-fusion RISP and GST-fusion C-terminal eS6, see Supplementary Materials and Methods.

Viral infection

Virus infection was achieved using an agroinfectible construct derived from WT CaMV isolate CM1841 and kindly provided by Dr. Kappei Kobayashi (pFastWt; Kobayashi and Hohn, 2003,

2004; Tsuge et al., 1994), which was designated in this study simply as CaMV. Full details of the construction of the agroinfectible clone are given in (Laird et al., 2013). Briefly, the hypervirulent *Agrobacterium* strain AGL1+virG (Vain et al., 2004) containing the WT viral construct was grown for 20 h at 28 °C in 5 mL of Luria–Bertani medium containing kanamycin (50 µg mL^{-1}) and rifampicin (100 µg mL^{-1}). Five mL of the saturated culture were resuspended in 95 mL of similar liquid medium and incubated overnight at 28 °C. The cells were washed in water, and incubated for 2 h in buffer A containing 10 mM $MgCl_2$, 10 mM MES pH 5.7 and 200 µM acetosyringone at room temperature. A final dilution at OD_{600}=0.8 was prepared and plants at the early eight-leaf stage were infiltrated equally on three different leaves.

Protein purification

Wheat germ eIF2 was kindly provided by Professor K. Browning (University of Texas at Austin, USA). GST-fusion and His-tagged proteins were expressed in Rosetta 2 DE3 pLysS (Novagen®) and purified by the batch Glutathione Sepharose 4B or the HisTrap HP column (GE Healthcare®) procedures, respectively, according to supplier protocol (see Supplementary Materials and Methods).

In Vitro GST Pull-Down Assay

The *in vitro* GST pull-down assay was performed as described previously (Park et al., 2001). Binding of GST or GST-RISP to wheat eIF2 (or GST-Cter eS6 to His-RISP) was carried out in a 300 µL reaction containing 50 mM HEPES pH 7.5, 50 mM KCl, 3 mM magnesium acetate, with either 5 µg of wheat eIF2 or 5 µg of His-RISP. The total bound fraction as well as 30 µL of the unbound fraction were separated by a 15% SDS-PAGE gel and stained by Coomassie blue.

Yeast two-hybrid assay

To test for interactions, yeast strain AH109 was cotransformed with purified plasmids using the Yeastmaker® yeast transformation system 2 (BD Biosciences Clontech®) according to the manufacturer's instructions. β-Galactosidase activity was measured by using the Gal-Screen® assay system (Tropix® by Applied Biosystems®, see Supplementary Materials and Methods). The values given are the means from more than three independent experiments.

Transient expression for protoplast GUS-assays

Protoplasts derived from *Arabidopsis thaliana* wild-type or *S6* mutant seedlings were prepared according to (Yoo et al., 2007) with some modifications (see Supplementary data) and samples

of 2 x 10^4 protoplasts were used for PEG-mediated transfection. For transactivation, 10 µg pbiGUS, 10 µg p*monoGFP* and either 10 µg pTAV (or 10 µg empty vector p35S) were transfected. p*monoGFP* expression was monitored by western blot with anti-GFP antibodies (Chromotek®). GFP fluorescence and GUS activity was measured using a FLUOstar OPTIMA fluorimeter (BMG Biotech, USA). The values given are the means from more than three independent experiments.

Assay for root gravitropism

Seeds were surface-sterilized with 75% (v/v) ethanol for 1 min, followed by 2% (v/v) NaClO bleach with 0.01% (v/v) Triton X-100 detergent for 20 min. After 2 rinses with sterile water, seeds were germinated and grown vertically on medium containing MS salts (Murashige and Skoog, 1962), 1% sucrose (w/v) and 1% (w/v) agar in Petri dishes. The Petri dishes were kept in the cold (4 °C) and dark for 4 days, then transferred to the growth chambers with 120 µmol s^{-1} m^{-2} fluorescent light in two 16 h-light/8 h-dark cycles at room temperature (22°C). For the root gravitropism assay, germinated seedlings were grown vertically in the dark at room temperature. After 4 days of growth, plates were rotated by 90° and images of root tips were captured (Canon EOS 350D digital) at 24 h or 48 h after reorientation. The angle of the root tip with respect to the gravity vector was measured from the pictures with Image J software.

Molecular modeling

The 3D structure of *Arabidopsis* RISP was created using Modeller (Sali et al., 1995) and represented graphically by PyMOL (http://www.pymol.org).

2.1.6 Acknowledgments

We are grateful to J-M Daviere and N. Baumberger for helpful assistance in plant genetics and protein analysis, respectively. This work was supported by French Agence Nationale de la Recherche—BLAN-2011_BSV6 010 03, France—for funding L.R., and CONACYT, Service de Coopération Universitaire de l'Ambassade de France au Mexique to E. M-M.

2.2 eS6 phosphorylation in response to TOR activation in planta

2.2.1 Introduction

In eukaryotic cells, the main rate-limiting step of translation is initiation, which is controlled by different signaling cascades activated by extracellular signals. Under diverse conditions of nutrient and energy sufficiency, and growth hormonal stimulation, TOR stimulates important translational regulators, such as the eIF4E-binding proteins (4E-BPs), and the 70 kDa ribosomal eS6 kinases 1 and 2 (S6Ks). S6K1 phosphorylates several substrates located in the cytoplasm, including the ribosomal protein eS6 (see details in pág. 65). eS6 is one of 33 proteins that comprise the 40S ribosomal subunit and represents the most extensively studied substrate of the cytoplasmic S6K1 for phosphorylation.

Because the initial discovery that liver-derived eS6 was phosphorylated (Gressner and Wool, 1974), mitogenic stimulation of cells was found to correlate with phosphorylation of eS6 suggesting the role of eS6 in mRNA translation control in dividing cells (Bandi et al., 1993) and attracted a lot of attention since its discovery more than four decades ago. eS6 phosphorylation sites have been mapped to five or six clustered residues that are conserved in metazoans, consisting of Ser235, Ser236, Ser240, Ser242, Ser244, and Ser247 at the C-terminal part of the protein (Krieg et al., 1988).

In mammals, carboxyl-terminal phosphorylation of eS6 is regulated by at least two signal transduction pathways. The TOR/S6K1 pathway plays a major role in eS6 C-terminus phosphorylation in response to insulin, serum, and amino acid stimulation (Meyuhas, 2008). S6K1 phosphorylates all five serines, particularly Ser240 and Ser244 (Roux et al., 2007). The RAS/ERK pathway also regulates eS6 phosphorylation through the activation of p90 ribosomal eS6K kinases, RSK1 and RSK2 (Pende et al., 2004). RSK1 and RSK2 phosphorylate eS6 on Ser235 and Ser236 in response to phorbol ester, serum, and oncogenic RAS (Roux et al., 2007).

The physiologic roles of eS6 phosphorylation have been investigated through the generation of a knock-in mouse encoding a mutant eS6 harboring Ala substitutions at all five C-terminal phosphorylation sites (Ruvinsky et al., 2005). eS6 knock-in animals exhibit strong physiologic abnormalities—reduced overall size, glucose intolerance, and muscle weakness (Ruvinsky and Meyuhas, 2006). eS6 knock-in mouse-derived embryo fibroblasts (MEFs) displayed *an increased rate of protein synthesis* and accelerated cell division, and they are significantly smaller than wild-type cells. Moreover, the size of eS6 knock-in cells, unlike wild-type MEFs, is not further decreased upon rapamycin treatment, indicating that eS6 is a downstream target of mTOR in regulation of cell size. Thus, a current model states that eS6 phosphorylation promotes translation and cell growth. Surprisingly, overall protein translation

was not significantly reduced in eS6 knock-in cells suggesting that *deregulation of specific mRNAs* may be responsible for observed phenotypes (Ruvinsky and Meyuhas, 2006). However, despite a large body of information on signal transduction pathways that phosphorylate eS6, it is surprising that the biological role of eS6 phosphorylation in translation remain largely mysterious.

In plants, the deletion of two eS6 isoforms, *RPS6A* and *RPS6B*, is vital, and both genes are *redundant and interchangeable* (Creff et al., 2010). Up to now the large-scale phosphoproteome studies in *Arabidopsis* revealed phosphorylation of seven sites in the eS6a isoform—Thr127, Ser229, Ser231, Ser237, Ser240, Ser247, Thr249—and phosphorylation of four serines in the eS6b isoform—Ser229, Ser231, Ser237 and Ser240— (Boex-Fontvieille et al., 2013; Reiland et al., 2009; Turkina et al., 2011). Nevertheless, the nature of inputs regulating eS6 phosphorylation and how phosphorylation contributes to protein synthesis remain unclear and requires further analysis.

The studies of phosphorylation patterns of ribosomal proteins in plants are complicated because of the ribosome heterogeneity. *Arabidopsis* ribosomal proteins are encoded by small gene families, of two to seven paralogs, representing a total of 249 genes (Barakat et al., 2001). Many of these paralogous ribosomal proteins are different by their developmental or conditional expression (Whittle and Krochko, 2009). Thus different phosphorylation pattern might be associated with plant extracts isolated from different cell types and plant tissues, or under different enviromental conditions, or using different purification methods, phosphopeptide enrichment protocols, mass-spectrometric detection and data analysis. This idea is supported by the fact that Giavalisco et al. (2005) observed expression of at least two family members of the ribosomal protein families—two or more distinct spots in the 2-D gel. In addition, multiple phosphorylated r-proteins that generate multiple phosphorylated peptides are notoriously difficult to detect by simple mass spectrometry (Carroll, 2013).

The model states—if multiple ribosomal protein paralogs are expressed simultaneously and paralogs have distinct functions in translation, individual ribosomes differ qualitatively with respect to the r-protein paralog selected—. Here we concentrated on identification of the eS6 phosphorylation pattern in either crude extract or isolated polysomes prepared from *Arabidopsis* seedlings that are characterized by a different TOR phosphorylation status.

2.2.2 Results

Isolation of r- proteins from A. thaliana seedlings treated with auxin or Torin-1

It was shown in our laboratory that plant hormone auxin triggers TOR activation followed by S6K1 phosphorylation at T449 in a manner sensitive to the TOR inhibitor Torin-1 (Schepetilnikov et al., 2013). To obtain *Arabidopsis* plants characterized by either high or low TOR phosphorylation status, 7 day after germination (dag) seedlings were treated by auxin or Torin-1 as described in Materials and Methods. Strikingly, TOR activation triggers its loading in polysomes, where TOR and its downstream target S6K1 maintain the high phosphorylation status of their targets such as eIFs. Thus, we compared the levels of both protein extraction and phosphorylation status between crude *Arabidopsis* extracts and polysomes isolated via the 60S ribosomal protein L18 (Zanetti et al., 2005). WT and *35S:HF-RPL18 Arabidopsis* seedlings were grown on MS agar plates under short-day conditions for 7-dag. Next, equal amount of plant material was incubated in a liquid medium containing appropriate concentrations of either auxin (NAA) or Torin-1 for 8 h in order to increase or decrease the phosphorylation status of TOR.

To established relatively efficient and fast protein isolation from crude extracts we compared two protein extraction protocols described for phosphoproteome analysis in *Arabidopsis*: TCA/acetone precipitation (Boex-Fontvieille et al., 2013) and a modified TRIzol® protein extraction method (see Table 2.2-1; Materials and Methods).

Selective immunopurification of polysomes (IP, Zanetti et al., 2005) was used as well. The method of affinity purification of *Arabidopsis* polysomal complexes based on expression of an epitope-tagged r-protein (in our case the 60S ribosomal protein FLAG-L18) provides a manner to isolate plant polyribosomes very fast thus providing a valuable tool for analysis of ribosomal and non-ribosomal proteins and their post-translational modifications. Protein elution of FLAG-L18-containing ribosomes and ribosomal subunits bound to anti-FLAG-Sepharose was done either by FLAG peptide at 4 °C (C) or in Laemmli buffer at either 95 °C (B) or 30 °C (D2; Table 2.2-1). In addition, two total crude extract samples prepared from NAA or Torin-1 treated seedlings were treated either by TCA/acetone (A1 and A2 conditions) or by Trizol (D1 condition; Table 2.2-1) and then immediately resuspended in urea-containing IEF buffer.

Table 2.2-1. Experimental conditions for phosphoproteomic analyses

Experiment (date)	Protein extraction method	Elution or resuspension conditions	Selective phospho-enrichment	Comments
A1	TCA/acetone	IEF buffer	IMAC 1	Low recovery of eS6 phosphopeptides.
A2	TCA/acetone	IEF buffer	IMAC 3	High recovery of eS6 phosphopeptides
B	IP	Elution by Laemmli buffer at 95 °C	TiO_2	Poor recovery of phosphopeptides in NAA sample but excellent identification of r- and non-r- proteins in both samples
C	IP	Elution by FLAG peptide at 4 °C	TiO_2	Poor quality in phosphopeptide spectra but good identification of r- and non-r- proteins in both samples
D1	Trizol	IEF buffer	TiO_2	Partial recovery of eS6 phosphopeptides but qualitative differences in phosphorylation status can be detected. Excellent identification of r- and non-r- proteins in both samples
D2	IP	Elution by Laemmli buffer at 30 °C	TiO_2	

In all cases, phosphopeptides were selectively enriched by using the Immobilized Metal Ion Affinity Chromatography (IMAC) and/or dioxide titanium columns (TiO_2), and the resulting phosphopeptide pools were analyzed by LC-MS/MS. To protect the natural phosphorylation state of r-proteins at all stages of preparations we used three different phosphatase inhibitors (1 mM sodium molybdate, 80 mM β-glycerol phosphate, and the PhosSTOP® Phosphatase Inhibitor cocktail [Roche]), according to earlier described procedures (Williams et al., 2003) and manufacture's guidelines. An overview of the experimental strategy is shown in (Table 2.2-1).

Characterization of the ribosomal and non-ribosomal proteins by nano-LC-MS/MS

For proteomic characterization protein samples were analyzed as described in Boex-Fontvieille et al., (2013). Peptides were methylated via formylation with labeled (deuterated) or nonlabeled formaldehyde and reduction with cyanoborohydride. Non-labeled and labeled peptides were mixed (the condition of interest (non-labeled) and the mix of all samples as a reference

(labelled) mixed with a 1:1 ratio, and underwent a SCX (Strong Cation Exchange) chromatography. The quantity of proteins was determined by direct LC-MS-MS analysis and data were separately analyzed using MASCOT search against the Swissprot database for *Arabidopsis*. The resulting sets of identified r-proteins present in the immunoprecipitated ribosomal complexes revealed the presence of 141 cytosolic r-proteins spanning different paralog genes identified by a single gene locus (Table 2.2-2). Surprisingly, the range of protein abundance in the mixtures (Mascot score; Figure 2.2-1) was larger than expected for a homogeneous and stable multicomplex made of 80 different proteins, revealing that some ribosomal peptides were particularly more abundant. Furthermore, we were able to detect 64 out of 80 ribosomal protein families composing the plant cytosolic ribosome (Table 2.2-3). In order to eliminate discrepancies in the nomenclature for eukaryotic ribosomal proteins, we used the new nomenclature system for r-proteins (Ban et al., 2014). Based on the sequence of each single gene accession number (TAIR data base, www.arabidopsis.org) and combining a set of bioinformatics tools (BLAST and BLink, http://blast.ncbi.nlm.nih.gov/Blast.cgi) it was possible to unambiguously assign each plant r-protein detected in IP samples to a family based on structural homology to yeast and human proteins.

Table 2.2-2. Eukaryotic r-proteins identified by nanoLC-MS/MS in ribosomal IP samples

Accession number	Name	MW [kDa]	pI	Meta Score[a]	# Spectra[b]	RMS [ppm][c]
AT3G09630.1	Ribosomal protein L4/L1 family	44.7	10.9	1457	67	6.46
AT5G07090.1	Ribosomal protein S4 (RPS4A) famil...	29.9	10.7	1249.5	58	6.19
AT5G02870.1	Ribosomal protein L4/L1 family	44.7	10.8	1246.2	63	7.17
AT3G05590.1	ribosomal protein L18, Symbols: RPL18	20.9	11.6	1223.3	99	7
AT1G43170.1	ribosomal protein 1, Symbols: ARP1...	44.5	10.7	1175.5	50	5.97
AT1G72370.1	40s ribosomal protein SA, Symbols:...	32.3	4.9	1139.7	47	7.51
AT5G20290.1	Ribosomal protein S8e family protein	25	10.9	1118.9	45	6.9
AT1G74060.1	Ribosomal protein L6 family protein	26	10.6	1097.2	52	6.18
AT5G27850.1	Ribosomal protein L18e/L15 superfa...	21	11.6	1081.5	83	7.13
AT2G27710.1	60S acidic ribosomal protein family	11.4	4.5	1059.7	39	7.44
AT3G53870.1	Ribosomal protein S3 family protein	27.3	10	1014.4	43	6.26
AT1G18540.1	Ribosomal protein L6 family protein	26.1	10.5	995	46	6.15
AT3G62870.1	Ribosomal protein L7Ae/L30e/S12e/G...	29	10.7	977.9	44	6.04
AT3G09200.1	Ribosomal protein L10 family protein	34.1	4.8	971.2	53	8.08
AT3G04840.1	Ribosomal protein S3Ae	29.8	10.4	954.2	31	7.4
AT5G35530.1	Ribosomal protein S3 family protein	27.4	10	947.4	41	5.98
AT3G25520.1	ribosomal protein L5, Symbols: ATL...	34.3	9.7	923.1	36	6.13
AT1G56070.1	Ribosomal protein S5/Elongation fa...	93.8	5.9	911	23	7.69
AT5G10360.1	Ribosomal protein S6e, Symbols: EM...	28.1	11.6	899.8	35	7.01
AT4G31700.1	ribosomal protein S6, Symbols: RPS...	28.3	11.3	889.7	37	6.69
AT2G47610.1	Ribosomal protein L7Ae/L30e/S12e/G...	29.1	10.7	872.7	39	6.15
AT1G33120.1	Ribosomal protein L6 f...	22	10.1	867.7	43	7.46
AT2G36160.1	Ribosomal protein S11 family protein	16.2	11.3	858.5	31	6.39
AT5G39740.1	ribosomal protein L5 B, Symbols: O...	34.4	9.6	851.4	32	6.19
AT2G18020.1	Ribosomal protein L2 family, Symbo...	27.8	11.7	849.2	71	5.23
AT2G01250.1	Ribosomal protein L30/L7 family pr...	28.2	10.4	828.7	36	7.18
AT1G01100.1	60S acidic ribosomal protein family	11.2	4.3	788.2	18	9.67

AT4G34670.1	Ribosomal protein S3Ae	29.8	10.3	783.8	25	7.07
AT4G36130.1	Ribosomal protein L2 family	27.9	11.7	766.9	53	5.54
AT2G27720.2	60S acidic ribosomal protein family	13	4.2	739	19	7.05
AT5G47700.1	60S acidic ribosomal protein family	11.2	4.3	716.3	15	9.89
AT2G44120.2	Ribosomal protein L30/L7 family pr...	28.5	10.3	715.8	27	6.37
AT3G52580.1	Ribosomal protein S11 family protein	16.2	11.3	714	26	6.06
AT2G34480.1	Ribosomal protein L18ae/LX family ...	21.3	11	690.3	21	7.54
AT4G39200.1	Ribosomal protein S25 family protein	12	11.2	679.3	34	7.32
AT4G27090.1	Ribosomal protein L14	15.5	10.5	657.4	34	7.66
AT3G05560.1	Ribosomal L22e protein family	14	10.1	653.8	42	6.32
AT5G27770.1	Ribosomal L22e protein family	14	10.1	649.1	42	6.13
AT3G11940.1	ribosomal protein 5A, Symbols: ATR...	22.9	10.2	637.4	28	7.56
AT1G22780.1	Ribosomal ...	17.5	11.1	634	42	6.86
AT2G37270.1	ribosomal protein 5B, Symbols: ATR...	23	10.3	632.7	28	7.19
AT1G04480.1	Ribosomal ...	15	11.4	603.3	32	7.12
AT1G08360.1	Ribosomal protein L1p/L10e family	24.5	10.5	598.5	27	4.78
AT5G18380.1	Ribosomal protein S5 domain 2-like...	16.6	11	584	23	7.06
AT3G07110.2	Ribosomal protein L13 family protein	23.6	11.2	563.5	20	6.31
AT4G00100.1	ribosomal protein S13A, Symbols: A...	17.1	10.9	558.4	20	6.53
AT2G09990.1	Ribosomal protein S5 domain 2-like...	16.6	11	557.7	19	6.31
AT5G16130.1	Ribosomal protein S7e family protein	22	10.2	551.8	16	8.29
AT3G13580.3	Ribosomal protein L30/L7 family pr...	28.4	10.4	548.4	22	6.5
AT4G13170.1	Ribosomal protein L13 family protein	23.6	11.1	546.6	20	6.07
AT5G48760.1	Ribosomal protein L13 family protein	23.6	11.1	541.7	20	6.18
AT3G60770.1	Ribosomal protein S13/S15	17.1	10.9	527.2	21	6.56
AT3G24830.1	Ribosomal protein L13 family protein	23.4	11.2	524.5	21	6
AT1G48830.1	Ribosomal protein S7e family protein	21.9	10.2	522.5	20	7.8
AT4G29410.1	Ribosomal L28e protein family	15.9	11.7	518.1	26	6.99
AT1G48630.1	receptor for activated C kinase 1B...	35.8	6.8	517.2	14	7.53
AT5G46430.1	Ribosomal protein L32e	15.5	11.4	513.9	20	5.89
AT3G18740.1	Ribosomal protein L7Ae/L30e/S12e/G...	12.3	10.3	513.1	20	7.81
AT1G15930.2	Ribosomal protein L7Ae/L30e/S12e/G...	15.4	5.3	511.3	21	7.52
AT4G18100.1	Ribosomal protein L32e	15.5	11.5	509.7	25	6.5
AT2G20450.1	Ribosomal protein L14	15.5	10.6	489.9	26	7.83
AT2G27530.1	Ribosomal protein L1p/L10e family,...	24.4	10.5	485.5	21	5.12
AT5G22440.1	Ribosomal protein L1p/L10e family	24.5	10.5	485.3	22	4.73
AT3G02080.1	Ribosomal protein S19e family protein	15.8	10.6	482.4	25	7.81
AT3G56340.1	Ribosomal protein S26e family protein	14.6	12.3	481.2	18	6.11
AT5G61170.1	Ribosomal protein S19e family protein	15.7	10.7	481.1	24	7.98
AT4G00810.1	60S acidic ribosomal protein family	11.3	4.2	481	9	10.86
AT5G15200.1	Ribosomal protein S4	23	10.6	477.5	25	6.11
AT2G37190.1	Ribosomal protein L11 family protein	17.9	9.8	472.7	22	6.12
AT2G21580.1	Ribosomal protein S25 family protein	12.1	11.2	466.4	23	5.58
AT1G27400.1	Ribosomal protein L22p/L17e family...	19.9	10.8	456	43	7.71
AT1G77940.1	Ribosomal protein L7Ae/L30e/S12e/G...	12.3	10.2	455.7	18	7.6
AT2G19730.1	Ribosomal L28e protein family	15.9	11.1	454.4	29	6.79
AT2G42740.1	ribosomal protein large subunit 16...	20.8	10.5	451.6	24	7.13
AT1G07770.1	ribosomal protein S15A...	14.8	10.4	451	22	6.46
AT2G40510.1	Ribosomal protein S26e family protein	14.8	12.3	450	20	6.12
AT1G14320.1	Ribosomal protein L16p/L10e family...	24.9	11.7	403.8	15	6.44
AT5G23740.1	ribosomal protein S11-beta, Symbol...	17.7	11.6	403.4	22	5.28
AT1G70600.1	Ribosomal protein L18e/L15 superfa...	16.4	11.2	397.1	18	7.06
AT3G18130.1	receptor for activated C kinase 1C...	35.8	6.8	396.4	11	8.34
AT3G45030.1	Ribosomal protein S10p...	13.9	10.4	387.5	31	6.17
AT3G04920.1	Ribosomal protein S24e family protein	15.4	11.2	387.4	12	8.07
AT5G02960.1	Ribosomal protein S12/S23 family p...	15.7	11	387	17	8.27
AT5G23900.1	Ribosomal protein L13e family protein	23.5	11.5	386.2	12	6.17
AT3G09500.1	Ribosomal L29 family protein	14.3	11.4	386	16	6.12
AT2G05220.1	Ribosomal S17 family protein	15.9	10.5	386	17	5.97

AT1G04270.1	cytosolic ribosomal protein S15, S...	17.1	10.8	383.7	25	7.8
AT2G32060.1	Ribosomal protein L7Ae/L30e/S12e/G...	15.3	5.5	377.1	15	5.72
AT3G46040.1	ribosomal protein S15A D, Symbols:...	14.8	10.5	372.3	13	5.93
AT1G23290.1	Ribosomal protein L18e/L15 superfa...	16.3	11.1	369.5	17	7.57
AT5G02450.1	Ribosomal protein L36e family protein	12.2	12.1	358.3	7	5.87
AT1G61580.1	R-protein L3 B, Symbols: RPL3B, ARP2	44.5	10.8	355.9	16	6.17
AT4G15000.1	Ribosomal L27e protein family	15.6	10.8	350.1	15	6.47
AT3G22230.1	Ribosomal L27e protein family	15.6	10.8	335.7	15	9.27
AT3G53740.2	Ribosomal protein L36e family protein	12.7	12.2	331.6	8	5.86
AT2G41840.1	Ribosomal protein S5 family protein	30.9	11	322.3	7	7.96
AT4G10450.1	Ribosomal protein L6 family	22	10.1	316.6	12	7.02
AT3G47370.2	Ribosomal protein S10p/S20e family...	13.7	10.4	309.6	21	6.29
AT3G55280.1	ribosomal protein L23AB, Symbols: ...	17.4	10.7	302.8	14	7.09
AT2G39390.1	Ribosomal L29 family protein	14.2	11.4	302	10	6.07
AT3G44590.2	60S acidic ribosomal protein family	11	4.4	296.4	6	6.26
AT3G02560.1	Ribosomal protein S7e family protein	22.2	10.2	292.8	11	7.04
AT4G16720.1	Ribosomal protein L23/L15e family ...	24.2	12.1	292.8	13	7.12
AT5G28060.1	Ribosomal protein S24e family protein	15.4	11.1	292.3	9	7.78
AT1G58380.1	Ribosomal protein S5 family protei...	30.7	11	285.8	8	7.67
AT2G36620.1	ribosomal protein L24, Symbols: RP...	18.8	11.4	280.8	16	6.73
AT1G41880.1	Ribosomal protein L35Ae family pro...	12.8	11.2	278.1	7	6.62
AT2G43460.1	Ribosomal L38e protein...	8.1	10.6	273.4	13	7.59
AT3G55750.1	Ribosomal protein L35Ae family pro...	12.8	11.2	216	6	6.08
AT3G27850.1	ribosomal protein L12-C, Symbols: ...	19.7	5.4	205.6	5	6.96
AT2G43030.1	Ribosomal protein L3 family protein	29.3	10.9	193.9	5	7.45
AT1G64880.1	Ribosomal protein S5 family protein	60.2	7.7	173.1	4	7.21
AT5G64140.1	ribosomal protein S28, Symbols: RPS28	7.3	11.7	164.8	4	7.34
AT3G25920.1	ribosomal protein L15, Symbols: RPL15	29.7	11.5	162.7	3	6.11
AT1G02780.1	Ribosomal protein L19e family prot...	24.6	11.9	159.3	5	14.1
AT1G07320.1	ribosomal protein L4, Symbols: RPL4	30.5	9.4	153	4	8.82
ATCG00830.1	ribosomal protein L2, ...	29.8	11.7	141.7	5	7.01
AT3G53890.1	Ribosomal protein S21e	9.1	9.2	140.3	5	8.58
AT5G27700.1	Ribosomal protein S21e	9.1	7.8	133.4	2	10.18
AT3G16780.1	Ribosomal protein L19e family protein	24.3	11.8	131.8	3	7.89
AT1G05190.1	Ribosomal protein L6 family, Symbo...	24.7	10.4	130.7	4	6.93
AT2G19750.1	Ribosomal ...	6.9	12.7	127.6	2	7.13
AT5G57290.1	60S acidic ribosomal protein family	11.9	4.3	124.5	8	5.83
AT1G78630.1	Ribosomal protein L13 family prote...	26.8	10.5	120.2	3	6.04
AT2G19740.1	Ribosomal protein L31e family protein	13.7	10.5	113.2	3	4.07
AT4G25890.1	60S acidic ribosomal protein family	11.8	4.3	109	2	7.11
AT5G40950.1	ribosomal protein large subunit 27...	21.7	10.5	105.7	4	8.43
AT3G63490.1	Ribosomal protein L1p/L10e family	37.6	9.9	102.7	3	6.46
AT1G26880.1	Ribosomal protein L34e superfamily...	13.7	12.2	97.7	4	6.73
AT5G09510.1	Ribosomal protein S19 family protein	17.1	10.8	95.3	27	9.6
AT4G02230.1	Ribosomal protein L19e family protein	24.2	12	92.4	3	17.14
AT5G30510.1	ribosomal protein S1, Symbols: RPS...	45.1	5	82.1	1	5.08
ATCG00820.1	ribosomal protein S19, Symbols: RPS19	10.6	10.8	79	2	7.85
ATCG00770.1	ribosomal protein S8, Symbols: RPS8	15.5	11.6	74.5	2	3.43
AT4G01310.1	Ribosomal L5P family protein	28.3	10.6	73.5	2	8.48
AT2G33800.1	Ribosomal protein S5 family protein	32.6	9.5	71.3	3	5.26
AT3G28900.1	Ribosomal protein L34e superfamily...	13.6	12	70.1	2	22.45
AT1G79850.1	ribosomal protein S17, Symbols: RP...	16.3	11.2	67.8	1	4.66
AT3G43980.1	Ribosomal ...	6.4	11.9	66.2	2	4.52
AT1G75350.1	Ribosomal protein L31, Symbols: em...	16	10.5	63.8	2	9.46
AT2G24090.1	Ribosomal protein L35	16.1	12.5	59	2	9.31

[a] This value gives a quantitative trend concerning the abundance of proteins in the mixture (Mascot score)
[b] The number of detected spectra correlates with the protein abundance (Spectral counting)
[c] Average error in ppm

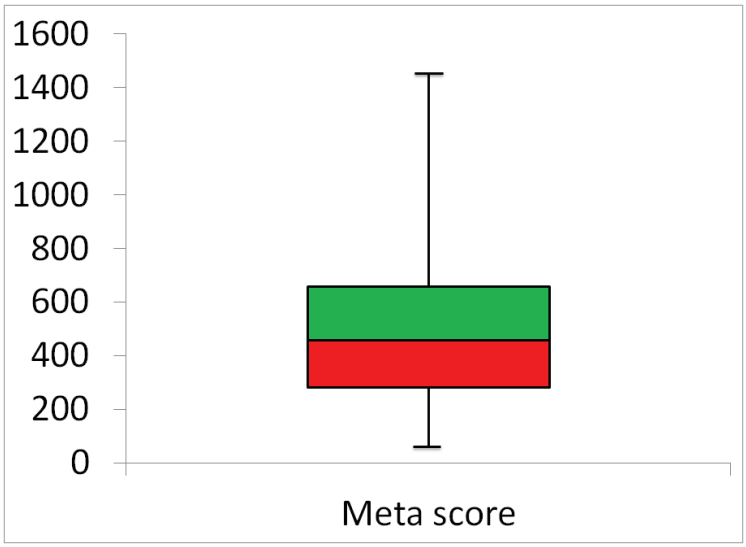

Figure 2.2-1. | **A box-and-whisker plot reveals a non-Gaussian distribution among Meta-score values for each ribosomal peptide in a single polyribosomal IP population.**

Table 2.2-3. Single plant r-protein families identified by nano LC-MS/MS

Subunit	Accession[a]	Generic name	Protein family name (new nomenclature)	MW [kDa]	pI
L	AT1G08360.1	Ribosomal protein L1p/L10e family	uL1	24.5	10.5
L	AT2G18020.1	Ribosomal protein L2 family, Symbo...	uL2	27.8	11.7
L	AT1G43170.1	ribosomal protein 1, Symbols: ARP1...	uL3	44.5	10.7
L	AT1G07320.1	ribosomal protein L4, Symbols: RPL4	L4	30.5	9.4
L	AT3G09630.1	Ribosomal protein L4/L1 family	uL4	44.7	10.9
L	AT2G42740.1	ribosomal protein large subunit 16...	uL5	20.8	10.5
L	AT1G18540.1	Ribosomal protein L6 family protein	eL6	26.1	10.5
L	AT1G05190.1	Ribosomal protein L6 family, Symbo...	uL6	24.7	10.4
L	AT3G09200.1	Ribosomal protein L10 family protein	uL10	34.1	4.8
L	AT2G37190.1	Ribosomal protein L11 family protein	uL11	17.9	9.8
L	AT5G23900.1	Ribosomal protein L13e family protein	eL13	23.5	11.5
L	AT1G78630.1	Ribosomal protein L13 family prote...	uL13	26.8	10.5
L	AT2G20450.1	Ribosomal protein L14	eL14	15.5	10.6
L	AT1G04480.1	Ribosomal ...	uL14	15	11.4
L	AT4G16720.1	Ribosomal protein L23/L15e family ...	eL15	24.2	12.1
L	AT1G23290.1	Ribosomal protein L18e/L15 superfa...	uL15	16.3	11.1
L	AT1G14320.1	Ribosomal protein L16p/L10e family...	uL16	24.9	11.7
L	AT3G05590.1	ribosomal protein L18, Symbols: RPL18	eL18	20.9	11.6
L	AT3G25520.1	ribosomal protein L5, Symbols: ATL...	uL18	34.3	9.7
L	AT1G02780.1	Ribosomal protein L19e family prot...	eL19	24.6	11.9
L	AT2G34480.1	Ribosomal protein L18ae/LX family ...	eL20	21.3	11
L	AT3G05560.1	Ribosomal L22e protein family	eL22	14	10.1
L	AT1G27400.1	Ribosomal protein L22p/L17e family...	uL22	19.9	10.8
L	AT3G55280.1	ribosomal protein L23AB, Symbols: ...	uL23	17.4	10.7

L	AT2G36620.1	ribosomal protein L24, Symbols: RP...	eL24	18.8	11.4
L	AT3G22230.1	Ribosomal L27e protein family	eL27	15.6	10.8
L	AT2G19730.1	Ribosomal L28e protein family	eL28	15.9	11.1
L	AT2G39390.1	Ribosomal L29 family protein	uL29	14.2	11.4
L	AT2G01250.1	Ribosomal protein L30/L7 family pr...	uL30	28.2	10.4
L	AT2G19740.1	Ribosomal protein L31e family protein	eL31	13.7	10.5
L	AT4G18100.1	Ribosomal protein L32e	eL32	15.5	11.5
L	AT1G41880.1	Ribosomal protein L35Ae family pro...	eL33	12.8	11.2
L	AT1G26880.1	Ribosomal protein L34e superfamily...	eL34	13.7	12.2
L	AT2G43460.1	Ribosomal L38e protein...	eL38	8.1	10.6
L	AT4G31985.1	Ribosomal protein L39 ...	eL39	6.4	12.8
L	AT3G53740.2	Ribosomal protein L36e family protein	eL36	12.7	12.2
L	AT1G01100.1	60S acidic ribosomal protein family	P1/P2	11.2	4.3
S	AT3G04840.1	Ribosomal protein S3Ae	eS1	29.8	10.4
S	AT1G72370.1	40s ribosomal protein SA, Symbols:...	uS2	32.3	4.9
S	AT3G53870.1	Ribosomal protein S3 family protein	uS3	27.3	10
S	AT5G07090.1	Ribosomal protein S4 (RPS4A) famil...	eS4	29.9	10.7
S	AT5G15200.1	Ribosomal protein S4	uS4	23	10.6
S	AT1G58380.1	Ribosomal protein S5 family protei...	uS5	30.7	11
S	AT4G31700.1	ribosomal protein S6, Symbols: RPS...	eS6	28.3	11.3
S	AT1G48830.1	Ribosomal protein S7e family protein	eS7	21.9	10.2
S	AT2G37270.1	ribosomal protein 5B, Symbols: ATR...	uS7	23	10.3
S	AT5G20290.1	Ribosomal protein S8e family protein	eS8	25	10.9
S	AT1G07770.1	Ribosomal protein S15A...	uS8	14.8	10.4
S	AT2G09990.1	Ribosomal protein S5 domain 2-like...	uS9	16.6	11
S	AT3G45030.1	Ribosomal protein S10p...	uS10	13.9	10.4
S	AT2G36160.1	Ribosomal protein S11 family protein	uS11	16.2	11.3
S	AT1G15930.2	Ribosomal protein L7Ae/L30e/S12e/G...	eS12	15.4	5.3
S	AT5G02960.1	Ribosomal protein S12/S23 family p...	uS12	15.7	11
S	AT3G60770.1	Ribosomal protein S13/S15	uS15	17.1	10.9
S	AT2G05220.1	Ribosomal S17 family protein	eS17	15.9	10.5
S	AT1G79850.1	ribosomal protein S17, Symbols: RP...	uS17	16.3	11.2
S	AT3G02080.1	Ribosomal protein S19e family protein	eS19	15.8	10.6
S	AT1G04270.1	cytosolic ribosomal protein S15, S...	uS19	17.1	10.8
S	AT3G53890.1	Ribosomal protein S21e	eS21	9.1	9.2
S	AT3G04920.1	Ribosomal protein S24e family protein	eS24	15.4	11.2
S	AT2G21580.1	Ribosomal protein S25 family protein	eS25	12.1	11.2
S	AT2G40510.1	Ribosomal protein S26e family protein	eS26	14.8	12.3
S	AT5G64140.1	ribosomal protein S28, Symbols: RPS28	eS28	7.3	11.7
S	AT1G48630.1	Receptor for activated C kinase 1B...	RACK1	35.8	6.8

[a] This column shows only an example of one r-protein encoding paralog

Moreover, we have identified several non-ribosomal proteins associated with ribosomal proteins. In addition, five eukaryotic translation factors were detected, including initiation factors eIF4A-1, eIF4A-2, eIF5A, eIF6 and the translation elongation factor eEF1B. In addition two isoforms of a protein with homology to the human receptor for activated protein C-kinase and yeast Asc1p (RACK1-B and RACK1-C; Gandin et al., 2013) and two proteins involved in tRNA aminoacylation, [a glutamyl/glutaminyl-tRNA synthetase (AT5G26710.1) and an aminoacyl tRNA synthase complex-interacting multifunctional protein 1 (AT2G40660.1)] were detected.

Mapping of phosphorylation sites in the ribosomal proteins

Total peptides were quantified before chromatography purification and selected phospho-peptide fractions were subsequently purified by SCX chromatograpy followed by IMAC using different solvent agents and then analyzed by nanoLC-MS/MS. Phospho-peptides were identified with X!Tandem and quantified by MassChroQ.

Aliquots of each of the SCX fractions corresponding to positively charged peptides were subjected to enrichment by IMAC and TiO_2 using several solvent systems and extraction methods. In order to be consistent we created two enrichment methods for IMAC, one containing 250 mM acetic acid (termed in Table 2.2-1 IMAC-1) and one containing 6% TFA (termed in Table 2.2-1 IMAC-3). An IMAC-3-TiO_2 approach was used also for selective enrichment. The SCX fractions were subjected to enrichment by each method and then analyzed by LC-MS/MS where each precursor was subjected to both CID and ETD fragmentation events. When samples were prepared by a total protein extraction protocol, the three methods IMAC-1, IMAC-3, IMAC-3-TiO_2, yielded 19 (experiment A1), 413 (experiment A2) and 1180 (mean of samples from experiment D1) unique protein identifications originating 4, 67 and 24 phosphoproteins, respectively. Considering that the IMAC-3 and the IMAC-3-TiO_2 methods identified more phosphopeptides than the IMAC-1 method, TFA was routinely used as solvent agent. However, we also observed that recovery of phosphopeptides was affected by extraction methods (Table 2.2-1). Below we highlight the most representative and accurate data from different phosphoproteomic experimental sets.

In the experiment “A”, we analyzed two similar TCA/acetone crude total extracts from NAA treated seedlings, using acetic acid or trifluoroacetic acid (TFA) as solvent agents for sample resuspension during IMAC-based selective enrichment (IMAC-1 and IMAC-3 respectively). As mentioned before, results of these analyses revealed that using TFA as solvent during preparative manipulations increased the abundance of phosphopeptides when analyzed by LC-MS/MS. Comparing with polyribosomal IP samples, where recovery of phosphopeptides was not efficient (Experiments B, C and D2, see details in Table 2.2-1), we found that IMAC in combination with TFA in the loading buffer, outperformed all other methods tested, enabling the identification of around of 67 unique phosphopeptides from high concentrated TCA/acetone total protein extracts (Table 2.2-4), indicating that higher initial protein concentrations render the analytical system more robust for phosphopeptide detection. This experimental approach identified eS6 to be the main phosphorylation target in the translational machinery under NAA conditions, represented by 20 phosphorylated hits which indicated phosphorylation at Ser231,

Ser237 and Ser240 over the two eS6 paralogs (for a complete description of eS6 phosphorylation pattern see below). Interestingly, the protein phosphatase 2A regulatory subunit (PR55) was found to be phosphorylated under NAA conditions (Experiment A2) at Ser550 and Ser560, which are located in a similar S6K1-specific phosphorylation context (RALS^{550}SITRV and RVVSRGS^{560}ES), suggesting that TOR-dependent PR55 phosphorylation may play a role in regulation of PP2A activity. Moreover, analyses of protein composition in polyribosomal immunopurified complexes (Experiment B) revealed that PR55 is bound to translational machinery in Torin-1 treated seedlings where TOR is inactive but not in NAA treated polyribosomes (TOR activation conditions).

Fortunately the experiment D1 (Trizol/IMAC3-TiO_2 experimental set up) allowed us to get a set of highly accurate data of phosphorylated peptides for both NAA and Torin-1 samples. The translationally related phosphopeptides we observed in the phosphoproteomic analysis are listed in Table 2.2-5, in which significant (i.e., with statically significant changes under NAA/Torin-1 conditions), insignificant and punctual (i.e., punctually phosphorylated with little repeatability or no significant changes under NAA/Torin-1 conditions) sites are distinguished. Phosphorylation sites were mapped using MS spectra and searching with the MASCOT engine, thus giving obvious phosphorylated residues in peptides. In some instances, however, ambiguous cases occurred, in which the nature of the phosphorylated residue could not be determined (many undistinguishable possibilities were reported by using the “or” conjunction, see “validation” column Table 2.2-5). This was the case for peptides from eS6a/eS6b that include two or more phosphorylatable Ser residues. Already reported phosphorylation sites were detected in at least three Ser of the eS6 C-terminal domain, including Ser231, Ser237 and Ser240, with mono Ser231, mono Ser240 in both paralogs and bis-phosphorylated Ser237/Ser240 in eS6a. In this case, the specific nature of the r-protein eS6a or b could be solved due to small differences in sequence identity. We also detected a new N(α)-acetylated/phosphorylated peptide located in the most proximal N-terminal Ser of eIF5A under TOR inactivation conditions. The biological significance of this N-terminal modification varies with the particular protein, with some proteins requiring acetylation for function, whereas others do not N-terminal acetylation can also affect protein stability (Hwang et al., 2010) and protein localization (Starheim et al., 2009). It has been also found that the protein synthesis activity of yeast hypo-acetylated ribosomes was decreased by 27%, as compared to that of the normal strain (Kamita et al., 2011). In addition, we also detected a phosphorylated site in eIF4A2 (Thr145) but any significant TOR-dependent change was observed.

Interestingly, the two metabolic-related enzymes fructose-2,6-bisphosphatase (FBPase) and phosphoenolpyruvate carboxylase 2 (PEP carboxylase) appear to be differentially phosphorylated upon Torin-1 treatment, with Ser303 and Ser11 becoming dephosphorylated respectively. Indeed, dephosphorylated state of these two enzymes has been correlated with higher levels of carbon fixation (PEP carboxylase) and negative effects on glycolysis (FBPase). In addition, both new phospho-sites are located in a good S6K1-specific phosphorylation context (K.SLS^{303}ASSFLIDTK.Q in FBPase and K.MAS^{11}IDAQLR.L in PEP carboxylase). Although these preliminary observations obtained in this high-throughput screen need still to be confirmed, they suggest the very interesting possibility that TORC1 signals directly impinge upon this key nodes of carbon metabolism.

2.2.3 Discussion

To summarize, we identify three phosphorylation sites in eS6 C-terminal helix that are sensitive to Torin-1 – Ser231, Ser237 and Ser 240 (Table 2.2-5). The residue Ser240 was predominantly phosphorylated upon TOR activation. However, it was not possible to distinguish which residue was more affected. Nevertheless, I conclude that phosphorylation of Ser231, Ser237 and Ser240 is regulated by TOR, because all these residues were highly phosphorylated in TOR favorable conditions in Torin-1 sensitive manner. Thus I will perform an additional set of experiments to further verify this hypothesis. The best experimental conditions are chosen and all experiments are in progress.

Table 2.2-4. Phosphopeptides identified in NAA conditions (Experiment A2-IMAC-3)

Accession	Protein	Range	Sequence	Modifi
AT5G54430.1	Adenine nucleotide alpha hydrolase...	16 - 23	K.IHHPPSPR.H	Phospho
AT1G74910.1	ADP-glucose pyrophosphorylase fami...	216 - 227	R.VSSFEALQPATR.I	Phospho
AT5G43830.1	Aluminium induced protein with YGL...	241 - 251	R.VDSSQNWAGHI.-	Phospho
AT3G22850.1	Aluminium induced protein with YGL...	238 - 246	R.VGSVQNWSK.Q	Phospho
AT5G43830.1	Aluminium induced protein with YGL...	8 - 29	K.TVANSPEALQSPHSSESAFALK.D	Phospho
AT5G43830.1	Aluminium induced protein with YGL...	214 - 233	R.VDSSGDVCGATFKVDAETKR.E	Carbami
AT2G37180.1	Aquaporin-like superfamily protein...	275 - 280	K.SLGSFR.S	Phospho
AT2G37180.1	Aquaporin-like superfamily protein...	275 - 285	K.SLGSFRSAANV.-	Phospho
AT2G37550.1	ARF-GAP domain 7, Symbols: ASP1, AGD7	184 - 198	R.GAPAKSKSSEDIYSR.S	Phospho
ATCG00140.1	ATP synthase subunit C family prot...	2 - 41	M.NPLVSAASVIAAGLAVGLASIGPGVGQGTAAGQAVEGIAR.Q	Phospho
AT1G29910.1	chlorophyll A/B bindin...	44 - 57	K.GPSGSPWYGSDRVK.Y	Phospho
AT1G29910.1	chlorophyll A/B bindin...	38 - 55	K.TVAKPKGPSGSPWYGSDR.V	Phospho
AT4G24280.1	chloroplast heat shock protein 70-...	524 - 529	K.SLGSFR.L	Phospho
AT2G21660.1	cold, circadian rhythm, and rna bi...	105 - 125	R.SGGGGGYSGGGGSYGGGGGRR.E	Phospho
AT1G20440.1	cold-regulated 47, Symbols: COR47,...	107 - 126	R.SNSSSSSSSDEEGEEKKEKK.K	Phospho
AT1G20440.1	cold-regulated 47, Symbols: COR47,...	107 - 125	R.SNSSSSSSSDEEGEEKKEK.K	Phospho
AT1G76850.1	exocyst complex component sec5, Sy...	203 - 224	R.LITESSGSPSKAEKVDNTLREK.L	Phospho
AT4G38710.2	glycine-rich protein	260 - 280	R.RREESGAANGSPPPSGGSRPR.L	Phospho
AT5G50820.1	NAC domain containing protein 97, ...	138 - 145	R.LLSSRATR.W	Phospho
AT3G05900.1	neurofilament protein-related	651 - 660	K.AIIGRSPSSK.T	Phospho
AT3G05900.1	neurofilament protein-related	656 - 673	R.SPSSKTITTEEPKEEIKV.-	Phospho
AT4G13350.1	NSP (nuclear shuttle protein)-inte...	158 - 172	R.SSPGGRSPGFETGSR.N	Phospho
AT4G05150.1	Octicosapeptide/Phox/Bem1p family ...	261 - 289	R.EVSTLSDPGSPRRDVPSPYGSTSSAPVMR.I	Phospho
AT4G05150.1	Octicosapeptide/Phox/Bem1p family ...	258 - 289	K.IQREVSTLSDPGSPRRDVPSPYGSTSSAPVMR.I	Phospho
AT5G62810.1	peroxin 14, Symbols: PEX14, ATPEX1...	310 - 327	R.SASPPAAPADSSAPPHPK.S	Phospho
AT4G37870.1	phosphoenolpyruvate carboxykinase ...	60 - 86	K.KRSAPTTPINQNAAAAFAAVSEEERQK.I	Phospho
AT2G46820.1	photosystem I P subunit, Symbols: ...	64 - 88	R.ATTEVGEAPATTTEAETTELPEIVK.T	Phospho
ATCG00710.1	photosystem II reaction center pro...	2 - 15	M.ATQTVEDSSRSGPR.S	Phospho
ATCG00710.1	photosystem II reaction center pro...	2 - 11	M.ATQTVEDSSR.S	Phospho
ATCG00270.1	photosystem II reaction center pro...	2 - 7	M.TIALGK.F	Acetyl: 1
ATCG00020.1	photosystem II reaction center pro...	2 - 8	M.TAILERR.E	Acetyl: 1
ATCG00270.1	photosystem II reaction center pro...	2 - 10	M.TIALGKFTK.D	Acetyl: 1

AT3G11330.1	plant intracellular ras group-rela...	470 - 497	R.TTSKLKTYVADVSEYLGSNSPRDPYLER.Q	Phospho
AT3G11330.1	plant intracellular ras group-rela...	20 - 26	R.LPSFTAK.S	Phospho
AT4G35100.1	plasma membrane intrinsic protein ...	270 - 280	K.ALGSFRSNATN.-	Phospho
AT1G51690.3	protein phosphatase 2A 55 kDa regu...	555 - 577	R.VVSRGSESPGVDGNTNALDYTTK.L	Phospho
AT1G51690.3	protein phosphatase 2A 55 kDa regu...	548 - 554	R.ALSSITR.V	Phospho
AT1G01050.1	pyrophosphorylase 1, Symbols: AtPP...	22 - 29	R.ILSSLSRR.S	Phospho
AT1G01050.1	pyrophosphorylase 1, Symbols: AtPP...	22 - 28	R.ILSSLSR.R	Phospho
AT4G31700.1	ribosomal protein S6, Symbols: RPS...	228 - 236	R.RSESLAKKR.S	Phospho
AT4G31700.1	ribosomal protein S6, Symbols: RPS...	237 - 250	R.SRLSSAAAKPSVTA.-	Phospho
AT5G10360.1	Ribosomal protein S6e, Symbols: EM...	237 - 249	R.SRLSSAPAKPVAA.-	Phospho
AT5G10360.1	Ribosomal protein S6e, Symbols: EM...	228 - 236	R.RSESLAKKR.S	Phospho
AT5G10360.1	Ribosomal protein S6e, Symbols: EM...	237 - 249	R.SRLSSAPAKPVAA.-	Phospho
AT1G20110.1	RING/FYVE/PHD zinc finger superfam...	277 - 285	R.SISFSSSGR.D	Phospho
AT4G17720.1	RNA-binding (RRM/RBD/RNP motifs) f...	255 - 275	R.VHLSESPKAASSTQEAERESK.L	Phospho
AT1G33470.1	RNA-binding (RRM/RBD/RNP motifs) f...	89 - 102	R.SKPSSPIHGHVGGR.G	Phospho
AT5G55850.2	RPM1-interacting protein 4 (RIN4) ...	53 - 70	K.KTGGKPGSPGKSSEGHVK.S	Phospho
AT5G55850.2	RPM1-interacting protein 4 (RIN4) ...	54 - 70	K.TGGKPGSPGKSSEGHVK.S	Phospho
AT2G39730.1	rubisco activase, Symbols: RCA	73 - 89	R.GLAYDTSDDQQDITRGK.G	Phospho
AT2G39730.1	rubisco activase, Symbols: RCA	73 - 87	R.GLAYDTSDDQQDITR.G	Phospho
AT4G39680.1	SAP domain-containing protein	430 - 446	R.DFSRSDSSVSEDGPKER.V	Phospho
AT4G39680.1	SAP domain-containing protein	434 - 446	R.SDSSVSEDGPKER.V	Phospho
AT3G14350.1	STRUBBELIG-receptor family 7, Symb...	360 - 376	K.KLDTSLSMNLRPPPSER.H	Phospho
AT3G11820.1	syntaxin of plants 121, Symbols: S...	262 - 277	R.ASSFIRGGTDQLQTAR.V	Phospho
AT1G01320.1	Tetratricopeptide repeat (TPR)-lik...	1,389 - 1,413	K.NSVVSLGKSPSYKEVALAPPGSIAK.Y	Phospho
AT5G41950.1	Tetratricopeptide repeat (TPR)-lik...	477 - 491	R.NLSGKAETMSTNVER.K	Phospho
AT1G01320.1	Tetratricopeptide repeat (TPR)-lik...	1,397 - 1,413	K.SPSYKEVALAPPGSIAK.Y	Phospho
AT5G41950.1	Tetratricopeptide repeat (TPR)-lik...	477 - 492	R.NLSGKAETMSTNVERK.T	Phospho
AT4G23040.1	Ubiquitin-like superfamily protein	357 - 369	R.TQRPPSPSLTAQR.L	Phospho
AT4G11740.1	Ubiquitin-like superfamily protein...	388 - 401	R.AQPRPPSPSLTAQR.L	Phospho
AT3G47070.1	unknown protein	57 - 73	K.KVDEKEGTTTGGRGTVR.G	Phospho
AT3G47070.1	unknown protein	58 - 76	K.VDEKEGTTTGGRGTVRGGK.N	Phospho
AT3G47070.1	unknown protein	58 - 73	K.VDEKEGTTTGGRGTVR.G	Phospho
AT5G04000.2	unknown protein	21 - 32	R.VLSPGGSKIEER.Q	Phospho
AT5G39570.1	unknown protein	337 - 349	R.SGSGDDEEGSYGR.K	Phospho
AT1G78150.3	unknown protein	177 - 201	K.QLSDAKYKEISGQNIFAPPPEIKPR.S	Phospho
AT3G01390.1	vacuolar membrane ATPase 10, Symbo...	1 - 28	-.MESNRGQGSIQQLLAAEVEAQHIVNAAR.T	Acetyl: 1

Table 2.2-5. Plant translationally-related phosphopeptides regulated by TOR

Protein	Treatment	Accession	Ortholog	Range	Sequence	Modifications	Mascot
eIF5A	Torin-1	AT1G26630.1	eIF5A	2-17	M.SDDEHHFEASESGASK.T	Acetyl: 1; Phospho: 1	55.
eIF4A2	Torin-1	AT1G54270.1	eIF4A2	138 - 148	K.VHACVGGTSVR.E	Carbamidomethyl: 4; Phospho: 8	66.
	NAA	AT1G54270.1	eIF4A2	138 - 148	K.VHACVGGTSVR.E	Carbamidomethyl: 4; Phospho: 8	61.
eS6	Torin-1	AT4G31700.1	eS6a	237 - 250	R.SRLSSAAAKPSVTA.-	Phospho: 4	49.
		AT4G31700.1	eS6a	237 - 250	R.SRLSSAAAKPSVTA.-	Phospho: 4	39.
		AT5G10360.1	eS6b	237 - 249	R.SRLSSAPAKPVAA.-	Phospho: 4	35.
	NAA	AT4G31700.1	eS6a	237 - 250	R.SRLSSAAAKPSVTA.-	Phospho: 4	49.
		AT4G31700.1	eS6a	237 - 250	R.SRLSSAAAKPSVTA.-	Phospho: 4	44.
		AT5G10360.1	eS6b	237 - 249	R.SRLSSAPAKPVAA.-	Phospho: 4	46.
		AT5G10360.1	eS6b	237 - 249	R.SRLSSAPAKPVAA.-	Phospho: 4	46.
		AT4G31700.1	eS6a	228 - 236	R.RSESLAKKR.S	Phospho: 4	55.
		AT4G31700.1	eS6a	237 - 250	R.SRLSSAAAKPSVTA.-	Phospho: 4	54.
		AT5G10360.1	eS6b	228 - 236	R.RSESLAKKR.S	Phospho: 4	47.
		AT5G10360.1	eS6b	237 - 249	R.SRLSSAPAKPVAA.-	Phospho: 4	63.
		AT4G31700.1	eS6a	237 - 250	R.SRLSSAAAKPSVTA.-	Phospho: 4	41
		AT4G31700.1	eS6a	237 - 250	R.SRLSSAAAKPSVTA.-	Phospho: 4	59.
RRM-containing protein	Torin-1	AT4G17720.1	RRM-containing protein	255 - 272	R.VHLSESPKAASSTQEAER.E	Phospho: 6	61.
	NAA	AT4G17720.1	RRM-containing protein	255 - 272	R.VHLSESPKAASSTQEAER.E	Phospho: 6	49.
		AT4G17720.1	RRM-containing protein	255 - 275	R.VHLSESPKAASSTQEAERESK.L	Phospho: 6	32.
		AT4G17720.1	RRM-containing protein	255 - 272	R.VHLSESPKAASSTQEAER.E	Phospho: 4	59.
		AT4G17720.1	RRM-containing protein	255 - 275	R.VHLSESPKAASSTQEAERESK.L	Phospho: 4	45.

2.3 Article 2: TOR and S6K1 promote translation reinitiation of uORF-containing mRNAs via phosphorylation of eIF3h

Mikhail Schepetilnikov, Eder Mancera-Martínez[1], Maria Dimitrova[1], Angèle Geldreich, Mario Keller and Lyubov A Ryabova

Institut de Biologie Moléculaire des Plantes du CNRS, Université de Strasbourg, Strasbourg Cedex, France

[1]These authors contributed equally to this work.

The EMBO Journal (2013) 32, 1087–1102
www.embojournal.org

SOURCE DATA | TRANSPARENT PROCESS

THE EMBO JOURNAL

TOR and S6K1 promote translation reinitiation of uORF-containing mRNAs via phosphorylation of eIF3h

Mikhail Schepetilnikov, Maria Dimitrova[1], Eder Mancera-Martínez[1], Angèle Geldreich, Mario Keller and Lyubov A Ryabova*

Institut de Biologie Moléculaire des Plantes du CNRS, Université de Strasbourg, Strasbourg Cedex, France

Mammalian target-of-rapamycin (mTOR) triggers S6 kinase (S6K) activation to phosphorylate targets linked to translation in response to energy, nutrients, and hormones. Pathways of TOR activation in plants remain unknown. Here, we uncover the role of the phytohormone auxin in TOR signalling activation and reinitiation after upstream open reading frame (uORF) translation, which in plants is dependent on translation initiation factor eIF3h. We show that auxin triggers TOR activation followed by S6K1 phosphorylation at T449 and efficient loading of uORF-mRNAs onto polysomes in a manner sensitive to the TOR inhibitor Torin-1. Torin-1 mediates recruitment of inactive S6K1 to polysomes, while auxin triggers S6K1 dissociation and recruitment of activated TOR instead. A putative target of TOR/S6K1—eIF3h—is phosphorylated and detected in polysomes in response to auxin. In TOR-deficient plants, polysomes were prebound by inactive S6K1, and loading of uORF-mRNAs and eIF3h was impaired. Transient expression of eIF3h-S178D in plant protoplasts specifically upregulates uORF-mRNA translation. We propose that TOR functions in polysomes to maintain the active S6K1 (and thus eIF3h) phosphorylation status that is critical for translation reinitiation.
The EMBO Journal (2013) **32,** 1087–1102. doi:10.1038/emboj.2013.61; Published online 22 March 2013
Subject Categories: signal transduction; proteins
Keywords: eIF3 subunit h phosphorylation; gravitropic response; phytohormone auxin; polyribosomes; TOR

Introduction

Eukaryotic cells respond to changing environments by utilizing various signal transduction pathways. Regulation can occur at the transcriptional level as well as post-transcriptionally, for example, via regulation of translation of specific messages (Nilsson *et al*, 2004). Regulating translation via upstream open reading frames (uORFs) in the 5′-untranslated region (5′-UTR) of mRNA is now recognised as a means of controlling potent proteins such as growth factors, protein kinases, and transcription factors (Morris and Geballe, 2000). uORFs can reduce protein expression typically by 30–80%, but have only a modest impact on mRNA levels (Calvo *et al*, 2009). uORFs are especially common in *Arabidopsis*, being present in at least 30% of full-length mRNAs (Zhou *et al*, 2010).

Short uORF length—more importantly, the short time required for translation—and a sufficient intercistronic distance between two consecutive ORFs are the main parameters boosting the reinitiation capacity of ribosomes (Luukkonen *et al*, 1995; Kozak, 2001; Hinnebusch, 2005). Reinitiation potential is also regulated by specific RNA *cis*-acting elements and *trans*-acting factors (Sachs and Geballe, 2006; Rahmani *et al*, 2009; Medenbach *et al*, 2011).

The need for rapid uORF translation may be related to problems with *de novo* recruitment of initiator tRNA ($tRNAi^{Met}$) in the ternary complex (TC; eIF2xGTPxMet-$tRNAi^{Met}$), and the 60S ribosomal subunit (60S) required for the reinitiation event. Translation initiation factors (eIFs) needed for resumption of scanning and/or recruitment of TC and 60S were proposed to remain loosely associated with the elongating ribosome for a short time of a few cycles, and, after termination, to support a subsequent initiation event (Kozak, 2001; Pöyry *et al*, 2004), thus explaining why reinitiation is precluded after a long elongation event. Reinitiation-promoting factors (RPFs) include eukaryotic initiation factor 3 (eIF3) and eIF4F (Pöyry *et al*, 2004; Cuchalová *et al*, 2010; Roy *et al*, 2010; Munzarová *et al*, 2011). eIF3 is composed of 13 distinct subunits in humans and plants, and orchestrates assembly of the 43S pre-initiation complex (43S PIC) on mRNA (Browning *et al*, 2001; Hinnebusch, 2006).

In plants, eIF3 non-core subunit h (eIF3h) and the 60S protein RPL24 increase the reinitiation competence of uORF-containing mRNAs (uORF-RNAs) encoding two families of transcriptional factors—auxin response factors (ARFs) and basic zipper transcription factors (bZIPs)—via as yet unknown mechanisms (Kim *et al*, 2004; Nishimura *et al*, 2005; Zhou *et al*, 2010). Critically, translation reinitiation and auxin-mediated organogenesis are compromised severely by mutations in either eIF3h or RPL24. eIF3 is recruited to promote a special case of reinitiation after long ORF translation by the Cauliflower mosaic virus protein translational transactivator/viroplasmin (TAV; Park *et al*, 2001). TAV accomplishes reinitiation via retention in polyribosomes (polysomes) of eIF3 and a novel reinitiation supporting protein (RISP) during the long elongation event, and reuse of these factors for reinitiation (Park *et al*, 2001; Thiébeauld *et al*, 2009). More recent evidence has linked TAV to activation of target-of-rapamycin (TOR) in plants (Schepetilnikov *et al*, 2011). When activated by TAV, TOR

*Corresponding author. Institut de Biologie Moléculaire des Plantes du CNRS, Université de Strasbourg, 12, rue du General Zimmer, Strasbourg Cedex 67084, France. Tel.: +33 3 67 15 53 31;
Fax: +33 3 88 61 44 42; E-mail: lyuba.ryabova@ibmp-cnrs.unistra.fr
[1]These authors contributed equally to this work.

Received: 7 January 2013; accepted: 15 February 2013; published online: 22 March 2013

associates with polysomes, ensuring the S6 kinase 1 (S6K1) and RISP phosphorylation that is essential for virus-activated reinitiation.

TOR—a critical sensor of nutritional and cellular energy and a regulator of cell growth (Gingras *et al*, 2001; Sengupta *et al*, 2010; Dobrenel *et al*, 2011)—is a large serine/threonine protein kinase. Mammalian TOR (mTOR) modulates the activity of two main substrate classes: 4E-binding proteins (4E-BPs) and protein kinases of RPS6 (S6Ks; Ma and Blenis, 2009). Recently, 4E-BPs were implicated in mTOR-dependent translation initiation control of mRNAs with 5′ terminal oligopyrimidine (TOP) motifs within the leader region (Thoreen *et al*, 2012). eIF3 works as a scaffold for mTOR and S6K1 binding (Holz *et al*, 2005). When inactive, S6K1, but not TOR, binds the non-polysome-associated eIF3 complex. Upon activation, TOR associates with eIF3 and phosphorylates S6K1, triggering its dissociation from eIF3 and further activation.

The *Arabidopsis* genome contains a single *TOR* gene (Menand *et al*, 2002), two *RAPTOR* genes (Menand *et al*, 2002; Mahfouz *et al*, 2006) and LST8 genes (Moreau *et al*, 2012) that encode components of the TOR complex. A TOR knockout mutant in *Arabidopsis* is embryo lethal, and altered TOR expression affects plant growth (Menand *et al*, 2002; Deprost *et al*, 2007). The *Arabidopsis* genome encodes two S6K1 homologues, S6K1 and S6K2; S6K1 is phosphorylated by TOR at hydrophobic motif residue T449 (Zhang *et al*, 1994; Schepetilnikov *et al*, 2011), while 4E-PBs remain illusive in plants.

An important question is what are the upstream effectors that trigger TOR activation in plants? Our data show that the phytohormone auxin can trigger TOR signalling pathway activation, thus providing a tool to study the role of TOR in plant translation control. Here, we uncover the role of the TOR signalling pathway in promoting reinitiation after uORF translation in *Arabidopsis*. Our data show that TOR and S6K1 contribute to assembly of reinitiation-competent ribosomes in response to auxin. We suggest that TOR functions in reinitiation via maintenance of eIF3h phosphorylation status in polysomes.

Results

Interaction of eIF3 with TOR or S6K1 is regulated by phytohormone auxin and TOR inhibitor, Torin-1

First, we asked if TOR and S6K1 form part of eIF3-containing complexes in *Arabidopsis*. Both TOR and S6K1 associate with eIF3-bound complexes immunoprecipitated with anti-eIF3c antibodies from *Arabidopsis* suspension cultures (Figure 1A). TOR immunoprecipitates contain an eIF3c marker, but not S6K1, suggesting that the TOR/eIF3 immunoprecipitation complex does not contain significant amounts of S6K1. Raptor—an important partner of TOR—was also found within TOR immunoprecipitates. In control experiments, the above proteins were not detected in non-immune RS complexes, and the control protein—ADP-ribosylation factor-GTPase (ARF GTPase)—did not co-immunoprecipitate with either TOR or eIF3c.

Then, we examined the phytohormone auxin as an upstream TOR effector. To verify auxin activation of TOR, we used Torin-1, which inhibits TOR phosphorylation activity (Thoreen *et al*, 2009; Schepetilnikov *et al*, 2011).

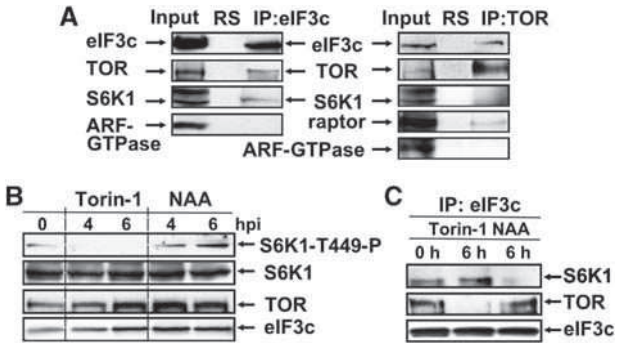

Figure 1 Auxin-induced phosphorylation of *At*S6K1 at TOR-specific residue T449 regulates interaction with eIF3. (**A**) eIF3c or TOR immunoprecipitated from WT extracts was assayed for complex formation between eIF3c, TOR, S6K1, raptor, and ARF-GTPase. Input, 5% of immunoprecipitation (IP) or normal rabbit serum (RS). (**B**) Suspension-culture cells treated with NAA or Torin-1 for 0, 4, and 6 h, lysed assayed by immunoblot analysis. (**C**) eIF3c immunoprecipitated from extracts in (**B**) and assayed for association with TOR and S6K1 by immunoblotting. Source data for this figure is available on the online supplementary information page.

Torin-1 abolished phosphorylation of recombinant *At*S6K1 at TOR-specific residue T449 in *Arabidopsis* extract, and triggered its rapid dephosphorylation (Supplementary Figure S1A). Next, the effect of the auxin analogue 1-naphthylacetic acid (NAA) or Torin-1 on S6K1 phosphorylation at T449, and TOR and S6K1 association with eIF3 was followed in stationary-phase suspension cultures. Phosphorylation of recombinant S6K1 at T449 was visualised by western blot using phospho-specific antibodies against mS6K1 phosphorylated at T389, which specifically recognises *At*S6K1-T449-P (Schepetilnikov *et al*, 2011). Although expression of S6K1 did not change significantly upon NAA treatment, the basal level of S6K1 phosphorylation at T449 increased about seven-fold 6 h after treatment, while it fell below the limit of detection upon Torin-1 treatment (Figure 1B; for quantification, see Supplementary Figure S1B). Thus, auxin can induce phosphorylation of S6K1 at TOR-specific T449. TOR was present in eIF3c immunoprecipitates only when suspension cultures were treated with auxin (Figure 1C). In contrast, S6K1 accumulated in the eIF3c pellet after a 6h incubation with Torin-1, but no S6K1 precipitation was seen 6 h after NAA treatment.

Overall, these results suggest that eIF3 associates with S6K1 upon Torin-1 treatment, and with TOR in the presence of auxin. Thus, plant eIF3-containing complexes can interact with TOR and S6K1 in a defined temporal order and may serve as a platform for S6K1 phosphorylation by TOR, likely within non-polysomal PICs, as suggested in mammals (Holz *et al*, 2005).

Auxin stimulation of polysomal loading of uORF-containing mRNAs in planta

Our studies of CaMV TAV-mediated polycistronic translation in plants revealed that the TOR signalling pathway is essential for activation of reinitiation after long ORF translation (Schepetilnikov *et al*, 2011). Here, we asked whether TOR could modulate the reinitiation capacity of uORF-containing mRNAs such as *ARF3*, *ARF5*, *ARF6*, *ARF11*, and *bZIP11* (Figure 2A). Translation of these messages requires reinitiation to translate the main ORF (Zhou *et al*, 2010). To determine the

effects of TOR on initiation *per se*, we included uORF-less mRNAs encoding actin or an auxin/indole-3-acetic acid 6 (IAA6) transcriptional inhibitor. Notably, the mRNAs used do not contain TOP motifs (Thoreen *et al*, 2012).

We quantified polysomal levels of selected endogenous uORF-mRNAs under conditions that affect TOR activation differentially *in planta*. mRNA mobilization was monitored by semi-quantitative RT–PCR (sqRT–PCR) of mRNA in polysome gradient fractions in extracts obtained from *Arabidopsis* seedlings treated with NAA or Torin-1 7 days after germination (dag). Possible translation repression mediated by uORF2b within the leader of *bZIP11* mRNA in response to sucrose was suppressed by using low sucrose levels (Wiese *et al*, 2004).

In non-treated seedlings, accumulation in polysomes of *bZIP11*, *ARF3, ARF5, ARF6*, and *ARF11* mRNAs was significantly lower than in ribosomal subunit fractions, while *actin* and *IAA6* mRNAs accumulated exclusively in polysomes (Figure 2B; band density quantification of results shown in Supplementary Figure S2A; for sqRT–PCR specificity control, see Supplementary Figure S2B). This correlates with the inhibiting effect of uORFs diminishing *ARF3* and *ARF5* mRNA translation levels to 50 and 12–15% in *Arabidopsis* protoplasts, respectively (Nishimura *et al*, 2005). Surprisingly, all our uORF-containing mRNAs, including *bZIP11* mRNA, accumulated to a high extent in polysome fractions in response to auxin (Figure 2B, WT/NAA). In contrast, TOR inactivation by Torin-1 reduced their accumulation in polysomes, and shifted uORF-mRNAs from polysomes to ribosomal fractions, mainly 40S (fractions 7 and 8). Note that Torin-1 did not abolish uORF-mRNA loading on 40S PICs in our conditions. Torin-1 did not affect the first initiation event significantly—heavy polysomal loading of both *actin* and *IAA6* mRNAs was practically the same. In contrast, Torin-1 greatly impaired uORF-mRNA complex formation with heavy polysomes, while light polysomes—with probably 2–3 ribosomes sitting on the uORFs—still formed. We concluded that uORF-mRNA abundance in polysomes is regulated by auxin in a TOR-dependent manner, not only for auxin-related genes, but also for *bZIP11*, suggesting a role for TOR in translation of these mRNAs.

To verify that the effect of auxin on polysomal loading of uORF-mRNAs was mediated by TOR activation, TOR was inactivated by Torin-1 in seedlings treated with NAA. Supplementary Figure S3A and B demonstrates that auxin treatment failed to support polysomal loading of uORF-mRNAs in conditions of TOR inactivation (WT/NAA + Torin-1), as compared with NAA treatment (WT/NAA). Again, loading of *Actin* and *IAA6* mRNAs was affected only slightly by NAA/Torin-1 application.

Comparative analysis of total mRNAs in extracts just prior to loading on sucrose gradients revealed no significant difference in mRNA levels 8 h after NAA or Torin-1-treatment (Figure 2C). In contrast, *IAA6* mRNA levels were significantly higher after NAA treatment, but there was no impact on polysomal loading.

Next, we verified whether auxin can promote protein synthesis from uORF-containing *ARF5::GFP* mRNA in *ARF5:ARF5::GFP* transgenic seedlings. There was a significant increase in accumulation of ARF5::GFP fusion protein in response to auxin, but not in the presence of Torin-1 (Figure 2E). To monitor the phosphorylation status of endogenous TOR during 4, 6, 8, and 10 h of auxin or Torin-1 treatment, we used phospho-specific antibodies against mTOR phosphorylated at S2448 (see Schepetilnikov *et al*, 2011; S6K1 is the major protein kinase responsible for S2448 phosphorylation of mTOR (Chiang, 2005); S2448 appears to be conserved in *Arabidopsis* TOR (see alignment in Figure 2D)). The partial TOR phosphorylation RxxS/T site (TGRDFS) can be phosphorylated as well (Jastrzebski *et al*, 2011). Strikingly, auxin triggered TOR phosphorylation after 4–6 h of NAA application, without altering TOR or eIF3c protein levels, while Torin-1 triggered TOR dephosphorylation (Figure 2E, TOR-P). In contrast, there was no significant effect of auxin on *Arabidopsis* ERK1/ERK2-like MAPK phosphorylation upon auxin application during 10 h (Supplementary Figure S3C), as shown by western blot with phospho-specific antibodies raised against *Arabidopsis* MPK3/4/6-P (Asai *et al*, 2002).

An effect of *ARF* mRNA leaders on GFP protein levels was studied in transgenic plants, with GFP placed downstream of the authentic *ARF* promoter/5′-UTR (Rademacher *et al*, 2011). As expected, GFP levels were elevated after auxin treatment (Supplementary Figure S3D).

TOR is phosphorylated and recruited to polysomes in response to auxin, while Torin-1 triggers TOR and S6K1 dephosphorylation, resulting in replacement of TOR by S6K1 in polysomes

Although reinitiation efficiency depends on retention of RPFs in polysomes after the preceding initiation event, TOR pathway activation also seems important. We analysed the distribution of TOR and S6K1 between non-polysomal 48S PIC and polysomes in extracts of *Arabidopsis* seedlings treated with NAA or Torin-1 for 8 h (Figure 3). The initial state of seedlings without treatment showed that TOR and S6K1 are distributed between polysomal and ribosomal fractions (Figure 3A), with TOR and S6K1 detected in 40S ribosomal subunit fractions, while in 80S and light polysomes TOR levels are at the limit of detection, and S6K1 seems to preferentially occupy polysomes. Interestingly, in response to auxin, TOR is phosphorylated and associates not only with 80S and ribosomal subunit fractions as expected, but also with polysomes (Figure 3B). Although S6K1 association with polysomes was fully disrupted in NAA-treated seedlings, we noted that some S6K1-T449-P remained associated with ribosomal fractions. Torin-1 treatment triggers TOR dephosphorylation and dissociation from polysomes and binding of inactive S6K1 instead (Figure 3C). Inactive S6K1 associated with 40S as well. We noted that phosphorylated TOR could be detected in 40S fractions—most likely due to incomplete TOR inactivation by Torin-1, which may explain why Torin-1 had no major effect on the first initiation event. We conclude that reinitiation after uORF translation may require active TOR loading onto polysomes. In control experiments, RNase treatment resulted in the disruption of polysomal complexes and the concomitant redistribution of S6K1 and TOR to lighter fractions of sucrose gradients (Figure 3D and E).

Partial depletion of TOR in planta maintains inactive S6K1 bound to polysomes defective in uORF-mRNA recruitment

We next tested whether TOR inactivation *in planta* is able to impair reinitiation events specifically. As an assay system we

employed plants ectopically expressing an RNAi construct targeting the TOR FRB domain (TOR-deficient RNAi line 35-7; Deprost *et al*, 2007; Schepetilnikov *et al*, 2011). Although TOR and *TOR* transcript accumulation are reduced by ~10-fold, mesophyll protoplasts derived from these plants promote translation initiation of uORF-less reporters as efficiently as wild-type protoplasts (Schepetilnikov *et al*, 2011), suggesting that the remaining TOR levels are sufficient to promote initiation events.

Accordingly, under conditions of partial TOR depletion (*TOR RNAi*) polysomal loading of uORF-less mRNAs revealed no significant differences in either *actin* or *IAA6* RNA with

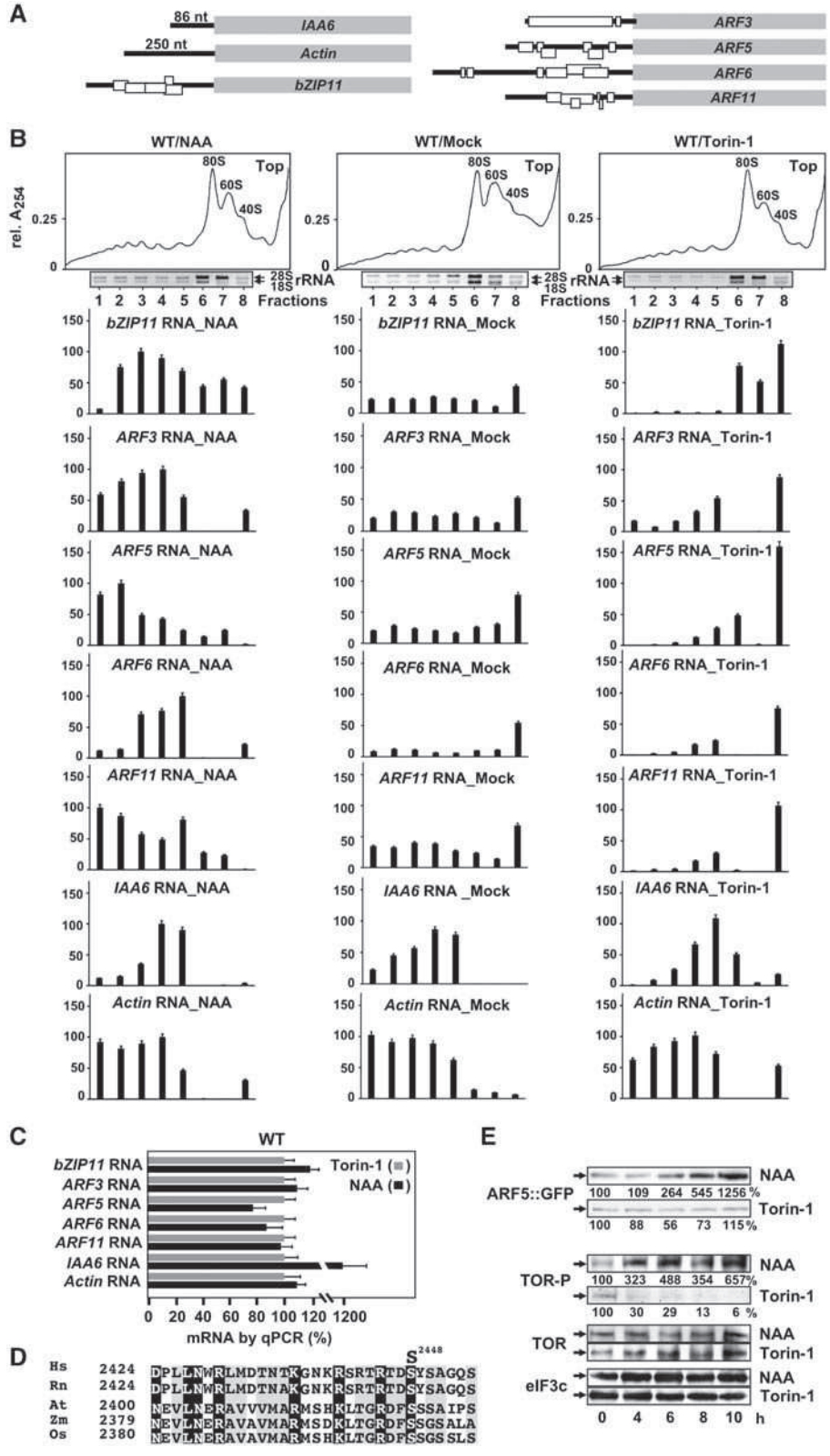

WT seedlings (Figure 2B), under any of the conditions applied (Mock/NAA/Torin-1 data shown in Figure 4A and Supplementary Figure S4A). In contrast, polysomal loading of uORF-mRNAs was reduced significantly in both non-treated (*TOR RNAi*/Mock) and NAA-treated conditions (cf Figures 2B and 4A). However, Torin-1 application reduced these levels even further.

In *TOR RNAi* seedlings, auxin treatment for 8 h augmented total *ARF* and *IAA6* mRNA levels as compared with after Torin-1 application (Figure 4B). As shown in Supplementary

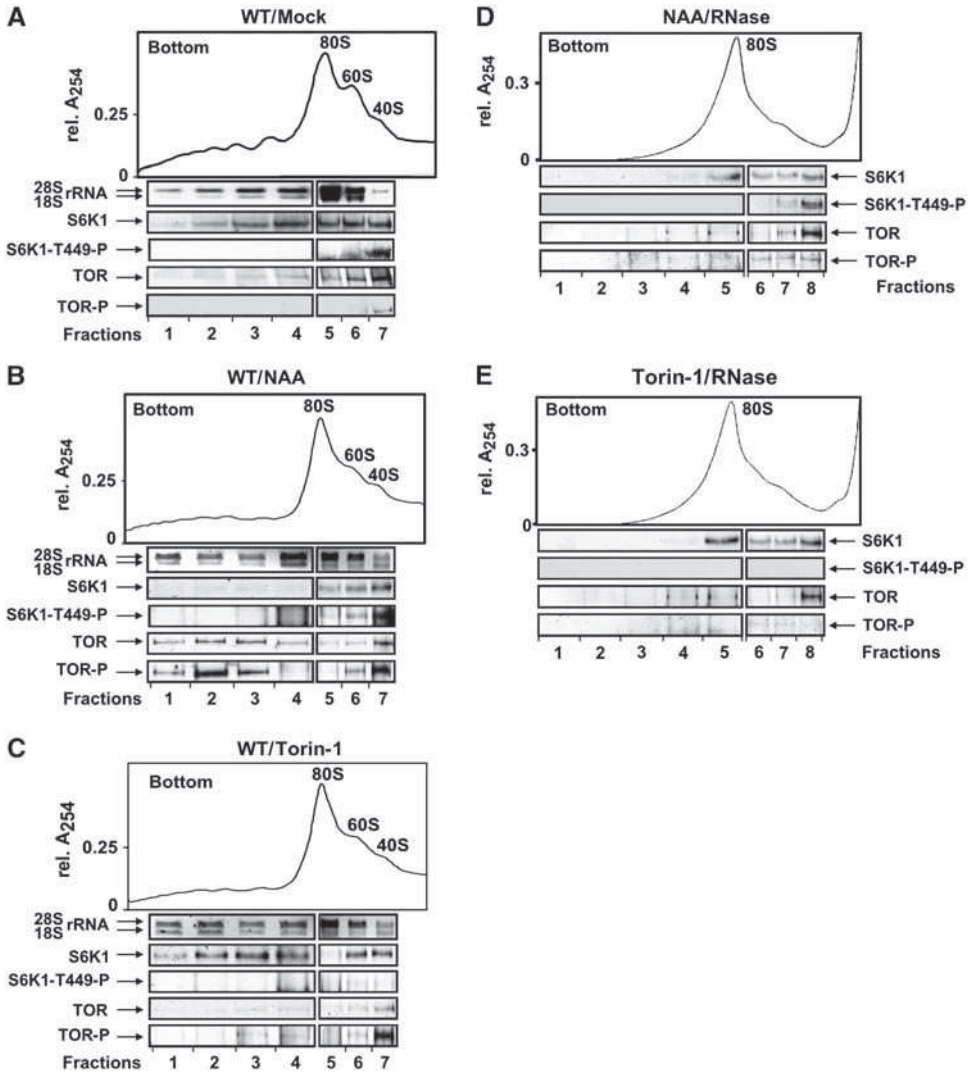

Figure 3 TOR and S6K1 are loaded on polysomes in an NAA- and Torin-1-sensitive manner. (**A**–**C**) Ribosomal profiles obtained from extracts prepared from 7-dag seedlings treated (or not, **A**) with either auxin (NAA, **B**) or Torin-1 (**C**) for 8 h. In all, 1 ml (1V, 80S/60S/40S) and 2 ml (2V, polysomes) aliquots were precipitated with 10% TCA; rRNA was analysed by agarose gel electrophoresis, and S6K1/TOR by immunoblot. Left (2V) and right (1V) panels below each profile are images from the same gel. Data shown are representative of three independent blots. (**D**, **E**) Ribosomal profiles of polyribosomes and ribosomal species from extracts prepared from auxin treated with RNase A (**D**) and Torin-1 treated with RNase A (**E**). Source data for this figure is available on the online supplementary information page.

Figure 2 uORF-mRNA abundance in polysomes is regulated by auxin and Torin-1. (**A**) Schematic representation of mRNAs coding for ARFs, bZIP11, IAA6, and Actin (*open rectangles* uORFs). (**B**) Distribution of mRNAs—*ARF3*, *ARF5*, *ARF6, ARF11*, *bZIP11*, *IAA6* and *Actin* analysed in polysome gradient fractions from extracts prepared from 7-dag seedlings treated (or not, Mock) with either auxin (NAA) or Torin-1 for 8 h. A set of graphs shows quantification of semi-quantitative RT–PCR (sqRT–PCR; Supplementary Figure S2A) corrected for polysome volume in non-, or NAA-, or Torin-1-treated ribosomal profiles. The highest value of each WT/NAA polysome-bound mRNA was set as 100%. Error bars indicate standard deviation of the mean of three replicates. (**C**) Quantitative RT–PCR (qRT–PCR) of each mRNA in total extracts as in (**B**). The RNA value in WT/Torin-1 extracts was set as 100%. Values, expressed in arbitrary units, are averages of two replicates, and error bars indicate s.d. (**D**) Alignment of phosphorylation site patterns from TOR homologues *Human*, *Rattus norvegicus*, *Arabidopsis*, *Zea mays*, and *Oryza sativa*. The human phosphorylation site S2448 within the motif is indicated. Similar residues are printed in reverse type and conserved residues are shaded in agreement with Blossom 62 and Jonson amino-acid substitution matrixes. (**E**) Time course of ARF5::GFP accumulation in 7-dag seedlings expressing GFP tag fused to *ARF5* under the control of the natural promoter (*ARF5:ARF5::GFP*) before (0 h) and after transfer to medium with NAA or Torin-1 analysed by immunoblot with anti GFP ABs (see quantification below the blot line). TOR-P, TOR, and eIF3c protein values in above conditions assayed by immunoblot and ARF5::GFP were corrected for loading control (LC; TOR phosphorylation was quantified). The value at 0 h (no incubation) for each line was set as 100%. Data shown are the means of three independent blots. Source data for this figure is available on the online supplementary information page.

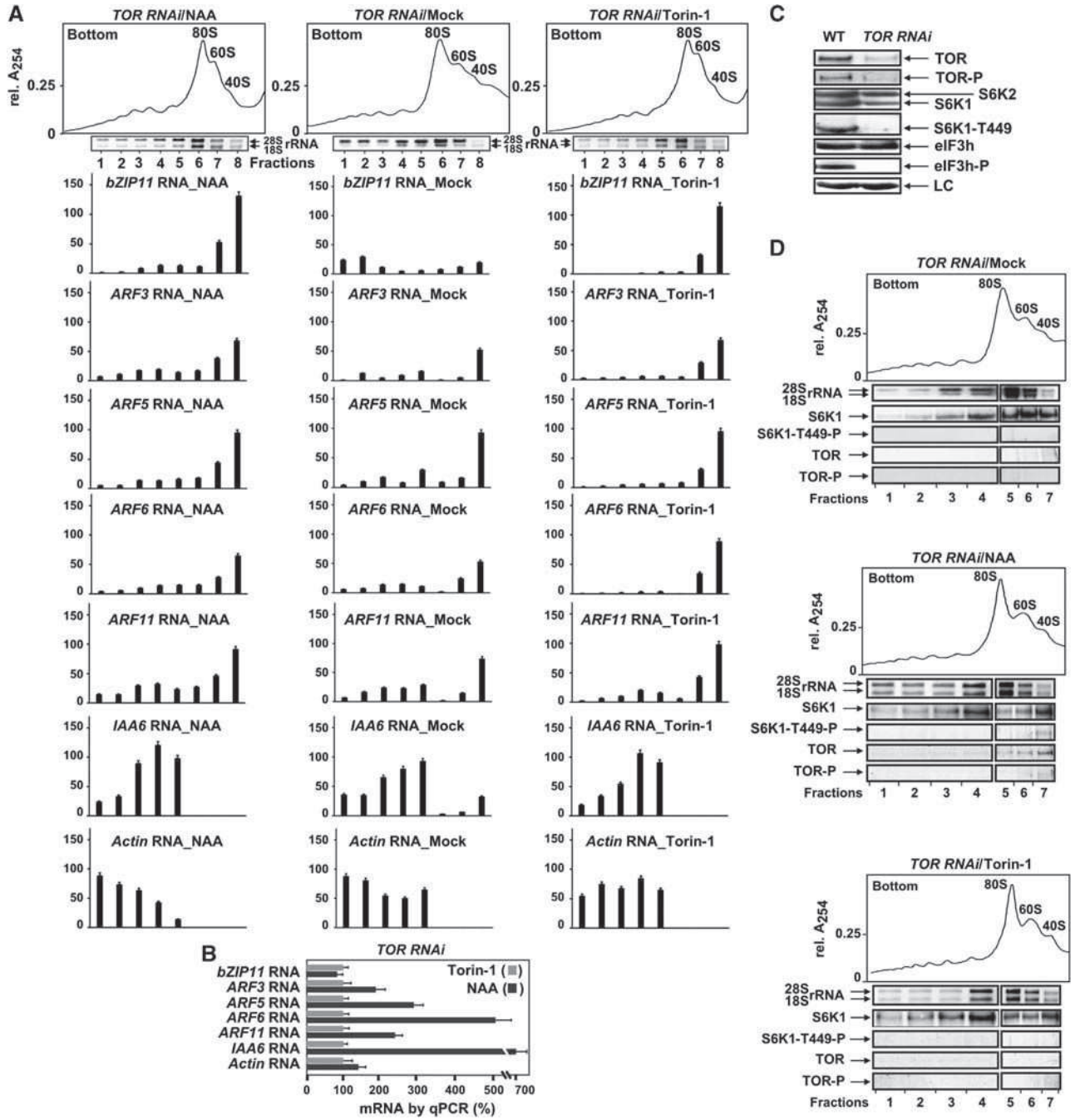

Figure 4 Polysomal loading of both uORF-mRNAs and TOR is impaired in *TOR RNAi* plants. (**A**) Comparison of uORF-RNA accumulation in polysomes in extracts prepared from 7-dag *TOR RNAi* seedlings treated (or not, Mock) with NAA or Torin-1 for 8 h. A set of graphs shows quantification of sqRT–PCR (Supplementary Figure S4A) corrected for polysome volume in non-, or NAA-, or Torin-1-treated ribosomal profiles. The highest value of each mRNA in polysomes from NAA/WT plants (Figure 2B) was set as 100%. Error bars indicate s.d. of the mean of three replicates. (**B**) qRT–PCR of mRNAs in total extracts prepared as in (**A**). The RNA value in *TOR RNAi*/Torin-1 extracts was set as 100%. Values are averages of three replicates. (**C**) Immunoblot analysis of TOR, S6K1, and eIF3h phosphorylation, as well as their accumulation levels in the control line (WT) and the TOR-deficient RNAi line. LC, loading control. (**D**) Ribosomal profiles from *TOR RNAi* were obtained as in (**B**). In all, 2 ml (2V, polysomes) and 1 ml (1V, 80S/60S/40S) were used to monitor distribution of rRNA on agarose gels and S6K1/TOR by immunoblot. Left (2V) and right (1V) panels of rRNA gel and immunoblot are from the same gel. Source data for this figure is available on the online supplementary information page.

Figure S4C, auxin can stimulate *ARF*, in contrast to *bZIP11* mRNAs, while after about 8 h *ARF* mRNAs become unstable and their levels drop to those in Mock seedlings. Similarly, auxin upregulates *ARF4* transiently in *Arabidopsis* plants (Marin *et al*, 2010). However, upon partial TOR depletion the auxin effect on *ARF* mRNA accumulation was delayed by about 2 h, resulting in elevated *ARF* mRNA levels at 8 h as compared with WT/NAA conditions (Supplementary Figure S4E). But the increase in *ARF*-mRNA levels in *TOR RNAi* seedlings failed to significantly shift uORF-RNA loading from 40S to polysomes (Figure 4A). Again, a seven-fold increase in *IAA6* mRNA levels did not further improve polysomal loading of this mRNA.

Next, we examined TOR and S6K1 levels and their phosphorylation status in *TOR RNAi* seedlings. Phosphorylated TOR and S6K1 were both detected in WT plants, while TOR levels were at the limit of detection in TOR-deficient plants (Figure 4C). As for phosphorylation of the TOR-dependent substrate S6K1, phosphothreonine 449 was high in WT plants, and below the limit of detection in *TOR RNAi* (see also Schepetilnikov *et al*, 2011). Accordingly, TOR partial depletion revealed defects in polysomal loading of mRNAs that require reinitiation, but is TOR present within polysomes in *TOR RNAi* plants? Strikingly, regardless of the conditions applied—mock, NAA, and Torin-1 (Figure 4D)—polysomes were prebound exclusively by S6K1 in its inactive dephosphorylated state. TOR association with ribosomal subunits could be detected after NAA treatment, but was below the limit of detection in Torin-1 conditions. Accordingly, *TOR RNAi* extracts were not active in *in vitro* phosphorylation of recombinant S6K1 (Supplementary Figure S1A, right panel).

Mutation of reinitiation factor eIF3h abolishes polysomal association of uORF-RNAs in the presence of a functional TOR signalling pathway

Translation initiation events are not reduced in *eif3h-1* plants (carrying carboxyl-terminal truncation alleles of eIF3h), but there is a serious defect in translation of uORF-mRNAs (Roy *et al*, 2010). Accordingly, polysomal loading of *ARF* and *bZIP11* mRNAs was fully abolished in non- (data not shown) and NAA/Torin-1-treated conditions (Figure 5A; band density quantification of results shown in Supplementary Figure S5A) in contrast to the recruitment of *actin* and *IAA6* mRNAs into polysomes in all conditions. Note that total mRNA levels in the *eif3h-1* mutant increased still further after 8 h of NAA treatment (Figure 5B), indicating that mRNA turnover is not responsible for the decrease in uORF-mRNA loading onto polysomes.

In *eif3h-1* seedlings lacking full-length eIF3h, the level of TOR and S6K1 as well as their phosphorylation status was largely unaffected (Figure 5C). Neither TOR/S6K1 phosphorylation status nor their ordered binding to polysomes in *eif3h-1* plants were significantly impaired: phosphorylated TOR was found in polysomes in response to NAA, and S6K1 was found after Torin-1 application (Figure 5D). Thus, while mRNA reinitiation capacity is severely affected in *eif3h-1* mutants, normal TOR signalling pathway behaviour was unimpaired. This led us to suggest that eIF3h functions downstream of TOR and S6K1 in promoting reinitiation, raising the question of whether eIF3h is part of the TOR pathway.

Finally, we compared total polysomes from WT, *TOR RNAi*, and *eif3h-1* treated with NAA or Torin-1 by superimposition of polysomal profiles (Supplementary Figure S5B). Interestingly, heavy polysomes in WT plants are often less pronounced in *TOR RNAi* or *eif3h-1* mutant plants, and small, but reproducible decrease in polysomal levels in response to Torin-1 was detected.

Auxin treatment of Arabidopsis seedlings triggers eIF3h phosphorylation and binding to polysomes in Torin-1-sensitive manner

Comparing plant and mammalian eIF3h sequences revealed similar motifs (REKNFS^{178}/KEKDFS^{183}, Figure 6A)—a pattern found in many Akt or S6K1 substrates (R/KxR/KxxS/T)—suggesting eIF3h phosphorylation via TOR signalling. Using the crystallographic structure of the MPN domain of hMov34 as template, a 3D model of *Arabidopsis* eIF3h was generated (Sali *et al*, 1995); S178 is positioned within a specific loop spanning well-conserved residues in the N-terminal domain, suggesting high accessibility for phosphorylation (Figure 6B). In 2D western blots of extracts prepared from WT seedlings treated with either auxin or Torin-1 (Figure 6C), one major phosphoisoform was identified by eIF3h antibodies in addition to the eIF3h spot, which was present only upon Torin-1 application. Phospho-specific antibodies confirmed the opposing effects of NAA and Torin-1 on eIF3h phosphorylation by recognising an eIF3h-P spot mainly in extracts treated with NAA (Figure 6C). Strikingly, in TOR-deficient extract (*TOR RNAi*), where S6K1 phosphorylation was significantly reduced, phosphorylation of eIF3h was also impaired (Figure 4C), strongly suggesting that eIF3h is a novel target of the TOR signalling pathway.

We next studied whether eIF3h, like TOR, is targeted to polysomes in response to auxin. Without treatment, eIF3h was found in sucrose gradient fractions of light polysomes and, in phosphorylated state (visualised by phospho-specific anti-(R/KxR/KxxS/T-P) antibodies), in 80S and ribosomal subunit fractions (Figure 6D). Strikingly, in response to auxin treatment, a significant fraction of phosphorylated eIF3h was found co-sedimenting with polysomes (Figure 6E). These signals are specific for eIF3h, and were not observed in extracts prepared from *eif3h-1* plants (Figure 6G). Importantly, unlike with auxin, we detected no eIF3h in polysomes after Torin-1 treatment; however, phosphorylated eIF3h co-sedimented with ribosomal subunits, again suggesting that Torin-1 did not fully abolish TOR phosphorylation in *Arabidopsis* seedlings in our conditions (Figure 6E).

Next, we monitored eIF3h in polysomal and non-polysomal complexes from TOR RNAi seedlings separated by sucrose gradient sedimentation (Figure 6F). As with TOR in *TOR RNAi* polysomes (Figure 4D), we found no eIF3h in polysomes, further suggesting that TOR is required for both eIF3h phosphorylation and association with polysomes. Again, eIF3h was found in ribosomal subunit fractions and was phosphorylated after NAA application, or dephosphorylated if Torin-1 was applied. As expected, full-length eIF3h was not detected in polysomes or non-polysomal fractions of *eif3h-1* mutant seedlings under any conditions tested (Figure 6G). To gain further evidence that eIF3h is the downstream target of TOR/S6K1, we show that eIF3h co-immunoprecipitates with S6K1 and/or TOR in *Arabidopsis* extracts (Figure 6H). In addition, S6K1 can interact physically with eIF3h as demonstrated by the yeast two-hybrid system (Supplementary Figure S6).

Reinitiation is upregulated by eIF3h phosphorylation in Arabidopsis protoplasts

To study directly TOR and eIF3h involvement in translation reinitiation, we first tested whether transient expression of a reporter gene harbouring a single uORF within the leader region is sensitive to Torin-1. Protoplasts prepared from *Arabidopsis* suspension cultures were transformed with two reporter plasmids: p*monoGFP*, containing a single GFP ORF (control for transformation efficiency), and either p*MAGRIS-GUS* with GUS (β-glucuronidase) reporting reinitiation after

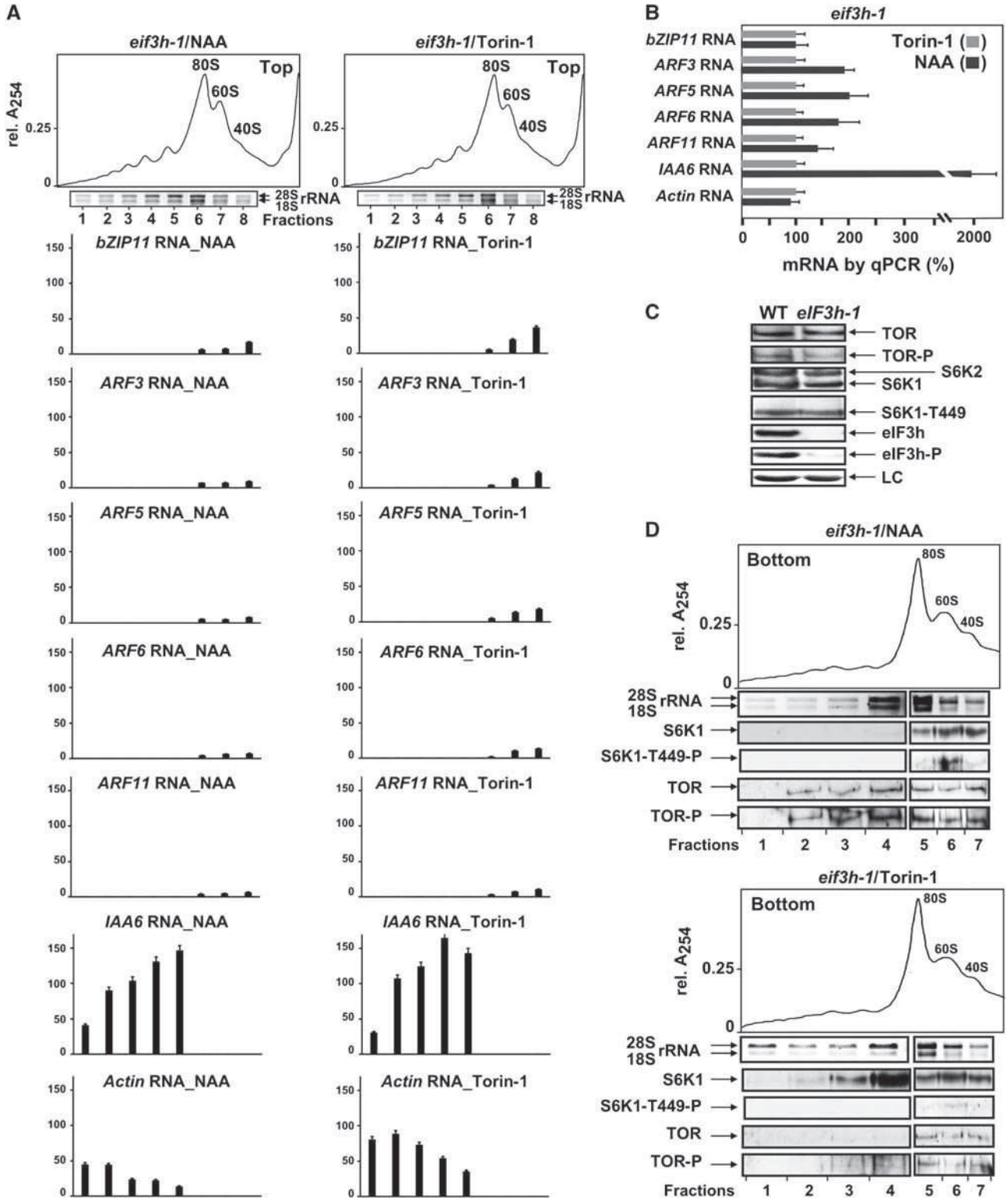

Figure 5 Polysomal loading of uORF-mRNAs, but not TOR signalling, is impaired in *eif3h-1* plants. (**A**) Comparison of uORF-RNA accumulation in polysomes in extracts prepared from 7-dag *eif3h-1* seedlings treated for 8 h with NAA or Torin-1. Quantification of sqRT–PCR data (Supplementary Figure S5A) corrected for polysome volume in NAA- or Torin-1-treated ribosomal profiles. The highest value of each mRNA in NAA/WT polysomes (Figure 2B) was set as 100%. Error bars indicate s.d. of the mean of two replicates. (**B**) qRT–PCR of mRNAs in total *eif3h-1* extracts prepared as in (**A**). The RNA value in *eif3h-1*/Torin-1 extracts was set as 100%. Each value is the average of two replicates. (**C**) Immunoblot analysis of TOR, S6K1, and eIF3h phosphorylation, as well as their accumulation levels in WT and the *eif3h-1* line. LC, loading control. (**D**) Ribosomal profiles from *eif3h-1* obtained as in (**A**). In all, 2 ml (2V, polysomes) and 1 ml (1V, 80S/60S/40S) were used to monitor rRNA and S6K1/TOR distribution by immunoblot. Left (2V) and right (1V) panels of rRNA gel and immunoblot are from the same gel. Source data for this figure is available on the online supplementary information page.

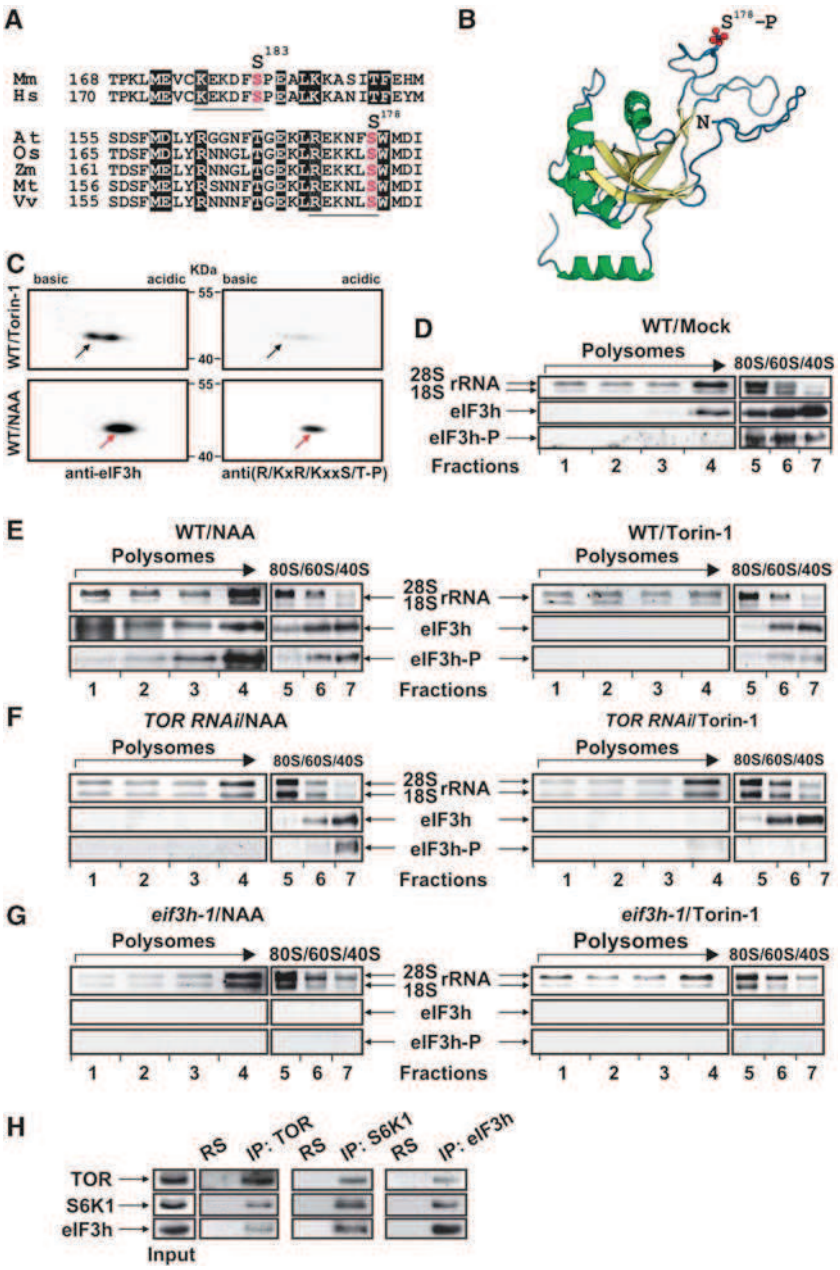

Figure 6 Auxin triggers eIF3h phosphorylation and association with polysomes in a Torin-1-sensitive manner. (**A**) Alignment of phosphorylation site patterns from eIF3h homologues *Mus musculus*, *Homo sapiens*, *Arabidopsis*, *Oryza sativa*, *Zea mays*, *Medicago truncatula*, and *Vitis vinifera*. Akt/S6K1 phosphorylation site consensus (R/KxR/KxxS/T) within the motif is underlined (putative phosphorylation residue in red). (**B**) The putative *At*eIF3h 3D structure was generated by PyMOL. The S178-P position within the conserved loop shown in (**A**) is highlighted in red, residues predicted to fold as helixes in green and β-sheets in yellow. (**C**) WT/NAA and WT/Torin-1 protein extracts were resolved in two dimensions and revealed by western blot with anti-eIF3h or anti-(R/KxR/KxxS/T-P) antibodies. Molecular masses are indicated. Arrow, eIF3h-P. (**D–G**) Ribosomal profiles from WT (**D**) not treated or WT, *TOR RNAi*, *eif3h-1* treated with NAA or Torin-1 (**E–G**, respectively) were obtained as in (Figure 3) and indicated by distribution of rRNA. In all, 2 ml (2V, polysomes) and 1 ml (1V, 80S/60S/40S) were used to monitor distribution of rRNA by agarose gel and eIF3h/eIF3h-P by immunoblot with antibodies as in (**C**). Left (2V) and right (1V) panels of rRNA gel and immunoblot are from the same gel. (**H**) Extracts prepared from WT seedlings were used for immunoblotting of eIF3h, TOR, or S6K1 present in Input, normal rabbit serum (RS), and the entire immunoprecipitate (IP). Source data for this figure is available on the online supplementary information page.

translation of the 6-amino-acid peptide MAGRIS, or p*monoGUS*, with GUS indicating initiation efficiency (Figure 7A). The 7-codon uORF MAGRIS is highly permissive for reinitiation in protoplasts and its translation does not reduce reinitiation of translation of further downstream ORF in mock conditions (Ryabova and Hohn, 2000).

To investigate the percentage of scanning ribosomes that could initiate at the MAGRIS uORF start codon, and thus would need to reinitiate to translate GUS, we employed a specific uORF from the *AdoMetDC* gene (Ruan *et al*, 1996) encoding the peptide MAGDIS, which stalls ribosomes at the *MAGDIS* uORF stop codon, and no reinitiation occurs (Ryabova and Hohn, 2000). The stalling effect can be suppressed by a single amino-acid substitution (D4R) within the *MAGDIS* uORF coding region resulting in uORF *MAGRIS*. The *MAGDIS* uORF diminished GUS expression to

10% of that of p*monoGUS* in mock conditions, indicating that most ribosomes initiated efficiently at *MAGDIS* uORF and thus are trapped at its stop codon (Figure 7A). Therefore, since the initiation context of the D4R mutant-coding uORF is identical, we expected to obtain similar high initiation efficiency for the *MAGRIS* ORF.

In control protoplasts reinitiation of *GUS* ORF from p*MAGRIS-GUS* as efficient as initiation from p*monoGUS* as expected for uORF *MAGRIS* (Figure 7A). Adding Torin-1 to the protoplast incubation medium inhibits p*MAGRIS-GUS* expression by about 2.5-fold, but does not reduce p*monoGUS* expression, suggesting that the reinitiation step is specifically

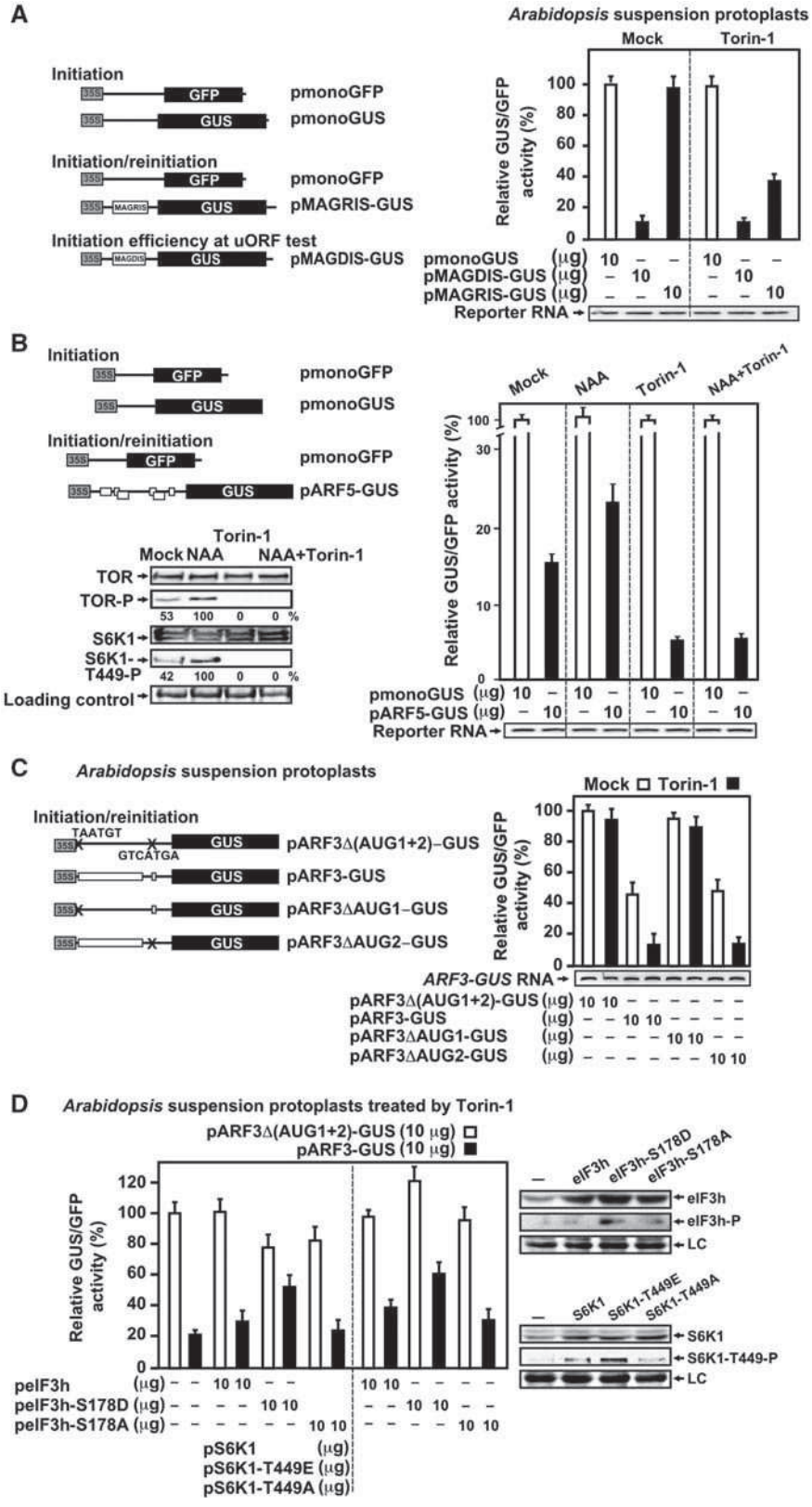

affected. Note that levels of *GUS*-containing RNAs were unaltered during protoplast incubations (Figure 7A). Our results suggest strongly that reinitiation after translation of a 7-codon uORF is sensitive to TOR inactivation.

In contrast to a single uORF, multiple uORFs within the *ARF5* leader fused to the *GUS* ORF in its authentic initiation context (p*ARF5-GUS*) reduced *GUS* ORF translation by about 80% as compared with that of p*monoGUS* (Mock, Figure 7B), suggesting that several uORFs become nearly reinitiation non-permissive in mock conditions. The low level of p*ARF5-GUS* expression was decreased further by Torin-1, and increased in response to NAA. Importantly, the protoplast response to NAA was abolished by Torin-1 (NAA + Torin-1 versus Torin-1, Figure 7B). p*monoGUS* expression was the same under all these conditions, indicating that normal initiation was unaffected.

Accordingly, TOR and S6K1, somewhat phosphorylated in protoplasts in mock conditions, were significantly dephosphoryated in the presence of Torin-1 with or without NAA (Figure 7B, left panel). In contrast, TOR and S6K1 phosphorylation increased by about two-fold in response to auxin. Thus, the GUS levels produced by *ARF5-GUS* mRNA correlate with TOR and S6K1 phosphorylation levels and all are determined by auxin or Torin-1 application.

Among uORF-containing leaders, *ARF3* harbours the longest uORF that codes for a 92-aa peptide and a short one encoding a 5-aa peptide (Figure 2A). To dissect the effect of TOR on reinitiation after the first and/or second uORF translation, the AUG start of either one or both uORFs was replaced by a stop codon (Figure 7C). Although the *ARF3* leader decreases the translation efficiency of the *GUS ORF* by 50% in mock and by 80% in Torin-1 conditions as compared with the uORF-less reporter, removal of uORF1 increases GUS up to the level of uORF-less or uORF2-containing reporters. Therefore, reinitiation of the GUS ORF after translation of uORF1, but not uORF2 is sensitive to Torin-1. However, the effect of Torin-1 on reinitiation is likely higher since uORF1/2 recognition can be decreased by a relatively weak initiation context of both uORF AUGs. Strikingly, *GUS ORF* translation from *ARF3-GUS* RNA in Torin-1 conditions can be increased by overexpression of eIF3h, or eIF3h-S178D (phosphorylation mimic), but not eIF3h-S178A (phosphorylation knock-out) or, similarly, by overexpression of S6K1 or S6K1-T449E, but less significantly by S6K1-S178A (Figure 7D). Here, uORF1/2-less *ARF3-GUS* RNA translation was somewhat improved also upon S6K1-T449E overexpression. In Torin-1 conditions, endogenous eIF3h/S6K1 phosphorylation levels were reduced significantly but, when overexpressed, these proteins display some phosphorylation albeit less than their phosphorylation mimics (Figure 7D, right panels).

As expected, mesophyll protoplasts prepared from *TOR RNAi* seedlings support similar levels of pmonoGUS expression as WT protoplasts and significantly less p*ARF5-GUS* transient expression in mock and NAA conditions (Figure 8A). Indeed, *GUS* expression levels from p*ARF5-GUS* obtained in WT (11% from p*monoGUS*) dropped to residual levels in *TOR RNAi* protoplasts. Furthermore, transient expression of p*ARF5-GUS*, but not p*monoGUS* in *eif3h-1* mesophyll protoplasts failed, but was rescued by eIF3h overexpression (Figure 8B), suggesting strongly that protoplast reinitiation competence under the conditions used depends on eIF3h.

To confirm further the significance of S178 phosphorylation for reinitiation, ribosome reinitiation capacity was compared in the presence of eIF3h, eIF3h-S178D, and eIF3h-S178A (Figure 8C). Strikingly, the eIF3h-S178D, when overexpressed, induces GUS functional activity by three-fold giving >30% of *ARF5* leader-containing mRNA expression as compared with *monoGUS* mRNA. Transient overexpression of eIF3h (less phosphorylated than eIF3h-S178D, upper panel) slightly supported GUS activity in mock conditions, while eIF3h-S178A has no impact. GUS activity from p*monoGUS* did not change significantly upon overexpression of eIF3h mutants. Since phosphorylation mimic of eIF3h is active in reinitiation, we expect to find it bound to polysomes, while eIF3h-S178A is not. Thus, we analysed polysomal association of eIF3h, eIF3h-S178D, or eIF3h-S178A mutants overexpressed in *eIF3h-1* mesophyll protoplasts (Supplementary Figure S7). Only eIF3h and its phosphorylation mimic were found in polysomal fractions, again indicating that eIF3h phosphorylation is a prerequisite for polysomal association.

Auxin responses to gravity are impaired by Torin-1

The above results, together with the finding that *eif3h-1* mutant plants display strong defects in root gravitropism (Figure 9A), raise the possibility that TOR may function in mediating the link between auxin signalling and root gravitropic response. Accordingly, a gravitropic defect was also seen in *TOR RNAi* seedlings after 24 h of 90° gravity stimulation (Figure 9B). We thus examined whether Torin-1 affects the slower phase of gravity root bending regulated by the

Figure 7 Auxin and Torin-1 regulate reinitiation after uORF translation in *Arabidopsis* suspension protoplasts. (**A**) Transient expression experiments in *Arabidopsis* suspension protoplasts included the two reporter plasmids (left panel): p*monoGFP* and p*monoGUS*; and p*monoGFP* and either p*MAGRIS-GUS*, or p*MAGDIS-GUS* in the amounts indicated below the graphs (right panel). After transfection, cells were incubated with Torin-1 or not (Mock) for 18 h, and GUS/GFP ratios are shown as open (p*monoGUS*/p*monoGFP*) and black (p*MAGRIS/MAGDIS-GUS*/p*monoGFP*) bars. p*monoGUS* expression in Mock protoplasts was set as 100% (197 800 RFU). Reporter mRNA levels were analysed by sqRT–PCR. (**B**) *Arabidopsis* suspension protoplasts were transformed with p*monoGFP* and either p*monoGUS* or *pARF5-GUS* (left panel). After transfection, cells were incubated or not (Mock) with Torin-1 or NAA or (NAA + Torin-1) for 18 h, and GUS/GFP ratios were calculated and shown as open (for p*monoGUS*/p*monoGFP*) and black bars (for p*ARF5-GUS*/p*monoGFP*). The GUS/GFP ratio found in Mock protoplasts (for p*monoGUS*/p*monoGFP*) was set as 100% (211 000 RFU). TOR, S6K1, and their phosphorylation status in protoplasts were assayed by immunoblotting (left panel). Densitometry was used to quantify western blot results from at least three independent replicates (NAA value set as 100%). (**C**) p*monoGFP* and either p*ARF3-GUS* or p*ARF3*Δ*(AUG1 + 2)-GUS* or p*ARF3*Δ*AUG1-GUS* or p*ARF3*Δ*AUG2-GUS* (left panel) were used for transformation. GUS/GFP ratios were calculated and shown as open (Mock) and black bars (Torin-1). The GUS/GFP ratio found in Mock protoplasts with uORF-less *ARF3* leader was set as 100% (150 000 RFU). (**D**) Protoplasts transformation with p*monoGFP* and either p*ARF3*Δ*(AUG1 + 2)-GUS* (open bars) or p*ARF3-GUS* (black bars) with or without additional plasmids indicated below the graphs. The GUS/GFP ratio found in Mock protoplasts with uORF-less *ARF3* leader was set as 100% (180 000 RFU). eIF3h, S6K1, and their phosphorylation status in protoplasts were assayed by immunoblotting (right panel). LC, loading control. Results in (**A**–**D**) represent the means of three independent experiments.

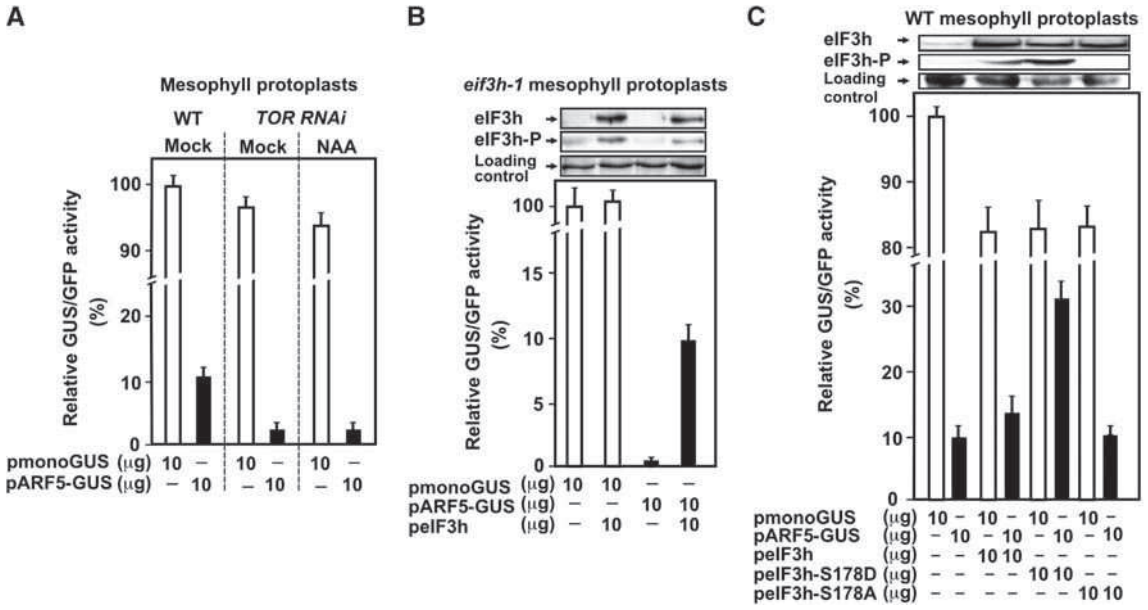

Figure 8 TOR partial depletion or eIF3h C-terminal deletion impair reinitiation after uORF translation in mesophyll protoplasts. (**A**) WT or *TOR RNAi* protoplasts were co-transformed with reporter plasmids, which are shown in Figure 7B. Activity of GUS synthesized in protoplasts transfected with p*monoGUS* was set as 100% (245 000 RFU). GUS/GFP ratios were calculated and shown as open (for p*monoGUS/pmonoGFP*) and black bars (for p*ARF5-GUS/pmonoGFP*). (**B**) *eif3h-1* mesophyll protoplasts were co-transformed with reporters shown in Figure 7B with or without plasmid expressing eIF3h as indicated. Activity of GUS synthesized in protoplasts transfected with p*monoGUS* was set as 100% (110 000 RFU). eIF3h and its phosphorylation status were assayed by immunoblotting (top panels). (**C**) WT mesophyll protoplasts were co-transfected with plasmids expressing eIF3h, or eIF3h-S178D, or S178A in addition to reporters shown in Figure 7B as indicated. The value of p*monoGUS* expression was set as 100% (205 000 RFU). eIF3h and its phosphorylation status at S178 were assayed by immunoblotting (top panels). Results shown in (**A**–**C**) represent the means obtained in three independent experiments. Source data for this figure is available on the online supplementary information page.

asymmetric distribution of auxin (Wolverton *et al*, 2002). Strikingly, 4-dag WT and *TOR RNAi* seedlings grown for 48 h on agar plates with Torin-1 lost gravity perception after turning the seedlings through 90°, showing no or a smaller bending angle after Torin-1 application (drawn schematically in Figure 9B). These results indicate that TOR may exert its effects on gravity sensing by triggering translation reinitiation of mRNAs that encode members of the ARF family, and thus auxin-responsive gene expression. If true, then this would predict that Torin-1 will affect transcription from promoters regulated by ARFs.

To test this hypothesis, we exploited an auxin-responsive promoter driving GFP expression (DR5:GFP) to follow *in situ* cellular activation of auxin-induced genes in gravity-stimulation experiments. Gravity determines auxin redistribution along the lower side of the root tip, creating supraoptimal auxin levels that inhibit cell elongation, causing the root to bend downwards (Takahashi *et al*, 2009). Four hours after gravity stimulation, the DR5:GFP signal was observed mainly in the columella, a stem-cell niche of the root meristem, and in a streak extending basipetally as expected (Figure 9C). As shown above, Torin-1 can block the gravity response, and here no asymmetry in DR5:GFP signal distribution was detected within cortical-endodermal cells in gravity-stimulated roots after 4 h. Torin-1 application had no effect on GFP redistribution along cortex/endodermal cells in response to gravity stimulation in a 35S:GFP *Arabidopsis* line.

Discussion

Protein synthesis is regulated intensively at the initiation stage by metabolic and signal transduction pathways in eukaryotes; however, this translational control is largely unexplored in plants. Here, we uncover a novel link between reinitiation of translation and the TOR signal transduction pathway. First, we found that the phytohormone auxin can specifically promote activation of TOR/S6K1 signalling in *Arabidopsis*. We demonstrated that reinitiation after uORF translation is controlled by the TOR signalling pathway in *Arabidopsis* plants. TOR can trigger translation reinitiation via phosphorylation of the plant reinitiation factor eIF3h—an RPF that, when phosphorylated, promotes translation of mRNAs harbouring uORFs within their leaders.

In plants, upstream TOR effectors are still unknown; however, auxin positively affects phosphorylation of S6 in maize (Beltrán-Peña *et al*, 2002) and S6K phosphorylation in *Arabidopsis* suspension culture (Turck *et al*, 2004). Here, we demonstrated that exogenous auxin can mediate TOR activation, triggering phosphorylation of S6K1 at the TOR-specific hydrophobic motif residue T449 followed by phosphorylation of eIF3h, which is critical for reinitiation in plants (Roy *et al*, 2010). Our data indicate that eIF3h functions in reinitiation under the control of TOR/S6K1.

Previous studies suggest that activated mTOR phosphorylates S6K1 at T389 in eIF3-PIC, triggering S6K1 dissociation (Holz *et al*, 2005). Examining TOR and S6K1 association with eIF3 revealed a similar scenario in *Arabidopsis*—auxin triggers both TOR association with eIF3-complexes and accumulation of phosphorylated S6K1 in a Torin-1-sensitive manner (Figure 1). Moreover, our results implicate polysomes as a second platform for S6K1 phosphorylation by TOR. When TOR is inactivated, S6K1 is dephosphorylated and occupies polysomes. Following an activating signal, such as auxin, TOR associates with polysomes, leading to

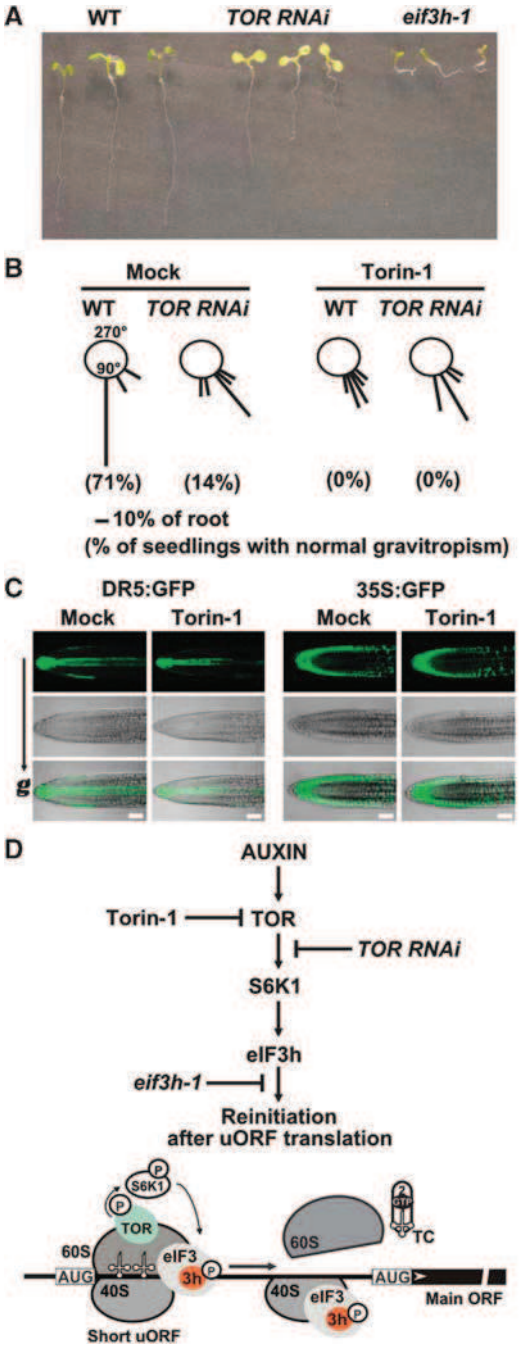

Figure 9 Torin-1 interferes with root gravitropic responses of wild type and abolishes that of *TOR RNAi* plants. (**A**) WT, *TOR RNAi*, and *eif3h-1* seedlings grown vertically for 7 dag. (**B**) *TOR RNAi*/Torin-1 and WT/Torin-1 plants display agravitropic phenotype. Seedlings described in (**A**) were grown on medium without (Mock) or with 250 nM Torin-1 and analysed 24 h after gravity stimulation. The orientation of root growth of 12 seedlings was measured by assigning to 1 of 12 30° sectors; the length of each bar represents the percentage of seedlings showing this direction of root growth within the sector. (**C**) Seven-dag seedlings homozygous for the DR5:GFP construct were analysed 4 h after gravity (*g*) stimulation on control medium without (Mock) and with 250 nm Torin-1. Scale bars, 25 mm. (**D**) Proposed scheme of auxin-responsive TOR function in reinitiation after uORF translation (see text for details). Torin-1 application, or TOR deficiency, or eIF3h C-terminal deletion inhibit reinitiation at the steps indicated.

phosphorylation of bound and inactive S6K1 at T449. Polysomal association of S6K1 is disrupted by its phosphorylation at T449. Concomitantly, eIF3h, when phosphorylated, occupies polysomes, where it can stimulate the reinitiation capacity of post-terminating ribosomes. According to our results, TOR and eIF3h recruitment to polysomes is a hallmark of efficient polysomal loading of uORF-containing mRNAs and thus translation reinitiation. The interaction of TOR with polysomes is dynamic, auxin-responsive, Torin-1 sensitive with or without auxin, and is blocked in TOR-deficient TOR RNAi plants. TOR activation improves polysomal loading not only for auxin-related ARFs, but also for auxin-unrelated *bZIP11*. All these data indicate a ubiquitous role for TOR in reinitiation after uORF translation.

Whether inactive S6K1 or activated TOR enters polysomes through direct interaction with ribosomes, or other polysomal components, remains unknown. In *S. cerevisiae*, TOR has the capacity to interact with 60S to accomplish TORC2 complex association with polysomes (Oh *et al*, 2010), and activation of TORC2 can also be triggered by the ribosome (Zinzalla *et al*, 2011). It is unlikely that eIF3h mediates TOR interaction with polysomes since, in *eIF3h-1*, activated TOR is recruited to polysomes (Figure 5D).

eIF3h seems to be a unique RPF that is critical for translation of uORF-mRNAs, but dispensable for translation of monocistronic messages in plants (Roy *et al*, 2010). In human cells, eIF3h is phosphorylated at S183 and, when overexpressed, triggers dysregulation of protein synthesis, where eIF3h phosphorylation at S183 is critical (Zhang *et al*, 2008). Phosphorylation of *At*eIF3h at S178 is also critical for uORF-mRNA reinitiation. S6K1 binds eIF3h *in vivo* and seems to be responsible for phosphorylation of eIF3h at S178—in TOR-deficient plants, S6K1 and eIF3h phosphorylation were nearly abolished. The effect of TOR on ribosomal reinitiation capacity is seen after a single (6-aa or 92-aa) uORF as well as multiple uORF translation. Since reinitiation competent uORF may become non-permissive if it has a secondary structure around uORF that would be expected to cause ribosome pausing or it is a further downstream uORF has to be initiated by the same ribosome, the effect of TOR may vary from case to case as well as modulated by the number, length, and nature of the uORF(s). It seems that inappropriately activated TOR/S6K1 signalling may trigger upregulation of uORF-mRNAs that encode proteins that are harmful when abundant.

The results obtained in this study allow us to postulate the following model for the role of TOR in translation of uORF-containing mRNAs (Figure 9D). During the rapid elongation event a set of RPFs recruited during the primary 5′-initiation event remain attached to the translating ribosome. One might expect that RPFs reinitiation competence while moving along the mRNA would require re-activation (eIF3h will undergo dephosphorylation). In response to auxin, TOR is activated, binds polysomes prebound by inactive S6K1 to phosphorylate S6K1 at T449. Activated S6K1 can maintain the phosphorylation state of eIF3h within polysomes.

How eIF3h contributes to translation reinitiation is unclear. Previous data suggest that the eIF3h C-terminal part is critical for eIF3h integration within eIF3, but not for eIF3 integrity—h-less eIF3 can still interact with 40S and participate in all initiation steps (Roy *et al*, 2010). Thus, we propose that eIF3h *per se* does not play an essential role in initiation steps. In contrast, it can provide a link between eIF3 and polysomes, thus ensuring polysomal retention of eIF3 via its N-terminus. Therefore, after termination, eIF3 bound to reinitiating

ribosomes can promote scanning or TC/60S recruitment. Indeed, retention of eIF3 on translationally active ribosomes increases their reinitiation capacity (Park *et al*, 2001; Pöyry *et al*, 2007). Functional roles for several eIF3 subunits in reinitiation were proposed in yeast, where subunits a/Tif32, g/Tif35, i/Tif34 were shown to support resumption of scanning of post-terminating ribosomes in addition to their essential roles in translation initiation (Cuchalová *et al*, 2010; Munzarová *et al*, 2011).

The hormone auxin is essential for many aspects of growth, development, and pattern formation in plants (Vanneste and Friml, 2009). Based on our data, we predict that at least some auxin responses proceed via the TOR signalling pathway in a Torin-1-sensitive manner in *Arabidopsis* seedlings. Thus, auxin signalling can target the cell translation machinery by activating the TOR signalling pathway in the cytosol/ER. Note the suggestion of auxin trafficking in the cytoplasm (Friml and Jones, 2010), thus auxin functioning in translation control in the cytoplasm adds another layer of complexity to the well-known pathway in the nucleus, where auxin regulates activation of ARF transcriptional factors (Mockaitis and Estelle, 2008; Leyser, 2006). These ARF proteins regulate expression of multiple auxin-responsive genes and thus a multitude of functions in plant development, including root gravitropism (Blancaflor and Masson, 2003).

Strikingly, a root gravitropic response that is dependent on polar auxin transport and ARF-controlled auxin responsive factors (Palme *et al*, 2006; Takahashi *et al*, 2009) can be altered by TOR inactivation via Torin-1. *TOR RNAi* seedlings defective in reinitiation display defects in the gravity-sensing machinery, suggesting that auxin-responsive function of TOR is critical for plant development.

To summarise, our report describes a novel translational mechanism in which the translational efficiency of genes harbouring multiple uORFs in their leader regions is controlled at multiple levels by auxin, TOR signalling, and eIF3h. The details of how this regulation functions and the possible involvement of other players open up a fascinating area for further study.

Materials and methods

Plant material and growth conditions

Transgenic lines and vector constructions are described in Supplementary data. For seedling growth, cell culture details, extract preparations, production of recombinant S6K1, and the *in vitro* kinase phosphorylation assay, see Supplementary data and Schepetilnikov *et al* (2011). Fourteen-day-old Arabidopsis cultures, 7-dag seedlings were incubated in MS medium containing no, or 20 nM NAA, or 250 nM Torin-1 for the times indicated. For growth details, extract preparation, and analysis, see Supplementary methods.

Protein assays

For immunoprecipitation assays, we used 7-dag *Arabidopsis* Col-0 seedlings or 14-day-old Arabidopsis cultures that were transferred into fresh MS medium containing no or 20 nM NAA, or 250 nM Torin-1 and grown at 24°C. Total protein extracts, IP fractions, and 2D gel analysis were as described in Supplementary data.

Polyribosome analysis

Polysomes were isolated from 18 h mesophyll protoplasts, 7-dag *Arabidopsis* Col-0 WT, *TOR RNAi*, and *eif3h-1* seedlings treated (or not) with NAA or Torin-1 for 8 h and analysed by density sucrose centrifugation (Supplementary data). *ARF*, *bZIP11*, *IAA6*, and *ACTIN* mRNA levels were analysed in ribosomal profiles by sqRT–PCR, and in total extracts by qRT–PCR, protein content by western blot.

Protoplast assays

Transient expression was analysed in protoplasts derived from an *Arabidopsis* suspension culture or 2-week *eif3h-1* or *TOR RNAi* plantlets incubated with no or NAA, or Torin-1. For transfection protocol, see Supplementary data.

Assay for root gravitropism

Seedlings were germinated vertically in the dark at 22°C for 4 days. The plants were then placed on fresh MS agar plates with or without 250 nM Torin-1 maintaining the same orientation and growth conditions and allowed to grow for a further 2 days. The plates were then turned through 90° and grown for a further 4 h. GFP fluorescence in roots was analysed after 4 h of a 90° gravistimulation in the dark as described in Supplementary data.

Molecular modelling

The 3D structure of *Arabidopsis* eIF3h was created using Modeller (Sali *et al*, 1995) and represented graphically by PyMOL (http://www.pymol.org). Support structure for modelling the central region (1–200 aa) of eIF3h was found with NIH BLAST.

Supplementary data

Supplementary data are available at *The EMBO Journal* Online (http://www.embojournal.org).

Acknowledgements

We are grateful to C Robaglia for *TOR RNAi* and A von Arnim for *eif3h-1*/anti eIF3h antibodies, D Weijers for providing ARF-encoding plasmids, M Yusupov and S Melnikov for help with molecular modelling, N Baumberger and P Hammann for helpful assistance in protein analysis. We thank A von Arnim and C Robaglia for comments on the manuscript. This work was supported by French Agence Nationale de la Recherche—BLAN06-2_135889 and BLAN-2011_BSV6 010 03, France—for funding LR.

Conflict of interest

The authors declare that they have no conflict of interest.

References

Asai T, Tena G, Plotnikova J, Willmann MR, Chiu W-L, Gomez-Gomez L, Boller T, Ausubel FM, Sheen J (2002) MAP kinase signalling cascade in Arabidopsis innate immunity. *EMBO J* **415:** 977–983

Beltrán-Peña E, Aguilar R, Ortíz-López A, Dinkova TD, De Jiménez ES (2002) Auxin stimulates S6 ribosomal protein phosphorylation in maize thereby affecting protein synthesis regulation. *Physiol Plant* **115:** 291–297

Blancaflor EB, Masson PH (2003) Plant gravitropism. Unraveling the ups and downs of a complex process. *Plant Physiol* **133:** 1677–1690

Browning KS, Gallie DR, Hershey JWB, Hinnebusch AG, Maitra U, Merrick WC, Norbury C (2001) Unified nomenclature for the subunits of eukaryotic initiation factor 3. *Trends Biochem Sci* **26:** 284

Calvo SE, Pagliarini DJ, Mootha VK (2009) Upstream open reading frames cause widespread reduction of protein expression and are polymorphic among humans. *Proc Natl Acad Sci USA* **106:** 7507–7512

Chiang GG (2005) Phosphorylation of mammalian target of rapamycin (mTOR) at Ser-2448 is mediated by p70S6 kinase. *J Biol Chem* **280:** 25485–25490

Cuchalová L, Kouba T, Herrmannová A, Dányi I, Chiu WL, Valášek L (2010) The RNA recognition motif of eukaryotic translation initiation factor 3g (eIF3g) is required for resumption of scanning of posttermination ribosomes for reinitiation on GCN4 and together with eIF3i stimulates linear scanning. *Mol Cell Biol* **30:** 4671–4686

Deprost D, Yao L, Sormani R, Moreau M, Leterreux G, Nicolai M, Bedu M, Robaglia C, Meyer C (2007) The Arabidopsis TOR kinase links plant growth, yield, stress resistance and mRNA translation. *EMBO Rep* **8:** 864–870

Dobrenel T, Marchive C, Sormani R, Moreau M, Mozzo M, Montané MH, Menand B, Robaglia C, Meyer C (2011) Regulation of plant growth and metabolism by the TOR kinase. *Biochem Soc Trans* **39:** 477–481

Friml J, Jones AR (2010) Endoplasmic reticulum: the rising compartment in auxin biology. *Plant Physiol* **154:** 458–462

Gingras AC, Raught B, Sonenberg N (2001) Regulation of translation initiation by FRAP/mTOR. *Genes Dev* **15:** 807–826

Hinnebusch A (2006) eIF3: a versatile scaffold for translation initiation complexes. *Trends Biochem Sci* **31:** 553–562

Hinnebusch AG (2005) Translational regulation of GCN4 and the general amino acid control of yeast. *Annu Rev Microbiol* **59:** 407–450

Holz MK, Ballif BA, Gygi SP, Blenis J (2005) mTOR and S6K1 mediate assembly of the translation preinitiation complex through dynamic protein interchange and ordered phosphorylation events. *Cell* **123:** 569–580

Jastrzebski K, Hannan KM, House CM, Hung SSC, Pearson RB, Hannan RD (2011) A phospho-proteomic screen identifies novel S6K1 and mTORC1 substrates revealing additional complexity in the signaling network regulating cell growth. *Cell Signal* **23:** 1338–1347

Kim TH, Kim BH, Yahalom A, Chamovitz DA, Arnim von AG (2004) Translational regulation via 5' mRNA leader sequences revealed by mutational analysis of the Arabidopsis translation initiation factor subunit eIF3h. *Plant Cell* **16:** 3341–3356

Kozak M (2001) Constraints on reinitiation of translation in mammals. *Nucleic Acids Res* **29:** 5226–5232

Leyser O (2006) Dynamic integration of auxin transport and signaling. *Curr Biol* **16:** 424–433

Luukkonen BG, Tan W, Schwartz S (1995) Efficiency of reinitiation of translation on human immunodeficiency virus type 1 mRNAs is determined by the length of the upstream open reading frame and by intercistronic distance. *J Virol* **69:** 4086–4094

Ma XM, Blenis J (2009) Molecular mechanisms of mTOR-mediated translational control. *Nat Rev Mol Cell Biol* **10:** 307–318

Mahfouz MM, Kim S, Delauney AJ, Verma DP (2006) Arabidopsis TARGET OF RAPAMYCIN interacts with RAPTOR, which regulates the activity of S6 kinase in response to osmotic stress signals. *Plant Cell* **18:** 477–490

Marin E, Jouannet V, Herz A, Lokerse AS, Weijers D, Vaucheret H, Nussaume L, Crespi MD, Maizel A (2010) miR390, Arabidopsis TAS3 tasiRNAs, and their AUXIN RESPONSE FACTOR targets define an autoregulatory network quantitatively regulating lateral root growth. *Plant Cell* **22:** 1104–1117

Medenbach J, Seiler M, Hentze MW (2011) Translational control via protein-regulated upstream open reading frames. *Cell* **145:** 902–913

Menand B, Desnos T, Nussaume L, Berger F, Bouchez D, Meyer C, Robaglia C (2002) Expression and disruption of the Arabidopsis TOR (target of rapamycin) gene. *Proc Natl Acad Sci USA* **99:** 6422–6427

Mockaitis K, Estelle M (2008) Auxin receptors and plant development: a new signaling paradigm. *Annu Rev Cell Dev Biol* **24:** 55–80

Moreau M, Azzopardi M, Clément G, Dobrenel T, Marchive C, Renne C, Martin-Magniette ML, Taconnat L, Renou JP, Robaglia C, Meyer C (2012) Mutations in the Arabidopsis homolog of LST8/GβL, a partner of the target of rapamycin kinase, impair plant growth, flowering, and metabolic adaptation to long days. *Plant Cell* **2:** 463–481

Morris DR, Geballe AP (2000) Upstream open reading frames as regulators of mRNA translation. *Mol Cell Biol* **20:** 8635–8642

Munzarová V, Pánek J, Gunišová S, Dányi I, Szamecz B, Valášek LS (2011) Translation reinitiation relies on the interaction between eIF3a/TIF32 and progressively folded cis-acting mRNA elements preceding short uORFs. *PLoS Genet* **7:** e1002137

Nilsson J, Sengupta J, Frank J, Nissen P (2004) Regulation of eukaryotic translation by the RACK1 protein: a platform for signalling molecules on the ribosome. *EMBO Rep* **5:** 1137–1141

Nishimura T, Wada T, Yamamoto KT, Okada K (2005) The Arabidopsis STV1 protein, responsible for translation reinitiation, is required for auxin-mediated gynoecium patterning. *Plant Cell* **17:** 2940–2953

Oh WJ, Wu CC, Kim SJ, Facchinetti V, Julien LA, Finlan M, Roux PP, Su B, Jacinto E (2010) mTORC2 can associate with ribosomes to promote cotranslational phosphorylation and stability of nascent Akt polypeptide. *EMBO J* **29:** 3939–3951

Palme K, Dovzhenko A, Ditengou FA (2006) Auxin transport and gravitational research: perspectives. *Protoplasma* **229:** 175–181

Park HS, Himmelbach A, Browning KS, Hohn T, Ryabova LA (2001) A plant viral ''reinitiation'' factor interacts with the host translational machinery. *Cell* **106:** 723–733

Pöyry TA, Kaminski A, Connell EJ, Fraser CS, Jackson RJ (2007) The mechanism of an exceptional case of reinitiation after translation of a long ORF reveals why such events do not generally occur in mammalian mRNA translation. *Genes Dev* **21:** 3149–3162

Pöyry TA, Kaminski A, Jackson RJ (2004) What determines whether mammalian ribosomes resume scanning after translation of a short upstream open reading frame? *Genes Dev* **18:** 62–75

Rademacher E, Möller B, Lokerse AS, Llavata-Peris CI, van den Berg W, Weijers D (2011) A cellular expression map of the Arabidopsis AUXIN RESPONSE FACTOR gene family. *Plant J* **68:** 597–606

Rahmani F, Hummel M, Schuurmans J, Wiese-Klinkenberg A, Smeekens S, Hanson J (2009) Sucrose control of translation mediated by an upstream open reading frame-encoded peptide. *Plant Physiol* **150:** 1356–1367

Roy B, Vaughn JN, Kim BH, Zhou F, Gilchrist MA, von Arnim AG (2010) The h subunit of eIF3 promotes reinitiation competence during translation of mRNAs harboring upstream open reading frames. *RNA* **16:** 748–761

Ruan H, Shantz LM, Pegg AE, Morris DR (1996) The upstream open reading frame of the mRNA encoding S-adenosylmethionine decarboxylase is a polyamine-responsive translational control element. *J Biol Chem* **271:** 29576–29582

Ryabova LA, Hohn T (2000) Ribosome shunting in the cauliflower mosaic virus 35S RNA leader is a special case of reinitiation of translation functioning in plant and animal systems. *Genes Dev* **14:** 817–829

Sachs MS, Geballe AP (2006) Downstream control of upstream open reading frames. *Genes Dev* **20:** 915–921

Sali A, Potterton L, Yuan F, van Vlijmen H, Karplus M (1995) Evaluation of comparative protein modeling by MODELLER. *Proteins* **23:** 318–326

Schepetilnikov M, Kobayashi K, Geldreich A, Caranta C, Robaglia C, Keller M, Ryabova LA (2011) Viral factor TAV recruits TOR/S6K1 signalling to activate reinitiation after long ORF translation. *EMBO J* **30:** 1343–1356

Sengupta S, Peterson TR, Sabatini DM (2010) Regulation of the mTOR complex 1 pathway by nutrients, growth factors, and stress. *Mol Cell* **40:** 310–322

Takahashi H, Miyazawa Y, Fujii N (2009) Hormonal interactions during root tropic growth: hydrotropism versus gravitropism. *Plant Mol Biol* **69:** 489–502

Thiébeauld O, Schepetilnikov M, Park HS, Geldreich A, Kobayashi K, Keller M, Hohn T, Ryabova LA (2009) A new plant protein interacts with eIF3 and 60S to enhance virus-activated translation re-initiation. *EMBO J* **28:** 3171–3184

Thoreen CC, Chantranupong L, Keys HR, Wang T, Gray NS, Sabatini DM (2012) A unifying model for mTORC1-mediated regulation of mRNA translation. *Nature* **485:** 109–113

Thoreen CC, Kang SA, Chang JW, Liu Q, Zhang J, Gao Y, Reichling LJ, Sim T, Sabatini DM, Gray NS (2009) An ATP-competitive mammalian target of rapamycin inhibitor reveals rapamycin-resistant functions of mTORC1. *J Biol Chem* **284:** 8023–8032

Turck F, Zilbermann F, Kozma SC, Thomas G, Nagy F (2004) Phytohormones participate in an S6 kinase signal transduction pathway in Arabidopsis. *Plant Physiol* **134:** 1527–1535

Vanneste S, Friml J (2009) Auxin: a trigger for change in plant development. *Cell* **136:** 1005–1016

Wiese A, Elzinga N, Wobbes B, Smeekens S (2004) A conserved upstream open reading frame mediates sucrose-induced repression of translation. *Plant Cell* **16:** 1717–1729

Wolverton C, Ishikawa H, Evans ML (2002) The kinetics of root gravitropism: dual motors and sensors. *J Plant Growth Regul* **21:** 102–112

Zhang L, Smit-McBride Z, Pan X, Rheinhardt J, Hershey JWB (2008) An oncogenic role for the phosphorylated h-subunit of human translation initiation factor eIF3. *J Biol Chem* **283:** 24047–24060

Zhang SH, Lawton MA, Hunter T, Lamb CJ (1994) Atpk1, a novel ribosomal protein kinase gene from Arabidopsis. I. Isolation, characterization, and expression. *J Biol Chem* **269:** 17586–17592

Zhou F, Roy B, von Arnim AG (2010) Translation reinitiation and development are compromised in similar ways by mutations in translation initiation factor eIF3h and the ribosomal protein RPL24. *BMC Plant Biol* **10:** 193

Zinzalla V, Stracka D, Oppliger W, Hall MN (2011) Activation of mTORC2 by association with the ribosome. *Cell* **144:** 757–768

3. Final conclusion and perspectives

During my PhD I have studied how reinitiation-supporting protein—RISP—participates in translation initiation, particularly in the virus-activated reinitiation process. RISP has been suggested to assist eIF3 in recruitment of the ternary complex de novo to 43S PIC and to ensure 60S ribosomal subunit joining or 60S re-use during the reinitiation event (Thiébeauld et al., 2009). Although RISP can be immunoprecipitated by either anti-eIF2β, anti-eS6, or anti-eIF3c antibodies, strongly suggesting that RISP is a part of 48S PIC, the functional role of RISP within the complex remains unclear. Here, we identified a physical association between RISP and eIF2, and suggested that, together with the previously identified interaction of RISP with eIF3, RISP participates in eIF2 and thus in TC recruitment to 43S PIC during cap-dependent translation initiation. Interestingly, eIF2 and eIF3 seem to interact preferentially with RISP before its phosphorylation, suggesting a role for TOR also in eIF2 recruitment. Taking into account that S6K1 phosphorylation by TOR occurs within the 48S PIC—43S PIC loaded onto the eIF4F-bound mRNA, one might expect that phosphorylation of RISP by activated S6K1 would also proceed in close proximity to 48S PIC (see Schepetilnikov et al., 2011).

In contrast, RISP, when phosphorylated, interacts preferentially with TAV and 60S via eL24 (Schepetilnikov et al., 2013) and 40S via eS6. Thus, there is a possibility that, in plants, RISP can either link C-terminal helices of eS6 and eL24, providing the intersubunit bridge between 40S and 60S, or stabilize the eS6-eL24 bridge. Confocal microscope immunoanalysis revealed that RISP co-localizes only with a fraction of ribosomes suggesting that RISP binding to 60S is somewhat controlled (Thiébeauld et al., 2009).

I expect that phosphorylated RISP-Ser267-P is involved in interactions with both eS6-P and eL24 C-terminal domains on the ribosome, and experiments to test this hypothesis are in progress.

Another future task will be to reveal partners of RISP before and after phosphorylation in planta. For this purpose I have started generation of several transgenic lines (*rispa* mutant background) expressing tagged RISP phosphorylation mutants (analysis of T1 seeds is in progress). Although phosphorylation of eS6 at Ser231, Ser237 and Ser240 was demonstrated in *Arabidopsis*, and our data suggest their preferential phosphorylation in conditions of TOR activation, how phosphorylation of eS6 at these sites affect its interaction with RISP *in vivo* is not known. We currently have several *Arabidopsis* transgenic lines expressing different combinations of phosphorylation mimic and knockout eS6 at Ser231, Ser237 and Ser240 in WT and s6a mutant *Arabidopsis* plants. An encouraging result is that the phenotype of plants with double knockout of Ser237 and Ser240 is severely affected.

CaMV employs very unusual mechanism for translation of its polycistronic pregenomic RNA via reinitiation. And as expected, virus replication depends on reinitiation promoting factors (RPFs) that are required to overcome cell barriers to reinitiation. Indeed, RPFs like TOR (Schepetilnikov et al., 2011) and eIF3h (unpublished lab results) are strictly required for viral infection. Here, eS6 is such RPF, where knockout of one copy (rpS6a mutant) practically abolished CaMV infection despite that as we know from protoplasts experiments, the cap-dependent initiation is positively supported in this mutant, while TAV-mediated reinitiation is inhibited. My data identify eS6 as a factor that is crucial for TAV-mediated reinitiation after long ORF translation, and suggest the role of eS6 in reinitiation after short ORF translation as well.

In addition, eS6 is the most intriguing ribosomal protein that functions under the control of the TOR signaling pathway. Although phosphorylation of eS6 was suggested to play a role in regulation of a specific class of mRNAs containing so called TOP-motif at the 5'-end, knocking out these sites did not interfere with the above-mentioned control. Despite the fact that knockout of phosphorylation sites strongly affects cell growth and physiology in humans and plants, the functional role of phosphorylation is an open question. My results indicate that eS6 participates in reinitiation at the step of 60S recruitment, but it might be more critical for the ribosome to resume scanning without losing 60S—the same 60S will be used during repeated reinitiation events. Thus, the role of eS6 in reinitiation after either short or long ORF translation is the most interesting aspect for future research. We hope that our investigations into the viral model of RISP and eS6-eL24 intersubunit bridge function will help understand the mechanism of 60S function during cellular translation initiation and reinitiation after short ORF translation.

4. Materials and Methods

4.1 Materials

4.1.1 Chemical and Molecular Biological Materials

Unless stated otherwise, all chemicals and reagents used in this study were purchased from BioRad Laboratories Ltd. (Marnes-la-Coquette, France), Ozyme Inc. (St Quentin en Yvelines, France), ThermoFisher Scientific Ltd. (Illkirch, France), GE Healthcare (Strasbourg, France), Life Technologies Ltd. (Saint Aubin, France), Qiagen Ltd. (Courtaboeuf, France), Sigma-Aldrich Ltd. (Illkirch, France) and Macherey-Nagel (Hoerdt, France).

Enzymes and reagents used for molecular biology were purchased from New England Biolabs Ltd. (Évry, France), Promega Ltd. (Charbonnieres, France), Roche Diagnostics Ltd. (Meylan, France), and Ozyme Inc. (St Quentin en Yvelines, France).

Bacterial [*Escherichia coli* (*E.coli*)] and yeast (*S.cerevisiae*)] growth media components were purchased from Ozyme Inc. (St Quentin en Yvelines, France) and Sigma-Aldrich Ltd. (Illkirch, France). Antibiotics used in this study are listed in Table 4.1-1. Antibiotics used in this study and were purchased from Sigma-Aldrich Ltd. (Illkirch, France). All antibiotics were prepared as water, 50% alcoholic or DMSO stock solutions and stored at -20 °C.

Table 4.1-1. Antibiotics used in this study

Antibiotic	[Stock]	[Final]
Ampicillin sodium salt	100 mg/mL in 50% EtOH	100 µg/mL
Kanamycin disulfate salt	50 mg/mL in dH_2O	50 µg/mL
Streptomycin sulfate salt	50 mg/mL in dH_2O	50 µg/mL
Chloramphenicol	50 mg/mL in 50% EtOH	25 or 50 µg/mL
Spectomycin	100 mg/mL in dH_2O	100 µg/mL
Gentamycin	50 mg/mL in dH_2O	50 µg/mL
Rifampycin	100 mg/mL in DMSO	50 µg/mL
Zeocin®	100 mg/mL in dH_2O	25 µg/mL
Higromycin	35 mg/mL in dH_2O	35 µg/mL
Cefotoxin	250 mg/mL in dH_2O	250 µg/mL

4.1.2 Bacterial and yeast strains

Bacterial (*E. coli*, and *Agrobacterium tumefaciens*), and yeast (*S. cerevisiae*) strains used in this study are listed in Table-4.1-2. Strains used in this study. Plasmids were propagated in either One Shot® TOP10, DH5α, or XL1-Blue *E.coli*. Rosseta2 (DE3) pLys *E.coli* was routinely used for the production of recombinant fusion proteins. Strains having the designation DE3 are lysogenic for a lambda prophage that contains an IPTG-inducible T7 RNA polymerase under lacUV5 promoter. They are required for expression from vectors with T7 promoter. Strains having pLysS designation carry a plasmid (pACYC184-derived, CamR) that encodes T7 lysozyme, which is a natural inhibitor of T7 RNA polymerase that serves to repress basal expression of target genes under control of T7 promoter. GV3101 *Agrobacterium* strain was used for the production of transgenic plants by floral dipping. The hypervirulent *Agrobacterium* strain AGL1 +virG (Vain et al., 2004) containing the WT CaMV isolate CM1841 was used for viral infection experiments.

Table-4.1-2. Strains used in this study

Strains	Genotype/Characteristics	Origin	Resistance
Escherichia coli			
One Shot® TOP10	F- *mcr*A Δ(*mrr-hsd*RMS-*mcr*BC) ϕ80*lac*ZΔM15 Δ*lac*X74 *rec*A1 *ara*D139 Δ(*ara-leu*)7697 *gal*U *gal*K *rps*L (StrR) *end*A1 *nup*G	LifeTechnologies	none
Rosetta 2 (DE3) pLysS	F- *omp*T *hsd*S_B(r_B- m_B-) *gal dcm* (DE3) pLysSRARE2 (CamR). Supply tRNAs for seven rare codons (AUA, AGG, AGA, CUA, CCC, GGA CGG)	Novagen	CamR (25µg/mL)
XL1-Blue	*rec*A1 *end*A1 *gyr*A96 *thi-1 hsd*R17 *sup*E44 *rel*A1 *lac* [F´ *pro*AB *lacI*^{q} ZΔM15 Tn*10* (TetR)].	Stratagene	TetR (12,5 µg/mL)
DH5α	F– Φ80*lac*ZΔM15 Δ(*lac*ZYA-*arg*F) U169 *rec*A1 *end*A1 *hsd*R17 (rK–, mK+) *pho*A *sup*E44 λ– *thi*-1 *gyr*A96 *rel*A1	Life Technologies	none
Agrobacterium tumefaciens			
GV3101	It carries a disarmed Ti plasmid that possesses the vir genes needed for T-DNA transfer, but has no functional T-DNA region of its own	Kindly provided by Jean-Michel Davierre (IBMP, Strasbourg)	RifR (50µg/mL) and GentR (50µg/mL)
AGL1	It contains the hypervirulent Ti plasmid, pTiBo542 harbouring additional vir genes originated from the *Agrobacterium* strain A281	Kindly provided by Dr. Kappei Kobayashi (Ehime University, Japan)	RifR (50µg/mL)
Saccharomyces cerevisiae			
AH109	*MATa, trp1-901, leu2-3, 112, ura3-52, his3-200, gal4Δ, gal80Δ, LYS2 : : GAL1UAS-GAL1TATA-HIS3, GAL2UAS-GAL2TATA-ADE2, URA3 : : MEL1UAS-MEL1 TATA-lacZ*	Clontech Laboratories Ltd.	none

4.1.3 Growth media

With the exception of Rosetta2 (DE3) pLys *E.coli* cells that were used for RISP-His recombinant protein expression (see below) bacterial cells were routinely grown in liquid LB media [1% (w/v) tryptone, 0.5% (w/v) yeast extract, 0.5% (w/v) NaCl] containing the appropriate antibiotic if required. Solid media was prepared by the addition of 2% (w/v) agar prior to autoclaving. For the purpose of routine recombinant fusion protein production (refer to Expression of recombinant fusion proteins), transformed Rosseta2 (DE3) pLys *E.coli* cells were grown in 1.5X LB medium containing 0.2% (w/v) glucose and the appropriate antibiotic (Table 4.1-1. Antibiotics used in this study). For expression of His-tagged recombinant RISP, LB medium was modified to increase the production of soluble proteins. The addition of 1% glucose completely suppresses the T7 promoter in the absence of IPTG. The LB medium is also supplemented with 600 mM sorbitol and 2.5 mM betaine to produce osmotic stress promoting expression of chaperone proteins that assist in proper folding of the recombinant proteins (Blackwell and Horgan, 1991). Yeast cells were grown non-selectively in YPD [1% (w/v) yeast extract, 2% (w/v) peptone, 2% (w/v) glucose], or selectively on minimal synthetic defined (SD) media [0.675% (w/v) yeast nitrogen base without amino acids, 2% (w/v) glucose] lacking the appropriate amino acids. As before, solid media was prepared by the addition of 2% (w/v) agar prior to autoclaving. Bacterial and yeast agar plates were poured in a sterile environment and routinely stored at 4 °C.

4.2 Molecular biology

4.2.1 Purification of plasmid DNA from E.coli

Plasmids used in this study are mentioned in Plasmid construction. DNA plasmid that was used as a template for PCR (refer to Polymerase Chain Reaction) or bacterial and yeast cell transformations (see Transformation of competent yeast cells) was purified using the microcentrifugation protocol provided with the NucleoSpin® Plasmid Miniprep kit. This protocol is based on a modified alkaline lysis procedure initially described by Birnboim and Doly (1979). Purification was performed as outlined in the manufacturer's instruction manual. Purified plasmid DNA was routinely stored at -20 °C.

4.2.2 Agarose gel electrophoresis

DNA samples were analyzed by agarose gel electrophoresis. Agarose powder [0.5-2% (w/v)] was dissolved in TBE buffer (100 mM Tris, 90 mM boric acid, 2.5 mM EDTA, pH 8.0) by heating in a microwave. The gel solution was allowed to cool to approximately 54 °C prior to the addition of ethidium bromide to a final concentration of 0.5 µg/mL. The gel was cast into an ultraviolet (UV)-transparent plastic tray positioned directly on top of the BioRad Mini-Cell® GT agarose gel electrophoresis unit stage. An 8- or 15-well comb was positioned near the cathode and the gel was left to solidify (approximately 30 minutes). The gel was submerged in TBE buffer and the DNA samples were prepared by adding 6X DNA loading dye [0.25% (w/v) bromophenol blue, 0.25% (w/v) xylene cyanol FF, 30% (v/v) glycerol]. Loading dye was omitted for all PCR reactions containing 5X Green GoTaq® reaction buffer. The DNA samples were loaded into the wells contained within the gel and a constant electric potential of 90 volts (V) was applied for 20-40 minutes. 5 µL of either a 100 base pair (bp) or 1 kilobase pair (kb) DNA marker was routinely included as a DNA standard. Resolved DNA samples were visualized with an UV transilluminator and digital images were on-site printed.

4.2.3 Gel extraction and purification of DNA

DNA fragments that were resolved by agarose gel electrophoresis (refer to Agarose gel electrophoresis) that were to be used for subsequent procedures were excised from the gel with a clean scalpel and transferred to a 1.5 mL eppendorf tube. DNA was then extracted and purified from the agarose gel matrix using the NucleoSpin® Gel and PCR Clean-up extraction kit as outlined in the manufacturer's instruction manual.

4.2.4 Polymerase Chain Reaction

Oligonucleotide primer pairs were designed to amplify desired DNA sequences by PCR. Primers were synthesised by Sigma Ltd. and were routinely diluted to 100 µM in dH_2O prior to storage at -20 °C. The PCR reaction mix was typically made up to a total volume of 25 or 50 µL in a 0.2 mL thin-walled PCR tube. Either GoTaq® Flexi or Phusion® High-Fidelity DNA polymerase combined with their respective buffers were used. All PCR products were analyzed by agarose gel electrophoresis (refer to Agarose gel electrophoresis). An example of a standard PCR mix used in this study is shown in Table-4.2-1 Standard PCR reaction mix. Standard PCR conditions were employed as outlined in Table-4.2-2. Standard PCR conditions.

Table-4.2-1 Standard PCR reaction mix

Component	Volume (µL)
5X Buffer	10
$MgCl_2$ (C_{stock}=25 mM C_{final}=2mM)[a]	4
dNTPs (C_{stock}=10 mM C_{final}=0.2 mM)[b]	1
Forward primer (C_{stock}=100 µM C_{final}=0.5 µM)[c]	0.25
Reverse primer (C_{stock}=100 µM C_{final}=0.5 µM)[c]	0.25
dH_2O	33.25
GoTaq® Flexi DNA polymerase	0.25
DNA template (50-100 ng)	1
Total	50

[a] MgCl2 was excluded for all PCR reactions where Phusion® DNA polymerase 10X Buffer was used.
[b] dNTP mix contained 10 mM of each of dATP, dCTP, dGTP and dTTP.
[c] For PCR-driven overlap extension, details about concentrations of the DNA template and PCR-derived primers are described below.

Table-4.2-2. Standard PCR conditions

Step	Temperature[a]	Time[a] (min)	Number of cycles
1.Initial denaturation	95/98°C	2/0.5	1
2. Denaturation	95/98°C	0.5/0.17	
3. Anneal	44 °C-55 °C[b]	0.5	Repeat steps 2-4 for 25-30 cycles
4. Extension	72°C	x [c]	
5. Final extension	72°C	5/10	1
6. Hold	4 °C	Indefinite	

[a] Numbers on the left side correspond to GoTaq® conditions. On the right side the Phusion® cycle conditions are reported.
[b] Annealing temperature was optimized for each primer set based on the primer T_m.
[c] The size of amplified DNA determined the extension time according to manufacturer's instruction manual.

4.2.5 Site-directed mutagenesis by PCR-driven overlap extension

Extension of overlapping gene segments by PCR was used as a simple and versatile technique for site-directed mutagenesis (Heckman and Pease, 2007). Initial PCRs generate overlapping gene segments that are then used as template DNA for another PCR to create a full-length product. Internal primers generate overlapping, complementary 3' ends on the intermediate segments and introduce nucleotide substitutions, insertions or deletions for site-directed mutagenesis gene segments. Overlapping strands of these intermediate products hybridize at this 3' region in a subsequent PCR and are extended to generate the full-length product amplified by flanking primers that can include restriction enzyme sites for inserting the product into an expression vector for cloning purposes.

This approach was used to obtain the phosphorylation mimic RISP-encoding pGAD plasmid. Briefly, site-directed mutagenesis was accomplished by using mutagenic primers (primer b: 5'-TCACTTTCATCTTCCAACCT-3' and primer c: 5'-AGGTTGGAAGATGAAAGTGA-3') and flanking primers (primer a: 5'-gaattccatatgTCGAGTAATTGGGGAAGTAGC-3' and primer d: 5'-gcgggatcc TTATACAGCAGGAAGAGGAAC-3', where lowercase nucleotides are NdeI and BamHI specific

restriction sites, respectively), to generate intermediate PCR products AB and CD that are overlapping fragments of the entire product AD. Products AB and CD were denatured when used as template DNA for the second PCR; strands of each product were hybridized at their overlapping, complementary regions that also contain the desired mutation (indicated by the underlined nucleotides in primers b and c). Amplification of product AD in PCR #2 is driven by primers a and d. Final product AD was inserted into a pGADT7 yeast vector to obtain pGAD-RISP-S267D.

4.2.6 Restriction endonuclease digestion of DNA

Plasmid DNA was digested using either a single restriction endonuclease or two simultaneously. The latter was only performed where both enzymes exhibited maximum activity in the same buffer. Sequential digestions were performed in the case where two different buffers were required for maximum enzyme activity. DNA from the first digest was recovered by gel extraction (refer to Gel extraction and purification of DNA). Agarose gel electrophoresis (refer to Agarose gel electrophoresis) was employed to analyze recovered DNA prior to use in subsequent reactions. Digestion reactions were prepared in 1.5 mL eppendorf tubes and in a total volume of 50 µL. These were routinely incubated for 2-4 hours at 37 °C. Linearized DNA fragments were analyzed by agarose gel electrophoresis (refer to Agarose gel electrophoresis). The restriction enzyme digestions were performed according to manufacturer's instruction manual.

4.2.7 Ligation of DNA

DNA fragments that were either amplified using PCR (refer to Polymerase Chain Reaction) or excised from existing vectors by restriction endonuclease digestion (refer to Restriction endonuclease digestion of DNA) were ligated into plasmids that had also been digested with the appropriate restriction endonuclease(s) to produce compatible ends for ligation.

Linearized plasmid and insert DNA was resolved by agarose gel electrophoresis (refer to Agarose gel electrophoresis) following digestion, excised and isolated by gel extraction (described in Gel extraction and purification of DNA). Purified insert and plasmid DNA were subsequently used at a 3:1 molar ratio for ligation reactions as outlined in Table-4.2-3. DNA ligation reaction. Negative controls containing either DNA insert or plasmid DNA alone, or no DNA were routinely included. Ligation reactions were carried out for at least 2 hours or up to overnight at room temperature prior to transformation into XL1-Blue, TOP10 or DH5α

competent bacterial cells (described in Transformation of competent bacterial cells). Transformations were selected on solid LB media containing the appropriate antibiotic. Plasmid DNA was subsequently purified from resultant colonies (described in Purification of plasmid DNA from E.coli) and analyzed by either restriction endonuclease digestion (section Restriction endonuclease digestion of DNA) or PCR colony checking (section Polymerase Chain Reaction). The resulting products were resolved alongside appropriate controls by agarose gel electrophoresis (described in section Agarose gel electrophoresis).

Table-4.2-3. DNA ligation reaction

Component	Volume (µL)
DNA insert (300 ng)	x
Plasmid DNA (150 ng)	x
10X T4 DNA ligase buffer	2
T4 DNA ligase	1
dH20 up to	**20**

4.2.8 General Gateway cloning strategy

Gateway technology is a universal cloning technology, which takes advantage of the site-specific recombination properties of bacteria lambda. The first step of this cloning is inserting a gene of interest into the Gateway, pENTRY vector. In order to produce the pENTRY vector a "BP" reaction was performed using 1:1 ratio of the PCR product of the gene of interest flanked with attB1 and attB2 sites and pDONOR vector (pDONR-Zeo) containing attP sites. The 5µl BP reaction consisted of 75 ng of the PCR fragment containing the gene of interest, 75 ng of pDONR-Zeo vector, 0.5 µL of 10X TE buffer, 0.5 µL of BP clonase enzyme mix (Invitrogen). The mixture was incubated on the bench (~20 °C) for 1 h, followed by incubation with Proteinase K (0.5 µL of Proteinase K at 37 °C for 15 min. The entire BP reaction was used to transform 50µl of *E.coli* DH5α cells (by heat shock) and spread on LB agar plates containing 25 µg/mL zeomycin®, the colonies were inoculated in to 5 mL LB containing 25 µg/mL zeomycin® overnight with shaking (250 rpm) at 37 °C. The plasmid was extracted according section Purification of plasmid DNA from E.coli.

In the second step in Gateway® cloning the gene cassette in the pENTRY vector is moved into a Gateway destination vector (binary expression vector). In order to generate an expression vector, a 5 µL LR reaction was performed between the pENTRY clone containing the gene of interest flanked by attL sites and a destination vector containing attR sites. The mix was

prepared as follows: 75 ng of pENTRY clone, 75 ng of destination vector, 0.5 µL of 10X TE buffer and 1 µL of LR clonase. The reaction was performed at 25 °C for 1h and followed by a Proteinase K step (0.5 µL of Proteinase K at 37 °C for 10 min). The entire LR reaction was used to transform DH5α *E.Coli* cells and selected on the LB agar plate with the appropriate antibiotic. Colonies were inoculated in 5 mL of LB at 37 °C overnight and plasmid DNA was extracted as in section Purification of plasmid DNA from E.coli.

4.2.9 Plasmid construction

The construct pbiGUS was described in Bonneville et al. (1989). Plasmids pGAD-RISP and pGAD-RISP-S267A, pmonoGUS, pmonoGFP, pTAV, were described previously (Thiébeauld et al., 2009; Schepetilnikov et al., 2011).

Plasmids for yeast two hybrid assays

PCR products corresponding to eIF2 subunits were amplified from eIF2α (AT5G05470.1), eIF2β (AT5G20920.1) and eIF2γ (AT1G04170.1) cDNAs with pairs of specific primers and cloned into the pGBKT7 vector (Clontech®) as in-frame fusion with the BD-domain to obtain the pBD-eIF2 subunit variants. eIF2β deletion mutants (eIF2βN, aa 1-121; eIF2βΔ124, aa 1-144 and eIF2βC, aa 121-268) fused to the BD-domain in the pGBKT7 vector were produced by deletion mutagenesis of the pGBK-eIF2β.

RISP (AT5G61200.3) and its deletion mutants (NRISP, aa 1-190; MRISP, aa 120-280; CRISP, aa 190-389; RISPΔH1, aa 120-389 and RISPΔH2, with a deletion of aa 120-190) fused to AD were produced by PCR from the original pGAD-RISP (Thiébauld et al., 2009) and cloned between the NdeI and BamHI sites of pGADT7 (Clontech®). PCR product corresponding to RISP-S267D was generated by substitution of Ser at position 267 to Asp (S267D) from pGAD-RISP by PCR-driven overlap extension, and cloned into pGADT7 vector to obtain the pGAD-RISP-S267D construct.

PCR product corresponding to eS6 was amplified from eS6 cDNA (AT5G10360.1) with pairs of specific primers and cloned between the NdeI and BamHI sites into the pGBKT7 vector (Clontech®) as in-frame fusion with the BD-domain to obtain the pGBK-S6 full-length variant. eS6 deletion mutants (NS6, aa 1-83; MS6, aa 83-177; CS6, aa 177-249 and ICS6 130-249) fused to the BD-domain in the pGBKT7 vector were produced by deletion mutagenesis of the pGBK-S6. PCR products corresponding to S6- or C'S6-Ser231A, -Ser231D, -Ser237A, -Ser237D, -Ser231A/Ser237D, Ser231D/Ser237A, -Ser240A and -Ser240D were generated by substitution of Ser at these positions to Ala (A) or Asp (D) from pGBK-S6 by PCR-driven site directed

mutagenesis, and cloned into pGBKT7 vector to obtain pGBK-S6 or -CS6 phosphorylation knockout/mimetic constructs.

Plasmids for recombinant protein expression

PCR product corresponding to the eS6 C-terminal domain (CS6) was amplified from pGBK-S6 with pairs of specific primers and cloned into pGEX-6P-3 as in-frame fusion with the GST-domain to obtain pGEX-CS6.

PCR product corresponding to RISP was amplified from pGAD-RISP with pairs of specific primers and cloned into pGEX-6P-3 as in-frame fusion with the GST-domain to obtain pGEX-RISP. pHis-RISP was constructed by cloning a RISP full-length PCR product from the pGAD-RISP plasmid into the pHGWA expression vector using Gateway® technology (Busso et al., 2005)), which provides an N-terminal hexahistidine tag.

Binary plasmids for generation of transgenic plants

PCR products corresponding to S6-Ser231A, -Ser231D, -Ser237A, -Ser237D, -Ser231A/Ser237D, Ser231D/Ser237A, -Ser237/240/241A and -Ser237/240/241D were generated by substitution of Ser at these positions to Ala (A) or Asp (D) from mutant pGBK-S6 variants by PCR-driven site directed mutagenesis, with primers incorporating attB1 and attB2 sequences and introduced into the pDONR-Zeo by BP clonase reaction according to manufacturer's instructions (Invitrogen®). The resulting pDONR clones were transformed into the *E. coli* strain DH5-alpha and sequenced. DNA fragments were transferred to the destination binary vector pGWB2 (kindly provided by Dr. Tsuyoshi Nakagawa, Shimane University, Matsue, Japan) by LR clonase reaction according to the manufacture instructions (Invitrogen®). The product of recombination reaction (LR reaction) was used to transform *Agrobacterium* as described later.

In a similar way, PCR products corresponding to phosphorylation RISP mutant—RISP-S267A and RISP-S267D—were cloned by Gateway® cloning technology to get N terminal HA-tag fusion proteins. The resulting pDONR clones were transformed into the *E. coli* strain DH5-alpha and sequenced. DNA fragments were transferred to the destination binary vectors pGWB5, pGWB14 and pGWB15 (kindly provided by Dr. Tsuyoshi Nakagawa, Shimane University, Matsue, Japan) by LR clonase reaction according to the manufacture instructions (Invitrogen®).

All pGWB vectors we used for this study (Table-4.2-4. The pGWB series used in this study) confer resistance to both kanamycin and hygromycin in plant and contain the 35S promoter upstream

of the cloning site. The N- or C-terminal tags are automatically fused subsequent to the LR reaction (except for pGWB2 where there is no tag-encoding sequence).

Table-4.2-4. The pGWB series used in this study

Plasmid	Context
pGWB2	[(35S promoter, no tag) (--35S promoter–R1-CmR-ccdB-R2--)]
pGWB5	[(35S promoter, C-sGFP) (--35S promoter–R1- CmR-ccdB-R2–sGFP--)]
pGWB14	[(35S promoter, C-3xHA) (--35S promoter-R1- CmR-ccdB-R2-3xHA--)]
pGWB15	[(35S promoter, N-3xHA) (--35S promoter-3xHA-R1- CmR-ccdB-R2--)]

Cloramphenicol resistance (CmR) and suicide gene (ccdB) are substituted by the gene of interest

4.3 Protein analysis

4.3.1 SDS-polyacrylamide gel electrophoresis

Proteins were resolved according to their electrophoretic mobility using discontinuous sodium dodecyl sulphate polyacrylamide gel electrophoresis (SDS-PAGE) as described previously. Gels were prepared in a vertical mould with a thickness of 1.0 or 1.5 cm and were composed of a lower resolving region [7.5%-15% (v/v) acrylamide, 750 mM Tris-HCl (pH 8.8), 0.2% (w/v) SDS] and an upper stacking region [5% (v/v) acrylamide, 250 mM Tris-HCl (pH 6.8), 0.2% (w/v) SDS]. Polymerization was catalysed by the addition of ammonium persulfate (APS) and tetramethylenediamine (TEMED) to a final concentration of 8 mM and 200 nM, respectively. The gels were transferred to an electrophoresis unit and submerged in running buffer [25 mM Tris-base, 190 mM glycine, 0.1% (w/v) SDS]. Samples containing the proteins to be analyzed were loaded into wells contained within the stacking region and a constant electric potential of 100-150 V was applied for the duration of the gel run. ProSieve® (Quadcolor®) standard was routinely included in the analysis. Resolved proteins contained within the gel were subjected to either Coomassie™ blue staining or immunoblot analysis.

4.3.2 Coomassie™ blue staining

Proteins resolved using SDS-PAGE were visualized by submerging the gel in Coomassie™ blue staining solution [0.25% (w/v) Brilliant Blue R-250, 40% (v/v) methanol, 10% (v/v) acetic acid] for 1 hour on a shaking platform. The resolved proteins were subsequently visualized by distaining the gel under constant motion in a solution of 15% (v/v) ethanol, 15% (v/v) acetic acid.

4.3.3 Western blot transfer

Resolved proteins after SDS-PAGE were made accessible to antibody detection by transferring and immobilizing protein bands contained within the acrylamide gel onto Immobilion® nitrocellulose membranes (0.45 µm pore size) (Millipore®, France). The protein gel and membrane was sandwiched between two layers of Whatman 3 mm filter paper pre-soaked in transfer buffer [30 mM Tris base, 230 mM glycine, 20% (v/v) ethanol]. The sandwich was compiled inside of a BioRad Criterion® Blotter electrophoretic transfer cell. Air bubbles were carefully removed by rolling over the completed sandwich. The cathode was carefully positioned in place and a constant voltage of 100 V was applied for 1 h. The transfer efficiency was evaluated by observing optimal transfer of the colored molecular marker.

4.3.4 Immunological detection of proteins

Nitrocellulose membranes were blocked in 5% non-fat dried milk (w/v) in PBS-T [140 mM NaCl, 3 mM KCl, 1.5 mM KH_2PO_4, 8 mM Na_2HPO_4, 0.1% (v/v) Tween-20] for 1 h to prevent non-specific antibody binding to the membrane in subsequent steps. Membranes were rinsed 15 min 3 times in PBS-T prior to overnight incubating with primary antibody diluted in PBS-T with indicated vehicles (Table-4.3-1 Antibody collection) at 4 °C. Primary antibody solutions were poured off and non-specifically bound primary antibody was washed off with PBS-T three times, with each washing interval lasting 15 min. The appropriate secondary antibody conjugated to horseradish peroxidase (HRP) (listed in Table-4.3-1 Antibody collection) was diluted in 5% (w/v) non-fat dried milk in PBS-T and incubated with gentle mixing for 1 hour at room temperature. Excess secondary antibody was washed from the membrane as before and proteins were visualised using enhanced chemiluminescence (ECL). Membranes were exposed on Fujifilm general purpose blue medical X–ray film (Fujifilm®, France) and developed using an automatic film processor.

4.3.5 Antibodies

Polyclonal phospho-(Ser/Thr) Akt/S6K1 substrate (R/KxR/KxxS/T-P) antibody described in Schepetilnikov et al. (2011) and used for eS6-P and RISP-P detection was obtained from Cell Signaling Technology®. Rabbit polyclonal antibodies raised against RISP, eS6, and CaMV coat protein (CP; anti-RISP, anti-eS6, and anti-CP respectively) were described previously (Thiébeauld et al., 2009). Rabbit polyclonal anti-TAV IgGs were a kind gift from Dr. Kappei Kobayashi (Ehime

University at Ehime, Japan). Primary and secondary antibodies used in this study are listed in Table-4.3-1 Antibody collection.

Table-4.3-1 Antibody collection

Antibody	Description	Dilution	Reference/Source	Buffer[a]
Primary				
anti-HA	Mouse monoclonal antibody against residues (YPYDVPDYA) of the human influenza virus haemagglutinin	1:10000	Sigma-Aldrich	A
anti-cMyc	Rabbit monoclonal IgG against residues 408-439 (EQKLISEEDL) of the human p62c-Myc protein	1:2500	Santa Cruz Biotechnology	A
anti-Phospho-(Ser/Thr) Akt/S6K1 substrate	Rabbit polyclonal antibody against the phosphorylated Ser/Thr signature (R/K)X(R/K)XX(T*/S*)	1:500	Cell Signaling	C
anti-eS6	Rabbit polyclonal antibody against the 30 kDa eS6 recombinant protein	1:5000	Home made	A
anti-P0	Goat polyclonal antibody against the 15 kDa recombinant human P0	1:1000	Home made	A
anti-tubulin	Mouse polyclonal antibody		Pr. Anne-Catherine Schmit	A
IgG anti-TAV (diluted 1:2 in glycerol)	Rabbit polyclonal IgG fraction against the 70 kDa recombinant TAV	1:20000	Dr. Kappei Kobayashi	A
anti-CP (p37)	Rabbit polyclonal antibody against the 37 kDa recombinant coat protein	1:10000	Pr. Mario Keller	A
anti-RISP	Rabbit polyclonal antibody against the 50 kDa recombinant protein	1:2500	Home made	A
anti-GFP	Rabbit polyclonal IgG fraction	1:5000	Life Technologies (Chromotek)	A
Secondary				
anti-mouse	HRP conjugated whole IgG from goat	1:10000 or 1:20000	ThermoFisher Scientific	A/C
anti-rabbit	HRP conjugated whole IgG from goat	1:10000 or 1:20000	ThermoFisher Scientific	A/C

[a] (A) 5% (w/v) non-fat dried milk in PBS-T, (C) PBS-T

4.4 General yeast methods

4.4.1 Cryopreservation and maintenance of yeast cell stock

Yeast strains were prepared for long-term storage as follows. 5 mL of YPD or the appropriate selective SD media was inoculated with a single colony of the desired yeast strain and incubated overnight in a 30 °C shaking incubator. The next day, 1.5 mL of the overnight culture were transferred into a 2 mL cryovial and 8% (v/v) DMSO (dimethyl sulfoxide) was added. The content of the vial was thoroughly mixed, the vial labeled and stored at -80 °C. Yeast strains were recovered by streaking a small amount of the frozen stock out onto YPD or selective agar plates.

The plates were sealed and incubated at 30 °C for 3 days to allow colonies to develop. Stock plates were subsequently kept at 4 °C for up to 3 weeks.

4.4.2 Preparation of competent yeast cells

Chemically competent yeast cells were prepared as follows. A single fresh colony of the AH109 yeast strain was used to inoculate a 50 mL culture of YPD media and grown overnight in a shaking incubator at 30 °C and 250 rpm. The overnight culture was diluted to an OD_{600} of 0.2-0.3 the following day and was further incubated during 3 h at 30 °C until an OD_{600} of 0.5. The cells were harvested by centrifugation at 1000 g for 10 min. The supernatant was discarded and the cell pellet was washed by resuspension in 50 mL 1X TE buffer [10 mM Tris-HCl (pH 7.5), 1 mM EDTA] before pelleting again. The cells were resuspended in 1.5 mL of 1X TE/LiAc buffer [10 mM Tris-HCl (pH 7.5), 1 mM EDTA, 100 mM lithium acetate] and kept in ice until transformation.

4.4.3 Transformation of competent yeast cells

Competent yeast cells (refer to section Preparation of competent yeast cells) were transformed using the lithium acetate/single-stranded carrier DNA/polyethylene glycol protocol. Briefly, 100 µL of competent cells were mixed with 1 µg of the BD-bait encoding DNA, 1 µg of the AD-prey encoding DNA and 0.1 mg of herring testes carrier DNA. A volume of 600 µL of PEG/LiAc solution [40% (v/v) polyethylene glycol-3350, 10 mM Tris-HCl (pH 7.5), 1 mM EDTA, 100 mM lithium acetate] was added per transformation. The contents of the tubes were mixed by gentle vortexing. The transformation mix was incubated in a 30 °C shaking incubator for 30 min at 250 rpm. Seventy µL of DMSO were added to each transformation mix and this was followed by a 20 min heat shock incubation period at 42 °C before pelleting the cells by centrifugation at 14000 rpm for 5 sec. The supernatant was discarded and the cell pellet was resuspended in 200 µL sterile dH20. The entire transformation mix was spread onto solid selective minimal SD media lacking the appropriate amino acids to allow for the selection of successfully transformed cells. The agar plates were incubated at 30 °C for 3-5 days to allow colonies to develop.

4.4.4 Preparation of yeast whole cell lysates

Yeast whole cell lysates were prepared using the urea/SDS protein extraction method. For the purpose of direct immunoblot analysis (sections SDS-polyacrylamide gel electrophoresis, Western blot transfer, Immunological detection of proteins) to assess the BD-bait and AD-prey

expression levels and their phosphorylation states, yeast cell lysates were prepared using a rapid urea/SDS lysis procedure (see below). Details regarding this protocol are outlined below.

Five yeast cell colonies were used to inoculate 5 mL of the appropriate selective media. Each culture was incubated overnight in a 30 °C shaking incubator at 250 rpm and diluted to an OD_{600} of 0.3 in the appropriate volume of fresh YPD media the next day. The culture was further incubated at 30 °C until it reached an OD_{600} of 0.8. 1.5 mL of cells were harvested by centrifugation at 1000 x g for 5 min at 4 °C in duplicates. Immediately after, 80 µL of 425-600 µm glass beads were added to each tube and samples were frozen by placing the tube in liquid nitrogen.

Following the initial freezing step, glass bead lysates were prepared by resuspending the cell pellet in 150 µL of urea/ SDS cracking buffer [8 M urea, 5% (w/v) SDS, 40 mM Tris-HCl (pH 6.8), 0.1 mM EDTA, 0.4 mg/mL bromophenol blue] supplemented with cOmplete® protease inhibitor cocktail (Roche®) and PhosSTOP Phosphatase Inhibitor cocktail (Roche®) according to manufacturer's guidelines and 1 mM sodium molybdate, 1mM sodium fluoride and 80 mM β-glycerol phosphate as phosphatase inhibitors. Samples were incubated at 70 °C for 10 min and processed on a mini-Precellys24 Homogenizer at one 30 sec cycle of 6500 x g. Cell lysates were then incubated in a Thermomixer® (Eppendorf®, France) for 10 min at 95 °C 1500 rpm. Cell debris was pelleted at 14000 rpm for 5 min at 4 °C. Whole cell lysates were analyzed for protein expression levels or TOR-specific phosphoryation by loading equal volumes onto an SDS-PAGE gel (section SDS-polyacrylamide gel electrophoresis) followed by immunoblot analysis (section Immunological detection of proteins).

4.5 Purification of recombinant fusion proteins from *E.coli*

4.5.1 Preparation of competent bacterial cells

Chemically competent bacterial cells were either purchased from Invitrogen or Novagen or prepared in–house as follows. 10 mL of 2YT containing relevant antibiotic was inoculated with the desired bacterial strain and incubated in a 37 °C shaking incubator overnight. The cells were diluted 1:100 in a total volume of 300 mL 2YT the next day. This culture was further incubated at 37 °C until an OD_{600} of 0.6. Cells were harvested by centrifugation at 1000 x g for 10 min and subsequently resuspended in 150 mL ice-cold 0.1 M $CaCl_2$ before being incubated on ice for 30

min. The cells were harvested as before and resuspended in 40 mL of ice-cold 0.1 M $CaCl_2$ containing 15% (v/v) glycerol. 100 µL aliquots of competent cells were prepared and stored at -80 °C.

4.5.2 Transformation of competent bacterial cells

Chemically competent bacterial cells (section Preparation of competent bacterial cells) were transformed according to traditional protocol. Briefly, cells were thawed on ice for 15 minutes. 500 ng of purified plasmid DNA (section Purification of plasmid DNA from E.coli) or the entire DNA ligation reaction (sections Ligation of DNA and Transformation of competent bacterial cells) was added to 50 µL of competent *E.coli* cells in 1.5 mL eppendorf tubes. The transformation mix was incubated on ice for 20 min. To facilitate the uptake of DNA into the competent cells, the cells were heat shocked for 90 sec at 42 °C before aseptically adding 500 µL of LB media. The cells were incubated for 1 hour at 37 °C to allow recovery and were then plated out onto solid LB containing the appropriate antibiotic. The plates were incubated overnight at 37 °C to allow for the selection of successfully transformed cells.

4.5.3 Cryopreservation and maintenance of plasmid DNA

E. coli harboring plasmid constructs were prepared for long-term storage as follows. A single colony of cells containing the desired transformed plasmid was inoculated into 10 mL LB supplemented with the appropriate antibiotic and incubated overnight in a 37 °C shaking incubator. 1.5 mL of the overnight culture was transferred into a 2 mL cryovial and glycerol was added to a final concentration of 25% (v/v), thoroughly mixed and transferred to -80 °C for storage. Frozen stocks could be used directly for subsequent inoculations to purify plasmid DNA (section Purification of plasmid DNA from E.coli)

4.5.4 Expression of recombinant fusion proteins

Wheat germ eIF2 was kindly provided by Professor K. Browning (University of Texas at Austin, Austin, USA). GST-fusion and His-tagged proteins were expressed in Rosetta 2 DE3 pLysS (Novagen®) and purified by the batch Glutathione Sepharose 4B or the HisTrap HP column (GE Healthcare®) procedures respectively, according to supplier protocol (see below).

A single colony of *Escherichia coli* Rosetta2-pLysS(DE3) cells transformed with the desired plasmid was used to inoculate 50 mL of LB or enriched LB medium (section Growth media) containing the appropriate antibiotic and incubated overnight in a 37 ˚C shaking incubator.

Escherichia coli Rosetta2-pLysS(DE3) cells harboring the pGEX-CS6 or -RISP-His expression plasmids were diluted in 2 L of the same original medium containing 100 μg mL^{-1} ampicillin and 25 μg mL^{-1} chloramphenicol and incubated at 30 °C until the OD_{600} reached 0.5. The temperature was shifted to 25 °C and isopropyl β-d-1-thiogalactopyranoside (IPTG) was added to a final concentration of 0.5 mM. Growth was continued for 3 h, after which the cells were harvested by centrifugation for 20 min at 4 °C at 8000 rpm, resuspended in 30 mL of buffer NET [50 mM Tris–HCl pH 7.5, 150 mM NaCl, 0.1 mM EDTA, 0.5 % v/v Igepal 360® (Sigma-aldrich®) and cOmplete® protease inhibitor cocktail (Roche®)] for GST-fusion protein purification, or 30 mL of buffer A (50 mM Tris–HCl pH 8, 300 mM NaCl, 20 mM imidazole, 1 mM DTT, 5% glycerol, 0.1% (v/v) Igepal 360 and cOmplete® protease inhibitor cocktail) for 6xHis-tagged protein purification at 4 °C. Cells were sonicated by six 30 sec-cycles at 40% of amplification power. Lysates were clarified by centrifugation at 16000 x g for 15 min at 4 °C and filtration through a 45 μm filter and processed as follows.

4.5.5 Purification of GST fusion proteins

GST binds to glutathione with high affinity and it is this property that is widely utilized to purify recombinant GST fusion proteins produced in *E. coli* using glutathione coated beads as described below.

Glutathione Sepharose beads were washed three times by NET buffer. Lysate was added to the beads and incubated for 2 h or overnight at 4 °C under constant rotation. Glutathione beads and bound recombinant GST fusion proteins were pelleted by centrifugation at 1000 g for 1 min. Glutathione beads were washed five times with 10 mL of NET300 buffer (NET buffer at 300 mM NaCl) and resuspended in an equal volume of NET300 buffer. 50 μL of the resuspended beads (bound fraction, B) and 30 μl the first supernatant (unbound fraction, U) were used for sample analysis by SDS-PAGE followed by immunoblotting and Coomassie™ blue staining.

Extracts containing GST, GST-RISP and GST-CS6 samples were incubated with Glutathione Sepharose 4B beads (GE Healthcare®) in binding buffer (20 mM Tris, pH 7.5, 300 mM NaCl, 0.1 mM EDTA, and 0.5% (v/v) Igepal 360®) overnight at 4 °C. Following binding, beads were extensively washed by the binding buffer to remove unbound proteins and stored in ice until GST-pull down assays.

The fraction of recombinant RISP-His was loaded on the Ni-column (1 mL) followed by application of (1) a linear gradient of imidazole from 20 to 100 mM in buffer E (50 mM Tris–HCl pH 8, 300 mM NaCl and 5% (v/v) glycerol) and then (2) a 3-step gradient (100 mM, 200 mM and 500 mM imidazole). The RISP-His fractions were analyzed by 12% SDS–PAGE and western blotting (data no shown). Three peak RISP-His containing fractions were pooled and stored at -80 °C.

4.6 Protein interaction assays

4.6.1 GST pull-down assays

Equivalent molar ratios of purified GST-fusion or GST-less recombinant proteins were incubated in 500 µL of prewashed Glutathione beads at 4 °C; after incubation, beads were washed 3 times by 3 mL NET300 buffer.

Pull-down assays were set up as follows. Molar equivalents of purified protein were incubated with the immobilized GST or GST-protein fusion at 4 °C for 2 h under constant rotation. Sepharose beads and associated proteins (bound fraction, B) were recovered by centrifugation at 500 g for 5 min and thoroughly washed as before (4 washing steps). 30 µL of the first unbound fraction (U) solution and bound fraction were used for SDS-PAGE analysis.

Binding of GST or GST-RISP to wheat eIF2 (or GST-Cter eS6 to His-RISP) was carried out in a 300 µL reaction containing 50 mM HEPES pH 7.5, 50 mM KCl, 3 mM magnesium acetate, with either 5 µg of wheat eIF2 or 5 µg of His-RISP. The total bound fraction as well as 30 µL of the unbound fraction were separated by a 15% SDS-PAGE gel and stained by Coomassie™ blue staining.

4.6.2 Yeast two-hybrid assay

The yeast two-hybrid assay is used for detection of protein-protein interactions (Fields and Song, 1989). It relies on the ability of Gal4 DNA binding domain (BD) or activation domain (AD) each fused to a corresponding reporter to restore its transcription activity, if reports interact. Thus wild type protein and its deletion mutants fused to either GAL4 BD- and AD-domains were co-transformed into *S.cerevisiae* strain AH109 as outline under section Transformation of competent yeast cells. Cotransformed yeast auxotrophs were subsequently selected for on solid media lacking the appropriate combination of amino acids. Colonies from successfully cotransformed AH109 yeast cells were replica plated onto the appropriate fresh solid double

amino acid drop-out media. Overnight saturated cultures from these stock plates were prepared in the appropriate liquid selective media and were incubated at 30 °C overnight. The cultures were equilibrated to the same optical density using water.

For the yeast two-hybrid interaction assay a series of two dilutions (ranging from 0.1 and 0.01) were prepared in a 96-well plate. This was followed by spotting 5 µL of the different diluted samples in triplicate onto the appropriate double (+his), triple amino acid drop-outs (-his or -ade) or quadruple (-his and -ade) selective agar. Agar plates containing the diluted samples were allowed to dry at room temperature prior to incubation at 30 °C for 3 to 5 days to allow growth.

To confirm expression of Gal4 BD and AD fusion proteins cracked lysates were prepared as outlined under section Preparation of yeast whole cell lysates and subjected to SDS-PAGE (section SDS-polyacrylamide gel electrophoresis) followed by immunoblot analysis (sections Immunological detection of proteins) using antibodies against cMyc and HA epitope tags.

4.6.3 β-galactosidase assay

Liquid cultures were assayed for β-galactosidase levels to verify and quantify two-hybrid interactions. Because of their quantitative nature, liquid assays can be used to compare the relative strength of the protein-protein interactions observed in selected transformants. We assume that there is some correlation between β-galactosidase activity and the strength of an interaction.

To test for interactions, yeast strain AH109 was cotransformed with purified plasmids by using the Yeastmaker® yeast transformation system 2 (BD Biosciences Clontech®) according to the manufacturer's instructions (section Transformation of competent yeast cells). β-Galactosidase activity was measured by using the Gal-Screen® assay system (Tropix® by Applied Biosystems®, see below). The values were the means from more than three independent experiments.

For this study a Gal-Screen® chemiluminescent reporter gene assay system was used because it allowed a rapid, simple and sensitive detection of β-galactosidase reporter enzyme directly in micro-well cultures of yeast cells. The Gal-Screen reporter assay system incorporates the Galacton-Star® substrate with a luminescence enhancer to generate glow and highly stable light emission kinetics. A single reagent—cell lysis components and luminescent substrate and enhancer, was added directly to cells in culture medium. These reagents provided a sensitive assay system for semi-automated high throughput quantification of interactions, enabling simple processing and measurement of multiple microplates.

Briefly, five yeast cell colonies were used to inoculate 5 mL of the appropriate selective media. Each culture was incubated overnight in a 30 °C shaking incubator at 250 rpm and diluted to an OD_{600} of 0.3 in the appropriate volume of fresh YPD media the next day. The culture was further incubated at 30 °C for 3-4 h until it reached an OD_{600} of 0.8. A hundred microliters of reaction buffer were added to a white 96-well microplate containing 100 µL/well of cells in culture medium. The mixtures were incubated at 26 °C for 60-90 min or until constant light emission was reached and values were measured in a luminometer for 0.1-1 sec/well.

4.7 Plant in-vivo assays

4.7.1 Plant material, growth conditions and expression vectors

Arabidopsis thaliana ecotype Columbia (Col-0) was used as the wild-type model in this study. SALK_048825 (*S6a*), SALK_012147 (*S6b*) and the *S6a*/+,*S6b*/+ double heterozygote lines were kindly provided by Dr. Thierry Desnos (CEA-Université Aix-Marseille-II at Marseille, France) and all of them are in the Col-0 background. Genotype details of these lines are described in Creff et al., (2010). For immunopurification of polysomal complexes we used transgenic plants expressing a *Cauliflower mosaic virus 35S:HF-RPL18* transgene, which over-express a translational fusion of the r-protein L18 with a His_6-FLAG dual epitope tag. Plasmids and expression constructions are described in section Binary plasmids for generation of transgenic plants.

4.7.2 Plant growth conditions

Seeds were sawn on humid freshly prepared *Arabidopsis* culture soil, covered with a plastic lid and stored for three to seven days at 4 °C. *Arabidopsis thaliana* plants were grown under long-day conditions (16 h of light, 8 h of darkness) between 18 and 25 °C under standard greenhouse conditions and the lid was removed after three to four days.

Arabidopsis seedlings were vertically cultured on MS agar (Murashige and Skoog medium with MSMO-salt mixture; Sigma®) and pictures were taken at 14 days after germination (14 dag). All plants were grown in the greenhouse under standard conditions.

4.7.3 Seed sterilization

The seeds were sterilized by 10 min incubation in 3% $NaClO_3$ solution containing 0.1% triton X-100 and 70% (v/v) ethanol and after that incubated 20 min in absolute ethanol. Finally the seeds were washed two to three times with sterile water and then plated under a sterile hood on appropriate MS-Agar plates

4.7.4 Viral infection

Virus infection was achieved using an agroinfectible construct kindly provided by Dr. Kappei Kobayashi derived from the wild-type CaMV isolate CM1841 (pFastWt; Kobayashi and Hohn, 2003, 2004; Tsuge et al., 1994), which was designated in this study simply as CaMV. Full details of the construction of the agroinfectible clone are given in (Laird et al., 2013). Briefly, the hypervirulent *Agrobacterium* strain AGL1+virG (Vain et al., 2004) containing the WT viral construct was grown 20 h at 28 °C in 5 mL of Luria–Bertani medium containing kanamycin (50 µg mL^{-1}) and rifampicin (100 µg mL^{-1}). Five mL of the saturated culture were resuspended in 95 mL of similar liquid medium and overnight incubated at 28 °C. The cells were washed by water, and incubated for 2 h in buffer A containing 10 mM $MgCl_2$, 10 mM MES pH 5.7 and 200µM acetosyringone at room temperature. A final dilution at OD_{600}=0.8 was prepared and plants at the early eight-leaf stage were equally infiltrated on three different leaves.

4.7.5 Transient expression for protoplast GUS-assays

Protoplasts derived from *Arabidopsis thaliana* wild-type or *S6* mutant seedlings were prepared under sterile conditions according to Yoo et al. (2007) with some modifications (see below) and samples of 2 x 10^4 protoplasts were used for PEG mediated transfection. For transactivation, 10 µg pbiGUS, 10 µg p*monoGFP* and either 10 µg pTAV (or 10 µg empty vector p35S) were transfected. p*monoGFP* expression was monitored by western blot with anti-GFP antibodies (Chromotek®). GFP fluorescence and GUS activity was measured using a FLUOstar OPTIMA fluorimeter (BMG Biotech, USA). The values given are the means from more than three independent experiments.

Briefly, leaves from 8-15 dag seedlings were collected and placed in Petri dishes with 5 mL of the 45 µM-filtered cell wall digestion enzyme solution [1.5% (w/v) cellulase R10 (Yakult Pharmaceutical®), 0.4% (w/v) macerozyme R10 (Yakult Pharmaceutical®), 0.4 M mannitol, 20 mM KCl, 20 mM MES (pH 5.7)] previously warmed for 10 min at 55 °C to inactivate DNAse and

proteases and enhance enzyme solubility, and complemented with 10 mM $CaCl_2$ and 0.1% BSA. Seedling leaves were finely and slightly cut by tapping tissue on the top with a scalpel and 15 mL of digestion enzyme solution were added at the end of cutting. Digestion mixtures were vacuum infiltrated for 10 min using a desiccator.

The mixtures were incubated at 28 °C with gentle rotation (40 rpm on a platform shaker). Protoplasts were then transferred to Falcon tubes by passing samples through a Miracloth membrane previously submerged in W5 solution [2 mM MES (pH 5.7), 154 mM NaCl, 125 mM $CaCl_2$ and 5 mM KCl] and centrifuged for 2 min 150 x g at 4 °C without brake. Then, protoplasts were washed twice with 15 mL W5 solution and immediately resuspended in 1–5 mL of MMG solution [0.4 M mannitol, 15 mM $MgCl_2$, 4 mM MES (pH 5.7)]. The final volume was adjusted to obtain the optimal concentration of 2×10^5 cells mL^{-1}. Protoplasts were incubated on ice for 15 min. For routine experiments, seedlings from 50 µL of seeds digested in 20 mL of the enzyme solution gave 1-2 x 10^6 protoplasts.

For transfection 100 µL of protoplasts were mixed with a maximum of 5-10 µg of plasmid diluted in 10 µL and 110 µL of PEG solution [30% (w/v) PEG 4000 (Fluka®); 200 mM mannitol; 100 mM $CaCl_2$] and incubated for 15 min at room temperature. One milliliter of W5 solution was added. Protoplasts were pelleted by gentle centrifugation (2 min, 300 x g), re-suspended immediately in 1 mL of WI solution [0.5 M mannitol; 20 mM KCl; 4 mM MES (pH 5.7)] and transferred into 6-well culture Greiner® plates. Protoplasts were analyzed after 16 h of incubation at 26 °C under darkness conditions.

For the GUS-activity quantification, protoplasts were centrifuged at 1000 x g for 2 min and supernatants were discarded. Pellets were resuspended in 180 µL of dH_2O and transferred into fresh 1.5 mL tubes containing 20 µL of 10X GUS extraction buffer [500 mM Tris-HCl (pH 7.5), 100 mM EDTA (pH 8.0), 1% (v/v) Triton X-100 and 1% (v/v) Igepal 360 ®]. Then samples were vortexed for 15 sec at high speed and incubated for 10 min at room temperature. After centrifugation (14000 rpm for 5 min) supernatants were carefully transferred into fresh new tubes.

GUS activity was measured by monitoring cleavage of the β-glucuronidase substrate 4-methylumbelliferyl β-D-glucuronide (MUG) (Jefferson et al., 1987). The assay was adapted so that large numbers of samples could be assayed and measured in a 96-well plate format. The assay reaction consisted of 150 µL sample extract and 150 µL 2X GUS Assay Buffer [10X GUS extraction buffer containing 2 mM 4-methylumbelliferyl β-D-glucuronide (MUG, Sigma®), 0.1% (w/v) BSA and 1 mM DTT]. The reaction was carried out in a dark microplate incubator (model

Stat-Fax 2200, Awareness technology®) at 37 °C with orbital mixing at 600 rpm. After 20 minutes, 50 µL of the reaction was transferred to 50 µL of 2X Stop Buffer [400 mM sodium carbonate] in an opaque 96-well plate. Before addition of MUG substrate, GFP-generated fluorescence was measured on a FLUO-star plate reader (BMG Lab technologies Inc., France®) at 485 nm when excited at 520 nm. A standard time curve corresponding to 1, 15, 30 and 45 min was set up with every sample by duplicate and used to calculate GFP/GUS relative units corresponding to the linear range slope over the time kinetic assay. GUS fluorescence was read at 355 nm when excited at 460 nm. Values from the fluorescence assay were converted to GUS relative units and then standardized by GFP protein fluorescence to accommodate differences in protoplast transfection efficiency.

4.7.6 Assay for root gravitropism

Seeds were surface-sterilized with 75% (v/v) ethanol for 1 min, followed by 2% (v/v) NaClO bleach with 0.01% (v/v) Triton X-100 detergent for 20 min. After 2 rinses with sterile water, seeds were germinated and vertically grown on a medium containing MS salts (Murashige and Skoog, 1962), 1% sucrose (w/v) and 1% (w/v) agar in Petri dishes. The Petri dishes were kept in the cold (4 °C) and dark for 4 days, then transferred to the growth chambers with 120 µmol s^{-1} m^{-2} fluorescent light in two 16 h-light/8 h-dark cycles at room temperature (22 °C). For root gravitropism assay, germinated seedlings were grown vertically under darkness conditions at room temperature. After 4 days of growth, plates were rotated by 90° and images of root tips were captured (Canon EOS 350D digital) at 24 h or 48 h after reorientation. The angle of the root tip with respect to the gravity vector was measured from the pictures with Image J software.

4.7.7 TOR signaling stimulation and inhibition in Arabidopsis seedlings

For total protein extraction or immunopurification of polyribosomal complex isolation (see methods below) we used 7 dag *Arabidopsis* wild-type Col-0 WT or the *35S:HF-RPL18* transgenic seedlings not treated (Mock), or treated with 100 nM NAA (NAA) or 250 nM Torin-1 during 8 h.

4.7.8 Protein Extraction and In-solution Digestion by the TCA/Acetone method

Treated *Arabidopsis* seedlings (see section TOR signaling stimulation and inhibition in *Arabidopsis* seedlings) were finely ground with liquid nitrogen. Protein extraction was carried out by using the TCA/acetone method. Briefly, the powder was incubated in a precipitating solution (10% TCA, 0.07% β-mercaptoethanol in acetone) for 1h at -20 °C. After centrifugation (5000 rpm for 15 min at 4 °C), the pellet was rinsed once in 0.07% β-mercaptoethanol in acetone, and two times in acetone, and then spin-dried. It was then suspended in a solubilization solution made of 7 M urea, 2 M thiourea, 4% CHAPS (w/v) and 20 mM Tris-HCl pH 8.5 and cell debris was eliminated by centrifugation. Total protein content was determined using the 2-D Quant-kit (GE Healthcare®). 2 mg of proteins were reduced by adding 10 mM DTT and then alkylated by adding 40 mM iodoacetamide. The samples were diluted to 1 M urea by adding 50 mM ammonium bicarbonate, and protein digestion (sequencing grade modified trypsin, Promega®) was performed at an enzyme/substrate ratio of 1:30 (w/w) by overnight incubation at 37 °C, and stopped by adding 1% formic acid (v/v). Stable isotope dimethyl labeling of tryptic peptides, peptide fractionation (SCX), selective enrichment of phosphopeptides using immobilized metal ion affinity chromatography (IMAC) and LC-MS/MS analysis, were performed according to Boex-Fontvieille et al. (2013) by the IBMC (Strasbourg) proteomic platform under the direction of Dr. Philippe Hammann.

4.7.9 Trizol total protein extraction

Briefly, 0.5 g of seedlings were homogenized by adding 1 mL of Trizol solution. Trizol extracts were incubated for 5 min at RT and then 200 µL of chloroform were added to samples. After vortexing for 15 sec and incubation for 3 min at room temperature, extracts were centrifuged for 15 min at 4 °C and 12000 x g, and the remaining aqueous phase was aspirated completely. DNA was precipitated with 100% ethanol and sedimented by centrifuging from the organic phase. The phenol ethanol supernatant obtained is critical for protein. Isopropanol was added to this supernatant to precipitate protein. This protein precipitate was washed thrice with 0.3 M guanidine hydrochloride in 95% ethanol and once with absolute ethanol. Further, the protein precipitate was vacuum-dried and dissolved in solubilization solution made of 7 M urea, 2 M thiourea, 4% CHAPS (w/v) and 20 mM Tris-HCl pH 8.5. After extraction, proteins were treated similarly to TCA/Acetone samples for further MS/MS analyses.

4.7.10 Immunopurification of polyribosomal complexes

After harvesting, equal amount of fresh material was frozen and ground in liquid nitrogen. For ready-to-immunopurification cytoplasmic extracts, 1.5 mL of powder was resuspended in 1.5 mL of ice-cold IP^N buffer. For polyribosomal immunopurification, 1 mL of powder was resuspended in 2 mL of the Ribo IP buffer of choice, depending on the downstream experimental out-puts. Compositions of the appropriate Ribo IP buffers and corresponding washing buffers are described in Table-4.7-1

Table-4.7-1. Composition of IP buffers

Application	Buffer	Composition
Normal IP		
	IP^N	50 mM Tris-HCl (pH 8.8), 250 mM NaCl, 0.5% (v/v) Igepal 360®, 1% (v/v) glycerol, 2 mM DTT, 10 nM MG-132 (Sigma-Aldrich®), cOmplete® Protease and PhosSTOP® Phosphatase Inhibitor cocktails (Roche®)
	$Washing^N$	Same that IP^N
Ribo IP with magnetic beads		
	Ribo IP^M	200 mM Tris-HCl (pH 8.8), 200 mM KCl, 25 mM EGTA, 36 mM $MgCl_2$, 50 µg/mL, 0.5 mg/mL Heparin, 1 % (v/v) Triton X-100®, 1% (v/v) Tween20®, 0.1% (w/v) Brij® 35, 0.1% (v/v) Igepal 360®, 1 mM sodium molybdate, 80 mM β-glycerol phosphate, 10 nM MG-132, cOmplete® protease inhibitor and PhosSTOP Phosphatase Inhibitor cocktails (Roche®)
	$Washing^M$	200 mM Tris-HCl, pH 9.0, 200 mM KCl, 25 mM EGTA, 36 mM $MgCl_2$, 50 mg/mL chloramphenicol, 1 mM sodium molybdate, 80 mM β-glycerol phosphate, cOmplete® Protease and PhosSTOP® Phosphatase Inhibitor cocktails (Roche®)
Ribo IP with agarose beads		
	Ribo IP^A	200 mM Tris-HCl (pH 8.8), 200 mM KCl, 25 mM EGTA, 36 mM $MgCl_2$, 50 µg/mL, 0.5 mg/mL Heparin, 1 % (v/v) Triton X-100®, 1% (v/v) Tween20®, 1% (w/v) Brij® 35, 1% (v/v) Igepal 360®, 1% (w/v) deoxicolic acid, 5 mM DTT, 1 mM sodium molybdate, 80 mM β-glycerol phosphate, 10 nM MG-132, cOmplete® Protease and PhosSTOP® Phosphatase Inhibitor cocktails (Roche®)
	$Washing^A$	200 mM Tris-HCl, pH 9.0, 200 mM KCl, 25 mM EGTA, 36 mM $MgCl_2$, 50 mg/mL chloramphenicol, 5mM DTT, 1 mM sodium molybdate, 80 mM β-glycerol phosphate, cOmplete® Protease and PhosSTOP® Phosphatase Inhibitor cocktails (Roche®)

Samples were homogenized 30 min at 4 °C rotating at 10 rpm. Cell debris was removed by double centrifugation at 16000 x g for 10 min and 15 min respectively. Then, extracts were incubated with 100 µL of EZ-View anti-FLAG® agarose beads, or 100 µL Anti-FLAG® M2 magnetic beads (Sigma-Aldrich®) at 4 °C for 2 h with gentle shaking. The unbound fraction was recovered, and the beads were washed four times for 5 min at 4 °C with 2 mL of appropriate washing buffer according to manufacturer's guidelines.

Magnetic-bead bound complexes were eluted by incubation of the magnetic beads with 200 µL of 1X Laemmli buffer [complemented with 5% β-mercaptoethanol, and cOmplete® Protease and

PhosSTOP Phosphatase inhibitor cocktails] pre-incubated at 95 °C or 30 °C. Agarose-bead bound complexes were eluted with 200 µL of 400 µg/mL of $[FLAG]_3$ peptide (Sigma-Aldrich®) at 4 °C for 30 min. Eluted material was stored at -80 °C the day before prior to MS/MS analyses. Aliquots collected during the elution steps were analyzed by SDS-PAGE followed by immunoblot analysis and Coomassie™ blue staining to analyze the presence of ribosomal specific proteins.

4.7.11 Molecular modeling

The 3D structure of *Arabidopsis* RISP was created using Modeller (Sali et al., 1995) and represented graphically by PyMOL (http://www.pymol.org). eS6 and aIF2 structures were obtained from the PDB database (3U5C and 2QMU respectively) and represented graphically with some color modifications by PyMOL.

4.7.12 Agrobacterium transformation

One µL of plasmid DNA (100-300µg/µL) was added to 40 µL of electro-competent *Agrobacterium* GV3101 cells and incubated on ice for 10 min. Electroporation was carried out in an ice-chilled electroporation cuvette and 1mL of appropriate LB liquid media was added immediately after the electroporation in the Biorad Micro Pulser. The bacterial suspension was incubated for 2 hours at 28 °C with gentle agitation. The cells were collected by gentle centrifugation (600 rpm) and spread on LB agar plates containing appropriate antibiotics. Colonies were incubated for 2-3 days at 28 °C.

4.7.13 Plant transformation

Plants were transformed according to the “floral dip” method (Clough and Bent, 1998). To obtain resistant stems, plants were allowed to grow at 18 °C until the first flowers appeared at stalks of approximately 10 cm in length. Two days before plant transformation a starter culture was prepared by inoculating 50 mL of selective LB medium with the desired *Agrobacterium* transformed clone and incubated for 24 h at 28 °C and 250 rpm. This preculture was used to inoculate a final 500 mL culture which was incubated for 6 h at 28 °C until it reached an OD_{600} of 0.8-1.2. *Agrobacterium* cells were collected by centrifugation at 4000g for 10 min at room temperature and resuspended in 20 mL of 10 mM $MgSO_4$. Ten min before transformation, plants were sprayed by water and placed into a mini-greenhouse, and cells were gently resuspended in 200 mL of freshly made MS liquid medium containing 5% (w/v) sucrose. Eighty

µL of Silwett L-77 were added before dipping. The early developing inflorescences of *Arabidopsis* plants were dipped in the *Agrobacterium* cell suspensions for 1 min with gentle agitation. After that plants were covered with the lid of the mini-greenhouse and kept in darkness conditions for 36 h. The lid was removed on the next day after those plants were treated as usual.

4.7.14 Screen for the primary transformants (Higromycin-based selection)

A rapid method for identifying transformed seedlings was used. *Arabidopsis* T1 seeds obtained after floral dip transformation are plated on 1% agar containing MS medium and hygromycin B and cefotoxine (250 µg/mL), as appropriate. After a 2-day stratification period, seeds were subjected to a regime of 4–6 h light, 48 h dark and 24 h light. Hygromycin B-resistant seedlings are easily identified as they had long hypocotyls (0.8–1.0 cm) whereas non-resistant seedlings have short hypocotyls (0.2–0.4 cm).

Briefly, seeds were surface sterilized and sown onto 1% agar containing MS medium and hygromycin B at a concentration of 35 µg/mL. Excess surface liquid was drained from the plates. Seeds were then stratified for 2 days in the dark at 4 °C. After stratification seeds were transferred to a growth chamber and incubated for 4–6 h at 22 °C in continuous white light (120 µmol m^{-2} s^{-1}) in order to stimulate germination. The plates were then wrapped in aluminum foil and incubated for 2 days at 22 °C. The foil was removed and seedlings were incubated for 24–48 h at 22 °C in continuous white light (120 µmol m^{-2} s^{-1}). The final 24–48 h light incubation need not be continuous; selection worked well when seedlings were placed in a 16 h light, 8 h dark regime although 24 h total light was required for optimum selection.

Total number of transformants was counted and after 2-3 weeks 20 seedlings were transferred to soil and grown to maturation and T1 seeds collected. The independent transformant T1 lines were grown to maturation and T2 seeds were collected and grown in soil in a controlled environment for phenotypic analysis. The homozygosity or heterozygosity of the transformants was assessed using a PCR genotyping assay.

5. Synthèse (en français)

5.1 Résumé

Des études dans notre laboratoire ont démontré que la protéine cellulaire appelée RISP est un composant de la machinerie de traduction cellulaire. Cette dernière est détournée par le virus de la mosaïque du chou-fleur (CaMV) pour assurer, ensemble avec la protéine virale TAV (transactivator/viroplasmin), la traduction de l'ARN 35S polycistronique viral. TAV active le mécanisme de réinitiation, après la traduction d'un cadre de lecture ouvert (ORF, open reading frame), en interagissant avec le facteur d'initiation de la traduction eIF3 et avec RISP et, en les recrutant au niveau des polysomes afin d'assurer la réinitiation de la traduction de l'ORF, situé en aval sur le même ARN messager. D'après les résultats que nous avons obtenus *in vitro*, le complexe formé par RISP et eIF3 peut s'associer avec la sous-unité ribosomique 40S alors que la protéine RISP seule est incapable de se lier au complexe eIF3-40S. Le CaMV est le premier virus pour le quel on a montré qu'une protéine virale, en l'occurrence TAV, est capable d'interagir directement avec la protéine kinase cellulaire TOR et ainsi, d'activer sa voie de signalisation qui stimule la traduction. La protéine RISP a été identifiée comme une nouvelle cible de la voie de signalisation de TOR et il a été montré que la phosphorylation de la sérine 267 (Ser267) par TOR est requise pour promouvoir la réinitiation de la traduction activée par TAV. Cependant, le rôle exact de RISP dans la traduction cellulaire ainsi que dans le processus d'activation par TAV, fait encore l'objet d'investigations.

Les résultats que j'ai obtenus au cours de mon travail de thèse suggèrent que RISP intervient ensemble, avec eIF3, au niveau du complexe de pré-initiation 43S (43S PIC) pour recruter le complexe ternaire (TC ; eIF2/GTP/Met-tRNAi^{Met}), ainsi que dans les changements conformationels du ribosome 80S en cours de traduction, en faisant un pont entre les sous-unités ribosomiques 40S et 60S. Dans un premier temps, j'ai démontré que RISP est capable

d'interagir *in vitro* avec la sous-unité β du facteur d'initiation eIF2 et qu'elle peut être immunoprécipitée spécifiquement avec des anticorps anti-eIF2α à partir d'extrait de plantes. Des résultats préliminaires indiquent que la phosphorylation de RISP n'est pas critique pour la formation du complexe entre RISP et eIF2β. Mais par contre, la mutation de la sérine 267 de RISP en alanine (RISP-S267A) qui empêche la phosphorylation, permet à RISP de s'associer à eIF2β plus efficacement que la substitution de cette même sérine par un acide aspartique (RISP-S267D) qui mime l'état de phosphorylation de RISP. L'ensamble de nos résultats nous permet de proposer un modèle où la protéine RISP relie eIF3 et eIF2 au sein du complexe de pré-initiation 43S pour promouvoir le recrutement du TC au niveau de la sous-unité 40S.

La protéine TAV du CaMV intéragit non seulement avec RISP et eIF3 mais aussi avec des protéines ribosomiques dont eL24. La structure cristallographique du ribosome 80S de la levure a révélé que le domaine N-terminal de la protéine ribosomique eL24 se trouve à l'interface de la sous-unité 60S alors que son hélice α C-terminale qui interagit avec RISP, émerge de la sous-unité 60S en direction de la sous-unité 40S. L'analyse du ribosome suggère que la protéine eL24 et la protéine ribosomique eS6 de la sous-unité 40S pourraient former un pont entre les deux sous-unités du ribosome. La protéine eS6 est connue depuis longtemps pour être une cible de la voie de TOR mais la fonction de la phosphorylation de eS6 demeure inconnue. De ce fait, nous avons investigué l'interaction éventuelle entre eS6 et eL24 ainsi que le rôle de RISP dans l'association entre les sous-unités 40S et 60S. Bien que nous n'ayions trouvé aucun lien direct entre eS6 et eL24, il s'est avéré que RISP a la capacité, lorsqu'elle est phosphorylée, d'interagir non seulement avec eL24 mais également avec eS6 chez la plante *Arabidopsis thaliana*. L'hélice C-terminale de la protéine eS6 d'*A. thaliana* contient 5 sérines dont au moins trois pourraient être phosphorylées par la voie de TOR. Nos résultats suggèrent que la phosphorylation de la protéine eS6 joue un rôle dans sa liaison à RISP, ainsi que dans la transactivation traductionnelle chez le CaMV. En effet, des plantes d'*Arabidopsis*, dans lesquelles une des deux copies du gène codant eS6 a été inactivée (plantes knock-out), sont plus résistantes à l'infection par le CaMV et moins efficaces dans la transactivation traductionnelle assurée par TAV. Nos résultats indiquent que la liaison entre les sous-unités ribosomiques 60S et 40S sous l'effet de RISP, est régulée par la voie de TOR et qu'elle joue un rôle important dans le contrôle de la réinitiation de la traduction.

Les résultats obtenus au cours de mon travail de thèse contribuent à clarifier le mécanisme d'initiation et de réinitiation de la traduction chez les plantes de même que la stratégie utilisée par les virus pour franchir les barrières qui limitent la réinitiation de la

traduction chez les eucaryotes. De manière inattendue, mes résultats apportent également un éclaircissement sur le rôle de la protéine ribosomale eS6 et sa phosphorylation par la voie de TOR dans l'initiation de la traduction et lors de l'infection de la plante par le CaMV. Ainsi, nous commençons enfin à comprendre l'importance et le rôle des ORFs présents dans la région 5' non-traduite de près de 35% des ARNm qui sont traduits par un mécanisme de réinitiation chez *Arabidopsis thaliana*.

[Mots-clés]: (Réinitiation; ARNs polycistroniques; sORF; Pararetrovirus; TAV; RISP; protéine ribosomique eS6, voie de signalisation de TOR)

5.2 Introduction

L'initiation de la traduction de la pluspart des ARNm chez les eucaryotes commence par le recrutement du complexe de pré-initiation 43S (43S PIC) au niveau de la coiffe, à l'extrémité 5' de l'ARNm. Cette dernière est spécifiquement reconnue par le complexe formé des facteurs d'initiation de la traduction, eIF4F contenant 4E, 4G et 4A, pour former, associé au complexe 43S PIC, un nouveau complexe de pré-initiation 48S (48S PIC) sur la région non-traduite de l'ARNm. Ce complexe balaye ensuite linéairement la région 5' non traduite (5'UTR) jusqu'à ce que l'anticodon du Met- ARNt^{Met} interagisse avec un codon initiateur AUG situé dans un contexte favorable, où il s'associe avec la sous-unité ribosomique 60S pour assembler le ribosome complet (80S ; Kozak, 1999). Au cours de ce processus, chacun des facteurs d'initiation a un rôle précis qui permet au final de positionner un ribosome compétent pour la traduction sur le « bon » codon d'initiation. Chez les eucaryotes, le facteur eIF2 fixe une molécule de GTP et se lie à l'ARNt initiateur aminocylé afin de former un complexe ternaire actif eIF2-GTP-Met-ARNt^{Met} (TC) qui sera chargé sur la sous-unité 40S. Le 43S PIC est assemblé soit par liaison séquentielle des facteurs d'initiation de la traduction (eIFs) 1, 1A, 5 et 3, suivie par le recrutement assisté par eIF3 du TC, sur la sous-unité ribosomique 40S (Sokabe et al., 2012), soit, par l'interaction directe entre un complexe préformé contenant les eIFs 1, 1A, 5, 3 et TC et la sous-unité ribosomique 40S (Hinnebusch and Lorsch, 2012). Lors de l'appariement du codon AUG avec le Met- ARNt^{Met}, localisé dans le site P de la sous-unité ribosomique 40S, le complexe eIF2, constitué de trois sous-unités, α, β et γ, hydrolyse la molécule de GTP, stimulé par eIF5, produisant le complexe eIF2-GDP qui se détachera par la suite du ribosome 80S. Le complexe

eIF5B-GTP se lie à la sous-unité 40S et favorise, grâce à l'hydrolyse de son GTP, l'association des sous-unités 40S et 60S pour former le ribosome 80S (Pestova et al., 2000), puis eIF5B-GDP se dissocie des ribosomes ayant peu d'affinité pour eux (Jackson et al., 2010). Afin de reformer un complexe ternaire actif, eIF2-GDP est recyclé en eIF2-GTP par le facteur d'initiation eIF2B qui possède une activité GEF (GTP Exchanging Factor). Le complexe eIF2-GTP pourra ensuite se lier à un nouveau Met-ARNt^{Met} et participer à une nouvelle initiation de la traduction. Il est admis que les facteurs restants se détachent graduellement, au cours des premiers cycles d'élongation après la formation du ribosome 80S (Kozak, 2001).

Après la terminaison de la traduction, les deux sous-unités ribosomiques se dissocient de l'ARNm et recommencent un nouveau cycle de traduction. Dans certains cas, la sous-unité 40S reste fixée sur l'ARNm après la traduction de l'ORF et poursuit sa migration et initie la traduction à un deuxième codon initiateur situé en aval du premier. Toutefois, les mécanismes permettant la réinitiation de la traduction semblent différents selon la longueur du premier ORF traduit, inférieure ou supérieure à 30 codons. Les ORFs, en général de petite taille, présents dans la région 5'UTR de l'ARNm, encore appelée région leader, sont désignés uORFs (upstream ORF). Selon une analyse des séquences de la région 5' UTR de gènes de protéines de mammifères (Suzuki et al., 2000), des uORFs sont présents dans environ 20-50% des ARNm. Ils sont particulièrement fréquents dans les transcrits codant pour les oncoprotéines, les facteurs de croissance et les récepteurs cellulaires. De même, environ 30% des ARNm de la plante *Arabidopsis thaliana* possèdent des uORFs dans leur séquence leader (Calvo et al., 2009; Zhou et al., 2010), notamment ceux codant pour des régulateurs de la transcription (Kawaguchi and Bailey-Serres, 2005). Ces uORFs permettent de moduler la stabilité des ARNm et/ou l'efficacité de la traduction des ORFs majeur(s) localisé(s) en aval par réinitiation de la traduction ou en bloquant les ribosomes sur l'ARNm par le truchement du peptide naissant codé par un uORF (revue, Morris and Geballe, 2000). Souvent, la présence d'un ou plusieurs uORFs dans la région leader des ARNm constitue une barrière pour les ribosomes en cours de balayage, ce qui diminue les taux de traduction de l'ORF principal présent en aval, suite à la dissociation des ribosomes lors du premier cycle traductionnel (Ingolia, 2014).

L'étape limitante de la réinitiation de la traduction est la réacquisition *de novo* de facteurs nécessaires à l'initiation de la traduction tel que le TC au cours du balayage entre l'uORF et l'ORF principal. La distance entre ces deux ORFs est essentielle, car plus elle est importante, plus la probabilité de réacquisition du TC par les ribosomes est grande (Kozak, 1987; Fütterer et Hohn, 1991). Chez la levure, le temps nécessaire à cet effet est inversement

proportionnel à la concentration du TC (Hinnebusch, 1997). Chez les mammifères, un paramètre important pour que le ribosome puisse réinitier la traduction est le temps qu'il met pour traduire l'uORF (Kozak, 2001). La présence d'un long uORF (supérieur à 30 codons) ou d'une structure de type pseudonoeud, provoque une pause de l'élongation et prévient ainsi la réinitiation de la traduction (Rajkowitsch et al., 2004). Si la traduction de l'uORF est suffisamment rapide, certains facteurs impliqués dans la réinitiation de la traduction (RPFs) demeurent sur le ribosome et fournissent le balayage, l'acquisition du TC et enfin, le recrutement de la sous-unité ribosomique 60S afin de permettre la réinitiation de la traduction au prochain codon initiateur (Pöyry et al., 2004).

Le facteur eIF3, avec ses 13 sous-unités différentes, est certainement l'un des RPFs les plus sophistiqués ; il est impliqué dans la formation des complexes de préinitiation de la traduction 43S et 48S, sur l'ARNm (Burks et al., 2001; Hinnebusch, 2006). Dans la réinitiation de la traduction, le facteur eIF3 stimule la liaison entre le TC et la sous-unité ribosomique 40S chez les mammifères, les levures et les plantes (Cuchalová et al., 2010; Hershey and Merrick, 2000; Munzarova et al., 2011; Park et al., 2001). Il a été montré, en se fondant sur des études réalisées *in vitro* dans un système animal, que le facteur eIF4F ou eIF4G associé à eIF4A, persiste quelques temps sur la sous-unité 40S, probablement par l'intermédiaire de eIF3, après avoir participé à l'initiation de la traduction de l'uORF (Pöyry et al., 2004). En effet, les interactions entre la sous-unité 40S, eIF3 et eIF4G doivent être modifiées après la jonction de la sous-unité 60S et donc être plus labiles. Si ces interactions sont perdues avant la fin de la traduction de l'uORF, la sous-unité 40S n'étant plus stabilisée par les facteurs d'initiation, se dissocie de l'ARNm. Une fonction de type RPF a été aussi mise en évidence pour la sous-unité h du facteur eIF3 (eIF3h) et la protéine ribosomique L24 de la sous-unité ribosomique 60S (eL24), étant donné que ces protéines sont impliquées dans la réinitiation de la traduction après un uORF chez les plantes (Kim et al., 2004; Nishimura et al., 2005). En effet, la réinitiation de la traduction de deux familles de facteurs transcriptionnels de plantes, a savoir, les facteurs en réponse à l'auxine (ARF, auxin response factor) et les facteurs de transcription à glissière basique (bZIP, basic zipper transcription factor), impliqués dans le contrôle de l'organogénèse, est sévèrement affectée par des mutations dans eIF3h ou eL24 (Kim et al., 2004; Nishimura et al., 2005; Schepetilnikov et al., 2013; Zhou et al., 2010). L'analyse du ribosome a révélé que la protéine eL24, qui est impliquée dans le processus de recrutement de la sous-unité 60S lors de l'initiation de la traduction chez la levure (Baronas-Lowell and Warner, 1990; Dresios et al., 2000), et la protéine eS6 de la sous-unité 40S, pourraient former un pont entre les deux sous-unités du

ribosome (Anger et al., 2013; Armache et al., 2010; Ben-Shem et al., 2011). De ce fait, ces deux protéines pourraient jouer un rôle important dans le recrutement de la sous-unité 60S.

Des données récentes ont montré que la réinitiation de la traduction après un uORF chez les plantes est contrôlée par la protéine sérine/thréonine kinase TOR (Target of Rapamycin, (Schepetilnikov et al., 2013). TOR est un senseur critique de la suffisance énergétique et nutritionnelle, et un régulateur principal de la croissance cellulaire (Gingras et al., 2001; Senguptaet al., 2010; Dobrenel et al., 2011).

Chez *Arabidopsis*, il a été montré que TOR active S6K1, la protéine kinase ribosomique eS6, en phosphorylant la même thréonine que chez les animaux (T449) (Mahfouz et al., 2006; Schepetilnikov et al., 2011; Xiong and Sheen, 2012). Par ce biais, la formation d'un site de liaison pour la protéine kinase PDK1 (pleckstrin-dependent kinase 1) devient possible pour compléter son activation (Mahfouz et al., 2006).

L'apport de la phytohormone auxine active la protéine kinase TOR et entraine une augmentation du degré de phosphorylation de la sérine 178 de la sous-unité h du facteur eIF3 ce qui déclenche l'activation de la traduction des uORF-ARNm par un mécanisme encore inconnu (Schepetilnikov et al., 2013).

Le virus de la mosaïque du chou fleur (CaMV) a développé une stratégie de réinitiation de la traduction après la traduction d'un ORF long appelée transactivation traductionnelle (Ryabova et al., 2006) pour synthétiser l'ensemble des protéines virales à partir de son ARN pre-génomique 35S (35S pgRNA). Cet ARN polycistronique est coiffé en 5' et polyadenylé en 3' et renferment plusieurs uORFs dans sa région leader. La stratégie de réinitiation, encore peu comprise, consiste à exploiter la machinerie traductionnelle grâce à la protéine virale TAV (transactivator/ viroplasmin), qui est synthétisée principalement à partir de l'ARN monocistronique 19S.

Pour réinitier la traduction après un ORF long, la protéine TAV interagit avec plusieurs partenaires de la machinerie traductionnelle dont le facteur eIF3, la protéine RISP et la protéine ribosomique eL24 de la sous unité 60S, ce qui permet à ce complexe de rester attaché avec les ribosomes lors du premier évènement de traduction, assurant ainsi la régénération de complexes ribosomiques aptes pour la réinitiation après la terminaison de la traduction (Park et al., 2001; Thiébeauld et al., 2009). Il a été montré que la protéine TAV du CaMV active la traduction des ARN polycistroniques chez les plantes grâce à sa capacité de recruter égalment au niveau des ribosomes actifs, la protéine kinase TOR (Target of Rapamycin ; Schepetilnikov et al., 2011). L'interaction de TAV avec TOR provoque l'hyperactivation de TOR ce qui conduit à la

phosphorylation de la thréonine 449 de la protéine kinase S6K1 et la sérine 267 de la protéine RISP et ainsi, à l'activation de la transactivation traductionnelle (Schepetilnikov et al., 2011).

La fonction de la kinase TOR dans la réinitiation de la traduction semble être de maintenir un état élevé de la phosphorylation de RISP et eIF3h au niveau des polysomes (Schepetilnikov et al., 2011, 2013). Au cours des travaux de recherche dans notre laboratoire, il a été montré que la sous-unité ribosomique 60S est un acteur critique impliqué dans la formation du complexe de réinitiation de la traduction *via* des interactions entre TAV et les protéines L18 et L13, localisées à la surface de la sous-unité ribosomique 60S (Leh et al., 2000; Bureau et al., 2004; respectivement). Une autre interaction déterminante dans la transactivation traductionnelle a été décrite entre TAV et la protéine ribosomique eL24. Des études entreprises pour caractériser les domaines d'interaction, montrent que la protéine RISP interagit fortement avec la sous unité 60S, *via* la partie C-terminale de la protéine ribosomique eL24 et avec la partie C-terminale du domaine minimal de TAV, requis pour la transactivation. Le complexe entre TAV et RISP peut donc se former et se stabiliser sur la sous-unité 60S par l'intermédiaire de la protéine ribosomique eL24, étant donné que cette dernière est un partenaire d'interaction commun aux deux protéines TAV et RISP. Toutes ces observations témoignent de l'importance que pourrait avoir ce complexe dans le recrutement efficace de la sous-unité 60S par la sous-unité 40S lors de la traduction afin de favoriser la réinitiation de la traduction. En effet, il faut en particulier tenir compte de l'interaction entre TAV et RISP et du rôle de la protéine eL24 dans le recrutement de la sous-unité 60S (Baronas-Lowell et Warner, 1990) et dans la formation d'un pont entre les deux sous-unités ribosomiques 40S et 60S (Ben-Shem et al., 2011). RISP seule peut servir en tant que protéine d'échafaudage, car elle est capable d'interagir avec eIF3 *via* les sous-unités a / c, la sous-unité ribosomique 40S (si RISP est déjà associée à eIF3), et la sous-unité ribosomique 60S par l'intermédiaire de l'extrémité C-terminale de la protéine ribosomique eL24, ce qui suggère qu'elle possède sa propre fonction de initiation de la traduction chez *Arabidopsis* (Thiébeauld et al., 2009).

In vivo, le cofacteur RISP est co-immunoprécipité à partir d'extraits bruts d'*Arabidopsis* non seulement avec eIF3 et la sous-unité 40S, mais aussi avec eIF2α, ce qui suggère fortement que RISP peut faire partie du complexe de pré-initiation 43S. Cependant, la protéine RISP se trouve dans la fraction ribosomique 60S de germe de blé, et elle co-localise avec des particules contenant la sous-unité 60S dans des cellules BY-2 de *Nicotiana tabacum*, ce qui suggère que RISP peut aussi être constitutive des complexes contenant la sous-unité ribosomique 60S (Thiébeauld et al., 2009).

Au cours de cette étude, nous rapportons deux nouvelles interactions de RISP qui contribuent à la réalisation de ses fonctions dans le complexe de pré-initiation 43S et sur la sous-unité ribosomique 60S pour favoriser le recrutement du TC et le recyclage de la sous-unité 60S. Grâce à sa structure hélicoïdale, RISP est capable d'interagir avec le facteur d'initiation de la traduction eIF2 ou le pont « intraribosomique » 40S/60S établi par les protéines ribosomiques eS6-eL24, et ce, dans un ordre évènementiel dynamique contrôlé par l'état de phosphorylation de RISP et eS6. Par conséquent, nos résultats sont compatibles avec l'idée que, chez les plantes, RISP joue un rôle important dans l'initiation et la réinitiation de la traduction.

5.3 Résultats et discussion

Jusqu'à présent, il a été difficile de savoir comment RISP participe à l'initiation de traduction et en particulier dans le processus de la transactivation traductionnelle activée par la protéine TAV du CaMV. Le rôle de la protéine RISP pourrait être d'aider eIF3 dans le recrutement du TC au niveau du complexe de pré-initiation 43S et de promouvoir la liaison entre le complexe 40S-eIF3 et la sous-unité 60S du ribosome. Au cours de ces travaux, nous avons pu révéler que RISP fonctionne comme une protéine d'échafaudage dynamique qui peut interagir avec eIF2 afin de favoriser l'assemblage du complexe de pré-initiation 43S et avec le pont « intraribosomique » eS6/eL24 pour accoupler les deux sous-unités ribosomiques. Il a été frappant de constater que l'interaction entre la protéine RISP et les facteurs eIF2 et/ou eIF3 est modulée par la phosphorylation de la sérine 267 de RISP par la voie de signalisation de TOR, et que ceci pourrait induire son détachement du complexe d'initiation de la traduction 43S. En plus, la phosphorylation de la sérine 267 conduit RISP à se lier préférentiellement à la forme phosphorylée de la protéine eS6 et à la protéine eL24 de la sous-unité 60S. La façon dont la phosphorylation de cette sérine perturbe la liaison entre RISP et eIF2/eIF3 et favorise l'interaction avec la forme phosphorylée des protéines ribosomiques eS6 et eL24 sur le ribosome fait l'objet d'investigations.

5.3.1 RISP et ses interactions avec le complexe de pré-initiation 43S

La protéine RISP est liée aux complexes d'initiation contenant la sous-unité ribosomique 40S de manière spécifique et stable. En effet, RISP peut être spécifiquement immunoprécipitée à partir d'extraits d'*Arabidopsis* avec des anticorps dirigés contre eIF2α, eIF3c et eS6 (Thiébeauld et al., 2009). Dans cette étude, nous avons démontré que RISP est capable, grâce à des interactions inter-hélicoïdales, de se lier à la sous-unité β du facteur eIF2 au niveau de son hélice centrale qui se situe dans l'interface entre eIF2β et eIF2α (voir la structure du facteur aIF2 d'*Archaea* dans la Figure 2.1-2E; Schmitt et al., 2010). Étant donné que RISP peut contacter à la fois eIF3 et eIF2 dans le complexe 43S, nous concluons que RISP, lorsque elle est attachée à eIF3, peut aider à eIF3 dans la capture de eIF2 *via* sa sous-unité β, stimulant ainsi le recrutement du complexe ternaire par le 43S PIC.

Dans les cellules animales, la phosphorylation de S6K1 par mTORC1 se produit au niveau des complexes de pré-initiation contenant le facteur eIF3 (Holz et al., 2005). Chez *Arabidopsis*, S6K1 est pleinement activée de façon similaire par PDK1 (Mahfouz et al., 2006; Otterhag et al., 2006) et de ce fait, elle devient capable de phosphoryler à son tour, la sous-unité h du facteur eIF3, la protéine ribosomique eS6 et le cofacteur de transactivation RISP. Ceci revêt une importance indiscutable car de cette manière, S6K1 peut être placée dans une position adéquate pour phosphoryler RISP à proximité du facteur eIF3.

Lorsque RISP est phosphorylée, elle se lie à l'hélice α C-terminale de la protéine ribosomique eS6. Bien que les sites de phosphorylation (S231 et S237) de l'hélice C-terminale de eS6 considérés comme probablement sensibles à l'activation ou l'inhibition de la voie de TOR chez les plantes, n'aient pas été encore confirmés, il se trouve que les motifs qui encadrent ces sites de phosphorylation correspondent en partie à ceux trouvés dans nombreux substrats de la kinase S6K1 chez les plantes. Ensemble avec la sérine 240, ces sites de phosphorylation ont été sélectionnés pour des analyses moléculaires d'interaction quantitatives chez la levure (essai de l'activité de la β-galactosidase). Nos données expérimentales chez la levure indiquent que la phosphorylation de ces sites peut fortement contribuer à la capacité de RISP de se lier à la protéine ribosomique eS6. Cependant, la signification fonctionnelle de ces sites de phosphorylation et l'effet de leur mutation sur le développement de la plante, requièrent une exploration plus exhaustive *in planta*.

5.3.2 RISP et son interaction avec la sous-unité ribosomique 60S

Les structures tridimensionnelles du ribosome 80S récemment publiées (Ben-Shem et al., 2011) montrent que les sous-unités 40S et 60S sont reliées par les deux longues hélices-alpha des protéines ribosomique eL19 et eL24, qui émergent respectivement depuis les côtes gauche (pont eB12) et droit (pont eB13, situé près du site principal de liaison des eIFs de la sous-unité 60S) du ribosome. Le pont eB13 est formé par l'hélice C-terminale de la protéine eL24 et une deuxième hélice C-terminale de la protéine eS6 qui émerge de l'interface de la sous-unité 40S. Bien que l'interaction entre eS6 et eL24 ait été proposée, jusqu'à présent, aucune preuve expérimentale de ce contact n'a pas été clairement établie chez les plantes.

Les résultats obtenus avant et au cours de ma thèse suggèrent que RISP peut interagir avec les sous-unités ribosomiques 60S et 40S grâce à sa capacité d'interagir avec les protéines ribosomiques eL24 et eS6, respectivement. Une mutation qui mime l'état de phosphorylation de RISP (S267D), permet à RISP de s'associer à la forme phosphorylée de l'hélice C-terminale d'eS6 de manière plus efficace qu'une mutation qui empêche la phosphorylation (S267A). De cette manière, la structure super enroulée de RISP peut être placée dans une position idéale pour interagir avec eL24 *via* son hélice alpha C-terminale qui émerge de la sous-unité 60S en direction de la sous-unité 40S. Encore une fois, la liaison entre RISP et le pont intraribosomique établi par eL24 et eS6 peut avoir lieu grâce par des interactions hélice-hélice.

Ainsi, nos résultats suggèrent un rôle pour le pont eB13 dans les dernières étapes de l'initiation de traduction, en particulier lors du recrutement de la sous-unité 60S. Cette architecture particulière de la protéine eL24 appuie son rôle dans la transactivation traductionnelle, car son domaine C-terminal a été proposé comme un médiateur de la rétention du facteur eIF3 sur le ribosome. De la même manière, la protéine eS6 pourrait interagir avec des facteurs qui adhèrent sur le segment d'extension $ES6^S$ et agir dans l'initiation ou la réinitiation traductionnelle (Ben-Shem et al., 2011). Ainsi, tenant compte de nos résultats, RISP peut être un de ces facteurs.

Différentes approches *in vitro* n'ont pas permis de révéler une liaison stable entre RISP et la sous-unité ribosomique 40S, contrairement à ce que l'on observe lorsqu'on combine la sous-unité 60S et RISP (Thiébeauld et al., 2009). Cependant, le fait que eS6 ne puisse pas toujours être localisée et par conséquent modélisée dans la structure du ribosome 80S, suggère que la protéine eS6 n'est pas systématiquement présente dans la sous-unité ribosomique 40S et / ou qu'elle soit indisponible pour l'interaction. Tenant compte du fait que les niveaux de phosphorylation de la kinase TOR sont faibles dans les plantes (sa phosphorylation est à peine

détectée par les anticorps utilisés ; Schepetilnikov et al, 2013), il est envisagé ce soit aussi le cas pour l'hélice C-terminale de la protéine ribosomique eS6, et que par conséquent, cela diminuerait la liaison entre RISP et la sous-unité ribosomique 40S, particulièrement *in vitro*. En revanche, le traitement par l'auxine de plantes d'*Arabidopsis* affecte positivement la liaison entre RISP et les sous-unités 40S (Schepetilnikov et al., 2011).

La protéine eS6 a été connue depuis longtemps pour être une cible de la voie de TOR est sa phosphorylation est extrêmement contrôlée car elle est essentielle chez la pluspart des eucaryotes. Depuis sa découverte, cette phosphorylation a suscité beaucoup d'intérêt mais jusqu'au présent, sa fonction biologique demeure inconnue. Dans ce contexte, nos données suggèrent que, en réponse à l'activation de la voie de TOR, la phosphorylation d'eS6 peut renforcer l'association entre les deux sous-unités ribosomiques (40S/60S) par la liaison de la forme phosphorylée de RISP au niveau du pont établi par les protéines eS6 et eL24. Cela pourrait affecter négativement la liaison d'autres ligands au cours de l'étape d'élongation de la traduction, et à l'inverse, promouvoir le recyclage ou la réutilisation des sous-unités ribosomiques 60S pour un nouvel événement d'initiation.

À ce stade, nous pouvons proposer un modèle de travail pour le rôle de RISP dans l'assemblage du complexe de pré-initiation 43S et la transactivation traductionnelle activée par la protéine virale du CaMV (Figure 2.1-8). RISP est recruté pour le complexe de pré-initiation 43S sous la forme d'un complexe avec le facteur eIF3, dont les sous-unités a et / ou c contactent l'hélice-alpha 2 de RISP (Figure 2.1-8A; Thiébeauld et al., 2009). D'après les études d'Holz et col. (2005), la protéine kinase TOR, lorsqu'elle est activée, peut phosphoryler S6K1, qui est liée au facteur eIF3, au niveau des complexes de pré-initiation 48S. Donc, il est probable que la phosphorylation de RISP par la kinase S6K1 aurait également lieu à proximité du complexe de pré-initiation 48S (voir Schepetilnikov et al., 2011). Bien que RISP reste attachée au complexe eIF2-eIF3 lorsqu'elle n'est pas phosphorylée, sa phosphorylation pourrait déclencher son recrutement par la protéine virale TAV, et la relocalisation de RISP-P (P pour phosphorylée) ou du complexe RISP-P / TAV en direction du domaine C-terminal de la protéine ribosomique eS6 (Figure 2.1-8B). Une possibilité intéressante est que l'interaction entre eS6, RISP et TAV pourrait servir à la rétention du facteur eIF3 (via l'extrémité N-terminale d'eIF3g) dans les polysomes lors d'un premier événement d'élongation long. Plus tard, au cours de la reprise du balayage, les contacts découverts dans cette étude entre RISP et la protéine eS6 de la sous-unité 40S, pourraient assurer la rétention et la réutilisation de la sous-unité 60S *via* le réseau d'interaction entre eL24, eS6 et RISP (Figure 2.1-8C). Si RISP et TAV participent à la stabilisation du pont

intraribosomique établi par les protéines eS6 et eL24, les sous-unités 60S pourraient être utilisées pour des événements consécutifs de réinitiation. Cependant, pour que ça soit possible il faudrait que la voie de signalisation de TOR puisse rester active en permanence. En effet, en présence de TAV, l'activation constitutive de la kinase S6K1 maintient élevé l'état de phosphorylation de RISP au niveau des polysomes (Schepetilnikov et al., 2011). Le recrutement du TC *de novo* peut se faire soit par le facteur eIF3 seul ou par l'intermédiaire de son complexe avec RISP, à condition que RISP non phosphorylée soit disponible. De manière intéressante, il a été démontré que le facteur eIF3 est impliqué dans la réinitiation traductionnelle chez la levure, et que les sous unités a, g et i jouent un rôle important dans la reprise du balayage des complexes ribosomiques après la terminaison de la traduction chez la levure (Cuchalová et al., 2010; Munzarova et al., 2011).

5.3.3 Le rôle de RISP dans la transactivation traductionnelle

Nos données suggèrent que la protéine ribosomique eS6 joue un rôle dans la transactivation traductionnelle activée par la protéine TAV du CaMV et qu'elle est clairement indispensable pour l'infection des plantes par le CaMV. Étant donné que TAV maintient la protéine kinase TOR dans un état constitutivement phosphorylé, RISP et eS6 sont également susceptibles d'être phosphorylée lors de l'infection par le CaMV. Ainsi, TOR, lorsqu'elle est active, créerait des conditions favorables pour la liaison de RISP avec la protéine eL24 de la sous-unité 60S et pourrait stabiliser son interaction avec la protéine ribosomique eS6 de la sous-unité 40S. À cette fin, TAV renforcerait le lien entre les deux sous-unités grâce à sa capacité de liaison avec l'extrémité N-terminale de la protéine ribosomique eL24 et l'hélice C-terminale (hélix 4) de RISP. Une fois liée à proximité du principal site de liaison de facteurs de traduction, sur l'interface de la sous-unité ribosomique 60S, TAV pourrait interférer avec les événements d'élongation, mais au même temps, elle pourrait égalment promouvoir le balayage du ribosome 80S, lorsqu'il est sous la conformation « ouverte » 40S-60S comme nous l'avons proposé précédemment (Thiébeauld et al., 2009). En effet, l'idée d'un balayage du ribosome 80S a été avancée récemment par le groupe de Tatiana Pestova (Skabkin et al., 2013). De plus, la transactivation traductionnelle induite par TAV est stimulée par la surexpression d'une forme libre de la protéine ribosomique eL24 (Park et al., 2001). Chez les plantes, il y a une certaine hétérogénéité au sein de la population ribosomique de la cellule (Giavalisco et al., 2005), et de ce fait, la surexpression de eL24 pourrait augmenter la fraction de ribosomes contenant cette protéine.

Conformément à cette hypothèse, l'inactivation d'une des deux copies du gène codant eS6 réduit l'efficacité de la transactivation traductionnelle assurée par TAV (Figure 2.1-6D).

Bien que la transactivation traductionnelle soit essentielle pour la réplication virale, l'inactivation de la sous-unité h du facteur eIF3, qui n'est pas cruciale pour la cellule, de même que l'inactivation de protéines essentielles comme TOR et eS6, qui elles, sont essentielles pour la réinitiation après la traduction d'un ORF long, affectent ou limitent l'infection des plantes hôtes, en occurrence *Arabidopsis*, par le CaMV. Dans l'ensemble, les gènes de résistance aux virus dans les plantes sont souvent hérités de manière récessive, ce qui rend ces gènes avantageux comme outils dans les programmes de sélection pour contrôler les maladies virales des plantes. Divers études révèlent un nombre croissant de gènes de résistance récessifs codant pour des facteurs d'initiation qui appartient aux familles 4E (eIF4E) et 4G (eIF4G) (Robaglia and Caranta, 2006). Dans notre étude, des plantes d'*Arabidopsis thaliana*, dans lesquelles une des deux copies du gène codant eS6 a été inactivée (plantes knock-out), sont plus résistantes à l'infection par le CaMV dû à une réduction dans l'efficacité de la transactivation traductionnelle assurée par TAV. Encore une fois, dans les plantes knock-out *eS6a* la traduction coiffe dépendante ne présente pas d'altération évidente, bien au contraire, elle semble être plus efficace (Figure 2.1-6D). De cette manière, un bon nombre de gènes dont les mutations confèrent de résistance au CaMV, codifient des protéines impliquées dans la machinerie de la traduction de la plante.

5.3.4 eS6, eL24 et d'autres RPFs chez la plante

Des analyses statistiques ont montré que les uORFs sont nettement plus long chez les plantes que chez les autres organismes, ce qui indique une plus grande capacité de réinitiation de la traduction dans la cellule végétale. Des mutations dans deux RPFs décrits chez la plante, à savoir eL24 et eIF3h, qui coopèrent pour favoriser la réinitiation de la traduction, provoquent certaines anomalies communes dans le développement du système vasculaire au niveau des cotylédons et les valves du fruit (Zhou et al., 2010). En plus des anomalies dans la réinitiation de la traduction, d'autres défauts de la fonction des ribosomes pesant sur la synthèse des protéines pourraient contribuer aux phénotypes observés. En effet, des mutations dans plusieurs protéines ribosomiques perturbant le développement de la plante de la même façon (Byrne, 2009), pourraient ne pas être impliquées dans le processus de la réinitiation de la traduction *per se*. Par ailleurs, toutes les mutations inactivant la fonction des RPFs qui ont été étudiés, comme par exemple la kinase TOR, eIF3h (Schepetilnikov et al., 2013) et dans cette étude, la protéine

ribosomique eS6, induisent des anomalies gravitropiques, suggérant leur rôle dans la transduction des signaux par la voie du TOR qui ont pour objectif de stimuler la traduction d'ARNm qui contiennent des ORFs au sein de leur région 5'UTR. Nous prévoyons que d'autres mutants de protéines impliquées dans la réinitiation de la traduction pourraient induire des défauts dans le gravitropisme des racines.

5.4 Matériel et méthodes

5.4.1 Matériel végétal, conditions de croissance et vecteurs d'expression

L'écotype Columbia (Col-0) d'*Arabidopsis thaliana* a été utilisé comme modèle dans cette étude. Nos expériences ont été réalisées avec la plante d'*A. thaliana* sauvage, et les plantes d'*Arabidopsis* déficientes pour la protéine eS6, appelées *S6a* (SALK_048825)*, S6b* (SALK_012147) et *S6a/+, S6b/+* (lignées doubles hétérozygotes), qui ont été aimablement fournies par Dr. Thierry Desnos (CEA-Université Aix-Marseille-II, Marseille, France). Les détails du génotype de ces lignées sont décrites par Creff et al., (2010). Les plasmides et les constructions pour les expériences d'expression de protéines sont décrits dans les données supplémentaires. Pour les conditions de croissance des semis, et de la culture de cellules d'*Arabidopsis*, la préparation des extraits de protéines et la production recombinante des protéines RISP et eS6 étiquetées par une extension de histidines ou par la protéine GST, voir la section de Matériel et Méthodes de cette thèse.

5.4.2 Infection virale

L'infection par le virus CaMV a été réalisée en utilisant une construction binaire dérivée de l'isolat WT du CaMV CM1841 qui a été aimablement fournie par Dr. Kappei Kobayashi (pFastWt; Kobayashi et Hohn, 2003, 2004; Tsuge et al., 1994), et qui a été désignée dans cette étude simplement comme CaMV. Tous les détails de la construction contenant le génome du CaMV sont indiqués dans l'article publié par Laird et al., (2013). En résumé, la souche hypervirulente d'*Agrobacterium* AGL1 + virG (Vain et al., 2004) contenant le clone viral WT du CaMV a été cultivée pendant 20 h à 28 °C dans 5 mL de milieu Luria-Bertani contenant de la kanamycine (50 µg ml^{-1}) et de la rifampicine (100 µg ml^{-1}). Cinq mL de la culture saturée ont été remis en suspension dans 95 mL du même milieu liquide et la nouvelle culture a été incubée pendant une

nuit à 28 °C. Les cellules ont été lavées avec de l'eau, et mises en incubation pendant 2 h dans du tampon A contenant 10 mM de $MgCl_2$, 10 mM de MES pH 5,7 et 200 µM d'acétosyringone, à température ambiante. Une dilution finale à DO_{600} = 0,8 a été préparée et les plantes au stade de 8 feuilles ont été infiltrées de manière homogène sur trois feuilles différentes.

5.4.3 Purification des protéines

Le facteur eIF2 des germes de blé a été gracieusement fourni par le professeur K. Browning (Université du Texas à Austin, Etats-Unis). Les protéines de fusion avec la GST et marquées par histidines ont été exprimées chez la souche d'*E.coli* Rosetta 2 DE3 pLysS (Novagen®) et purifiées par la méthode de « batch » avec la glutathion Sepharose 4B ou la colonne HisTrap HP (GE Healthcare®), respectivement, selon le protocole du fournisseur (voir la section de Matériel et Méthodes de cette thèse).

5.4.4 Analyses par GST-pull down

Ces analyses ont été réalisées comme il a été décrit précédemment par Park et al. (2001). La liaison de GST ou GST-RISP à eIF2 de blé (ou GST-Cter-eS6 à His-RISP) a été réalisée dans une réaction de 300 µL contenant 50 mM de HEPES pH 7,5, KCl 50 mM, acétate de magnésium 3 mM, avec soit 5 µg du facteur eIF2 ou 5 µg de la protéine His-RISP. La fraction liée totale, ainsi que 30 µL de la fraction non liée ont été séparées par SDS-PAGE sur un gel à 15% et les protéines ont été colorées par le bleu de Coomasie.

5.4.5 Analyses par la technique de double hybride

Pour tester les interactions, la souche de levure AH109 a été co-transformée avec les plasmides purifiés à l'aide du système de transformation de levure Yeastmaker® 2 (BD Biosciences Clontech®) selon les instructions du fabricant. L'activité de la β-galactosidase a été mesurée en utilisant le système Gal-Screen (TROPIX® par Applied Biosystems®, voir la section de Matériel et Méthodes de cette thèse). Les valeurs indiquées sont les moyennes de plus de trois expériences indépendantes.

5.4.6 Expression transitoire en protoplastes et quantification de l'activité de GUS

Des protoplastes provenant d'*Arabidopsis thaliana* sauvage ou de plantes mutantes *S6a* ont été préparés selon Yoo et al. (2007) avec quelques modifications (voir la section de Matériel et Méthodes de cette thèse) et des échantillons contenant 2 x 10^4 protoplastes, ont été utilisés pour la transfection par PEG. Pour les analyses de la transactivation traductionnelle, 10 µg des plasmides d'intérêt ont été utilisés pour la transfection. L'expression de pmonoGFP a été surveillée par Western blot avec des anticorps anti-GFP (Chromotek®). La fluorescence de la GFP et l'activité GUS ont été mesurées en utilisant un fluorimètre FLUOstar OPTIMA (BMG Biotech, USA). Les valeurs indiquées sont les moyennes de plus de trois expériences indépendantes.

5.4.7 Essai de gravitropisme en racines

Les surfaces des graines ont été stérilisées avec 75% (v/v) d'éthanol pendant 1 min, suivi de 2% (v/v) de javel avec 0,01% (v/v) de Triton X-100 pendant 20 min. Après deux rinçages avec de l'eau stérile, les graines ont été mises à germer puis cultivées sur un milieu solide verticale contenant des sels MS (Murashige et Skoog, 1962), 1% de saccharose (p/v) et 1% (p/v) d'agarose dans des boîtes de Pétri. Les boîtes de Pétri ont été conservées dans le froid (4 °C) en conditions d'obscurité pendant 4 jours, puis transférées dans des chambres de croissance avec 120 pmol s^{-1} m^{-2} de lumière fluorescente pour deux cycles 16 h-lumière/8h-obscurité à température ambiante constante (22 °C). Pour l'analyse de la réponse gravitropique dans les racines, les plantules germées ont été cultivées verticalement dans l'obscurité à température ambiante constante. Après 4 jours de croissance, les plaques ont subi une rotation de 90 ° et des images de l'extrémité des racines ont été prises (Canon EOS 350D) à 24 h ou 48 h après réorientation. L'angle de la pointe de la racine par rapport au vecteur de gravité a été mesuré à partir des images avec le logiciel Image J.

5.4.8 Modélisation moléculaire

La structure 3D de la protéine RISP d'*Arabidopsis* a été créée en utilisant Modeller (Sali et al., 1995) et représentée graphiquement par le logiciel PyMOL (http://www.pymol.org).

6. Bibliography

Acker, M.G., Shin, B.-S., Dever, T.E., and Lorsch, J.R. (2006). Interaction between eukaryotic initiation factors 1A and 5B is required for efficient ribosomal subunit joining. J. Biol. Chem. *281*, 8469–8475.

Acker, M.G., Shin, B.-S., Nanda, J.S., Saini, A.K., Dever, T.E., and Lorsch, J.R. (2009). Kinetic analysis of late steps of eukaryotic translation initiation. J. Mol. Biol. *385*, 491–506.

Ahn, C.S., Lee, H.-S., and Pai, H.-S. (2011). Molecular functions of the PP2A regulatory subunit Tap46 in plants. Plant Signal. Behav. *6*, 1067–1068.

Aitken, C.E., and Lorsch, J.R. (2012). A mechanistic overview of translation initiation in eukaryotes. Nat. Struct. Mol. Biol. *19*, 568–576.

Algire, M.A., Maag, D., and Lorsch, J.R. (2005). Pi release from eIF2, not GTP hydrolysis, is the step controlled by start-site selection during eukaryotic translation initiation. Mol. Cell *20*, 251–262.

Alone, P.V., and Dever, T.E. (2006). Direct binding of translation initiation factor eIF2gamma-G domain to its GTPase-activating and GDP-GTP exchange factors eIF5 and eIF2B epsilon. J. Biol. Chem. *281*, 12636–12644.

Anderson, G.H., Veit, B., and Hanson, M.R. (2005). The *Arabidopsis* AtRaptor genes are essential for post-embryonic plant growth. BMC Biol. *3*, 12.

Anger, A.M., Armache, J.-P., Berninghausen, O., Habeck, M., Subklewe, M., Wilson, D.N., and Beckmann, R. (2013). Structures of the human and *Drosophila* 80S ribosome. Nature *497*, 80–85.

Armache, J.-P., Jarasch, A., Anger, A.M., Villa, E., Becker, T., Bhushan, S., Jossinet, F., Habeck, M., Dindar, G., Franckenberg, S., et al. (2010). Localization of eukaryote-specific ribosomal proteins in a 5.5-Å cryo-EM map of the 80S eukaryotic ribosome. Proc. Natl. Acad. Sci. U. S. A. *107*, 19754–19759.

Asano, K., Krishnamoorthy, T., Phan, L., Pavitt, G.D., and Hinnebusch, A.G. (1999). Conserved bipartite motifs in yeast eIF5 and eIF2Bepsilon, GTPase-activating and GDP-GTP exchange factors in translation initiation, mediate binding to their common substrate eIF2. EMBO J. *18*, 1673–1688.

Asano, K., Clayton, J., Shalev, A., and Hinnebusch, A.G. (2000). A multifactor complex of eukaryotic initiation factors, eIF1, eIF2, eIF3, eIF5, and initiator tRNA(Met) is an important translation initiation intermediate *in vivo*. Genes Dev. *14*, 2534–2546.

Asano, K., Shalev, A., Phan, L., Nielsen, K., Clayton, J., Valásek, L., Donahue, T.F., and Hinnebusch, A.G. (2001). Multiple roles for the C-terminal domain of eIF5 in translation initiation complex assembly and GTPase activation. EMBO J. *20*, 2326–2337.

Ban, N., Beckmann, R., Cate, J.H.D., Dinman, J.D., Dragon, F., Ellis, S.R., Lafontaine, D.L.J., Lindahl, L., Liljas, A., Lipton, J.M., et al. (2014). A new system for naming ribosomal proteins. Curr. Opin. Struct. Biol. *24*, 165–169.

Bandi, H.R., Ferrari, S., Krieg, J., Meyer, H.E., and Thomas, G. (1993). Identification of 40 S ribosomal protein S6 phosphorylation sites in Swiss mouse 3T3 fibroblasts stimulated with serum. J. Biol. Chem. *268*, 4530–4533.

Barakat, A., Szick-Miranda, K., Chang, I.-F., Guyot, R., Blanc, G., Cooke, R., Delseny, M., and Bailey-Serres, J. (2001). The organization of cytoplasmic ribosomal protein genes in the arabidopsis genome. Plant Physiol. *127*, 398–415.

Baronas-Lowell, D.M., and Warner, J.R. (1990). Ribosomal protein L30 is dispensable in the yeast *Saccharomyces cerevisiae*. Mol. Cell. Biol. *10*, 5235–5243.

Baughman, G.A., Jacobs, J.D., and Howell, S.H. (1988). *Cauliflower mosaic virus* gene VI produces a symptomatic phenotype in transgenic tobacco plants. Proc. Natl. Acad. Sci. U. S. A. *85*, 733–737.

Beauchamp, E.M., and Platanias, L.C. (2013). The evolution of the TOR pathway and its role in cancer. Oncogene *32*, 3923–3932.

Beltrán-Peña, E., Aguilar, R., Ortíz-López, A., Dinkova, T.D., and De Jiménez, E.S. (2002). Auxin stimulates S6 ribosomal protein phosphorylation in maize thereby affecting protein synthesis regulation. Physiol. Plant. *115*, 291–297.

Berthelot, K., Muldoon, M., Rajkowitsch, L., Hughes, J., and McCarthy, J.E.G. (2004). Dynamics and processivity of 40S ribosome scanning on mRNA in yeast. Mol. Microbiol. *51*, 987–1001.

Birnboim, H.C., and Doly, J. (1979). A rapid alkaline extraction procedure for screening recombinant plasmid DNA. Nucleic Acids Res. *7*, 1513–1523.

Blackwell, J.R., and Horgan, R. (1991). A novel strategy for production of a highly expressed recombinant protein in an active form. FEBS Lett. *295*, 10–12.

Boex-Fontvieille, E., Daventure, M., Jossier, M., Zivy, M., Hodges, M., and Tcherkez, G. (2013). Photosynthetic control of *Arabidopsis* leaf cytoplasmic translation initiation by protein phosphorylation. PLoS ONE *8*.

Bonneville, J.M., Sanfaçon, H., Fütterer, J., and Hohn, T. (1989). Posttranscriptional trans-activation in *Cauliflower mosaic virus*. Cell *59*, 1135–1143.

Broglio, E.P. (1995). Mutational analysis of *Cauliflower mosaic virus* gene VI: changes in host range, symptoms, and discovery of transactivation-positive, noninfectious mutants. Mol. Plant-Microbe Interact. MPMI *8*, 755–760.

Browning, K.S. (1996). The plant translational apparatus. Plant Mol. Biol. *32*, 107–144.

Browning, K.S. (2004). Plant translation initiation factors: it is not easy to be green. Biochem. Soc. Trans. *32*, 589–591.

Browning, K.S., Fletcher, L., Lax, S.R., and Ravel, J.M. (1989). Evidence that the 59-kDa protein synthesis initiation factor from wheat germ is functionally similar to the 80-kDa initiation factor 4B from mammalian cells. J. Biol. Chem. *264*, 8491–8494.

Budkevich, T., Giesebrecht, J., Altman, R.B., Munro, J.B., Mielke, T., Nierhaus, K.H., Blanchard, S.C., and Spahn, C.M.T. (2011). Structure and dynamics of the mammalian ribosomal pretranslocation complex. Mol. Cell *44*, 214–224.

Bureau, M., Leh, V., Haas, M., Geldreich, A., Ryabova, L., Yot, P., and Keller, M. (2004). P6 protein of *Cauliflower mosaic virus*, a translation reinitiator, interacts with ribosomal protein L13 from *Arabidopsis thaliana*. J. Gen. Virol. *85*, 3765–3775.

Burks, E.A., Bezerra, P.P., Le, H., Gallie, D.R., and Browning, K.S. (2001). Plant initiation factor 3 subunit composition resembles mammalian initiation factor 3 and has a novel subunit. J. Biol. Chem. *276*, 2122–2131.

Busso, D., Delagoutte-Busso, B., and Moras, D. (2005). Construction of a set Gateway-based destination vectors for high-throughput cloning and expression screening in *Escherichia coli*. Anal. Biochem. *343*, 313–321.

Byrne, M.E. (2009). A role for the ribosome in development. Trends Plant Sci. *14*, 512–519.

Calvo, S.E., Pagliarini, D.J., and Mootha, V.K. (2009). Upstream open reading frames cause widespread reduction of protein expression and are polymorphic among humans. Proc. Natl. Acad. Sci. U. S. A. *106*, 7507–7512.

Carroll, A.J. (2013). The *Arabidopsis* cytosolic ribosomal proteome: from form to function. Front. Plant Sci. *4*.

Carroll, A.J., Heazlewood, J.L., Ito, J., and Millar, A.H. (2008). Analysis of the *Arabidopsis* cytosolic ribosome proteome provides detailed insights into its components and their post-translational modification. Mol. Cell. Proteomics MCP *7*, 347–369.

Casati, P., and Walbot, V. (2004). Crosslinking of ribosomal proteins to RNA in maize ribosomes by UV-B and its effects on translation. Plant Physiol. *136*, 3319–3332.

Chen, J., Zheng, X.F., Brown, E.J., and Schreiber, S.L. (1995). Identification of an 11-kDa FKBP12-rapamycin-binding domain within the 289-kDa FKBP12-rapamycin-associated protein and characterization of a critical serine residue. Proc. Natl. Acad. Sci. U. S. A. *92*, 4947–4951.

Cheng, S., and Gallie, D.R. (2006). Wheat eukaryotic initiation factor 4B organizes assembly of RNA and eIFiso4G, eIF4A, and poly(A)-binding protein. J. Biol. Chem. *281*, 24351–24364.

Chiu, W.-L., Wagner, S., Herrmannová, A., Burela, L., Zhang, F., Saini, A.K., Valásek, L., and Hinnebusch, A.G. (2010). The C-terminal region of eukaryotic translation initiation factor 3a (eIF3a) promotes mRNA recruitment, scanning, and, together with eIF3j and the eIF3b RNA recognition motif, selection of AUG start codons. Mol. Cell. Biol. *30*, 4415–4434.

Clemens, M.J. (2001). Translational regulation in cell stress and apoptosis. Roles of the eIF4E binding proteins. J. Cell. Mol. Med. *5*, 221–239.

Clough, S.J., and Bent, A.F. (1998). Floral dip: a simplified method for *Agrobacterium*-mediated transformation of *Arabidopsis thaliana*. Plant J. Cell Mol. Biol. *16*, 735–743.

Creff, A., Sormani, R., and Desnos, T. (2010). The two *Arabidopsis* RPS6 genes, encoding for cytoplasmic ribosomal proteins S6, are functionally equivalent. Plant Mol. Biol. *73*, 533–546.

Cuchalová, L., Kouba, T., Herrmannová, A., Dányi, I., Chiu, W.-L., and Valásek, L. (2010). The RNA recognition motif of eukaryotic translation initiation factor 3g (eIF3g) is required for resumption of

scanning of posttermination ribosomes for reinitiation on GCN4 and together with eIF3i stimulates linear scanning. Mol. Cell. Biol. *30*, 4671–4686.

Dar, A.C., Dever, T.E., and Sicheri, F. (2005). Higher-order substrate recognition of eIF2alpha by the RNA-dependent protein kinase PKR. Cell *122*, 887–900.

Dempsey, J.M., Mahoney, S.J., and Blenis, J. (2010). 1 - mTORC1-Mediated Control of Protein Translation. In The Enzymes, Fuyuhiko Tamanoi and Michael N. Hall, ed. (Academic Press), pp. 1–20.

Dennis, M.D., Person, M.D., and Browning, K.S. (2009). Phosphorylation of plant translation initiation factors by CK2 enhances the in vitro interaction of multifactor complex components. J. Biol. Chem. *284*, 20615–20628.

Deprost, D., Truong, H.-N., Robaglia, C., and Meyer, C. (2005). An *Arabidopsis* homolog of RAPTOR/KOG1 is essential for early embryo development. Biochem. Biophys. Res. Commun. *326*, 844–850.

Deprost, D., Yao, L., Sormani, R., Moreau, M., Leterreux, G., Nicolai, M., Bedu, M., Robaglia, C., and Meyer, C. (2007). The *Arabidopsis* TOR kinase links plant growth, yield, stress resistance and mRNA translation. EMBO Rep. *8*, 864–870.

Dever, T.E., and Green, R. (2012). The elongation, termination, and recycling phases of translation in eukaryotes. Cold Spring Harb. Perspect. Biol. *4*, a013706.

Dey, M., Cao, C., Sicheri, F., and Dever, T.E. (2007). Conserved intermolecular salt bridge required for activation of protein kinases PKR, GCN2, and PERK. J. Biol. Chem. *282*, 6653–6660.

Díaz-Troya, S., Florencio, F.J., and Crespo, J.L. (2008). Target of rapamycin and LST8 proteins associate with membranes from the endoplasmic reticulum in the unicellular green alga Chlamydomonas reinhardtii. Eukaryot. Cell *7*, 212–222.

Dobrenel, T., Marchive, C., Sormani, R., Moreau, M., Mozzo, M., Montané, M., Menand, B., Robaglia, C., and Meyer, C. (2011). Regulation of plant growth and metabolism by the TOR kinase. Biochem. Soc. Trans. *39*, 477–481.

Dong, J., Qiu, H., Garcia-Barrio, M., Anderson, J., and Hinnebusch, A.G. (2000). Uncharged tRNA activates GCN2 by displacing the protein kinase moiety from a bipartite tRNA-binding domain. Mol. Cell *6*, 269–279.

Dreher, T.W., and Miller, W.A. (2006). Translational control in positive strand RNA plant viruses. Virology *344*, 185–197.

Dresios, J., Derkatch, I.L., Liebman, S.W., and Synetos, D. (2000). Yeast ribosomal protein L24 affects the kinetics of protein synthesis and ribosomal protein L39 improves translational accuracy, while mutants lacking both remain viable. Biochemistry (Mosc.) *39*, 7236–7244.

Dufner, A., and Thomas, G. (1999). Ribosomal S6 kinase signaling and the control of translation. Exp. Cell Res. *253*, 100–109.

Duprat, A., Caranta, C., Revers, F., Menand, B., Browning, K.S., and Robaglia, C. (2002). The *Arabidopsis* eukaryotic initiation factor (iso)4E is dispensable for plant growth but required for susceptibility to potyviruses. Plant J. Cell Mol. Biol. *32*, 927–934.

Enchev, R.I., Schreiber, A., Beuron, F., and Morris, E.P. (2010). Structural insights into the COP9 signalosome and its common architecture with the 26S proteasome lid and eIF3. Struct. Lond. Engl. 1993 *18*, 518–527.

Erickson, F.L., Nika, J., Rippel, S., and Hannig, E.M. (2001). Minimum requirements for the function of eukaryotic translation initiation factor 2. Genetics *158*, 123–132.

Erzberger, J.P., Stengel, F., Pellarin, R., Zhang, S., Schaefer, T., Aylett, C.H.S., Cimermančič, P., Boehringer, D., Sali, A., Aebersold, R., et al. (2014). Molecular architecture of the 40S·eIF1·eIF3 translation initiation complex. Cell *158*, 1123–1135.

Fekete, C.A., Mitchell, S.F., Cherkasova, V.A., Applefield, D., Algire, M.A., Maag, D., Saini, A.K., Lorsch, J.R., and Hinnebusch, A.G. (2007). N- and C-terminal residues of eIF1A have opposing effects on the fidelity of start codon selection. EMBO J. *26*, 1602–1614.

Fields, S., and Song, O. (1989). A novel genetic system to detect protein□protein interactions. Nature *340*, 245–246.

Flynn, A., Oldfield, S., and Proud, C.G. (1993). The role of the beta-subunit of initiation factor eIF-2 in initiation complex formation. Biochim. Biophys. Acta *1174*, 117–121.

Franco, R., and Rosenfeld, M.G. (1990). Hormonally inducible phosphorylation of a nuclear pool of ribosomal protein S6. J. Biol. Chem. *265*, 4321–4325.

Fraser, C.S., Lee, J.Y., Mayeur, G.L., Bushell, M., Doudna, J.A., and Hershey, J.W.B. (2004). The j-subunit of human translation initiation factor eIF3 is required for the stable binding of eIF3 and its subcomplexes to 40 S ribosomal subunits in vitro. J. Biol. Chem. *279*, 8946–8956.

Friml, J., Vieten, A., Sauer, M., Weijers, D., Schwarz, H., Hamann, T., Offringa, R., and Jürgens, G. (2003). Efflux-dependent auxin gradients establish the apical–basal axis of *Arabidopsis*. Nature *426*, 147–153.

Fütterer, J., and Hohn, T. (1991). Translation of a polycistronic mRNA in the presence of the *Cauliflower mosaic virus* transactivator protein. EMBO J. *10*, 3887–3896.

Futterer, J., and Hohn, T. (1992). Role of an upstream open reading frame in the translation of polycistronic mRNAs in plant cells. Nucleic Acids Res. *20*, 3851–3857.

Futterer, J., Gordon, K., Sanfacon, H., Bonneville, J.M., and Hohn, T. (1990). Positive and negative control of translation by the leader sequence of *Cauliflower mosaic virus* pregenomic 35S RNA. EMBO J. *9*, 1697–1707.

Gandin, V., Senft, D., Topisirovic, I., and Ronai, Z.A. (2013). RACK1 Function in Cell Motility and Protein Synthesis. Genes Cancer *4*, 369–377.

Gazo, B.M., Murphy, P., Gatchel, J.R., and Browning, K.S. (2004). A novel interaction of Cap-binding protein complexes eukaryotic initiation factor (eIF) 4F and eIF(iso)4F with a region in the 3'-untranslated region of satellite tobacco necrosis virus. J. Biol. Chem. *279*, 13584–13592.

Giavalisco, P., Wilson, D., Kreitler, T., Lehrach, H., Klose, J., Gobom, J., and Fucini, P. (2005). High heterogeneity within the ribosomal proteins of the *Arabidopsis thaliana* 80S ribosome. Plant Mol. Biol. *57*, 577–591.

Gingras, A.-C., Gygi, S.P., Raught, B., Polakiewicz, R.D., Abraham, R.T., Hoekstra, M.F., Aebersold, R., and Sonenberg, N. (1999). Regulation of 4E-BP1 phosphorylation: a novel two-step mechanism. Genes Dev. *13*, 1422–1437.

Gressner, A.M., and Wool, I.G. (1974). The stimulation of the phosphorylation of ribosomal protein S6 by cycloheximide and puromycin. Biochem. Biophys. Res. Commun. *60*, 1482–1490.

Gromadski, K.B., and Rodnina, M.V. (2004). Kinetic determinants of high-fidelity tRNA discrimination on the ribosome. Mol. Cell *13*, 191–200.

Guertin, D.A., and Sabatini, D.M. (2009). The pharmacology of mTOR inhibition. Sci. Signal. *2*, pe24.

Haas, M., Geldreich, A., Bureau, M., Dupuis, L., Leh, V., Vetter, G., Kobayashi, K., Hohn, T., Ryabova, L., Yot, P., et al. (2005). The open reading frame VI product of Cauliflower Mosaic Virus is a nucleocytoplasmic protein: its n terminus mediates its nuclear export and formation of electron-dense viroplasms. Plant Cell *17*, 927–943.

Hanfrey, C., Elliott, K.A., Franceschetti, M., Mayer, M.J., Illingworth, C., and Michael, A.J. (2005). A dual upstream open reading frame-based autoregulatory circuit controlling polyamine-responsive translation. J. Biol. Chem. *280*, 39229–39237.

Harding, H.P., Zhang, Y., and Ron, D. (1999). Protein translation and folding are coupled by an endoplasmic-reticulum-resident kinase. Nature *397*, 271–274.

Hardtke, C.S., and Berleth, T. (1998). The *Arabidopsis* gene MONOPTEROS encodes a transcription factor mediating embryo axis formation and vascular development. EMBO J. *17*, 1405–1411.

Harms, U., Andreou, A.Z., Gubaev, A., and Klostermeier, D. (2014). eIF4B, eIF4G and RNA regulate eIF4A activity in translation initiation by modulating the eIF4A conformational cycle. Nucleic Acids Res. gku440.

Hashem, Y., des Georges, A., Dhote, V., Langlois, R., Liao, H.Y., Grassucci, R.A., Hellen, C.U.T., Pestova, T.V., and Frank, J. (2013). Structure of the mammalian ribosomal 43S preinitiation complex bound to the scanning factor DHX29. Cell *153*, 1108–1119.

Hashimoto, N.N., Carnevalli, L.S., and Castilho, B.A. (2002). Translation initiation at non-AUG codons mediated by weakened association of eukaryotic initiation factor (eIF) 2 subunits. Biochem. J. *367*, 359–368.

Hay, N., and Sonenberg, N. (2004). Upstream and downstream of mTOR. Genes Dev. *18*, 1926–1945.

Heckman, K.L., and Pease, L.R. (2007). Gene splicing and mutagenesis by PCR-driven overlap extension. Nat. Protoc. *2*, 924–932.

Heisler, M.G., Ohno, C., Das, P., Sieber, P., Reddy, G.V., Long, J.A., and Meyerowitz, E.M. (2005). Patterns of auxin transport and gene expression during primordium development revealed by live imaging of the *Arabidopsis* inflorescence meristem. Curr. Biol. *15*, 1899–1911.

Heitman, J., Movva, N.R., and Hall, M.N. (1991). Targets for cell cycle arrest by the immunosuppressant rapamycin in yeast. Science *253*, 905–909.

Hershey, J.W.B., and Merrick, W.C. (2000). The pathway and mechanism of initiation of protein synthesis. In Translational Control of Gene Expression, N. Sonenberg, J.W.B. Hershey, and M.B. Mathews, eds. (Cold Spring Harbor: Cold Spring Harbor Laboratory), pp. 33–88.

Hilbert, M., Kebbel, F., Gubaev, A., and Klostermeier, D. (2011). eIF4G stimulates the activity of the DEAD box protein eIF4A by a conformational guidance mechanism. Nucleic Acids Res. *39*, 2260–2270.

Himmelbach, A., Chapdelaine, Y., and Hohn, T. (1996). Interaction between *Cauliflower Mosaic Virus* Inclusion Body Protein and Capsid Protein: Implications for Viral Assembly. Virology *217*, 147–157.

Hinnebusch, A.G. (1997). Translational regulation of yeast GCN4. A window on factors that control initiator-trna binding to the ribosome. J. Biol. Chem. *272*, 21661–21664.

Hinnebusch, A.G. (2005). Translational regulation of GCN4 and the general amino acid control of yeast. Annu. Rev. Microbiol. *59*, 407–450.

Hinnebusch, A.G. (2006). eIF3: a versatile scaffold for translation initiation complexes. Trends Biochem. Sci. *31*, 553–562.

Hinnebusch, A.G. (2011). Molecular mechanism of scanning and start codon selection in eukaryotes. Microbiol. Mol. Biol. Rev. MMBR *75*, 434–467, first page of table of contents.

Hinnebusch, A.G. (2014). The Scanning Mechanism of Eukaryotic Translation Initiation. Annu. Rev. Biochem. *83*, 779–812.

Hinnebusch, A.G., and Lorsch, J.R. (2012). The mechanism of eukaryotic translation initiation: new insights and challenges. Cold Spring Harb. Perspect. Biol. *4*.

Hiraishi, H., Oatman, J., Haller, S.L., Blunk, L., McGivern, B., Morris, J., Papadopoulos, E., Gutierrez, W., Gordon, M., Bokhari, W., et al. (2014). Essential role of eIF5-mimic protein in animal development is linked to control of ATF4 expression. Nucleic Acids Res. *42*, 10321–10330.

Hohn, T., and Rothnie, H. (2013). Plant pararetroviruses: replication and expression. Curr. Opin. Virol. *3*, 621–628.

Holz, M.K., Ballif, B.A., Gygi, S.P., and Blenis, J. (2005). mTOR and S6k1 mediate assembly of the translation preinitiation complex through dynamic protein interchange and ordered phosphorylation events. Cell *123*, 569–580.

Huang, H.K., Yoon, H., Hannig, E.M., and Donahue, T.F. (1997). GTP hydrolysis controls stringent selection of the AUG start codon during translation initiation in *Saccharomyces cerevisiae*. Genes Dev. *11*, 2396–2413.

Hutchins, A.P., Roberts, G.R., Lloyd, C.W., and Doonan, J.H. (2004). In vivo interaction between CDKA and eIF4A: a possible mechanism linking translation and cell proliferation. FEBS Lett. *556*, 91–94.

Hutchinson, J.A., Shanware, N.P., Chang, H., and Tibbetts, R.S. (2011). Regulation of ribosomal protein S6 phosphorylation by Casein Kinase 1 and Protein Phosphatase 1. J. Biol. Chem. *286*, 8688–8696.

Hwang, C.-S., Shemorry, A., and Varshavsky, A. (2010). N-Terminal acetylation of cellular proteins creates specific degradation signals. Science *327*, 973–977.

Ingolia, N.T. (2014). Ribosome profiling: new views of translation, from single codons to genome scale. Nat. Rev. Genet. *15*, 205–213.

Ingolia, N.T., Ghaemmaghami, S., Newman, J.R.S., and Weissman, J.S. (2009). Genome-wide analysis *in vivo* of translation with nucleotide resolution using ribosome profiling. Science *324*, 218–223.

Jackson, R.J., Hellen, C.U.T., and Pestova, T.V. (2010). The mechanism of eukaryotic translation initiation and principles of its regulation. Nat. Rev. Mol. Cell Biol. *11*, 113–127.

Jackson, R.J., Hellen, C.U.T., and Pestova, T.V. (2012). Termination and post-termination events in eukaryotic translation. Adv. Protein Chem. Struct. Biol. *86*, 45–93.

Jakubowicz, T. (1985). Phosphorylation-dephosphorylation changes in yeast ribosomal proteins S2 and S6 during growth under normal and hyperthermal conditions. Acta Biochim. Pol. *32*, 7–12.

Jefferson, R.A., Kavanagh, T.A., and Bevan, M.W. (1987). GUS fusions: beta-glucuronidase as a sensitive and versatile gene fusion marker in higher plants. EMBO J. *6*, 3901–3907.

Jennings, M.D., and Pavitt, G.D. (2010). eIF5 has GDI activity necessary for translational control by eIF2 phosphorylation. Nature *465*, 378–381.

Jivotovskaya, A.V., Valásek, L., Hinnebusch, A.G., and Nielsen, K.H. (2006). Eukaryotic translation initiation factor 3 (eIF3) and eIF2 can promote mRNA binding to 40S subunits independently of eIF4G in yeast. Mol. Cell. Biol. *26*, 1355–1372.

Kamita, M., Kimura, Y., Ino, Y., Kamp, R.M., Polevoda, B., Sherman, F., and Hirano, H. (2011). N(α)-Acetylation of yeast ribosomal proteins and its effect on protein synthesis. J. Proteomics *74*, 431–441.

Kawaguchi, R., and Bailey-Serres, J. (2005). mRNA sequence features that contribute to translational regulation in *Arabidopsis*. Nucleic Acids Res. *33*, 955–965.

Khandal, D., Samol, I., Buhr, F., Pollmann, S., Schmidt, H., Clemens, S., Reinbothe, S., and Reinbothe, C. (2009). Singlet oxygen-dependent translational control in the tigrina-d.12 mutant of barley. Proc. Natl. Acad. Sci. U. S. A. *106*, 13112–13117.

Khoshnevis, S., Gunišová, S., Vlčková, V., Kouba, T., Neumann, P., Beznosková, P., Ficner, R., and Valášek, L.S. (2014). Structural integrity of the PCI domain of eIF3a/TIF32 is required for mRNA recruitment to the 43S pre-initiation complexes. Nucleic Acids Res. *42*, 4123–4139.

Kim, B.-H., Cai, X., Vaughn, J.N., and von Arnim, A.G. (2007). On the functions of the h subunit of eukaryotic initiation factor 3 in late stages of translation initiation. Genome Biol. *8*, R60.

Kim, T.-H., Kim, B.-H., Yahalom, A., Chamovitz, D.A., and von Arnim, A.G. (2004). Translational regulation via 5? mRNA leader sequences revealed by mutational analysis of the *Arabidopsis* translation Initiation Factor subunit eIF3h. Plant Cell *16*, 3341–3356.

Klinge, S., Voigts-Hoffmann, F., Leibundgut, M., and Ban, N. (2012). Atomic structures of the eukaryotic ribosome. Trends Biochem. Sci. *37*, 189–198.

Kobayashi, K., and Hohn, T. (2003). Dissection of Cauliflower Mosaic Virus Transactivator/Viroplasmin reveals distinct essential functions in basic virus replication. J. Virol. *77*, 8577–8583.

Kobayashi, K., and Hohn, T. (2004). The avirulence domain of Cauliflower Mosaic Virus Transactivator/Viroplasmin Is a determinant of viral virulence in susceptible hosts. Mol. Plant. Microbe Interact. *17*, 475–483.

Kozak, M. (1987). An analysis of 5'-noncoding sequences from 699 vertebrate messenger RNAs. Nucleic Acids Res. *15*, 8125–8148.

Kozak, M. (1999). Initiation of translation in prokaryotes and eukaryotes. Gene *234*, 187–208.

Kozak, M. (2001). Constraints on reinitiation of translation in mammals. Nucleic Acids Res. *29*, 5226–5232.

Krieg, J., Hofsteenge, J., and Thomas, G. (1988). Identification of the 40 S ribosomal protein S6 phosphorylation sites induced by cycloheximide. J. Biol. Chem. *263*, 11473–11477.

Laird, J., McInally, C., Carr, C., Doddiah, S., Yates, G., Chrysanthou, E., Khattab, A., Love, A.J., Geri, C., Sadanandom, A., et al. (2013). Identification of the domains of *Cauliflower mosaic virus* protein P6 responsible for suppression of RNA silencing and salicylic acid signalling. J. Gen. Virol. *94*, 2777–2789.

Laplante, M., and Sabatini, D.M. (2012). mTOR Signaling. Cold Spring Harb. Perspect. Biol. *4*.

Laurino, J.P., Thompson, G.M., Pacheco, E., and Castilho, B.A. (1999). The beta subunit of eukaryotic translation initiation factor 2 binds mRNA through the lysine repeats and a region comprising the C2-C2 motif. Mol. Cell. Biol. *19*, 173–181.

Lax, S.R., Browning, K.S., Maia, D.M., and Ravel, J.M. (1986). ATPase activities of wheat germ initiation factors 4A, 4B, and 4F. J. Biol. Chem. *261*, 15632–15636.

Le, H., Browning, K.S., and Gallie, D.R. (2000). The phosphorylation state of poly(A)-binding protein specifies its binding to poly(A) RNA and its interaction with eukaryotic initiation factor (eIF) 4F, eIFiso4F, and eIF4B. J. Biol. Chem. *275*, 17452–17462.

Lecompte, O., Ripp, R., Thierry, J.-C., Moras, D., and Poch, O. (2002). Comparative analysis of ribosomal proteins in complete genomes: an example of reductive evolution at the domain scale. Nucleic Acids Res. *30*, 5382–5390.

Lee, B., Udagawa, T., Singh, C.R., and Asano, K. (2007). Yeast phenotypic assays on translational control. Methods Enzymol. *429*, 105–137.

LeFebvre, A.K., Korneeva, N.L., Trutschl, M., Cvek, U., Duzan, R.D., Bradley, C.A., Hershey, J.W.B., and Rhoads, R.E. (2006). Translation initiation factor eIF4G-1 binds to eIF3 through the eIF3e subunit. J. Biol. Chem. *281*, 22917–22932.

Leh, V., Yot, P., and Keller, M. (2000). The *Cauliflower mosaic virus* translational transactivator interacts with the 60S ribosomal subunit protein L18 of *Arabidopsis thaliana*. Virology *266*, 1–7.

Leiber, R.-M., John, F., Verhertbruggen, Y., Diet, A., Knox, J.P., and Ringli, C. (2010). The TOR pathway modulates the structure of cell walls in *Arabidopsis*. Plant Cell *22*, 1898–1908.

Lindqvist, L., Imataka, H., and Pelletier, J. (2008). Cap-dependent eukaryotic initiation factor-mRNA interactions probed by cross-linking. RNA N. Y. N *14*, 960–969.

Lingaraju, G.M., Bunker, R.D., Cavadini, S., Hess, D., Hassiepen, U., Renatus, M., Fischer, E.S., and Thomä, N.H. (2014). Crystal structure of the human COP9 signalosome. Nature *512*, 161–165.

Liu, Y., and Bassham, D.C. (2010). TOR is a negative regulator of autophagy in *Arabidopsis thaliana*. PLoS ONE *5*.

Lomakin, I.B., and Steitz, T.A. (2013). The initiation of mammalian protein synthesis and mRNA scanning mechanism. Nature *500*, 307–311.

Lomakin, I.B., Kolupaeva, V.G., Marintchev, A., Wagner, G., and Pestova, T.V. (2003). Position of eukaryotic initiation factor eIF1 on the 40S ribosomal subunit determined by directed hydroxyl radical probing. Genes Dev. *17*, 2786–2797.

Lorsch, J.R., and Dever, T.E. (2010). Molecular view of 43 S complex formation and start site selection in eukaryotic translation initiation. J. Biol. Chem. *285*, 21203–21207.

Luna, R.E., Arthanari, H., Hiraishi, H., Nanda, J., Martin-Marcos, P., Markus, M.A., Akabayov, B., Milbradt, A.G., Luna, L.E., Seo, H.-C., et al. (2012). The C-terminal domain of eukaryotic initiation factor 5 promotes start codon recognition by its dynamic interplay with eIF1 and eIF2β. Cell Rep. *1*, 689–702.

Luukkonen, B.G., Tan, W., and Schwartz, S. (1995). Efficiency of reinitiation of translation on human immunodeficiency virus type 1 mRNAs is determined by the length of the upstream open reading frame and by intercistronic distance. J. Virol. *69*, 4086–4094.

Ma, X.M., and Blenis, J. (2009). Molecular mechanisms of mTOR-mediated translational control. Nat. Rev. Mol. Cell Biol. *10*, 307–318.

Magnuson, B., Ekim, B., and Fingar, D.C. (2012). Regulation and function of ribosomal protein S6 kinase (S6K) within mTOR signalling networks. Biochem. J. *441*, 1–21.

Mahfouz, M.M., Kim, S., Delauney, A.J., and Verma, D.P.S. (2006). *Arabidopsis* Target of Rapamycin interacts with RAPTOR, which regulates the activity of S6 kinase in response to osmotic stress signals. Plant Cell *18*, 477–490.

Majumdar, R., Bandyopadhyay, A., and Maitra, U. (2003). Mammalian translation initiation factor eIF1 functions with eIF1A and eIF3 in the formation of a stable 40 S preinitiation complex. J. Biol. Chem. *278*, 6580–6587.

Makky, K., Tekiela, J., and Mayer, A.N. (2007). Target Of Rapamycin (TOR) signaling controls epithelial morphogenesis in the vertebrate intestine. Dev. Biol. *303*, 501–513.

Martineau, Y., Wang, X., Alain, T., Petroulakis, E., Shahbazian, D., Fabre, B., Bousquet-Dubouch, M.-P., Monsarrat, B., Pyronnet, S., and Sonenberg, N. (2014). Control of Paip1-Eukayrotic Translation Initiation Factor 3 interaction by amino acids through S6 kinase. Mol. Cell. Biol. *34*, 1046–1053.

Mayberry, L.K., Allen, M.L., Nitka, K.R., Campbell, L., Murphy, P.A., and Browning, K.S. (2011). Plant cap-binding complexes eukaryotic initiation factors eIF4F and eIFiso4F: molecular specificity of subunit binding. J. Biol. Chem. *286*, 42566–42574.

Menand, B., Desnos, T., Nussaume, L., Berger, F., Bouchez, D., Meyer, C., and Robaglia, C. (2002). Expression and disruption of the *Arabidopsis* TOR (Target of Rapamycin) gene. Proc. Natl. Acad. Sci. U. S. A. *99*, 6422–6427.

Meurs, E.F., Galabru, J., Barber, G.N., Katze, M.G., and Hovanessian, A.G. (1993). Tumor suppressor function of the interferon-induced double-stranded RNA-activated protein kinase. Proc. Natl. Acad. Sci. U. S. A. *90*, 232–236.

Meyuhas, O. (2008). Physiological roles of ribosomal protein S6: one of its kind. Int. Rev. Cell Mol. Biol. *268*, 1–37.

Mignone, F., Gissi, C., Liuni, S., and Pesole, G. (2002). Untranslated regions of mRNAs. Genome Biol. *3*.

Mitchell, S.F., Walker, S.E., Algire, M.A., Park, E.-H., Hinnebusch, A.G., and Lorsch, J.R. (2010). The 5'-7-methylguanosine cap on eukaryotic mRNAs serves both to stimulate canonical translation initiation and to block an alternative pathway. Mol. Cell *39*, 950–962.

Moreau, M., Sormani, R., Menand, B., Veit, B., Robaglia, C., and Meyer, C. (2010). Chapter 15 - The TOR complex and signaling pathway in plants. In The Enzymes, Michael N. Hall; Fuyuhiko Tamanoi, ed. (Academic Press), pp. 285–302.

Moreau, M., Azzopardi, M., Clement, G., Dobrenel, T., Marchive, C., Renne, C., Martin-Magniette, M.-L., Taconnat, L., Renou, J.-P., Robaglia, C., et al. (2012). Mutations in the *Arabidopsis* Homolog of LST8/GβL, a partner of the Target of Rapamycin kinase, impair plant growth, flowering, and metabolic adaptation to long days[C][W]. Plant Cell *24*, 463–481.

Morris, D.R., and Geballe, A.P. (2000). Upstream Open Reading Frames as Regulators of mRNA Translation. Mol. Cell. Biol. *20*, 8635–8642.

Muhs, M., Yamamoto, H., Ismer, J., Takaku, H., Nashimoto, M., Uchiumi, T., Nakashima, N., Mielke, T., Hildebrand, P.W., Nierhaus, K.H., et al. (2011). Structural basis for the binding of IRES RNAs to the head of the ribosomal 40S subunit. Nucleic Acids Res. *39*, 5264–5275.

Munzarova, V., Panek, J., Gunisova, S., Danyi, I., Szamecz, B., and Valasek, L.S. (2011). Translation Reinitiation Relies on the Interaction between eIF3a/TIF32 and Progressively Folded cis-Acting mRNA Elements Preceding Short uORFs. PLoS Genet. *7*.

Nakamura, Y., and Ito, K. (2003). Making sense of mimic in translation termination. Trends Biochem. Sci. *28*, 99–105.

Nanda, J.S., Cheung, Y.-N., Takacs, J.E., Martin-Marcos, P., Saini, A.K., Hinnebusch, A.G., and Lorsch, J.R. (2009). eIF1 controls multiple steps in start codon recognition during eukaryotic translation initiation. J. Mol. Biol. *394*, 268–285.

Nanda, J.S., Saini, A.K., Muñoz, A.M., Hinnebusch, A.G., and Lorsch, J.R. (2013). Coordinated movements of eukaryotic translation initiation factors eIF1, eIF1A, and eIF5 trigger phosphate release from eIF2 in response to start codon recognition by the ribosomal preinitiation complex. J. Biol. Chem. *288*, 5316–5329.

Naveau, M., Lazennec-Schurdevin, C., Panvert, M., Mechulam, Y., and Schmitt, E. (2010). tRNA binding properties of eukaryotic translation initiation factor 2 from Encephalitozoon cuniculi. Biochemistry (Mosc.) *49*, 8680–8688.

Nielsen, K.H., Szamecz, B., Valásek, L., Jivotovskaya, A., Shin, B.-S., and Hinnebusch, A.G. (2004). Functions of eIF3 downstream of 48S assembly impact AUG recognition and GCN4 translational control. EMBO J. *23*, 1166–1177.

Nielsen, K.H., Valásek, L., Sykes, C., Jivotovskaya, A., and Hinnebusch, A.G. (2006). Interaction of the RNP1 motif in PRT1 with HCR1 promotes 40S binding of eukaryotic initiation factor 3 in yeast. Mol. Cell. Biol. *26*, 2984–2998.

Nielsen, K.H., Behrens, M.A., He, Y., Oliveira, C.L.P., Jensen, L.S., Hoffmann, S.V., Pedersen, J.S., and Andersen, G.R. (2011). Synergistic activation of eIF4A by eIF4B and eIF4G. Nucleic Acids Res. *39*, 2678–2689.

Nilsson, J., Sengupta, J., Frank, J., and Nissen, P. (2004). Regulation of eukaryotic translation by the RACK1 protein: a platform for signalling molecules on the ribosome. EMBO Rep. *5*, 1137–1141.

Nishimura, T., Wada, T., Yamamoto, K.T., and Okada, K. (2005). The *Arabidopsis* STV1 protein, responsible for translation reinitiation, is required for auxin-mediated gynoecium patterning. Plant Cell *17*, 2940–2953.

Olsen, D.S., Savner, E.M., Mathew, A., Zhang, F., Krishnamoorthy, T., Phan, L., and Hinnebusch, A.G. (2003). Domains of eIF1A that mediate binding to eIF2, eIF3 and eIF5B and promote ternary complex recruitment *in vivo*. EMBO J. *22*, 193–204.

Otterhag, L., Gustavsson, N., Alsterfjord, M., Pical, C., Lehrach, H., Gobom, J., and Sommarin, M. (2006). *Arabidopsis* PDK1: identification of sites important for activity and downstream phosphorylation of S6 kinase. Biochimie *88*, 11–21.

Park, E.-H., Walker, S.E., Lee, J.M., Rothenburg, S., Lorsch, J.R., and Hinnebusch, A.G. (2011). Multiple elements in the eIF4G1 N-terminus promote assembly of eIF4G1•PABP mRNPs *in vivo*. EMBO J. *30*, 302–316.

Park, H.S., Himmelbach, A., Browning, K.S., Hohn, T., and Ryabova, L.A. (2001). A plant viral "reinitiation" factor interacts with the host translational machinery. Cell *106*, 723–733.

Park, H.-S., Browning, K.S., Hohn, T., and Ryabova, L.A. (2004). Eucaryotic initiation factor 4B controls eIF3-mediated ribosomal entry of viral reinitiation factor. EMBO J. *23*, 1381–1391.

Parsyan, A., Svitkin, Y., Shahbazian, D., Gkogkas, C., Lasko, P., Merrick, W.C., and Sonenberg, N. (2011). mRNA helicases: the tacticians of translational control. Nat. Rev. Mol. Cell Biol. *12*, 235–245.

Passmore, L.A., Schmeing, T.M., Maag, D., Applefield, D.J., Acker, M.G., Algire, M.A., Lorsch, J.R., and Ramakrishnan, V. (2007). The eukaryotic translation initiation factors eIF1 and eIF1A induce an open conformation of the 40S ribosome. Mol. Cell *26*, 41–50.

Pearce, L.R., Sommer, E.M., Sakamoto, K., Wullschleger, S., and Alessi, D.R. (2011). Protor-1 is required for efficient mTORC2-mediated activation of SGK1 in the kidney. Biochem. J. *436*, 169–179.

Pende, M., Um, S.H., Mieulet, V., Sticker, M., Goss, V.L., Mestan, J., Mueller, M., Fumagalli, S., Kozma, S.C., and Thomas, G. (2004). S6K1−/−/S6K2−/− mice exhibit perinatal lethality and rapamycin-sensitive 5?-terminal oligopyrimidine mRNA translation and reveal a Mitogen-Activated Protein Kinase-dependent S6 Kinase pathway. Mol. Cell. Biol. *24*, 3112–3124.

Pestova, T.V., and Kolupaeva, V.G. (2002). The roles of individual eukaryotic translation initiation factors in ribosomal scanning and initiation codon selection. Genes Dev. *16*, 2906–2922.

Pestova, T.V., Lomakin, I.B., Lee, J.H., Choi, S.K., Dever, T.E., and Hellen, C.U. (2000). The joining of ribosomal subunits in eukaryotes requires eIF5B. Nature *403*, 332–335.

Pestova, T.V., Lorsch, J.R., and Hellen, C.U. (2007). 4 The Mechanism of Translation Initiation in Eukaryotes. Cold Spring Harb. Monogr. Arch. *48*, 87–128.

Pfeiffer, P., and Hohn, T. (1983). Involvement of reverse transcription in the replication of *Cauliflower mosaic virus*: A detailed model and test of some aspects. Cell *33*, 781–789.

Pisarev, A.V., Kolupaeva, V.G., Yusupov, M.M., Hellen, C.U.T., and Pestova, T.V. (2008). Ribosomal position and contacts of mRNA in eukaryotic translation initiation complexes. EMBO J. *27*, 1609–1621.

Pisarev, A.V., Skabkin, M.A., Pisareva, V.P., Skabkina, O.V., Rakotondrafara, A.M., Hentze, M.W., Hellen, C.U.T., and Pestova, T.V. (2010). The role of ABCE1 in eukaryotic posttermination ribosomal recycling. Mol. Cell *37*, 196–210.

Plisson, C., Uzest, M., Drucker, M., Froissart, R., Dumas, C., Conway, J., Thomas, D., Blanc, S., and Bron, P. (2005). Structure of the mature P3-virus particle complex of *Cauliflower mosaic virus* revealed by cryo-electron microscopy. J. Mol. Biol. *346*, 267–277.

Pöyry, T.A.A., Kaminski, A., and Jackson, R.J. (2004). What determines whether mammalian ribosomes resume scanning after translation of a short upstream open reading frame? Genes Dev. *18*, 62–75.

Pullen, N., and Thomas, G. (1997). The modular phosphorylation and activation of p70s6k. FEBS Lett. *410*, 78–82.

Rabl, J., Leibundgut, M., Ataide, S.F., Haag, A., and Ban, N. (2011). Crystal structure of the eukaryotic 40S ribosomal subunit in complex with initiation factor 1. Science *331*, 730–736.

Radimerski, T., Mini, T., Schneider, U., Wettenhall, R.E., Thomas, G., and Jenö, P. (2000). Identification of insulin-induced sites of ribosomal protein S6 phosphorylation in *Drosophila* melanogaster. Biochemistry (Mosc.) *39*, 5766–5774.

Rahmani, F., Hummel, M., Schuurmans, J., Wiese-Klinkenberg, A., Smeekens, S., and Hanson, J. (2009). Sucrose control of translation mediated by an upstream open reading frame-encoded peptide. Plant Physiol. *150*, 1356–1367.

Rajagopal, V., Park, E.-H., Hinnebusch, A.G., and Lorsch, J.R. (2012). Specific domains in yeast translation initiation factor eIF4G strongly bias RNA unwinding activity of the eIF4F complex toward duplexes with 5'-overhangs. J. Biol. Chem. *287*, 20301–20312.

Rajkowitsch, L., Vilela, C., Berthelot, K., Ramirez, C.V., and McCarthy, J.E.G. (2004). Reinitiation and recycling are distinct processes occurring downstream of translation termination in yeast. J. Mol. Biol. *335*, 71–85.

Raught, B., Peiretti, F., Gingras, A.-C., Livingstone, M., Shahbazian, D., Mayeur, G.L., Polakiewicz, R.D., Sonenberg, N., and Hershey, J.W. (2004). Phosphorylation of eucaryotic translation initiation factor 4B Ser422 is modulated by S6 kinases. EMBO J. *23*, 1761–1769.

Reibarkh, M., Yamamoto, Y., Singh, C.R., del Rio, F., Fahmy, A., Lee, B., Luna, R.E., Ii, M., Wagner, G., and Asano, K. (2008). Eukaryotic initiation factor (eIF) 1 carries two distinct eIF5-binding faces important for multifactor assembly and AUG selection. J. Biol. Chem. *283*, 1094–1103.

Reiland, S., Messerli, G., Baerenfaller, K., Gerrits, B., Endler, A., Grossmann, J., Gruissem, W., and Baginsky, S. (2009). Large-scale *Arabidopsis* phosphoproteome profiling reveals novel chloroplast kinase substrates and phosphorylation networks. Plant Physiol. *150*, 889–903.

Reinhardt, D., Pesce, E.-R., Stieger, P., Mandel, T., Baltensperger, K., Bennett, M., Traas, J., Friml, J., and Kuhlemeier, C. (2003). Regulation of phyllotaxis by polar auxin transport. Nature *426*, 255–260.

Ren, M., Venglat, P., Qiu, S., Feng, L., Cao, Y., Wang, E., Xiang, D., Wang, J., Alexander, D., Chalivendra, S., et al. (2012). Target of Rapamycin Signaling regulates metabolism, growth, and life span in *Arabidopsis*[W][OA]. Plant Cell *24*, 4850–4874.

Richert-Pöggeler, K.R., Noreen, F., Schwarzacher, T., Harper, G., and Hohn, T. (2003). Induction of infectious petunia vein clearing (pararetro) virus from endogenous provirus in petunia. EMBO J. *22*, 4836–4845.

Robaglia, C., and Caranta, C. (2006). Translation initiation factors: a weak link in plant RNA virus infection. Trends Plant Sci. *11*, 40–45.

Robaglia, C., Thomas, M., and Meyer, C. (2012). Sensing nutrient and energy status by SnRK1 and TOR kinases. Curr. Opin. Plant Biol. *15*, 301–307.

Rodnina, M.V., and Wintermeyer, W. (2009). Recent mechanistic insights into eukaryotic ribosomes. Curr. Opin. Cell Biol. *21*, 435–443.

Rodnina, M.V., Fricke, R., and Wintermeyer, W. (1994). Transient conformational states of aminoacyl-tRNA during ribosome binding catalyzed by elongation factor Tu. Biochemistry (Mosc.) *33*, 12267–12275.

Rodnina, M.V., Fricke, R., Kuhn, L., and Wintermeyer, W. (1995). Codon-dependent conformational change of elongation factor Tu preceding GTP hydrolysis on the ribosome. EMBO J. *14*, 2613–2619.

Rodnina, M.V., Beringer, M., and Bieling, P. (2005). Ten remarks on peptide bond formation on the ribosome. Biochem. Soc. Trans. *33*, 493–498.

Roux, P.P., and Topisirovic, I. (2012). Regulation of mRNA translation by signaling pathways. Cold Spring Harb. Perspect. Biol. *4*.

Roux, P.P., Shahbazian, D., Vu, H., Holz, M.K., Cohen, M.S., Taunton, J., Sonenberg, N., and Blenis, J. (2007). RAS/ERK Signaling Promotes site-specific ribosomal protein S6 phosphorylation via RSK and stimulates cap-dependent translation. J. Biol. Chem. *282*, 14056–14064.

Roy, B., and von Arnim, A.G. (2013). Translational regulation of cytoplasmic mRNAs. Arab. Book Am. Soc. Plant Biol. *11*.

Rozovsky, N., Butterworth, A.C., and Moore, M.J. (2008). Interactions between eIF4AI and its accessory factors eIF4B and eIF4H. RNA N. Y. N *14*, 2136–2148.

Ruffel, S., Dussault, M.-H., Palloix, A., Moury, B., Bendahmane, A., Robaglia, C., and Caranta, C. (2002). A natural recessive resistance gene against potato virus Y in pepper corresponds to the eukaryotic initiation factor 4E (eIF4E). Plant J. Cell Mol. Biol. *32*, 1067–1075.

Ruvinsky, I., and Meyuhas, O. (2006). Ribosomal protein S6 phosphorylation: from protein synthesis to cell size. Trends Biochem. Sci. *31*, 342–348.

Ruvinsky, I., Sharon, N., Lerer, T., Cohen, H., Stolovich-Rain, M., Nir, T., Dor, Y., Zisman, P., and Meyuhas, O. (2005). Ribosomal protein S6 phosphorylation is a determinant of cell size and glucose homeostasis. Genes Dev. *19*, 2199–2211.

Ryabova, L.A., Pooggin, M.M., and Hohn, T. (2006). Translation reinitiation and leaky scanning in plant viruses. Virus Res. *119*, 52–62.

Saini, A.K., Nanda, J.S., Lorsch, J.R., and Hinnebusch, A.G. (2010). Regulatory elements in eIF1A control the fidelity of start codon selection by modulating tRNA(i)(Met) binding to the ribosome. Genes Dev. *24*, 97–110.

Salas-Marco, J., and Bedwell, D.M. (2004). GTP hydrolysis by eRF3 facilitates stop codon decoding during eukaryotic translation termination. Mol. Cell. Biol. *24*, 7769–7778.

Sali, A., Potterton, L., Yuan, F., van Vlijmen, H., and Karplus, M. (1995). Evaluation of comparative protein modeling by MODELLER. Proteins *23*, 318–326.

Scharf, K.D., and Nover, L. (1982). Heat-shock-induced alterations of ribosomal protein phosphorylation in plant cell cultures. Cell *30*, 427–437.

Schepetilnikov, M., Kobayashi, K., Geldreich, A., Caranta, C., Robaglia, C., Keller, M., and Ryabova, L.A. (2011). Viral factor TAV recruits TOR/S6K1 signalling to activate reinitiation after long ORF translation. EMBO J. *30*, 1343–1356.

Schepetilnikov, M., Mancera-Martínez, E., Dimitrova, M., Geldreich, A., Keller, M., and Ryabova, L.A. (2013). TOR and S6K1 promote translation reinitiation of uORF-containing mRNAs via phosphorylation of eIF3h. EMBO J. *32*, 1087–1102.

Schmitt, E., Naveau, M., and Mechulam, Y. (2010). Eukaryotic and archaeal translation initiation factor 2: a heterotrimeric tRNA carrier. FEBS Lett. *584*, 405–412.

Schmitt, E., Panvert, M., Lazennec-Schurdevin, C., Coureux, P.-D., Perez, J., Thompson, A., and Mechulam, Y. (2012). Structure of the ternary initiation complex aIF2–GDPNP–methionylated initiator tRNA. Nat. Struct. Mol. Biol. *19*, 450–454.

Schoelz, J., and Wintermantel, W. (1993). Expansion of viral host range through complementation and recombination in transgenic plants. Plant Cell *5*, 1669–1679.

Sessions, A., Nemhauser, J.L., McColl, A., Roe, J.L., Feldmann, K.A., and Zambryski, P.C. (1997). ETTIN patterns the *Arabidopsis* floral meristem and reproductive organs. Dev. Camb. Engl. *124*, 4481–4491.

Ben-Shem, A., Garreau de Loubresse, N., Melnikov, S., Jenner, L., Yusupova, G., and Yusupov, M. (2011). The structure of the eukaryotic ribosome at 3.0 Å resolution. Science *334*, 1524–1529.

Shin, B.-S., Kim, J.-R., Walker, S.E., Dong, J., Lorsch, J.R., and Dever, T.E. (2011). Initiation factor eIF2γ promotes eIF2-GTP-Met-tRNAi(Met) ternary complex binding to the 40S ribosome. Nat. Struct. Mol. Biol. *18*, 1227–1234.

Singh, C.R., Yamamoto, Y., and Asano, K. (2004). Physical association of eukaryotic initiation factor (eIF) 5 carboxyl-terminal domain with the lysine-rich eIF2beta segment strongly enhances its binding to eIF3. J. Biol. Chem. *279*, 49644–49655.

Siridechadilok, B., Fraser, C.S., Hall, R.J., Doudna, J.A., and Nogales, E. (2005). Structural roles for human translation factor eIF3 in initiation of protein synthesis. Science *310*, 1513–1515.

Skabkin, M.A., Skabkina, O.V., Hellen, C.U.T., and Pestova, T.V. (2013). Reinitiation and other unconventional posttermination events during eukaryotic translation. Mol. Cell *51*, 249–264.

Sokabe, M., Fraser, C.S., and Hershey, J.W.B. (2012). The human translation initiation multi-factor complex promotes methionyl-tRNAi binding to the 40S ribosomal subunit. Nucleic Acids Res. *40*, 905–913.

Sormani, R., Yao, L., Menand, B., Ennar, N., Lecampion, C., Meyer, C., and Robaglia, C. (2007). *Saccharomyces cerevisiae* FKBP12 binds *Arabidopsis thaliana* TOR and its expression in plants leads to rapamycin susceptibility. BMC Plant Biol. *7*, 26.

Spahn, C.M.T., Jan, E., Mulder, A., Grassucci, R.A., Sarnow, P., and Frank, J. (2004). Cryo-EM visualization of a viral internal ribosome entry site bound to human ribosomes: the IRES functions as an RNA-based translation factor. Cell *118*, 465–475.

Starheim, K.K., Gromyko, D., Evjenth, R., Ryningen, A., Varhaug, J.E., Lillehaug, J.R., and Arnesen, T. (2009). Knockdown of human N alpha-terminal acetyltransferase complex C leads to p53-dependent apoptosis and aberrant human Arl8b localization. Mol. Cell. Biol. *29*, 3569–3581.

Stavolone, L., Villani, M.E., Leclerc, D., and Hohn, T. (2005). A coiled-coil interaction mediates *Cauliflower mosaic virus* cell-to-cell movement. Proc. Natl. Acad. Sci. U. S. A. *102*, 6219–6224.

Stratford, R., and Covey, S.N. (1989). Segregation of *Cauliflower mosaic virus* symptom genetic determinants. Virology *172*, 451–459.

Sun, C., Todorovic, A., Querol-Audí, J., Bai, Y., Villa, N., Snyder, M., Ashchyan, J., Lewis, C.S., Hartland, A., Gradia, S., et al. (2011). Functional reconstitution of human eukaryotic translation initiation factor 3 (eIF3). Proc. Natl. Acad. Sci. U. S. A. *108*, 20473–20478.

Svitkin, Y.V., Pause, A., Haghighat, A., Pyronnet, S., Witherell, G., Belsham, G.J., and Sonenberg, N. (2001). The requirement for eukaryotic initiation factor 4A (eIF4A) in translation is in direct proportion to the degree of mRNA 5' secondary structure. RNA N. Y. N *7*, 382–394.

Szamecz, B., Rutkai, E., Cuchalová, L., Munzarová, V., Herrmannová, A., Nielsen, K.H., Burela, L., Hinnebusch, A.G., and Valásek, L. (2008). eIF3a cooperates with sequences 5' of uORF1 to promote resumption of scanning by post-termination ribosomes for reinitiation on GCN4 mRNA. Genes Dev. *22*, 2414–2425.

Szyszka, R., and Gasior, E. (1984). Phosphorylation of ribosomal proteins during differentiation of *Saccharomyces cerevisiae*. Acta Biochim. Pol. *31*, 375–382.

Takahashi, H., Shimamoto, K., Suzuki, M., and Ehara, Y. (1989). DNA sequence of gene VI of *Cauliflower mosaic virus* Japanese strain S (CaMV S-Japan). Nucleic Acids Res. *17*, 7981.

De Tapia, M., Himmelbach, A., and Hohn, T. (1993). Molecular dissection of the *Cauliflower mosaic virus* translation transactivator. EMBO J. *12*, 3305–3314.

Teale, W.D., Paponov, I.A., and Palme, K. (2006). Auxin in action: signalling, transport and the control of plant growth and development. Nat. Rev. Mol. Cell Biol. *7*, 847–859.

Thedieck, K., Polak, P., Kim, M.L., Molle, K.D., Cohen, A., Jeno, P., Arrieumerlou, C., and Hall, M.N. (2007). PRAS40 and PRR5-Like Protein are new mTOR interactors that regulate apoptosis. PLoS ONE *2*.

Thiébeauld, O., Schepetilnikov, M., Park, H.-S., Geldreich, A., Kobayashi, K., Keller, M., Hohn, T., and Ryabova, L.A. (2009). A new plant protein interacts with eIF3 and 60S to enhance virus-activated translation re-initiation. EMBO J. *28*, 3171–3184.

Thoreen, C.C., Chantranupong, L., Keys, H.R., Wang, T., Gray, N.S., and Sabatini, D.M. (2012). A unifying model for mTORC1-mediated regulation of mRNA translation. Nature *485*, 109–113.

Tiwari, S.B., Hagen, G., and Guilfoyle, T. (2003). The roles of Auxin Response Factor domains in auxin-responsive transcription. Plant Cell *15*, 533–543.

Torruella, M., Gordon, K., and Hohn, T. (1989). *Cauliflower mosaic virus* produces an aspartic proteinase to cleave its polyproteins. EMBO J. *8*, 2819–2825.

Treder, K., Pettit Kneller, E.L., Allen, E.M., Wang, Z., Browning, K.S., and Miller, W.A. (2008). The 3? cap-independent translation element of Barley yellow dwarf virus binds eIF4F via the eIF4G subunit to initiate translation. RNA *14*, 134–147.

Tsuge, S., Kobayashi, K., Nakayashiki, H., Okuno, T., and Furusawa, I. (1994). Replication of *Cauliflower Mosaic Virus* ORF I mutants in turnip protoplasts. Jpn. J. Phytopathol. *60*, 27–35.

Turck, F., Kozma, S.C., Thomas, G., and Nagy, F. (1998). A Heat-Sensitive *Arabidopsis thaliana* kinase substitutes for human p70s6k function *in vivo*. Mol. Cell. Biol. *18*, 2038–2044.

Turck, F., Zilbermann, F., Kozma, S.C., Thomas, G., and Nagy, F. (2004). Phytohormones Participate in an S6 Kinase Signal Transduction Pathway in *Arabidopsis*. Plant Physiol. *134*, 1527–1535.

Turkina, M.V., Klang Arstrand, H., and Vener, A.V. (2011). Differential Phosphorylation of Ribosomal Proteins in *Arabidopsis thaliana* Plants during Day and Night. PLoS ONE *6*.

Vain, P., Harvey, A., Worland, B., Ross, S., Snape, J.W., and Lonsdale, D. (2004). The effect of additional virulence genes on transformation efficiency, transgene integration and expression in rice plants using the pGreen/pSoup dual binary vector system. Transgenic Res. *13*, 593–603.

Valásek, L., Nielsen, K.H., Zhang, F., Fekete, C.A., and Hinnebusch, A.G. (2004). Interactions of eukaryotic translation initiation factor 3 (eIF3) subunit NIP1/c with eIF1 and eIF5 promote preinitiation complex assembly and regulate start codon selection. Mol. Cell. Biol. *24*, 9437–9455.

Vetter, I.R., and Wittinghofer, A. (2001). The guanine nucleotide-binding switch in three dimensions. Science *294*, 1299–1304.

Voigts-Hoffmann, F., Klinge, S., and Ban, N. (2012). Structural insights into eukaryotic ribosomes and the initiation of translation. Curr. Opin. Struct. Biol. *22*, 768–777.

Vornlocher, H.P., Hanachi, P., Ribeiro, S., and Hershey, J.W. (1999). A 110-kilodalton subunit of translation initiation factor eIF3 and an associated 135-kilodalton protein are encoded by the *Saccharomyces cerevisiae* TIF32 and TIF31 genes. J. Biol. Chem. *274*, 16802–16812.

Wang, A., and Krishnaswamy, S. (2012). Eukaryotic translation initiation factor 4E-mediated recessive resistance to plant viruses and its utility in crop improvement. Mol. Plant Pathol. *13*, 795–803.

Watanabe, R., Murai, M.J., Singh, C.R., Fox, S., Ii, M., and Asano, K. (2010). The eukaryotic initiation factor (eIF) 4G HEAT domain promotes translation re-initiation in yeast both dependent on and independent of eIF4A mRNA helicase. J. Biol. Chem. *285*, 21922–21933.

Whittle, C.A., and Krochko, J.E. (2009). Transcript profiling provides evidence of functional divergence and expression networks among ribosomal protein gene paralogs in *Brassica napus*. Plant Cell *21*, 2203–2219.

Williams, A.J., Werner-Fraczek, J., Chang, I.-F., and Bailey-Serres, J. (2003). Regulated phosphorylation of 40S ribosomal protein S6 in root tips of maize. Plant Physiol. *132*, 2086–2097.

Wilson, D.N., and Doudna Cate, J.H. (2012). The structure and function of the eukaryotic ribosome. Cold Spring Harb. Perspect. Biol. *4*.

Xiong, Y., McCormack, M., Li, L., Hall, Q., Xiang, C., and Sheen, J. (2013). Glc-TOR signalling leads transcriptome reprogramming and meristem activation. Nature *496*, 181–186.

Yaman, I., Fernandez, J., Liu, H., Caprara, M., Komar, A.A., Koromilas, A.E., Zhou, L., Snider, M.D., Scheuner, D., Kaufman, R.J., et al. (2003). The zipper model of translational control: a small upstream ORF is the switch that controls structural remodeling of an mRNA Leader. Cell *113*, 519–531.

Yanagiya, A., Svitkin, Y.V., Shibata, S., Mikami, S., Imataka, H., and Sonenberg, N. (2009). Requirement of RNA binding of mammalian eukaryotic translation initiation factor 4GI (eIF4GI) for efficient interaction of eIF4E with the mRNA cap. Mol. Cell. Biol. *29*, 1661–1669.

Yatime, L., Schmitt, E., Blanquet, S., and Mechulam, Y. (2004). Functional molecular mapping of archaeal translation initiation factor 2. J. Biol. Chem. *279*, 15984–15993.

Yatime, L., Mechulam, Y., Blanquet, S., and Schmitt, E. (2006). Structural switch of the gamma subunit in an archaeal aIF2 alpha gamma heterodimer. Struct. Lond. Engl. 1993 *14*, 119–128.

Yatime, L., Mechulam, Y., Blanquet, S., and Schmitt, E. (2007). Structure of an archaeal heterotrimeric initiation factor 2 reveals a nucleotide state between the GTP and the GDP states. Proc. Natl. Acad. Sci. U. S. A. *104*, 18445–18450.

Yoo, S.-D., Cho, Y.-H., and Sheen, J. (2007). *Arabidopsis* mesophyll protoplasts: a versatile cell system for transient gene expression analysis. Nat. Protoc. *2*, 1565–1572.

Yu, Y., Marintchev, A., Kolupaeva, V.G., Unbehaun, A., Veryasova, T., Lai, S.-C., Hong, P., Wagner, G., Hellen, C.U.T., and Pestova, T.V. (2009). Position of eukaryotic translation initiation factor eIF1A on the 40S ribosomal subunit mapped by directed hydroxyl radical probing. Nucleic Acids Res. *37*, 5167–5182.

Yu, Y., Sweeney, T.R., Kafasla, P., Jackson, R.J., Pestova, T.V., and Hellen, C.U. (2011). The mechanism of translation initiation on Aichivirus RNA mediated by a novel type of picornavirus IRES. EMBO J. *30*, 4423–4436.

Zanetti, M.E., Chang, I.-F., Gong, F., Galbraith, D.W., and Bailey-Serres, J. (2005). Immunopurification of Polyribosomal Complexes of *Arabidopsis* for Global Analysis of Gene Expression. Plant Physiol. *138*, 624–635.

Zeenko, V., and Gallie, D.R. (2005). Cap-independent translation of tobacco etch virus is conferred by an RNA pseudoknot in the 5'-leader. J. Biol. Chem. *280*, 26813–26824.

Zhang, S.H., Broome, M.A., Lawton, M.A., Hunter, T., and Lamb, C.J. (1994). atpk1, a novel ribosomal protein kinase gene from *Arabidopsis*. II. Functional and biochemical analysis of the encoded protein. J. Biol. Chem. *269*, 17593–17599.

Zhou, F., Roy, B., and von Arnim, A.G. (2010). Translation reinitiation and development are compromised in similar ways by mutations in translation initiation factor eIF3h and the ribosomal protein RPL24. BMC Plant Biol. *10*, 193.

Zijlstra, C., Schärer-Hernández, N., Gal, S., and Hohn, T. (1996). *Arabidopsis thaliana* expressing the *Cauliflower mosaic virus* ORF VI transgene has a late flowering phenotype. Virus Genes *13*, 5–17.

Zoncu, R., Efeyan, A., and Sabatini, D.M. (2011). mTOR: from growth signal integration to cancer, diabetes and ageing. Nat. Rev. Mol. Cell Biol. *12*, 21–35.

UNIVERSITÉ DE STRASBOURG

Eder Alberto MANCERA-MARTÍNEZ

Fonction de la protéine cellulaire RISP (Reinitiation Supporting Protein) dans la reinitiation de la traduction chez les plantes

École Doctorale des Sciences de la Vie et de la Santé STRASBOURG

Résumé

La protéine cellulaire appelée RISP est détournée par le virus de la mosaïque du chou-fleur (CaMV) pour assurer, ensemble avec la protéine virale TAV (transactivator/viroplasmin), la traduction de son ARN 35S polycistronique. Le CaMV est également le premier virus codant une protéine capable d'interagir directement avec la protéine kinase cellulaire TOR et ainsi activer sa voie de signalisation qui stimule la traduction. La protéine RISP a été identifiée comme une nouvelle cible de la voie de signalisation de TOR et il a été montré que cette phosphorylation de la sérine 267 est requise pour promouvoir la réinitiation de la traduction activée par TAV. Cependant, le rôle de RISP dans la traduction cellulaire de même que dans le processus d'activation par TAV fait encore l'objet d'investigations. Les résultats que j'ai obtenus au cours de mon travail de thèse suggèrent que RISP intervient ensemble avec eIF3, au niveau du complexe de pré-initiation 43S pour recruter le complexe ternaire (eIF2/GTP/Met-tRNAi^{Met}) grâce à l'interaction entre RISP et la sous-unité β du facteur eIF2, ainsi que dans le mouvement dynamique du ribosome 80S en cours de traduction, en faisant un pont entre les sous-unités ribosomiques 40S et 60S. Des résultats préliminaires indiquent que RISP non-phosphorylée s'associe à eIF2β plus efficacement que la forme phosphorylée. En plus, la structure cristallographique du ribosome 80S de la levure a révélé que le domaine N-terminal de la protéine ribosomique eL24 qui fixe TAV, est localisé à l'interface de la sous-unité 60S alors que l'hélice α C-terminale d'eL24 qui interagit avec RISP, émerge de la sous-unité 60S en direction de la protéine ribosomique eS6 de la sous-unité 40S. La protéine eS6 est connue depuis longtemps pour être une cible de la voie de TOR mais la fonction de cette phosphorylation demeure inconnue. De ce fait, nous avons investigué l'interaction éventuelle entre eS6 et eL24 ainsi que le rôle de RISP dans l'association entre les sous-unités 40S et 60S. Bien que nous n'ayons trouvé aucun lien direct entre eS6 et eL24, il s'est avéré que RISP a la capacité, lorsqu'elle est phosphorylée, d'interagir non seulement avec eL24 mais également avec eS6 chez *Arabidopsis*. Nos résultats suggèrent que la phosphorylation de la protéine eS6 joue un rôle dans sa liaison à RISP, ainsi que dans la transactivation traductionnelle chez le CaMV. En effet, des plantes d'*Arabidopsis*, dans lesquelles une des deux copies du gène codant eS6 a été inactivée, sont plus résistantes à l'infection par le CaMV et moins efficaces dans la reinitiation de la traduction assurée par TAV. Nos résultats indiquent que la liaison entre les sous-unités ribosomiques 60S et 40S sous l'effet de RISP, est régulée par la voie de TOR et qu'elle joue un rôle dans le contrôle de la réinitiation de la traduction.

Mots clés : Reinitiation de la traduction; Para-rétrovirus; TAV; RISP; Protéine ribosomique eS6; voie de signalisation de TOR

Résumé en anglais

A complex arrangement of factors is required to recruit the initiator tRNA (Met-tRNAiMet) and a 60S ribosomal subunit to the 40S ribosomal subunit preinitiation complex (40S PIC) initiating translation. This recruitment is normally strictly limited during reinitiation of translation if factors recruited during the primary translation event are shed from 40S. However, factor retention can occur during short ORF translation, or during long ORF translation if the Cauliflower mosaic virus (CaMV) reinitation factor TAV is present. TAV, together with retention of eIF3 and a cellular reinitiation-supporting factor (RISP) on the translating ribosome, mediates activation of the protein kinase TOR (Target of Rapamycin) to maintain ribosome-associated factors in their active phosphorylated state. RISP is a downstream target of TOR and found either within the 43S preinitiation complex (43S PIC), if bound to eIF3, and/or attached to 60S, if phosphorylated by TOR. We show here that RISP interacts physically with subunit β of eukaryotic initiation factor 2 (eIF2β) in vitro and in vivo. RISP lacking its phosphorylation site (RISP-S267A) binds eIF2β significantly more strongly. Thus RISP may function together with eIF3 in eIF2 recruitment to 43S PIC before being phosphorylated. In contrast, a RISP phosphorylation mimic interacts preferentially with the 40S ribosomal protein eS6. Full-length RISP is required to interact specifically with the eS6 C-terminal alpha helix. Critically, TOR activation up-regulates phosphorylation of both RISP and eS6 at its C-terminus as well as the binding of both factors. Since phosphorylated RISP also associates with the C-terminal α-helix of eL24, it may link both C-terminal tails, forming or stabilizing an intersubunit bridge within 80S. Importantly, eS6-deficient plants are less active in TAV-mediated reinitiation after long ORF translation and are thus less susceptible to CaMV infection. In addition, S6a-knockout plants display defects in root gravitropism typical of TOR-deficient plants as would be expected for TOR downstream targets. It is attractive to propose that eS6 phosphorylation contributes to retention and re-use of 60S during 40S scanning.

Keywords: 60S joining, TOR signaling pathway, S6K1, ribosomal protein eS6, CaMV, eIF3, gravitropic response